University of Novi Sad
FACULTY OF TECHNICAL SCIENCES
DEPARTMENT OF PRODUCTION ENGINEERING
21000 NOVI SAD, Trg Dositeja Obradovica 6, SERBIA

UDK 621 ISSN 1821-4932

JOURNAL OF

PRODUCTION ENGINEERING

Volume 20 Number 2

Novi Sad, December 2017

Journal of Production Engineering, Vol.20 (2017), Number 2

Publisher: FACULTY OF TECHNICAL SCIENCES
DEPARTMENT OF PRODUCTION ENGINEERING
21000 NOVI SAD, Trg Dositeja Obradovica 6
SERBIA

Manuscript submitted for publication: December 30, 2017.
Printing: 1st
Circulation: 300 copies

CIP classification:

CIP – Катаголизација у публикацији
Библиотека Матице српске, Нови Сад

621

JOURNAL of Production Engineering / editor in chief Pavel Kovač. – Vol. 12, No. 1 (2009)- . – Novi Sad : Faculty of Technical Sciences, Department for Production Engineering, 2009-. – 30 cm

Dva puta godišnje (2012-). Je nastavak: Časopis proizvodno mašinstvo = ISSN
0354-6446
ISSN 1821-4932

Printing by: FTN, Graphic Center ***GRID,*** *Novi Sad*

ISSN: 1821-4932

http://doi.org/10.24867/JPE-2017-02

INTERNATIONAL EDITORIAL BOARD

Editorial

The ***Journal of Production Engineering*** *dates back to 1984, when the first issue of the* ***Proceedings of the Institute of Production Engineering*** *was published in order to present its accomplishments. In 1994, after a decade of successful publication, the Proceedings changed the name into Production Engineering, with a basic idea of becoming a Yugoslav journal which publishes original scientific papers in this area.*

In 2009 year, our Journal finally acquires its present title - ***Journal of Production Engineering****. To meet the Ministry requirements for becoming an international journal, a new international editorial board was formed of renowned domestic and foreign scientists, refereeing is now international, while the papers are published exclusively in English. From the year 2011 Journal is in the data base Google scholar, COBISS and KoBSON presented.*

The Journal is distributed to a large number of recipients home and abroad, and is also open to foreign authors. In this way we wanted to heighten the quality of papers and at the same time alleviate the lack of reputable international and domestic journals in this area.

Editor in Chief

Professor Pavel Kovač, PhD,

Journal of Production Engineering
Vol.20 No.2

Contents

ORIGINAL SCIENTIFIC PAPER

http://doi.org/10.24867/JPE-2017-02-001

Journal of Production Engineering

Vol.20 No.2

JPE (2017) Vol.20 (2) Original Scientific Paper

Alabi, A.G.F., Aweda, J.O, Aluko, F.I.

INFLUENCE OF FERROSILICON MANGANESE ON THE SULPHUR CONTENT AND MICROSTRUCTURE IN THE PRODUCTION OF AUSTEMPERED DUCTILE IRON (ADI)

Received: 22 September 2017 / Accepted: 12 November 2017

Abstract: *This study considers the effect of ferrosilicon manganese addition to austempered ductile iron, (ADI) in order to reduce its sulphur level for improved engineering applications of the material. The cast samples were austenitised in a mixture of potassium chloride, sodium chloride and barium chloride solutions and austempered in sodium nitrate and potassium nitrate solutions. Ferrosilicon manganese was added to ADI in various amounts ranging from between 47 to 326 g. The study revealed that the sulphur level retained in ADI decreased from 0.088 wt % for as-cast to 0.027 wt % when 93 g of ferrosilicon manganese was added. Below this amount of ferrosilicon manganese addition, there was no significant reduction in the sulphur level recorded in ADI. The microstructure of the metal revealed bigger graphite nodules scattered in ferrite solutions for the situation when the sulphur level was 0.027 wt. %. From the study, it was discovered that addition of small amount of ferrosilicon manganese was required to produce ADI of low level sulphur content to make the metal more acceptable for other engineering applications.*

Key words: *Ductile iron, sulphur, austempering, nodularizer, ferrosilicon*

Uticaj ferosilikonskog mangana na sadržaj sumpora i mikrostrukturu u proizvodnji izotermalno poboljšanog gvožđa (ADI). *Ova studija razmatra uticaj dodatka ferozilicijevog mangana na izotermalno poboljšano gvožđe (ADI) kako bi smanjio nivo sumpora u cilju poboljšanja inženjerske primene materijala. Uzorci odlivaka su austenitizovani u mešavini kalijum hlorida, natrijum hlorida i rastvora barijum hlorida i austemperovani u rastvorima natrijum nitrata i kalijum nitrata. Ferosilicijum mangan je dodat u ADI u različitim količinama u rasponu od 47 do 326 g. Studija je utvrdila da je nivo sumpora zadržan u ADI je smanjen sa 0,088 tež.% za livenje na 0,027 tež.% kada je dodato 93 g ferosilikon mangana. Ispod ove količine ferosilicijevog manganskog dodatka, nije bilo značajnog smanjenja nivoa sumpora zabeleženog u ADI-u. Mikrostruktura metala otkrila je veće grafitne nodule raspršene u feritnim rastvorima za situaciju kada je nivo sumpora bio 0,027 tež. %. Studija je utvrdila da je dodatak male količine ferosilikovanog mangana potreban za proizvodnju ADI sadržaja sumpora na niskom nivou kako bi metal bio prihvatljiviji za druge inženjerske aplikacije.*

Ključne reči: *Nodularno gvožđe, sumpor, izotermalno poboljšanje, nodularizator, ferosilikon*

1. INTRODUCTION

Discovering new materials with improved mechanical properties meeting the required applications has engaged the attention of researchers worldwide. In recent years, Austempered Ductile Iron (ADI), obtained from ductile iron, has attracted considerable applications because of its good mechanical properties. Such properties include resistance to fatigue [1-4], good wear resistance [5, 6], high strength with good ductility [7-9] and good rolling contact resistance [10]. The density of ADI is lower than steel [8, 12] which makes it more applicable in the areas of production of engine blocks and other engineering components. ADI is used in the production of swivel pins, rail brakes and pressure pipes in the oil industry [13-16]. Thus, ADI has been found to have higher specific strength than steel [6, 17-21]. Austempered ductile iron products are used in the automobile and textile industries as crank shafts, cam shafts, gearwheels and thin wall castings reinforced parts [10, 16, 18, 26]. The production of ADI is cheaper when compared with forged steel by 20 % [27, 28]. Compared to steel, ADI exhibits improved properties in terms of machinability, tool life and machining speeds, surface finish, improved safeguard against failure (due to the lubricating effect provided by graphite) [17, 22], good ballistic properties [26], good resistance to bending fatigue [1], good damping capacity (better noise attenuation), amenability to heat treatment [6, 21, 24, 25], good corrosion resistance [24].

Therefore, ADI is considered as an economical substitute for wrought or forged steel in several structural applications [2, 3]. The metal loses less of its toughness than steel at sub-zero temperature. Austempered ductile iron usually work-hardens when stressed and has good vibration damping capability and heat transfer than other ferrous and non-ferrous alloys [18, 22, 26].

Liu [26] in his work suggested that an improved structure of ADI could be obtained by controlling the heat treatment process of nodular cast iron. The microstructure and mechanical properties of ADI can be influenced by the isothermal heat treatment and the temperature of austenite transformed [16]. The temperature of isothermal transformation is in the range of 250 and 450 ^{0}C [18]. When higher transformation

temperature above 450 ^{0}C is used, it resulted in lower strength and hardness but higher elongation and toughness and better fatigue characteristics [18, 23].

However, substantial amount of sulphur in ADI and other ferrous alloys have negative effect on their mechanical properties hence limiting their applications [1, 17, 18]. Other factors limiting the use of ADI include the low nodule count caused by long holding time in the furnace, prolonged pouring time and low carbon equivalent [11, 26] where the precipitating graphite was not adequate during cooling under inoculation or when pouring temperature is high.

In this work, standard method of producing austempered ductile iron was used while adding ferrosilicon manganese in varying quantities to it in the molten state. This was done such that the sulphur content in the produced ADI will be minimized which will consequently enhance the metal's applicability in engineering service.

2. MATERIALS AND METHOD

Grey cast iron scraps with percent weight of 0.199 of sulphur and other constituents from automobile engine blocks and graphite were collected and melted. The scraps were broken into smaller sizes to facilitate fast melting in the lift out crucible furnace used which was located in the foundry workshop of the Engineering Materials Development Institute (E.M.D.I), Akure, Nigeria.

2.1 Method of production

The production procedure of austempered ductile iron involved the processing of ductile iron casting that was austenized at temperatures between 800 and 950 ^{0}C. It was then quenched to a temperature of 250 – 400 ^{0}C in salt bath of potassium nitrate and sodium nitrate [17]. The rapid cooling referred to as austempering, was given to avoid the formation of pearlite or other micro-constituents to a temperature above martensite start (MS). It is possible to produce both compacted graphite irons and ductile iron from the same base iron by using cored wire containing a high magnesium and ferrosilicon. Magnesium ferrosilicon was used as nodularizer, while ferrosilicon was used as inoculants for the grey cast iron. The nodularizer was poured into the ladle while the inoculants were added in the prepared mould. Ferrosilicon manganese was added to the melt of the grey cast iron scraps in the furnace.

3. CASTING PROCEDURE

3.1 Melting process

The weights of the graphite, magnesium ferrosilicon and ferrosilicon manganese were measured using OHAUS-CS2000 electronic weighing machine at the foundry workshop of E.M.D.I., Akure. An Avery weighing scale of 250 kg capacity was employed in measuring the weight of the scraps that were melted in the rotary furnace. The furnace was 100 kg capacity oil fired designed and constructed locally by E.M.D.I. Akure. Eighteen grams each of powdered graphite and powdered ferrosilicon were introduced into the pocket of the mould before pouring of the molten metal in to the mould for casting. Magnesium, 700 g, and 18 g of powdered ferrosilicon were added as inoculants for all the melts. Ferrosilicon manganese with quantity ranging from between 47 g to 326 g was introduced in to the furnace for different melts. The temperature of the furnace was taken at an interval of ten minutes during melting process to ascertain that the material was completely molten. After the material had become molten, the tap hole of the furnace was opened. The ladle was brought near the furnace and the rotary furnace was tilted to pour the molten metal into the ladle. The ladle was preheated to a temperature slightly above 500^{0}C and maintained at this temperature through the period of pouring into the prepared mould. After pouring, the melt was allowed to solidify freely in the mould. All specimens were prepared while varying the amount of ferrosilicon manganese added from 47 g to 326 g. For the control, the same process was followed except that ferrosilicon manganese was not added in the process of melting.

The scraps used had the sulphur content as 0.199 percent weight and other components that was determined using Optical Emission Spectrometry. Table 1 shows the amount of sulphur in the initial ductile iron and final composition after the addition of varying amounts of ferrosilicon manganese.

Melt	Sulphur content in the scrap (% wt)	Ferrosilicon manganese added (g)	Final values of sulphur retained (% wt)
A	0.199	0	0.088
B	0.199	326	0.086
C	0.199	233	0.030
D	0.199	140	0.028
E	0.199	93	0.027
F	0.199	47	0.027

Table 1. The initial and the actual values of sulphur contents

4. RESULTS AND DISCUSSION

4.1 Effects of ferrosilicon manganese addition to ADI compositions

Figure 1 is the graph of various melts with composition of sulphur by weight % in the melts. With the addition of ferrosilicon manganese in varying amounts, the sulphur weights % retained were between 0.027 and 0.086. The highest value was recorded in melt A (0.088), the control and the least value of 0.027 g in Melts E and F. The sulphur content slightly reduced to 0.086 weight % for melt B when ferrosilicon manganese of 326 g was added. For melts C to F, when the added ferrosilicon manganese was reduced the sulphur content was greatly reduced from 0.030 to 0.027. There is no much difference between the sulphur weight percent of melts D to F as seen from the figure. The reduction in % weight composition of sulphur might have been through the addition of ferrosilicon manganese in smaller quantity where sulphur had reacted with manganese to form manganese sulphide, a slag that floated on the cast metal during casting. The graph also shows that with a

little amount of ferrosilicon manganese addition to the ductile iron not exceeding 93 % weight, the sulphur content is significantly reduced.

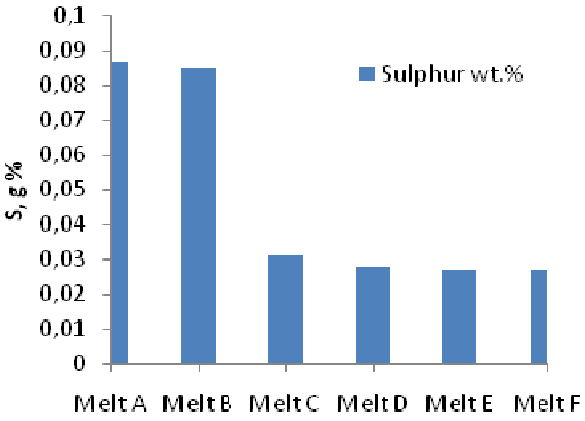

Fig. 1. Sulphur content in various melts

Figure 2 presents the composition of silicon percent weight in various melts as the quantity of ferrosilicon manganese added to ADI was varied for different melts. The silicon weight percent increased from Melt B to Melt E as the amount of ferrosilicon manganese added decreased. When 326 g of ferrosilicon manganese was added as in Melt B, the silicon retained was 1.87 g % wt this amount increased to 2.95 g when 93 g of ferrosilicon manganese was added as represented in Melt E. With the addition of 47 g of ferrosilicon manganese (Melt F), the amount of silicon retained reduced to 2.87 g % wt. The amount of silicon deposited was reduced because of the reduced quantity of ferrosilicon manganese that was added which led to less silicon available for the reaction.

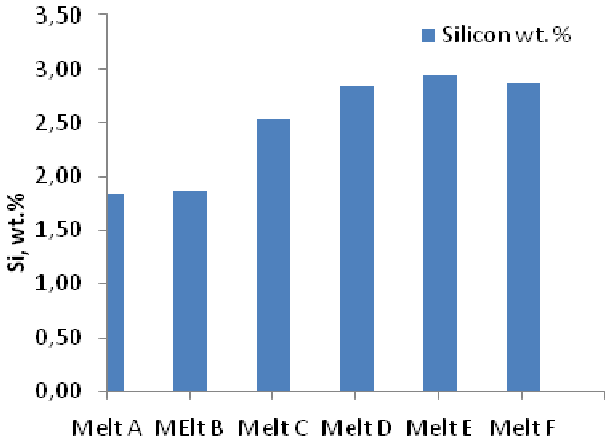

Fig. 2. Silicon content of vrious melts

From figure 3, the weight % of magnesium present in the ADI with the addition of ferrosilicon manganese ranged from between 0.0042 g for Melt A to 0.035 g for Melt F. Melt A which is the control, has the least weight % of 0.0042 g, while Melt F has the highest with 0.035 g. The weight % of magnesium present in ductile iron is usually not above 0.05 weight %. This amount obtained was likely due to the magnesium been deposited into the cast metal which resulted into the formation of magnesium ferrosilicon.

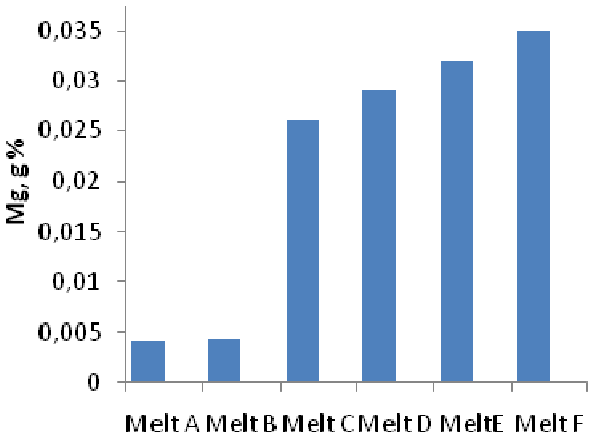

Fig. 3. Magnesium contents of various melts

Figure 4 represents the amount of iron retained in the melts with the addition of ferrosilicon manganese. The values of iron present in the melts were between 93.5 and 92.06 g for Melts A (control) and D respectively. The percentage change in the amount of iron present in the ADI from the control sample when ferrosilicon manganese was not added to that of Melt D when 140 g of ferrosilicon manganese was added is 1.5 %. This results show that addition of ferrosilicon manganese into ADI has no much influence on the % wt of iron in the metal.

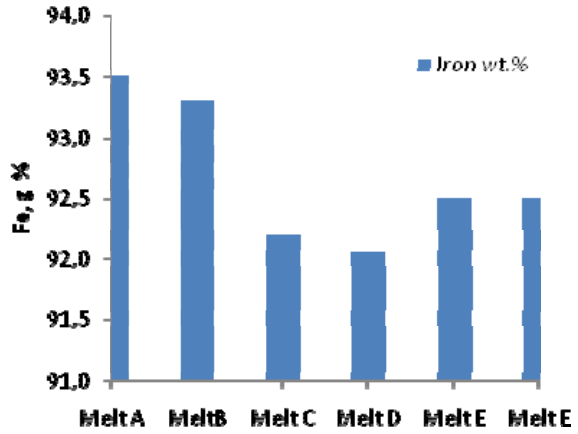

Fig. 4. Iron contents of various melts, wt.%

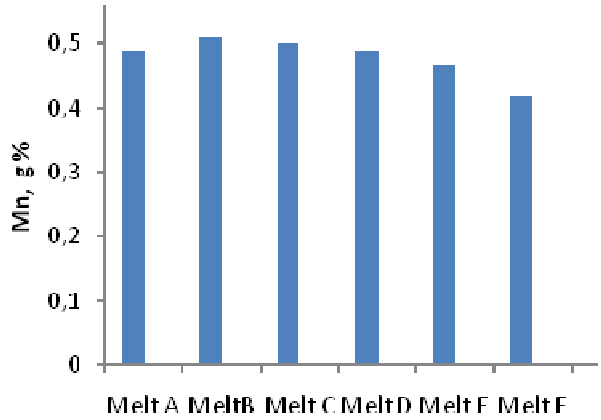

Fig. 5. Manganese contents of various melts, wt. %

The weight % of manganese present in the metal decreased from 0.510 to 0.419 g as shown in figure 5.

The amount of manganese retained after the casting was reduced from Melts B to F as the amount of ferrosilicon manganese added was reduced. Even though no ferrosilicon manganese was added to Melt A, about 0.488 weight % of manganese was recorded in the cast metal. The reason for the low manganese content in Melts B to F may be ascribed to the reactions that took place within the furnace where manganese and sulphur reacted to form manganese sulphide.

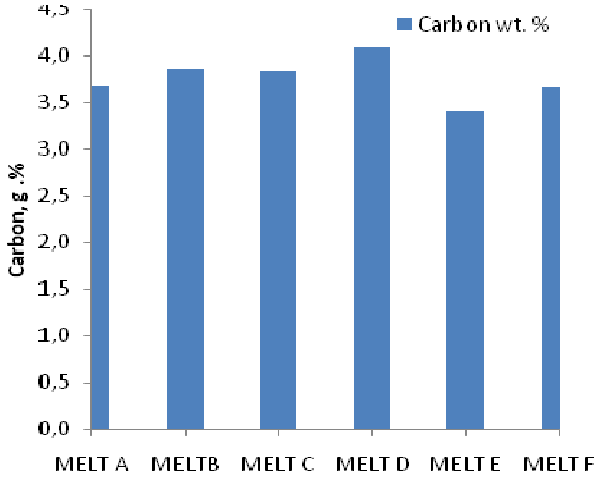

Fig. 6. Carbon contents in various Melts, wt %

Figure 6 depicts the carbon weight % of the sample which falls between 3.41 and 4.1 wt. percent with ferrosilicon addition in varying amounts. Melt D has the highest weight percent of 4.1 g while Melt E has the least, 3.41 g as reflected in the figure. Melts B and C have 3.87 and 3.84 weight % respectively. The control, Melt A grey cast iron has 3.68 weight %. This lower value may be an indication that some carbon might have reacted with oxygen to form carbon monoxide which would have diffused into the air. Melt D with highest carbon content may likely show improved mechanical properties

4.2 Effect of ferrosilicon manganese on microstructures

Figure 7a is the micrograph of Melt A when no ferrosilicon manganese was added to ADI. The microstructure revealed long graphite flakes within ferrite which probably is an indication that the metal will be soft and easy to machine.

Fig. 7a. Micrograph of Melt A

Figure 7b represents the micrograph of the metal with the addition of 326 g of ferrosilicon manganese where the graphite stripes turned to graphite nodules. The graphite nodules form lumps and are surounded by ferrite within the matrix. The lumped nodules are seen scatered within ferrite. This formation implies that the material is ductile iron. The silicon resulting from the added ferrosilicon has shown its potency for ferrite formation in the ductile iron

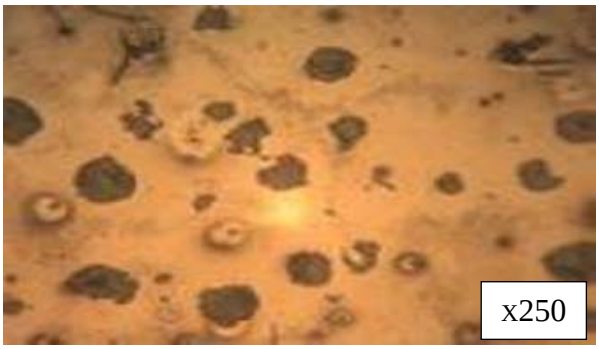

Fig. 7b. Micrograph of Melt B

Figure 7c is the microstructure of Melt D when 140 g of ferrosilicon manganese was added to ADI. The micrograph shows the presence of high concentration of graphite nodules within ferrites. Figure 7d represents the microgrph of Melt E when 93 g of ferrosilicon manganese was added showing bigger graphite nodules than that obtained for Melt D and relatively scattered all over the surface within ferrite confirming the results obtained by Alasoluyi *et al;*[12]

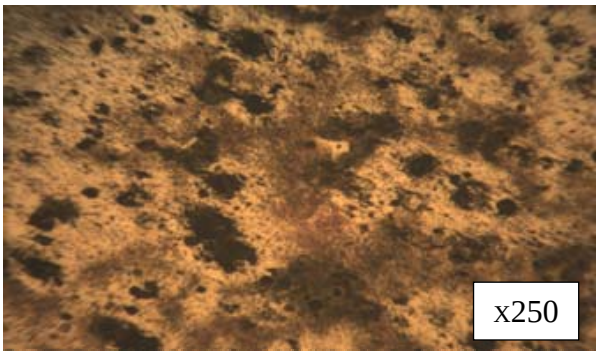

Fig. 7c. Micrograph of Melt D

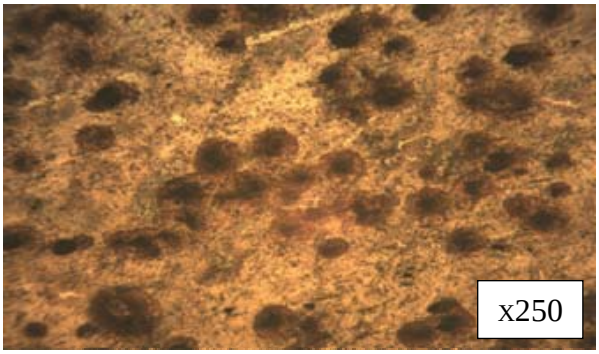

Fig. 7d. Micrograph of Melt E

Figure 7e is the situation when 47 g of ferrosilicon manganese was added to ADI. The microstructure as shown on the figure contained very few but big graphite

nodules with ferrites fairly scatered all over the surface. This similar effect was also observed by Alasoluyi *et al;* [6] in their work. The silicon from the ferrosilicon is seen to initiate the formation of the ferrite and tends to be slightly forming in the pearlite of the matrix. This also promotes the precipitation of the graphite nodules in pearlite matrix with little ferrite in existence. The figure reveals that the presence of ferrite is been usurped by the appearance of pearlite within the metal.

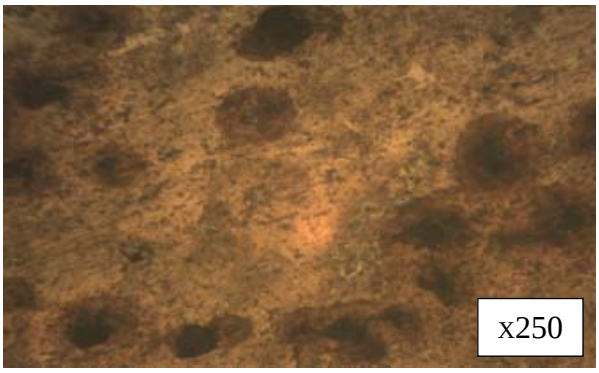

Fig. 7e. Micrograph of Melt F

5. CONCLUSIONS

Austempered ductile iron was produced by casting process through the addition of varying amount of ferrosilicon manganese in the ranges of 47, 93, 140, 233, 326 wt. % using lift out crucible furnace. The compositional analysis and microstructural examinations of the products were evaluated and compared with the as-cast. The following conclusions are made from the study;

1. Austempering of ductile iron in a lift out crucible furnace was successfully carried out.
2. Addition of ferrosilicon manganese to ADI has influence on the amount of sulphur and other constituent elements retained in the metal.
3. Addition of 47 g % wt. of ferrosilicon manganese to ADI shows significant lowering of sulphur retained in the metal after casting.

The microstructural examinations revealed that the graphite nodules were well distributed in the ADI

6. REFERENCES

[1] Yamanaka, M., Tamura, R., Inoue, K. and Narita, Y.: *Bending fatigue strength of austempered ductile iron spur gears,* Journal of Advanced Mechanical Design, Systems and Manufacturing, vol. 3(3), (2009), 203-211.

[2] Hassan, S.B.: Austempered Ductile cast Iron–An Alternative to steel and Aluminiums in Automotive Applications, Nigerian Mining Journal, 5(1), (2007), 32-39.

[3] Adewuyi, B.O., Afonja, A.A. and Adegoke, C.O.: *Effects of Isothermal Transformation on Fatigue strength of Austempered Ductile Iron*, Botswana Journal of Technology, vol. 14 No 2 (2005), 21-25.

[4] Aluko, F.I.: *Effect of Heat Treatment on Corrosion Properties of Gray Cast Iron in Paper making industries,* Nigerian Journal of Engineering Management, Besade Publishing press. Ondo, 5(1), (2004), 31-33.

[5] Rebasa, N., Dommarco, R., and Sikora, J.: *Wear Resistance of High Nodule Count Ductile Iron,* (T-8), Hokongghub, ElsevierScience, vol. 253, (2002), 855-861.

[6] Alasoluyi, J.O., Omotoyinbo, J.A., Olusunle, S.O.O. and Adewuyi, O.O.: *Investigation of Mechanical Properties of Ductile Iron Produced from Hybrid Innoculants using Rotary Furnace,* International Journal of Science and Engineering, vol. 2(5), (2013), 338-393.

[7] Keough, J.R. and Hayrynen, K.L.: *Designing with austempering ductile iron (ADI),* American Foundry Society, (2010), 1-15.

[8] Hassan, S.B.: The Effect of Chromium Additions on Microstructure and Mechanical Properties of Nodular Cast Iron, N.S.E.Technical Transaction, 41(3), (2006), 33-41.

[9] Behmani, M., Elliot, R. and Varehan, N.: *Austempered Ductile Iron: A Competitive Alternative for Forged Induction–Hardened Steel Crankshafts,* International Journal of Cast Metals Research, vol. 9, (1997), 249-257.

[10] Nofal, N.: *Advances in the metallurgy and applications of ADI,* Journal of Metallurgical Engineering (ME), vol. 2(1), (2013), 1-18.

[11] Shiokara, T.: *Effect of Graphite Nodules on Crack Growth Behavior of Austempered Ductile Cast Iron (ADI),* 59th Japan Ductile Cast Iron. Association Conference, Tokyo, Japan, (1978), 138-150.

[12] Alasoluyi, J.O., Omotoyinbo, J.A., Borode, J.A., Olusunle, S. O.O. and Adewuyi, O.O.: *Influence of Secondary Introduction of Carbon and Ferrosilicon on the Microstructure of Rotary Furnace Produced Ductile Iron,* International Journal of Science and Engineering, vol. 2(2), (2013), 211-217.

[13] Vechet, S., Kohout, J., Klakurkova, L.: *Fatigue Properties of Austempered Ductile Iron in Dependence Transformation Temperature,* Material Science (Medziagotyra), 14(4), (2008), 324-327.

[14] Trudel, A. and Gagne, A.: Effect of Composition and Heat Treatment Parameters on the Characteristics of ADI, Canadian Metallurgical, (1998), 289-298.

[15] Hassan, S.B. and Isah, L.A.: A study of relationship between Tensile Properties and Microstructure of low Alloy Austempered Ductile Iron Using Khaya Senegalensis Seed Oil as Quenchant, Journal of Metallurgy and Materials Engineering, 5 (2), (2010), 14–21.

[16] Bhople, N., Pahl, S. Harne, M. and Dhande, S.: *Austempering parameters and machinability of austempering ductile iron: A comprehensive review on effective parameters,* International Journal of Innovative Research in Science, Engineering and Technology, vol. 5(2), (2016), 1197-1211.

[17] Myszka, M. and Presz, W.: Microstructure transformations in austempered ductile iron during

deformation by dynamic hardness test, Computer methods in Materials Science, vol. 12(4), (2012), 259-263.
[18] Sikora, J. and Boeri, R.: Advances in ductile iron research: New metallurgical understanding and its Technological Significance, Archives of Foundry, vol. 5(15), (2005), 354-360.
[19] Kaczorowski, M. and Krzynska, A.: *Mechanical Properties and Structure of Austempered Ductile Iron-ADI,* Archives of Foundry Engineering, Publications of Foundry Commission of the Polish Academy, vol. 7, (2007), 161-166.
[20] Uma, B.: *Influence of composition and austempering temperature on machinability of austempered ductile iron,* International Journal of chemical, nuclear, Metallurgical and Materials Engineering, 7 (2), (2013), 116-121.
[21] Yawas, D.S.: Corrosion Characteristics of Mild Steel and Ductile Cast Iron Exposed to Different Media, N.S.E. Technical Transaction vol. 41 (3), (2006), 125-134.
[22] Bela, V. and Kovas, Sr.: *Autempered ductile iron: Facts and Friction,* Modern Casting, (1990), 38-41.
[23] Daramola, O.O. Adewuyi, B.O. and Oladele, I.O.: *Effect of Heat Treatment on the Mechanical properties of Rolled Medium Carbon Steel,* Journal of Minerals and Materials Characterization and Engineering, vol. 8, (2010), 693–708.
[24] Kovacs, B.: *The Effects of alloying Elements and their Segregation in ADI,* Proceedings of International Conference on Austempered Ductile Iron, vol.1. New York, USA, (1991), 241-252.
[25] Mszka, D.: *Austenite-martensite transformation in aus-tempered ductile iron,* Archives of Metallurgy and Materials, vol. 52, (2007), 475-480.
[26] Liu, J.: *Unique microstructure and excellent mechanical properties of ADI,* 8th International Symposium on Science and Processing of Cast Iron, Tsinghua University, (October), vol. 3 (4), (2006), 253-257.
[27] S. Balos, S., Radisavljevic, I., Rajnovic, D., Draicanin, M., Tabakovic, S., Eric-Cekic, O. and Sidjanin, L.: *Geometry, mechanical and ballistic properties of ADI material perforated plates,* Materials and Design, Elevier Series, vol. 83, (2015), 66-74.
[28] Myszka, D., Olejnik, L. and Klebizyk, M.: *Microstructure transformation during plastic deformation of the austempered ductile iron,* Archives of Foundry Engineering, Publication of Foundry Commission of the Polish Academy of Sciences, vol. 9, (2009), 169-174.

Acknowledgement
The permission granted by the authority of the Engineering Materials Development Institute, E.M.D.I., Akure, Nigeria to carry out the experimental works of this research in their workshop is highly appreciated.

Authors: **Professor A.G.F. Alabi, Ph.D.,** Kwara State University, College of Engineering and Technology, Department of Mechanical Engineering, Malete, **Dr. J.O. Aweda, Ph.D.,** University of Ilorin, Faculty of Engineering and Technology, Department of Mechanical Engineering, Ilorin. **Dr. F.I. Aluko, Ph.D.,** The Federal Polytechnic, School of Engineering, Department of Mechanical Engineering, Ado-Ekiti, Nigeria. Phone: +234 803 382 2017
E-mail: agfalabi@gmail.com
joaweda@unilorin.edu.ng
jacobaweda@gmail.com

http://doi.org/10.24867/JPE-2017-02-007

Journal of Production Engineering

Vol.20 No.2

JPE (2017) Vol.20 (2) Original Scientific Paper

Rizvi, S.A., Ali, W.

DETERMINATION THE EFFECT OF MACHINING PARAMETERS ON ROUGHNESS IN TURNING OPERATION OF DIN 17210 STEEL USING TAGUCHI TECHNIQUE

Received: 09 November 2017 / Accepted: 12 December 2017

Abstract: *In this research work an attempt has been made to try to investigate the effects of cutting parameters such as feed rate cutting speed and depth of cut on surface roughness in turning operation of 16MnCr5 steel, is a case hardening steel with by the support of Taguchi technique. An orthogonal array, signal to noise (S/N) ratio and analysis of variance (ANOVA) were used to determine the effects and contributions of cutting speed, feed rate and depth of cut on the response variable. Turning operations were carried out by Tungsten carbide coated cutting tool inserts. The experiments were conducted at three different cutting speeds (400, 600 and 800 rpm) with three different feed rates (0.06, 0.12 and 0.18 mm/rev) and a constant depth of cut (0.5, 1.0 and 1.5 mm). The cutting parameters are optimized using signal to noise ratio and the analysis of variance.obtained result data revelled that depth of cut has most significant effect over surface roughness followed by cutting speed while feed rate has lowest effect.*

Key words: *16MnCr5 steel, Regression analysis, Surface Roughness, Taguchi, optimization, ANOVA*

Određivanje uticaja parametara obrade na hrapavost pri operacijama struganja čelika DIN 17210 korišćenjem Taguchi tehnike. *U ovom istraživačkom radu napravljen je pokušaj da se ispita efekat parametara rezanja, kao što su pomak, brzina rezanja i dubina rezanja na hrapavosti površine pri struganju 16MnCr5 čelika, koji je ojačan, pomoću podrške Taguchi metode. Ortogonalni niz, odnos signala i šuma (S/N) i analiza varijanse (ANOVA) korišćeni su za određivanje uticaja i doprinosa brzine rezanja, pomaka i dubine rezanja na varijablu odziva. Pločice sa prevlakom od karbidnih vlakana su korišćene kao alat za rezanje. Eksperimenti su izvedeni sa tri različite brzine rezanja (400, 600 i 800 obrtaja u minuti) sa tri različita pomaka (0.06, 0.12 i 0.18 mm/o) i konstantne dubine rezanja (0.5, 1.0 i 1.5 mm). Parametri rezanja se optimiziraju korišćenjem odnosa šuma signala i analize varijanse. Dobijeni rezultati rezultata otkrivaju da dubina rezanja ima najznačajniji uticaj na hrapavost površine, nakon čega sledi brzina rezanja, dok pomak ima najmanji efekat.*

Ključne reči: *16MnCr5 čelik, regresiona analiza, površinska hrapavost, Taguchi, optimizacija, ANOVA*

1. INTRODUCTION

In modern industry the goal is to manufacture any item/products at low cost, with high quality in short time. Turning is a very important machining operation employed to remove the extra material from the periphery of work piece. Surface roughness is an important quality parameter of turned/machined surface. Selection of correct combination of cutting parameters will help the machinist to complete the operation in minimum possible time maintaining the required value of surface roughness.In turning operation, parameters such as cutting speed, feed, and depth of cut, cutting tool geometry and materials as well as use of any cutting fluids will impact the material removal rates and the machining qualities like the surface roughness, the roundness of circular and dimensional deviations of the product.

Carmita Camposeco-Negrete [1] conducted the experiments to optimize the cutting parameters for minimizing energy consumption in turning of AISI 6061 T6 Al with the support of orthogonal array, signal to noise (S/N) ratio and analysis of variance (ANOVA) and they observed that feed rate is the most significant factor for minimizing energy consumption and surface roughness. Srinivas Athreya and Y. D. Venkatesh [2] worked on lathe facing of mild steel. The objective of his work was to obtain optimum cutting conditions to get minimum surface roughness in facing of mild steel. Taguchi method was applied in this experimental design work. From the experiment it was finalised that, cutting speed has the most significant role on quality of surface roughness followed by depth of cut. D. Philip Selvaraj et al [3] optimized the surface roughness, cutting force and tool wear in tuning of duplex stainless steel and authors mentioned in their result that the feed rate is the more significant parameter influencing the surface roughness and cutting force and predicted results are found to be closer to experimental results within 8% deviations. Mathematical model developed with the help of RSM. K. Adarsh Kumar et al. [4] performed research work to analyze, how surface finish of EN-8 is affected by speed, feed, depth of cut on the basis of multiple regression analysis and analysis of variance. Chorng-Jyh Tzeng et al [5] coupled Taguchi technique with grey relation analysis to optimize machining parameters which affect the surface roughness of SKD 11 is a high carbon high chromium alloy tool steel and finally the identified that depth of cut was the most influence on the roughness average and the cutting speed was the most influential factor to the roughness

maximum and the roundness. Additionally, the analysis of variance (ANOVA) is also applied to identify the most significant factor. S. Arul [6] worked on optimization of machining parameters of glass fiber reinforced polymer. The data of machining parameters, tool life, thrust force and torque was analysed and optimized by using a algorithm which is based on group method data handling system. M.P. Jenarthanan [7] performed an experimental work to investigate the machining parameters in milling operation of glass fibers reinforced plastics (GFRP). For this tool used were solid carbide end mill tools. It was observed that, Feed rate was the machining parameter that has the highest influence on specific cutting force and surface roughness followed by the helix angle of the cutter. Saadat Ali Rizvi and Wajahat Ali [8] optimize the machining parameters in turning of IS2062 steel with Taguchi technique for dry turning operation and they mentioned in their result that cutting speed having significant effect on tool wear followed by feed rate.R. Suresh et al. [9] conducted experimental work on AISI 4340 steel with the help of RSM method. They concluded that to minimise surface roughness and cutting forces, it is necessary that low feed rate, high cutting speed, low depth of cut and short machining time are employed and to minimize tool wear low cutting speed and low feed rate required. S.Z. Chavoshi and M. Tajdari [10], worked on AISI 4140 steel by using CBN cutting tool on lathe machine. They analysed that hardness has most significant effect on roughness of surface produced after machining operation. Anil Gupta et al. [11] performed a research work and concluded that, the cutting speed of 160 m/min, feed 0.1 mm/rev, nose radius 0.8 mm, the depth of cut of 0.2 mm and a cryogenic environment are the most favourable machining parameters for the turning of AISI P -20 steel on CNC. Sahin et al. [12] worked on a model of the surface roughness for machining of mild steel by using TiN-coated carbide tool. In result they concluded that roughness of surface increases with increase in feed rate and surface roughness decreases with increase in depth of cut and depth of cut. Saadat Ali Rizvi, Wajahat Ali [13] optimized machining parameters which affect the surface roughness of EN 8steel in CNC turning operation, for this purpose they applied Taguchi technique and they produced a elation ship between the depth of cut and surface roughness and inform that on increasing the depth of cut surface roughness also increases. Murat Sarıkaya and Abdulkadir Güllü [14] studied the effect of the main turning parameters such as, cutting speed, feed rate, depth of cut and cooling condition on arithmetic average roughness (R_a) and average maximum height of the profile (R_z) when turning of AISI 1050 Steel and they informed that feed rate was most effective parameters on the surface roughness.

Cooling conditions are significantly effective on the surface roughness. MQL is a good tool in order to increase of the machined surface quality for cutting operations. M. Venkata Ramana and Y. ShanmukaAditya [15] worked on titanium alloys to determine the effect of process parameters on surface roughness during tuning operation and from result it was observed that feed rate is contributed more as compared to cutting speed and depth of cut to minimize surface roughness for both uncoated and coated tools.

2. TAGUCHI METHOD

This method is developed by Dr. Genichi Taguchi born in 1924 in Japan. This is a Fractional Factorial design method based on orthogonal array. In general main effects and interaction of two factors is considered and it is assumes that some higher order interactions are not much important. This method is used to find best set of values of controllable factors to make the design less sensitive with variation of noise, means Taguchi make a design more robust.

2.1 Signal-to-Noise ratio:

Main performance measuring character of Taguchi is signal-to-Noise ratio or simply known as S/N ratio. It is used to reduce variation of signal and to optimize the input factors for producing best possible response. There are three possible case for S/N ratio calculation-

i) Smaller-the-Better: It is used to minimize the response, means where output is undesirable.

$$SNR = -10\log_{10}\left[\frac{\sum y_i^2}{n}\right]$$

ii) Larger-the-Better: This is used to maximize the response, means where output is desirable. This case can be converted is Smaller-is-Better when we take reciprocal of all measured data and calculate the S/N ratio as Smaller-is-Better.

$$SNR = -10\log_{10}\left[\frac{\sum \frac{1}{y_i^2}}{n}\right]$$

iii) Nominal-the-Better: This is used when neither a smaller and nor a larger value is required for response.

$$SNR = 10\log_{10}\left[\frac{\bar{y}^2}{\sigma^2}\right]$$

Where:

y Measured output data of experiment
y_i Measured output data of i^{th} experiment
$\bar{y}$ Mean of measured output data of experiments
σ Standard deviation
σ^2 Variance

3. ANALYSIS OF VARIANCE

It is also known as ANOVA. It is used to check whether means of more than two set quantities are equal or not with the help of F-test. It is a statistical tool applied on result of Taguchi experiment to determine percentage contribution of factors. It use S/N ratio of Taguchi method for this calculation.

4. MATERIAL

Workpiece material used in presented work is 16MnCr5 which is a low alloy case hardening steel. It is used for the purpose of toughness and wear resistance. This material is used to manufacture camshaft, axle and crankshaft etc.fig 1 shown the work piece material after turning operation.

C %	Mn %	Si %	P %	S %	Cr %
0.14 to 0.19	1.00 to 1.30	0.40	0.035	0.035	0.80 to 1.10

Table 1. Chemical composition of 16MnCr5

Chemical composition and mechanical properties of parent material is shown in Table 1 and Table 2 respectively.

Young`s modulus	$2x10^5$ MPa
Tensile strength	650 – 880 MPa
Yield strength	350 – 550 MPa

Table 2. Mechanical Properties of 16MnCr5

Fig. 1. Work piece after turning

5. SELECTION OF FACTORS AND THEIR LEVELS

Cutting speed in rpm, feed in mm/rev and depth of cut in mm selected as factors for design of experiment and roughness of machined surface as response. The turning parameters used and their levels chosen are listed in Table 3.

Factors	Notation	Level 1	Level 2	Level 3
Speed (rpm)	N	400	600	800
Feed (mm/rev)	F	0.06	0.12	0.18
Depth of cut (mm)	D	0.5	1.0	1.5

Table 3. Factors and their levels

6. SELECTION OF ORTHOGONAL ARRAY

For design of experiment by using Taguchi method we select a L_{27} array. Total number of experiments performed in experimental work is equal to 27.

Sl. No.	Speed (rpm)	Feed (mm/rev)	Depth of Cut (mm)
1	400	0.06	0.5
2	400	0.06	1.0
3	400	0.06	1.5
4	400	0.12	0.5
5	400	0.12	1.0
6	400	0.12	1.5
7	400	0.18	0.5
8	400	0.18	1.0
9	400	0.18	1.5
10	600	0.06	0.5
11	600	0.06	1.0
12	600	0.06	1.5
13	600	0.12	0.5
14	600	0.12	1.0
15	600	0.12	1.5
16	600	0.18	0.5
17	600	0.18	1.0
18	600	0.18	1.5
19	800	0.06	0.5
20	800	0.06	1.0
21	800	0.06	1.5
22	800	0.12	0.5
23	800	0.12	1.0
24	800	0.12	1.5
25	800	0.18	0.5
26	800	0.18	1.0
27	800	0.18	1.5

Table 4. Taguchi L_{27} orthogonal array

7. EXPERIMENTAL PROCEDURE

In presented research work experimental setup consist CNC lathe machine, tungsten carbide insert, work piece, micrometer and surface roughness tester.

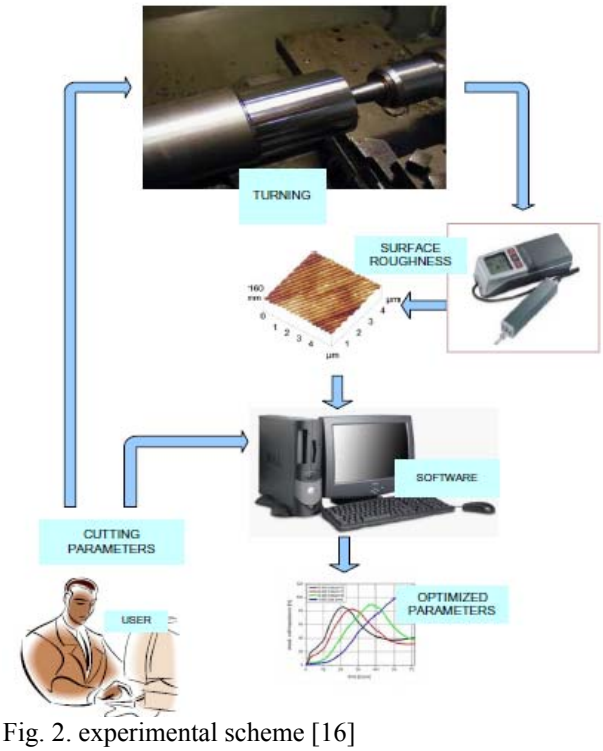

Fig. 2. experimental scheme [16]

Fig 2. shows the experimental arrangement and a graphical abstraction of the process is shown in fig 3.Turning operation is performed on 16MnCr5 material work piece in dry environment. There are total 27 experiments are carried on work piece with changing levels of three factors in each experiment. After that surface roughness was measured of each cut produced in different experiments.

Fig. 3. Graphical abstract

7.1 CNC Lathe Machine

CNC machine used in turning operation was universal turning machine MIDAS 8i by GALAXY MACHINARY PVT. LTD Rajkot. Turning operation is carried out on this machine, a dry environment was chosen because of environment safety. Fig 4 shows CNC machine used in turning process.


Fig. 4. CNC machine

7.2 CNC lathe machine specification

CNC lathe is used in this process is shown in fig 4 and the specification of machine is given in Table 5.

Turning diameter (max)	280 mm
Turning length (max)	522 mm
Speed	40 – 4000 rpm
No. of tool stations	8
Tailstock base travel	339 mm
CNC package	FANUC Oi "T"

Table 5. Specifications of CNC lathe used

8. RESULT AND DISCUSSION

The experimental results for average surface roughness, R_a corresponding to experimental layout using L_{27}, orthogonal array are listed in Table 6.Value for surface roughness represents the average value of three readings.

Sl. No	Ex. No.	N (rpm)	f (mm/rev)	d (mm)	Ra (µm)	SNR_{Ra} (db)
1	27	400	0.06	0.5	4.53	-13.1411
2	18	400	0.06	1.0	3.42	-10.6551
3	9	400	0.06	1.5	5.61	-14.9638
4	24	400	0.12	0.5	4.92	-13.8216
5	15	400	0.12	1.0	4.97	-13.9096
6	6	400	0.12	1.5	1.92	-5.5751
7	21	400	0.18	0.5	5.93	-15.4317
8	12	400	0.18	1.0	3.44	-10.6805
9	3	400	0.18	1.5	1.74	-4.9103
10	26	600	0.06	0.5	4.36	-12.8295
11	17	600	0.06	1.0	4.02	-12.0195
12	8	600	0.06	1.5	1.36	-2.7976
13	23	600	0.12	0.5	6.86	-16.7011
14	14	600	0.12	1.0	1.72	-4.7609
15	5	600	0.12	1.5	1.07	-0.5877
16	20	600	0.18	0.5	4.59	-13.2173
17	11	600	0.18	1.0	2.01	-5.4832
18	2	600	0.18	1.5	2.36	-7.4950
19	25	800	0.06	0.5	3.51	-10.8565
20	16	800	0.06	1.0	2.26	-7.1587
21	7	800	0.06	1.5	2.07	-6.2351
22	22	800	0.12	0.5	1.82	-5.2964
23	13	800	0.12	1.0	1.16	-1.1381
24	4	800	0.12	1.5	1.12	-0.7485
25	19	800	0.18	0.5	2.16	-6.6083
26	10	800	0.18	1.0	1.43	-3.1672
27	1	800	0.18	1.5	0.99	0.2646

Table 6. L27, Surface Roughness and S/N ration

Level	N	f	d
1	-11.454	-10.073	-11.989
2	-8.432	-6.949	-7.664
3	-4.549	-7.414	-4.783
Delta	6.905	3.124	7.206
Rank	2	3	1

Table 7. Response Table for S/N Ratios

Level	N	f	d
1	4.046	3.458	4.292
2	3.136	2.831	2.694
3	1.827	2.719	2.021
Delta	2.219	0.739	2.271
Rank	2	3	1

Table 8. Response Table for S/N Ratios

Table 7 and Table 8 show the response tables for S/N ratio and Means. Tables show the rank of factors according to their effect on response. A factor which has high delta value shows low rank value.

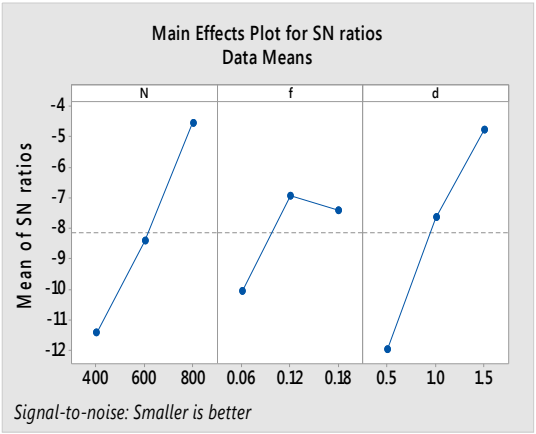

Fig. 5. Main effect plot for S/N ratio

Main effect plot shows the mean of surface roughness is decreases with increase in speed, feed and depth of cut. Mean of S/N ratio increases with increase in speed, for feed first increases up to feed 0.12 mm/rev and then decreases. S/N ratio increases with depth of cut.

The values ofthe surface roughness obtained from the 39 experimental trials, models presented in the work plotted in Fig 9.

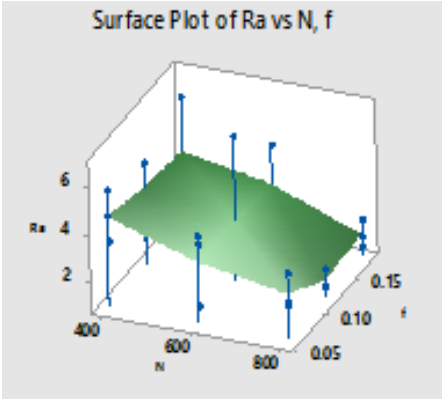

Fig. 6. Surface Plot of Ra vs N, f

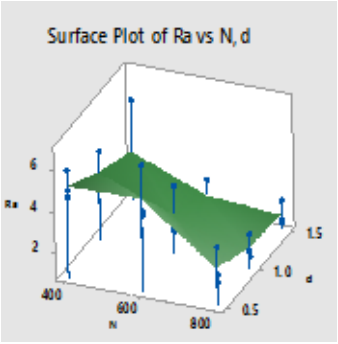

Fig. 7. Surface Plot of Ra vs N, d

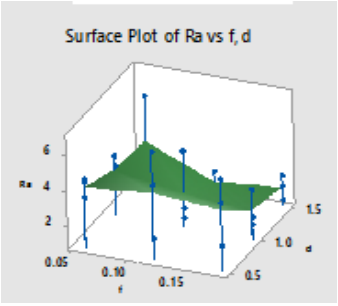

Fig. 8. Surface Plot of Ra vs f, d

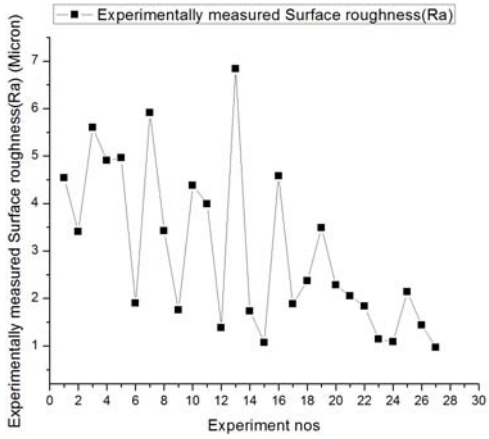

Fig. 9. Graph between experimental surface roughness and no of experiments perform

9. REGRESSION ANALYSIS

Regression Equation obtained from regression analysis is:

$$R_a = 9.34 - 0.00555\times N - 6.16\times f - 2.271\times d$$

Term	Coef	SE Coef	T-Value	P-Value	VIF
Constant	9.34	1.08	8.62	0.000	
N	-0.00555	0.00129	-4.30	0.000	1.00
f	-6.16	4.30	-1.43	0.165	1.00
d	-2.271	0.516	-4.41	0.000	1.00

Table 9. Regression analysis coefficient

10. ANOVA

The analysis of variance is used to find out which factor is more significant effect output response.

Table 10 shows depth of cut (P = 0.001) has highest effect on surface roughness. Second highest

effective factor is speed (P = 0.002) and feed (P = 0.347) has least effective factor for surface roughness.

Model Summary

S	R-sq	R-sq(adj)	R-sq(pred)
1.13113	66.03%	55.84%	38.09%

Source	DF	Adj SS	Adj MS	F-Value	P-Value	% contri-bution
N	2	22.394	11.197	8.75	0.002	29.73
f	2	2.854	1.427	1.12	0.347	3.78
d	2	24.493	12.246	9.57	0.001	32.51
Error	20	25.589	1.279			33.97
Total	26	75.330				

Table 10. ANOVA Table for R_a

11. CONCLUSIONS

Issues related with surface roughness during high speed machining of 16MnCr5 steel has been reported in this paper. Turning experiments were conducted at different speeds ranging i,e (400 rpm, 600 m/min, 8000 rpm). From investigation it was observed that depth of cut has highest effect on surface roughness followed by speed. Feed rate has lowest effect on surface roughness and Minimum surface roughness of were obtained at speed 800 rpm, feed 0.12 mm/rev and depth of cut 1.5 mm.During the investigation no major signs of tool damages were observed and Surface roughness obtained corresponding to optimum cutting parameters was 0.7543 µm.3-D figure represent effect of the turning parameters on surface roughness

12. REFERENCES

[1] Carmita Camposeco-Negrete "Optimization of cutting parameters for minimizing energy consumption in turning of AISI 6061 T6 using Taguchi methodology and ANOVA" Journal of Cleaner Production 53 (2013) 195-203

[2] S. Athreya, Venkatesh, "application of Taguchi method for optimization of process parameters in improving the surface roughness of lathe facing operation" International Refereed Journal of Engineering and Science (IRJES).1(3) 2012:13-19.

[3] D. Philip Selvaraj, P. Chandramohan , M. Mohanraj. "Optimization of surface roughness, cutting force and tool wear of nitrogen alloyed duplex stainless steel in a dry turning process using Taguchi method", Measurement 49 (2014) 205–215.

[4] K. Adarsh Kumar, Ch.Ratnam, BSN Murthy, B.Satish Ben,K. Raghu Ram Mohan Reddy." Optimisation of surface roughness in face turning operation in machining of EN-8" International Journal of Engineering Science and emerging technology Vol. 2, issue-4, 807-812, July-Aug 2012.

[5] Chorng-Jyh Tzeng, Yu-Hsin Lin, Yung-Kuang Yang, Ming-Chang Jeng. "Optimization of turning operations with multiple performance characteristics using the Taguchi method and Grey relational analysis" journal of materials processing technology 2 0 9 (2 0 0 9) 2753–2759.

[6] S. Arul,D.Samuel Raj,L.Vijayaraghavan, "Modeling and optimization of process parameters for defect toleranced drilling of GFRP composites", Materials and Manufacturing Process. 21 (4) (2006) 357-365.

[7] M.P. Jenarthanan, R. Jeyapaul, "Evaluation of machinability index on milling of GFRP composites with different fibre orientations using solid carbide end mill with modified helix angles", Int. J. Eng. Sci. Technol. 6 (4) (2014) 1-10.

[8] Saadat Ali Rizvi1, Wajahat Ali, Optimization of Machining Parameters in Dry Turning of IS 2062 with Taguchi Technique, IJIRSET, Vol. 4, Issue 8,(2015), 7722-7732.

[9] R. Suresh, S. Basavarajappa, V. N. Gaitonde, G.L. Samuel, Machinability investigations on hardened AISI 4340 steel using coated carbide insert, Int. J. Refract. Metals Hard Mater. 33 (2012) 75–86.

[10] S. Z. Chavoshi, M. Tajdari, Surface roughness modelling in hard turning operation of AISI 4140 using CBN cutting tool, Int. J. Mater. Form. 3 (4) (2010) 233–239.

[11] Anil Gupta, Hari singh, Aman Aggarwal "Taguchi-fuzzy multi output optimization (MOO) in high speed CNC truing of AISI P-20 tool steel", Expert System with Application : An International Journal, Vol.38 Issue 6, (2011),6822-6828.

[12] Y. Sahin, A. R. Motorcu, Surface roughness model for machining mild steel with coated carbide tool, Mater. Des. 26 (2005) 321–326.

[13] Saadat Ali Rizvi, Wajahat Ali," Optimization of machining parameters affecting surface roughness of EN8 Steel in CNC Turning by Using the Taguchi Technique" Journal of Mechanical and Mechanics Engineering Volume 2 Issue 3, (2016),59-71

[14] Murat Sarıkaya, Abdulkadir Güllü, "Taguchi design and response surface methodology based analysis of machining parameters in CNC turning under MQL" Journal of Cleaner Production 65 (2014) 604-616.

[15] M.VenkataRamana,Y.ShanmukaAditya,"Optimi zation and influence of process parameters on surface roughness in turning of titanium alloy" Materials Today: Proceedings 4 (2017) 1843–1851

[16] Ilhan Asilturk, Harun Akkus, Determining the effect of cutting parameters on surface roughness in hard turning using the Taguchi method, Measurement 44 (2011) 1697–1704.

Authors: **Saadat Ali Rizvi[a], Wajahat Ali[b],** [a] Research Scholar, Department of Mechanical Engineering, IIT (BHU), Varanasi (U.P) and faculty member in UP, Jamia Millia Islamia, New Delhi., Mobile No: 00917531026305, [b]Mechanical Engineering Department, SCRIET, CCS University, Meerut

E-mail: sarizvi1@jmi.ac.in, saritbhu@gmail.com

http://doi.org/10.24867/JPE-2017-02-013

Journal of Production Engineering

Vol.20 No.2

JPE (2017) Vol.20 (2) Original Scientific Paper

Tarić, M., Kovač, P., Nedić, B., Rodić, D., Ješić, D.

TOOL WEAR, CUTTING TEMPERATURE AND CUTTING FORCE DURING TURNING HARD STEEL

Received: 01 September 2017 / Accepted: 30 November 2017

Abstract: *In this study, cutting tool`s wear, temperature and forces during turning process were investigated. Used were two types of inserts HM and CBN were taken as cutting tools and round bar of EN 90MnCrV8 hardened steel was used as the workpiece. Since the life of the cutting tool material strongly depends upon cutting temperature, it is important to predict wear and heat generation in the tool. Determination of temperature field in tool was by thermal camera. Determined was dependence of temperature tool wear parameter for two cutting tool materials as well.*
Key words: *tool wear, cutting temperature, cutting force turning, hard steel.*

Habanje alata, temperature rezanja i sile rezanja za vreme obrade struganjem tvrdog čelika. *U radu je istraživano habanje alata temperature i sile za vreme struganja. Korišćene su dve vrste pločica za struganje i to tvrdi metal i kubni bor nitrid, a šipka od ojačanog čelika EN 90MnCrV8 kao obradak. Pošto postojanost alatnog materijala jako zavisi od temperature rezanja važno je odrediti temperaturu na alatu. Određivanje temperature je vršeno pomoću termalne kamere. Određena je zavisnost temperature od habanja alata za oba dva ispitivana alatna materijala.*
Ključne reči: *habanje alata, temperature rezanja, sile rezanja tvrdi čelik.*

1. INTRODUCTION

In the hard machining process, tool wear and cutting temperature is often of great concern due to its impact on the product performance. Tool wear cutting force and cutting temperature in the metal cutting process is a very important factor affecting production optimization [1]. Therefore, for a desired part performance, it is important to predict and control the development of this parameters and tool material of the hard machining parameters. The importance of temperature prediction for the machining processes has been well recognized in the machining research community, firstly, due to its effects on tool wear and its constraints on the productivity, and secondly, due to a significant impact it has on the integrity of workpiece surface such as residual stress, hardness, and surface roughness [2].

An important advantage in meeting this new challenge is being able to quickly acquire information on specific machining operations [3, 4]. Cutting temperature is the commonest index for determining tool wear [5]. Ay and Yang [6] monitored time wise change in the temperature of the work piece by using infrared thermo-vision to determine the effect of heat transfer on the tool. They concluded that if the tool's temperature is increased that leads to the acceleration of the wearing process. The high cost of specific cutting tools materials and the cost of downtime for tool changing must be minimized [7]. Tool wear plays a key role in the economy of machining operations. Jawahir et al. [8] maintain that knowing the optimum machining parameters is vital.

Hard turning has been receiving increased attention because it offers many possible benefits over grinding in machining hardened steel [9]. The cubic boron nitride inserts are commonly used in hard turning, because of the high cost of CBN inserts. It is minimized cutting temperature which directly influences the tool wear. In turning process, cutting temperature depends on the options and the suitability of different cutting speeds, feeds, cutting depth and it also affects the durability of the cutting tool [10]. Due to these aspects, measuring procedures are necessary as they permit one to establish the real state of tool wear and to manufacture parts with higher accuracy [11]. The thermo-graphic technique has commonly been used to measure the temperature of the cutting tool. Muller et a1. [12] measured the temperature distribution on the rake face of the diamond coated tool in turning using a thermo-graphic technique. This technique is used for researching the correlations between cutting parameters and temperature distribution in the zone of cutting [13].

Hardened steel is usually machined by grinding process and here is used the turning process which is a more effective machining process with a satisfied quality. Cutting temperature is an important issue in the machining processes and it is influenced by the process parameters such as tool geometry (i.e. nose radius, edge geometry, rake angle, tool tip radius, chamfer thickness, etc.), cutting conditions (cutting speed, feed, depth of cut, etc.) and workpiece properties. Contribution of this paper is seen in the fact that not only modeling is done by neural network, but the comparison of two CBN (cubic boron nitride) inserts with different tool geometry, a negative rake angle and zero angle, is shown. Comparative observation showed that zero angle gives slightly smaller deviation in the cutting temperature values for CBN than HM.

Cutting conditions during study were a = 0.22 mm, s = 0.1 mm/o, v = 90 m/min.

2. EXPERIMENTAL SETUP

The main aim of the experiments was to determine tool wear, cutting temperature and cutting force in the turning of cold working hardened steel for different tool materials. This steel was heat treated and hardness of 55 HRC was obtained in the machining zone of every workpiece. Machining was performed without cooling and lubrication agents.

Turning operations were realized with constant values of cutting speeds (v), feed (f), and the depth of cut (a) using cubic boron nitride (CBN) and hard metal (HM) tool inserts, table 1.

Inserts	γ [°]	α [°]	λ [°]	κ [°]	κ1 [°]	r [mm]
CNMA120404	-6	6	-6	91	5	0.4

Table 1. Specifications of tool insert

The workpiece material was EN 90MnCrV8 cold working tool steel with the following chemical composition: 0.90%C, 0.20%Si, 2.00%Mn, 0.40%Cr, and 0.10%V. Turning test was performed in longitudinal turning on the round bar with 34 mm diameters and 500 mm length using conventional lathe with 10 kW spindle power. During the turning test, and negative tool rake angle, cutting temperatures were recorded. A FLIR E50 thermal imaging camera was used to measure the cutting temperatures. Thermal camera was positioned and fixed on a tool holder. The camera moved with the tool and monitored the same area on it. The emission factor of 0.95 for steel was adopted as the highest temperature on the chip was measured. The thermal camera measured maximal temperature, minimal temperature and average temperature in the selected area. The temperature in the pointed spot on the tool was also measured and this temperature was used in calculations by ANN modeling. The temperature was monitored during the machining of one whole section on the workpiece and the value obtained after 5 seconds was used for the calculation.

Two types of inserts were used in these tests CBN and TM: CNMA120404 and CCMW120404 (table 1 and table 2). Through the use of tool holders, a negative rake angle y = -6° was obtained for the tool holder PCLNR2525M12.

2.1 The cutting force measurement

The acquisition system for measuring the cutting force applied for experimental research in this paper is characterized by the following components:

- Turning process (machine tool, cutting tool, worpiece),
- Measuring sensor (three-component dynamometer KISTLER Type 92651A1),
- Device for amplification of measuring signal (amplifier KISTLER type Ca5001),
- Acquisition module (AD converter converters) Burb Brown type 2000 and PC / AT 486 33MHz
- PC / AT 486 33MHz PC for software acquisition, software LT / CONTROL Ver. 5.02.

In order to monitor the process of machining and recording the signal to the computer disk, a user application was created that enabled the continuous graphical display of the signal components of the cutting force, its current numerical value, and the calculation of the mean value of the signal within the given limits.

In order to determine the character and size of wear process versus time, the width of the tool flank wear land on the back surface was performed after each passage of the 82 mm tool length, which lasted 70 seconds (1.16 min). The wear measurement was performed on the Zeiss tool microscope and images of wear progression was made as well.

The machine tool was a universal lathe - Prvomajska DK480. The universal was installed in the Metal Processing by cutting Laboratory at the Faculty of Mechanical Engineering in Kragujevac. The machine tool (universal lathe - Prvomajska DK480) has the following characteristics: power of the electric motor 10KW, the maximum machining diameter is 320 mm, the maximum machining length is 2000 mm.

3. RESULTS AND DISCUSSIONS

In accordance with the description in the previous section, the measurement of the width of flank wear land the VB versus cutting time for the HM tool insert material in the Figure 1 is presented, and for the CBN is presented in the Figure 3. Images of wear versus time for HM and shown in Figure 2 and in Figure 4 for CBN.

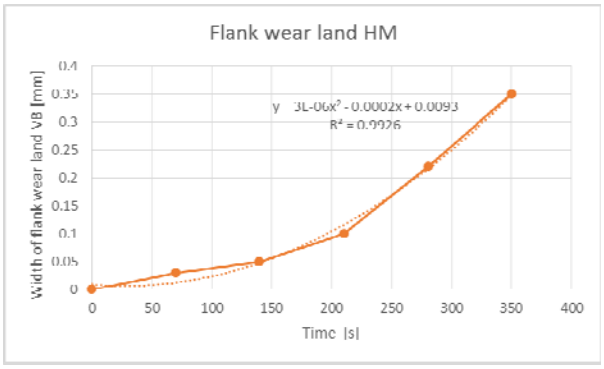

Fig. 1. Flank wear land HM

The cutting temperature versus time measured by the thermal camera is shown in Fig 5 for HM and Fig 6 for CBN.

The progresion of the cutting force versus time is more significant for HM Fig 7, than for CBN Fig 8, where values are significantly lower. Higher values are for cutting force component F2 than F1.

Dependence of the cutting temperature value in the function of tool wear for both tested materials is shown in the Fig 9 and Fig 10. The figures also show the dependencies that are valid for the high values of the coefficient of correlation.

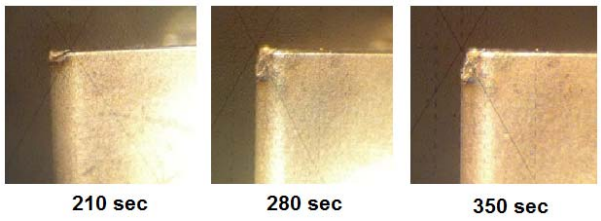

Fig. 2. Progresion of hard metal insert wear images

The width of flank wear land versus time can be represented by a second-order polynomial function with the higher value of correlation coefficient for both tool materials. On the basis of the analysis of the time progression of the tool wear, it can be concluded that the hard metal insert wear process is much faster than the CNB insert at a constant cutting conditions. The CBN insert was only slightly wear and the TM plates were completely wear (VB = 0.35 mm) after 350 seconds.

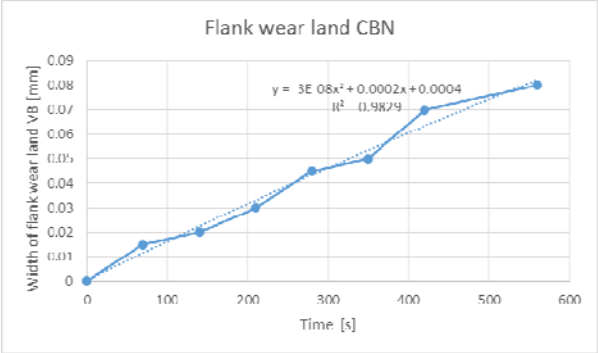

Fig. 3. Flank wear land CBN

The cutting-temperature time progression can also be represented by a second-order polynomial function. The cutting temperature for both tested tool materials has a similar value, but CBN is somewhat lower (330 ° C) than HM (for HM 360°C). The timing of the temperature change is similar to the change in wear and therefore there is a good correlation with the wear of the images.

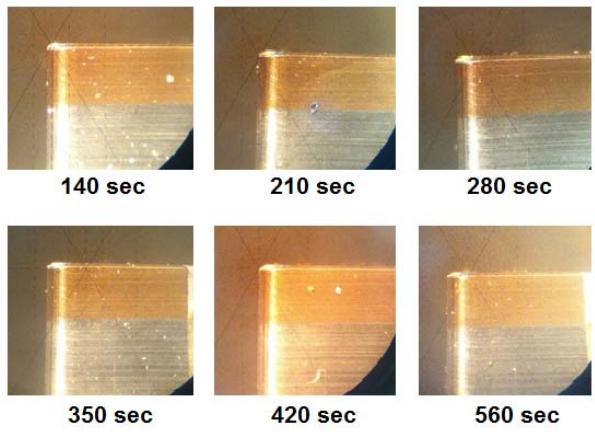

Fig. 4. Progression of CBN insert wear images

Progression of the cutting temperature value in the tool wear function for both examined materials shown in the Fig 9 and Fig 10, can be represented by linear regression and second-order polynomial and are valid with high values of correlation coefficients.

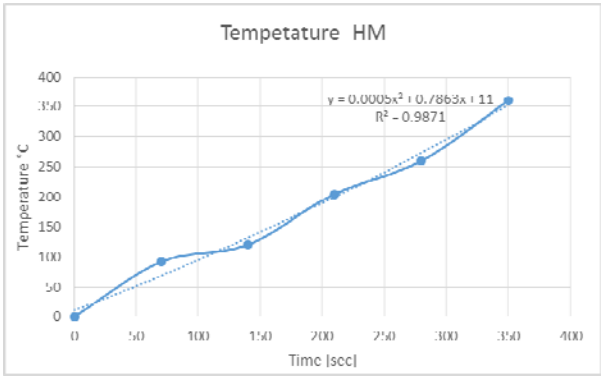

Fig. 5. Temperature versus time

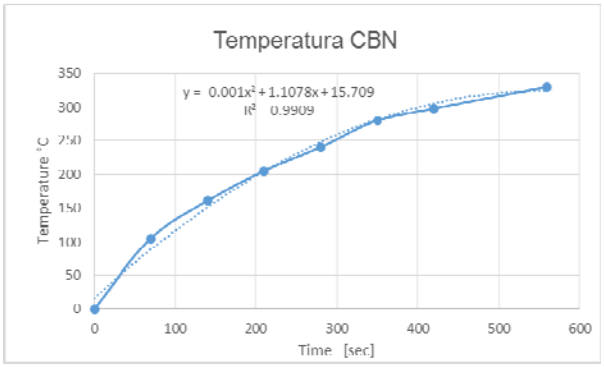

Fig. 6. Temperature versus time

Fig. 7. Cutting force versus time

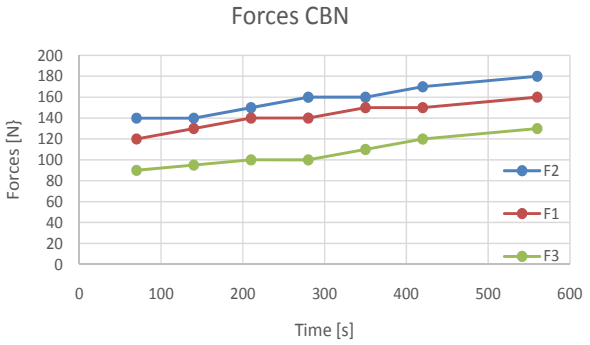

Fig. 8. Cutting force versus time

The higher values of the coefficient of correlation are find for the second-order polynomial model. The change of the cutting force in time is more significant for HM than CBN, where values are significantly lower. Higher values are for cutting force component F2 than F1. As wear progression go on For HM there is an abrupt jump of the cutting force components in time.

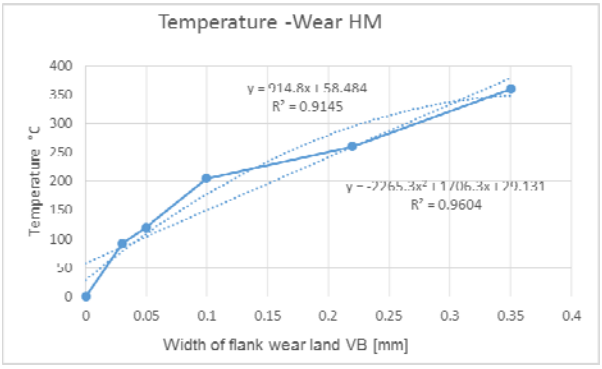

Fig. 9. Temperature versus wear

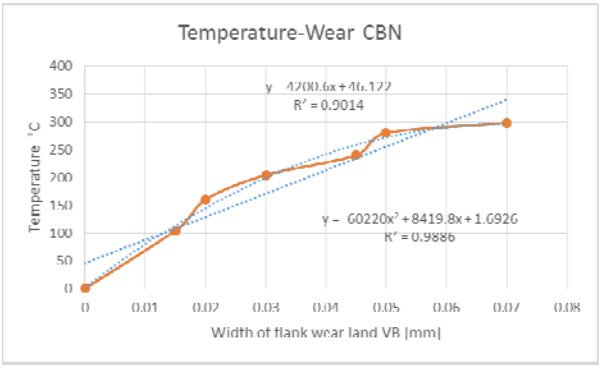

Fig. 10. Temperature versus wear

4. CONCLUSION

Equations On the basis of the analysis of the time progression of the tool wear, it can be concluded that the hard metal insert wear process is much faster than the CNB insert at a constant cutting conditions. The CBN insert was only slightly wear and the HM plates were completely wear (VB = 0.35 mm) after 350 seconds.

The change of the cutting force versus time is more significant for HM Fig 7, than for CBN Fig 8, where values are significantly lower. Higher values are for cutting force component F2 than F1.

Progression of the cutting temperature value in the tool wear function for both examined materials can be represented by linear regression and second-order polynomial and are valid with high values of correlation coefficients. The higher values of the coefficient of correlation are find for the second-order polynomial model.

5. REFERENCES

[1] Sharma, V.S., S.K. Sharma, and A.K. Sharma, Cutting tool wear estimation for turning. Journal of Intelligent Manufacturing, 2007. 19(1): p. 99-108.

[2] Kovac, P., et al., Application of fuzzy logic and regression analysis for modeling surface roughness in face milliing. Journal of Intelligent Manufacturing, 2012. 24(4): p. 755-762.

[3] Pontes, F.J., et al., Artificial neural networks for machining processes surface roughness modeling. The International Journal of Advanced Manufacturing Technology, 2009. 49(9-12): p. 879-902.

[4] Kovac, P., et al., Multi-output fuzzy inference system for modeling cutting temperature and tool life in face milling. Journal of Mechanical Science and Technology, 2014. 28(10): p. 4247-4256.

[5] Andjelkovic, B., et al., Modeling steady-state thermal defectoscopy of steel solids using two side testing. Thermal Science, 2016. 20 (suppl. 5): p. 1333-1343.

[6] Ay, H. and W.J. Yang, Heat transfer and life of metal cutting tools in turning. International Journal of Heat and Mass Transfer, 1998. 41(3): p. 613-623.

[7] Nedic, B. and M. Eric, Cutting temperature measurement and material machinability. Thermal Science, 2014. 18(suppl.1): p. 259-268.

[8] Jawahir, I.S., et al., Towards integration of hybrid models for optimized machining performance in intelligent manufacturing systems. Journal of Materials Processing Technology, 2003. 139(1-3): p. 488-498.

[9] Huang, Y. and T.G. Dawson, Tool crater wear depth modeling in CBN hard turning. Wear, 2005. 258(9): p. 1455-1461.

[10] Ueda, T., et al., Temperature on Flank Face of Cutting Tool in High Speed Milling. CIRP Annals - Manufacturing Technology, 2001. 50(1): p. 37-40.

[11] Ueda, T., et al., Temperature Measurement of CBN Tool in Turning of High Hardness Steel. CIRP Annals - Manufacturing Technology, 1999. 48(1): p. 63-66.

[12] Müller-Hummel, P. and M. Lahres, Infrared temperature measurement on diamond-coated tools during machining. Diamond and Related Materials, 1994. 3(4-6): p. 765-796.

[13] Tarić M., Kovač, P., Nedić, B., Rodić, D., Ješić, D. Monitoring and neural network modeling of cutting temperature during turning hard steel. Thermal Science, online first, doi: https://doi.org/10.2298/TSCI170606210T.

Authors: **[1]Mirfad Tarić, [2]Prof. Pavel Kovač PhD, [3]Prof. Bogdan Nedić PhD, [2]Dragan Rodić MSc, [4]Dušan Ješić PhD.** [1]Faculty of Mechanical Engineering, University of East Sarajevo, East Sarajevo, Bosnia and Herzegovina. [2]University of Novi Sad, Faculty of Technical Sciences, Department for Production Engineering, Trg Dositeja Obradovica 6, 21000 Novi Sad, Serbia. [3]Faculty of Engineering, University of Kragujevac, Kragujevac, Serbia. [4]MTM Academia, Novi Sad, Serbia.

E-mail: mirfad.taric@hotmail.com
pkovac@uns.ac.rs
nedic@kg.ac.rs
rodicdr@uns.ac.rs
dusanjesic@hotmail.com

http://doi.org/10.24867/JPE-2017-02-017

Journal of Production Engineering

Vol.20 No.2

JPE (2017) Vol.20 (2) Original Scientific Paper

Pejic, V., Sekulic, M., Jokanovic, S., Kovac, P., Gostimirovic, M.

MODELING OF CUTTING FORCES IN BALL-END MILLING PROCESS OF HARD (HARDENED) STEEL BY USING RESPONSE SURFACE METHODOLOGY

Received: 06 September 2017 / Accepted: 02 November 2017

Abstract: *The possibility of modeling the cutting forces provides an analytical basis for the planning of the machining process, for the construction of machine tool, the optimization of cutting tool geometry as well as on-line monitoring and process management. The planning and execution of the experiment was carried out on the basis of the rotatable central composite design-RCCD here for the input independent parameters the cutting speed was selected, i.e. the spindle speed (n), the feed per tooth (f_z), the axial (a_p) and radial (a_e) depth of cut. Cutting forces (F_x,F_y,F_z) and the resultant cutting force (F_R) for the responsive variables are selected. Using the RSM methodology, reliable mathematical models for cutting forces in the form of quadratic polynomials were obtained.*

Key words: *Modeling, Cutting Forces, Response Surface Methodology, Hard (Hardened) Steel, Ball-End Milling*

Razvoj modela za sile rezanja korištenjem metodologije odzivne površine pri glodanju tvrdih čelika vretenastim loptastim glodalima. *Mogućnost modelovanja sila rezanja daje analitičku osnovu za planiranje procesa obrade, za konstrukciju mašina alatki, optimizaciju rezne geometrije alata, kao i on-line praćenje i upravljanje procesom. Planiranje i izvođenje eksperimenta je realizovano na osnovu rotirajućeg centralnog kompozitnog plana eksperimenata, gde su za ulazne nezavisne parametre izabrani brzina rezanja, odnosno broj obrtaja alata (n), pomak po zubu (f_z), dubina rezanja (a_p) i širina rezanja (a_e). Za odzivne promenljive su izabrane komponente sila rezanja (F_x ,F_y ,F_z) i rezultujuća sila rezanja (F_R). Korištenjem metodologije odzivne površine (RSM) dobijeni su pouzdani matematički modeli za sile rezanja u obliku kvadratnog polinoma.*

Ključne reči: *Modelovanje, Sile rezanja, Metodologija odzivne površine, Tvrdi (kaljeni) čelik, Glodanje vretenastim loptastim glodalima*

1. INTRODUCTION

The field of application of modeling processing operations is extremely wide, as there are many different operations. For each operation, from different aspects, models may also be required from several different modeling techniques. The primary goal of modeling processing operations is to develop predictable processing performance capabilities in order to facilitate the effective planning of processing operations to achieve optimum productivity, quality and costs [1]. The cutting forces modeling are performed by using empirical, analytical, mechanistic, numerical and AI-based methods. At the moment, the analytical and mechanistic approach is most often used because of its speed and precision. In the future, these models are expected to be developed for new engineering materials, advanced geometry of tools and coatings. Milling is a mechanical processing operation where the tool has one or more teeth. In this era of globalization, milling is becoming popular because of its characteristics such as maximum productivity, minimal processing costs, and good quality of the treated surface. End milling with ball end mills plays an important role in three-dimensional machining, because it has the ability to easily handle three-dimensional curves. While the curved surface is milled, the tangential cutting speed is minimal (equal to zero) at the top of the ball, because of the rotation the tool radius is zero. The maximum radius value is on the periphery of a ball end mill. Changing the cutting speed along the blade causes the change in the cutting forces along the three-dimensional blade. This is the main difference between milling with end mills and ball-end mills. End milling with ball-end mills is commonly used in industry for the production of parts with a complicated free surface shape. These parts are very often made of hardened steel, and the process itself is carried out under conditions of high-speed processing.

2. RESPONSE SURFACE METHODOLOGY

Response Surface Methodology (RSM) is a set of statistical and mathematical methods that are useful for modeling and optimization engineering scientific problems. A measurable output performance of a process is called a response. The response is the measurable size of the processing process (the dependent variable size being tested). In this technique, the main goal is to optimization responses that are influenced by different input parameters of the machining. RSM also quantifies the relationship between the manageable input parameters and the received responses, or attempts to analyze the effect of independent variables on a specific dependent - response. In modeling and optimization manufacturing processes using RSM, it is enough to collect data using carefully designed experiments.

2.1 Response function

In the process of modeling the output performance of the process, it starts from the fact that the response function is unknown and it is approximated by the first-order polynomial:

$$\hat{y} = b_0 x_0 + \sum_{i=1}^{k} b_i x_i + \varepsilon \quad (1)$$

If it turns out that the first-order model is inadequate, then a model with interactions is analyzed:

$$\hat{y} = b_0 x_0 + \sum_{i=1}^{k} b_i x_i + \sum_{i<j}^{k} b_{ij} x_i x_j + \varepsilon \quad (2)$$

In case that this model is not adequate too, it continues with the approximation of the response function in the form of a second-order polynomial:

$$\hat{y} = b_0 x_0 + \sum_{i=1}^{k} b_i x_i + \sum_{i=1}^{k} b_{ii} x_i^2 + \sum_{i=1}^{k} \sum_{j>i}^{k} b_{ij} x_i x_j \pm \varepsilon \quad (3)$$

where:

- $\hat{y}$ – predicted system response
- k – number of factors
- b_0 – segment
- b_i – coefficient of tested factors
- b_{ij} – coefficient of factor interactions
- b_{ii} – coefficients of the squares of the tested factors effects
- ε – residual.

3. CUTTING FORCES

Based on the cutting forces that occurs in the milling process, it is possible to directly or indirectly evaluate the output performance of the process, such as the wear and tool life, the surface roughness, etc. The ability to model the cutting forces provides an analytical basis for planning the process, for machine tool construction, optimization cutting tool geometry, as well as on-line tracking and process management. Determining the cutting forces is often difficult due to the complexity of the process and the geometry of the cutting tool. Analytical determination of the cutting forces is difficult due to the large number of connected cutting parameters. A large number of connected cutting parameters that affect cutting forces (cutting speed, feed, cutting depth, cutting tool geometry, tool wear, physical and chemical properties of the workpiece, etc. make the finding of an appropriate model extremely difficult [2].

Below is a review of the significant results of previous research in the field of modeling of cutting forces in milling with ball end mills.

Yang and Park [3] developed a model for the prediction of the cutting forces based on the analysis of the cutting geometry of the ball end mills. The cutting edge of the ball end mills is observed as a series of infinite elements and the geometry of each cutting edge element is considered to be true. The slice cutting process is analyzed as an orthogonal cutting process in a level that contains cutting speeds and chips. Orthogonal cutting data were obtained from experiments in the scratching of thin-walled tubes.

Lee and Altintas [4], on the basis of orthogonal cutting experiments, including the end ball mills geometry and kinematics, determined with great accuracy the cutting forces in three orthogonal directions. The geometry of the mill is modeled analytically.

Milfelner and others [2] developed an equation for the calculation of maximum cutting force in the end ball milling using genetic programming. The developed intelligent model of maximum cutting force in axial depth, radial depth, feed per tooth and cutting speed showed good match of calculated values with experimental data.

4. EXPERIMENTAL PROCEDURES AND RESULTS

4.1 Experimental procedures

The experimental work was carried out at the company "ELMETAL" doo in Senta (Serbia). The experiments were conducted on vertical machining center type "HAAS VF-3YT" in dry condition, using a carbide coated (TiAlN-T3) ball-end mill with ∅6 mm diameter ("EMUGE FRANKEN" type 1877A). All experiments were carried out using hardened steel X210CR12 (Č4150) with hardness 58 HRC by orthogonal arrays with five levels (coded by:-2,-1,0,1 and 2), Table 1. The arrangement of workpiece preparation is shown in Fig. 1.

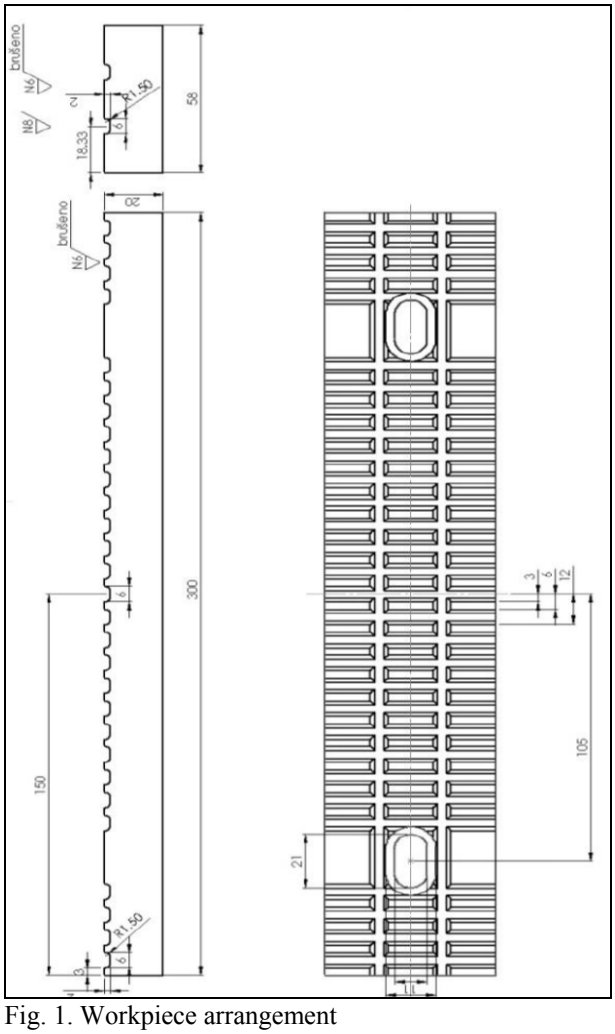

Fig. 1. Workpiece arrangement

Sym	Parameters	Levels				
		-2	-1	0	1	2
A	Spindle speed, n (min^{-1})	3981	4777	5573	6369	7169
B	Feed per tooth, f_z (mm/tooth)	0,018	0,024	0,030	0,036	0,042
C	Axial depth of cut, a_p (mm)	0,04	0,08	0,12	0,16	0,20
D	Radial depth of cut, a_e (mm)	0,20	0,40	0,60	0,80	1,00

Table 1. Machining parameters and their levels

4.2 The results

Experimental researches were first performed according to the central compositional plan and under the conditions described in the previous section. The measurement results for the central composite four-factor plan are shown in Table 2.

Ord. No.	Factor				Measurement results			
	n (min^{-1})	f_z (mm/z)	a_p (mm)	a_e (mm)	F_x (N)	F_y (N)	F_z (N)	F_R (N)
1	4777	0.024	0.08	0.40	41.02	38.52	50.04	65.24
2	6369	0.024	0.08	0.40	35.76	36.31	50.39	54.02
3	4777	0.036	0.08	0.40	45.42	37.91	53.51	67.94
4	6369	0.036	0.08	0.40	42.71	35.71	55.87	60.04
5	4777	0.024	0.16	0.40	65.56	46.32	65.32	96.06
6	6369	0.024	0.16	0.40	51.60	39.74	60.55	73.12
7	4777	0.036	0.16	0.40	77.49	53.75	69.44	110.01
8	6369	0.036	0.16	0.40	67.96	45.06	66.78	89.23
9	4777	0.024	0.08	0.80	61.22	35.24	68.73	72.61
10	6369	0.024	0.08	0.80	53.43	31.66	70.53	72.09
11	4777	0.036	0.08	0.80	71.91	36.18	77.13	83.20
12	6369	0.036	0.08	0.80	68.78	37.81	73.21	77.53
13	4777	0.024	0.16	0.80	89.03	48.26	76.70	118.21
14	6369	0.024	0.16	0.80	69.30	37.40	67.08	88.33
15	4777	0.036	0.16	0.80	90.92	80.06	78.22	121.87
16	6369	0.036	0.16	0.80	68.27	36.70	68.93	89.25
17	5573	0.030	0.12	0.60	53.50	24.48	57.74	66.40
18	5573	0.030	0.12	0.60	73.83	29.71	71.25	89.09
19	5573	0.030	0.12	0.60	65.44	34.26	75.96	86.75
20	5573	0.030	0.12	0.60	49.17	35.20	78.25	81.25
21	3981	0.030	0.12	0.60	65.37	37.56	59.23	84.30
22	7166	0.030	0.12	0.60	55.96	36.19	57.87	75.67
23	5573	0.018	0.12	0.60	51.45	24.12	69.36	76.45
24	5573	0.042	0.12	0.60	67.24	38.63	77.44	90.74
25	5573	0.030	0.04	0.60	44.89	29.39	56.45	61.01
26	5573	0.030	0.20	0.60	114.69	55.03	89.12	126.00
27	5573	0.030	0.12	0.20	64.90	43.72	55.83	70.81
28	5573	0.030	0.12	1.00	166.67	56.04	84.16	170.52
29	5573	0.030	0.12	0.60	59.51	48.78	74.87	92.31
30	5573	0.030	0.12	0.60	62.27	49.88	80.64	91.12

Table 2. Experimental results

The display of a separate enlarged part of the diagram of the measured values of the cutting forces components for one experimental point is given in Diagram 1.

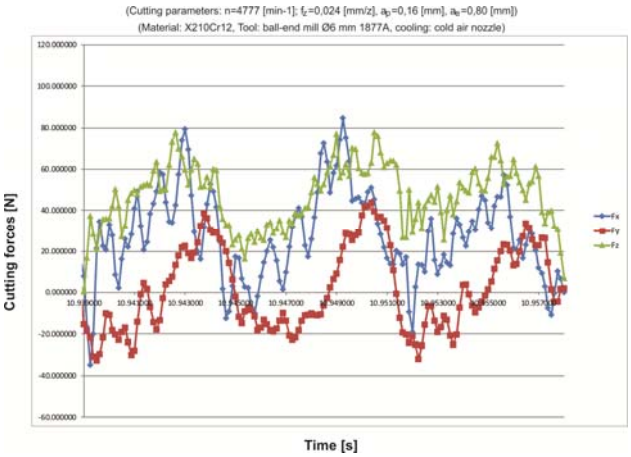

Diagram 1. Part of diagram of cutting forces

4.3 Mathematical models obtained using the response surface methodology (RSM)

For the statistical processing of experimental data, there are a lot of commercial software that greatly simplifies processing and data analysis. From the experiment planning software group, and for applying the response surface methodology, the Design-Expert v.7.0 software was used. In order to obtain reliable mathematical models based on the previously described procedures and experimental data obtained from the central compositional plan, the statistical processing and analysis was initiated. The significance of the model and the members of the response polynomial was determined by the analysis of the variance (ANOVA). After excluding minor members of the second degree polynomial, the variation analysis for the remaining members is given in Table 3:

Response 1 Fx
ANOVA for Response Surface Reduced Quadratic Model
Analysis of variance table [Partial sum of squares - Type III]

Source	Sum of Squares	df	Mean Square	F Value	p-value Prob > F	
Model	13448.18	5	2689.64	14.01	< 0.0001	significant
A-n	447.03	1	447.03	2.33	0.1400	
B-s_i	401.15	1	401.15	2.09	0.1612	
C-a	3737.01	1	3737.01	19.47	0.0002	
D-B	5071.55	1	5071.55	26.42	< 0.0001	
D^2	3791.43	1	3791.43	19.75	0.0002	
Residual	4606.42	24	191.93			
Lack of Fit	4222.94	19	222.26	2.90	0.1210	not significant
Pure Error	383.49	5	76.70			
Cor Total	18054.60	29				

Tabela 3. Analysis of the variance for a reduced square model of cutting force F_x

After the analysis, the F_x force model in the form of a reduced square polynomial in the decoded form has the appearance:

$$F_x = 89.32 - 5.42 \cdot 10^{-3} n + 681.39 f_z + 311.96 a_p - 271.53 a_e + 286.84 a_e^2 \quad (4)$$

The resulting model can also be presented using a contour or 3D diagram, which can be seen in Diagram 2 or Diagram 3.

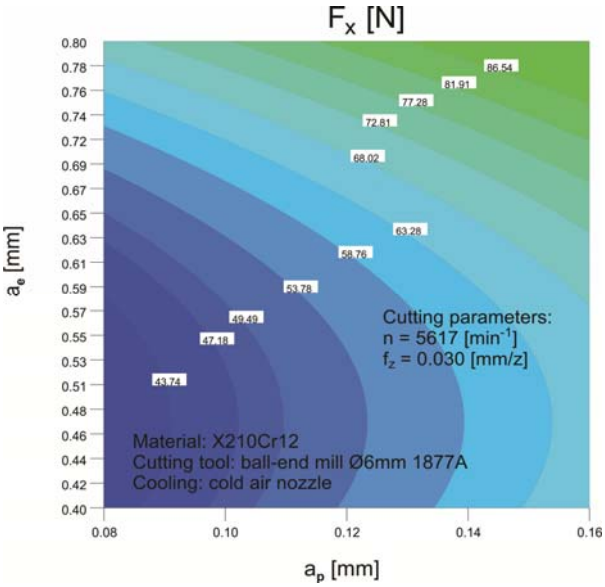

Diagram 2. Contour diagram of response surface for F_x cutting force

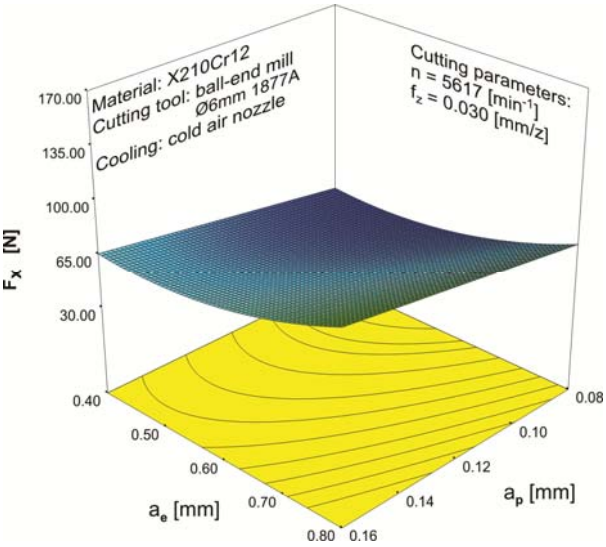

Diagram 3. 3D diagram of response surface for F_x cutting force

The same variance analysis methodology was also performed in the process of obtaining a model for cutting forces F_y , F_z *i* F_R:

$$F_y = -30.22 + 0.01n + 546.88f_z + 846.06a_p - 96.93a_e - 0.12na_p + 86.78a_e^2 \quad (5)$$

$$F_z = -185.19 + 0.067n + 346.60\, f_z + 362.73\, a_p + 82.20\, a_e - 398.05a_p\, a_e - 6.12\cdot 10^{-6}n^2 \quad (6)$$

$$F_R = 91.54 - 7.79\cdot 10^{-3}n + 610.90\, f_z + 378.53\, a_p - 168.50\, a_e + 193.69\, a_e^2 \quad (7)$$

The reliability of these models can be accomplished based on their relative deviation from the experimental data. The display is given in Table 4.

AVERAGE DEVIATION OF MODEL %			
F_x	F_y	F_z	F_R
11,98	13,86	5,51	10,13

Table 4. Relative deviation of the model from the experimental data

5. CONCLUSIONS

The structural form of mathematical models for the cutting forces F_x, F_y, F_z *i* F_R was determined by analysis of the second-order starting four-factor polynomial. Analysis of the ANOVA variance proved to be an excellent tool for determining the finite reduced structural forms of mathematical models by removing insignificant factors from the starting four-factor polynomials by "ejecting backwards". RSM has several advantages over conventional experimental methods. The first RSM offers a large amount of information from a small number of experiments. Second, in RSM it is possible to observe the interactive effect of independent parameters on the response. In addition, to obtain process information, an empirical model is used, which links the response to an independent variable. By analyzing the relative deviation of the model from the experimental results, a very good reliability of the obtained models can be established.

6. REFERENCE

[1] Luttervelt C.A., Childs T.H.C., Jawahir I.S., Klocke F., Venuvinod P.K., Altintas Y., Armarego E., Dornfeld D., Grabec I., Leopold J., Lindstrom B., Lucca D., Obikawa T., Shirakashi, Sato H.: Present Situation and Future Trends in Modelling of Machining Operations Progress Report of the CIRP Working Group: *Modelling of Machining Operations, CIRP Annals - Manufacturing Technology*, Vol. 47 (2), 1998., pp. 587–626

[2] Milfelner M., Kopac J., Cus F., Zuperl U.: Genetic equation for the cutting force in ball-end milling, *Journal of Materials Processing Technology* , Vol. 164–165, 2005., pp. 1554–1560.

[3] Yang M., Park H.: The prediction of cutting force in ball-end milling, *International Journal of Machine Tools and Manufacture*, Vol. 31 (1), 1991., pp. 45-54.

[4] Lee P., Altintas Y.: Prediction of ball-end milling forces from orthogonal cutting data, *International Journal of Machine Tools and Manufacture*, Vol. 36 (9), 1996., pp. 1059-1072.

[5] Pejic, V.: Modeling and optimization in the ball end milling process, *PhD dissertation*, University of Novi Sad, Faculty of Technical Sciences, Novi Sad, 2016.

Authors: **Assist. Prof. Vlastimir Pejic PhD,** College of business and technical education, Ozrenskih srpskih brigada 5A, 74000 Doboj, Bosnia and Herzegovina, Phone.: +387 53 208 600, E-mail: vlastimirpejic@gmail.com

Prof. Milenko Sekulić PhD, Prof. Marin Gostimirović PhD, Prof. Pavel Kovač PhD, University of Novi Sad, Faculty of Technical Sciences, Department of Production Engineering, Trg Dositeja Obradovica 6, 21000 Novi Sad, Serbia, Phone.: +381 21 450-366,

Assoc. Prof. Simo Jokanovic, University of Banja Luka, Faculty of Mechanical Engineering, 71 Vojvode Stepe Stepanovića Blvd., 510000 Banja Luka, Phone.: + +387 51 433 000.

http://doi.org/10.24867/JPE-2017-02-021

Journal of Production Engineering

Vol.20 No.2

JPE (2017) Vol.20 (2) Original Scientific Paper

Payal, H.

ANALYSIS OF TOOL MATERIAL ON METAL REMOVAL RATE IN ELECTRICAL DISCHARGE MACHINING

Received: 04 November 2017 / Accepted: 12 December 2017

Abstract: *H11 tool steel is an exceptional class of alloy steel, also known as chromium tool steel. It found applications in forging and extrusion dies, helicopter rotor blades etc. Electrical discharge machining (EDM) is one of the alternative processes to shape this material. This study exhibits the effect of discharge current (I_d) and gap voltage (Vg) on metal removal rate (MRR) during EDM of H11 tool steel by taking three different tool electrode materials. Experiments have been performed by varying I_d in four steps (4 A, 8A, 12 A, 16 A) and V_g in (25 V, 30 V, 35 V, 40 V) while keeping the values of other variable fixed. On the basis of experimental findings, it is concluded that tool properties of the electrode play a crucial role in machining characteristics of EDM process. The results show that graphite electrode offers the higher MRR followed by aluminium and copper electrode in EDM of H11 tool steel.*

Key words: *EDM, metal removal rate (MRR), H11 (hot die steel), discharge current, gap voltage*

Analiza uticaja alatnog materijala na količinu skinutog materijala kod mašina za elektro erozivonu obradu. *H11 alatni čelik je izuzetna klasa legiranog čelika, poznatog i kao hromski alatni čelik. Ovaj materijal je pronašao primenu kod kovanja i ekstruzije, rotacionih lopatica helikoptera itd. Elektro eroziona obrada (EDM) je jedan od alternativnih procesa za oblikovanje ovog materijala. Ova studija pokazuje uticaj struje pražnjenja (Id) i napona pažnjenja (Vg) na brzinu skidanja metala (MRR) tokom EDM obrade H11 alatnog čelika sa tri različita materijala alata elektrode. Eksperimenti su izvršeni promenom Id-a u četiri koraka (4A, 8A, 12 A, 16 A) i Vg u (25 V, 30 V, 35 V, 40 V) dok se vrednosti druge varijabli drže fiksne. Na osnovu eksperimentalnih nalaza, zaključeno je da svojstva alata elektrode igraju presudnu ulogu u mašinskim karakteristikama EDM procesa. Rezultati pokazuju da grafitna elektroda nudi veću količinu skinutog materijala MRR u odnosu na aluminijumsku i bakarnu elektrodu tokom obrade H11 alatnog čelika pomoću EDM.*

Ključne reči: *EDM, brzina skidanja metala (MRR), H11 (čelik za kalupe), struja pražnjenja, napon pražnjenja*

1. INTRODUCTION

H11, a special hot worked chromium tool steel with good hardness and toughness found suitable applications in the production of extrusion, forging and die casting dies etc. Due to its special class it found its usage in aerospace industries, helicopter rotor blades and shafts [1]. Due to its typical properties it found difficulty in the machining process by conventional methods. Non-conventional methods is found to be one of the options for machining H11 tool steel. EDM is an unconventional, non-contact machining process in which material removal takes place by the help of electrical discharges occurring between tool electrode and the work piece separated by dielectric medium. The amount of heat generated by the electrical sparks is around 8000-10000^{0}C which is sufficient to melt the material as well as electrode also. EDM is known for its thermal behavior which can machine any electrically conductive material regardless of its strength and hardness [2]. EDM is a stochastic process whose performance depends on the input parameters chosen. Thus, certain input parameters when varied directly effects the performance measures such as MRR, tool wear rate, surface roughness of the machined work piece. A lot of work has been reported in the literature with regard to high MRR in the field of EDM. Singh et al. [3] studied the influence of electrode type and material on the EDM process by taking EN-31 tool steel as a work piece and copper, copper-tungsten, aluminum, and brass as an electrode material. They reported that copper electrode showed better results related to MRR, diameter overcut, TWR and SR followed by the aluminium electrode. Muthuramalingam and Mohan [4] investigated the importance of tool electrode materials (copper, brass, tungsten carbide) on the machining performance of AISI 2020 stainless steel in EDM process. They reported that copper electrode produces higher MRR and tungsten carbide electrode showed better surface finish. Dewangan et al. [5] examined the effects of EDM parameters as well as tool electrode materials (copper, brass and graphite) onAISIP20 tool steel .They have reported that graphite tool showed better results in regards to white layer thickness, surface crack density and SR followed by brass, copper. Lee and Li [6] performed an experimental investigation on EDM for Tungsten carbide material using copper, copper tungsten and graphite as tool electrode material. They have taken MRR, SR, TWR as the performance measures. It was observed from the results that graphite electrode offers higher MRR whereas copper electrode showed higher TWR but better surface finish. They also reported that with negative tool polarity maximum MRR, minimum TWR and SR could be achieved. Payal

et al. [7-8] studied the machining characteristics of H11and H13 material by taking three electrode material i.e. aluminum, copper and graphite. They reported that copper electrode achieved the best surface finish among other electrodes.

In the present work, the objective is to investigate the machining characteristics of H11 tool steel material using three different electrode materials viz. copper(Cu), graphite (Gr), aluminum (Al). The discharge current and gap voltage has been varied in four steps to study the MRR.

2. EXPERIMENTATION

The experiments were conducted on EDM machine (S645CNC) of OSCARMAX a Taiwan company installed at Central Institute of Hand Tools, Jalandhar, India as shown in figure 1.The commercial grade EDM oil was used as a dielectric fluid. The work piece material was AISI H11 tool steel with rectangular in shape of 125mm x 100mm x 24mm size. Figure 2 shows the machining of H11 work piece Three different tool electrodes of cylindrically shaped namely Copper (Cu), Graphite (Gr) and aluminum as shown in figure 3 were used in the present study. Figure 4 depicts the machining by Cu electrode. Typical mechanical properties and chemical composition of H11 are depicted in table 1and table 2.

Fig. 1. Electric Discharge Machine (S645CNC)

Fig. 2. Hot die steel H11 during Machining

Fig. 3.Tool electrodes used

The input parameter discharge current and gap voltage has been varied in four steps. The MRR is taken as the performance measures. MRR is calculated by evaluating the weight loss of work piece using equation 1 respectively.

$$MRR = \frac{W_i - W_f}{\rho t} mm^3 / \min \qquad (1)$$

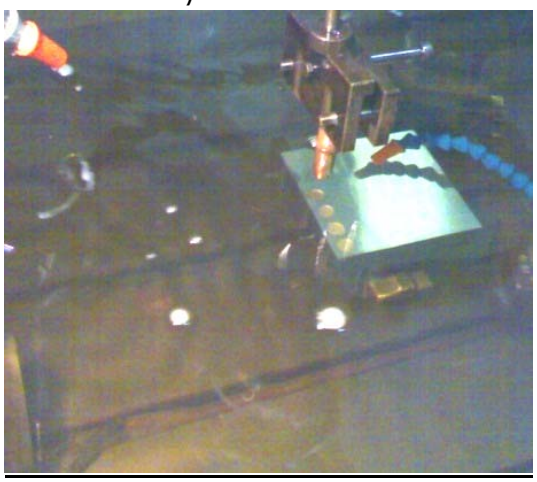

Fig. 4. Machining by Cu electrode

Property	Unit	Value
Density	g/cm^3	7.81
Melting Point	$^{\circ}C$	1427
Elastic modulus	GPa	207
Thermal expansion	(10-6/$^{\circ}C$)	11.9
Thermal conductivity	(W/m-K)	42.2
Hardness	HRC	57

Table 1. Mechanical properties of H11

Elements	Wt. % age
C	0.648
Si	0.603
Mn	0.262
P	0.0078
S	0.0145
Cr	5.17
Mo	1.23
V	0.756

Table 2. Chemical composition (wt %) of H11 material

3. RESULTS AND DISCUSSION

On the basis of experimental results, the effect of discharge current and gap voltage on MRR with different tool electrode materials has been shown in table 4 and 5and .Diagrammatic representation is shown in Figure 5 and 6. Figure 5 indicates that MRR increases with increase in discharge current for all the three electrode material. This is due to the fact that MRR is directly proportional to discharge current and another reason is that at higher discharge current the intensity of the sparks will increase which causes larger overcuts and more material is removed from the surface.

In the present work, the results depicts that graphite electrode exhibits higher MRR followed by aluminium and copper. This confirms that thermo physical properties of the electrode material play crucial role in MRR. The melting point of electrode material can also be linked up with the MRR of work piece. Figure 6 indicates the graph between gap voltage and MRR which indicates the increment in MRR with increase of gap voltage for all the three electrode materials. It was observed that an increase in gap voltage caused an increase in MRR for given constant parameters up to certain voltage. This is due to the fact that pulse energy increases with gap voltage.

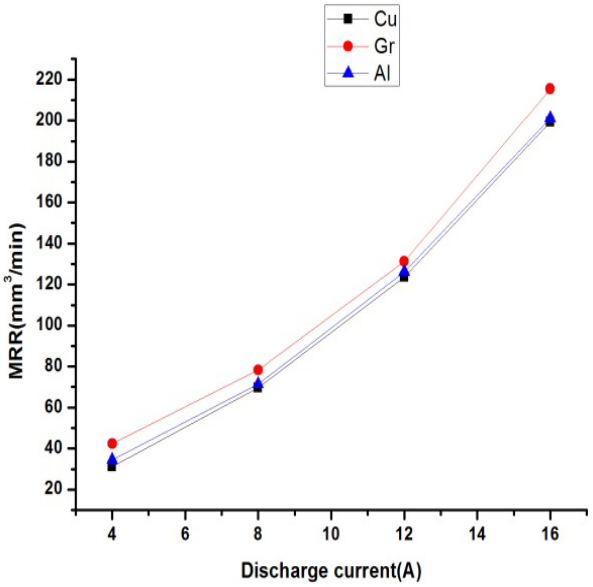

Fig. 5. MRR Vs Discharge Current

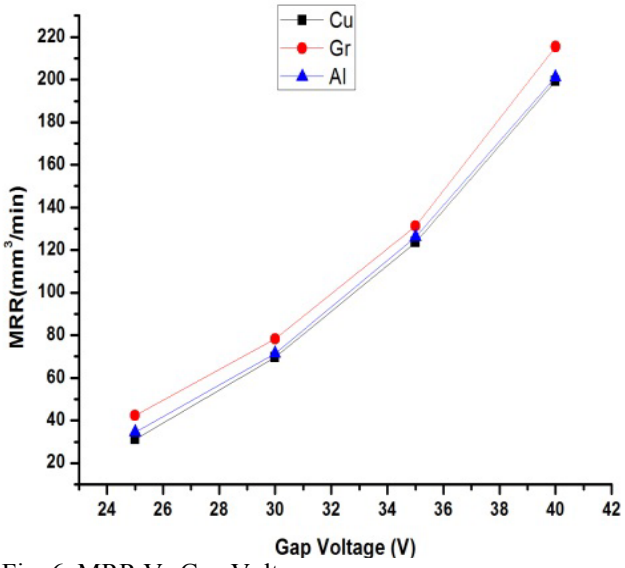

Fig. 6. MRR Vs Gap Voltage

Discharge Current (A)	MRR by Cu (mm^3/min)	MRR by Gr (mm^3/min)	MRR by Al (mm^3/min)
4	31.29	42.39	34.39
8	69.61	78.28	71.26
12	123.51	131.21	126.11
16	199.31	215.39	201.05

Table 3. Effect of discharge current on MRR for H11 material

Gap Voltage (V)	MRR by Cu (mm^3/min)	MRR by Gr (mm^3/min)	MRR by Al (mm^3/min)
25	31.29	42.39	34.39
30	69.61	78.28	71.26
35	123.51	131.21	126.11
40	199.31	215.39	201.05

Table 4. Effect of gap voltage on MRR for H11 material

4. CONCLUSION

The experimental study has been conducted to investigate the effect of discharge current and gap voltage during EDM of AISI H11 tool steel material by taking three different tool electrode materials. The value of MRR increases with increase in discharge current and gap voltage value. In the instant case, it is concluded that graphite offers the higher MRR followed by aluminium and copper.

5. REFERENCES

[1] Yamanaka, M., Tamura, R., Inoue, K. and Narita, Y.: *Bending fatigue strength of austempered ductile iron spur gears,* Journal of Advanced Mechanical Design, Systems and Manufacturing, vol. 3(3), (2009), 203-211.

[2] Qamar,Z.S.: *Effect of heat treatment on mechanical properties of H11 tool steel,*Journal of Achievements in Material and Manufacturing Engineering**,** 35/2, 115–120,2009

[3] Mathew,N.,Kumar,D., Beri ,N., Kumar,A., *Study Of Material Removal Rate Of Different Tool Materials During Edm Of H11 Steel At Reverse Polarity,* International Journal of Advance Engineering Technology,Vol.5(2),p.p-25-30,2014.

[4] Puertas,I.,Luis,J.C.,Villa,G.: *Space roughness parameter study on the EDM of silicon carbide*, Journal Material process technology 164-165, p.p.1590-1596, 2005.

[5] Muthuramalingam,.T., Mohan,.B.:*Influence of Tool Electrode Properties on Machinability in Spark Erosion Machining*, Materials and Manufacturing Processes, Vol.28, 939–943, 2013.

[6] Dewangan, S., Biswas, K.C.,Gangopadhyay, S.: *Influence of Different Tool Electrode Materials on EDMed Surface Integrity of AISI P20 Tool Steel,* Materials and Manufacturing Processes, Vol.29, 1387–1394, 2014.

[7] Lee.H.S.,Li.P.X.:Study of the effect of machining parameters on the machining characteristics in electrical discharge machining of tungsten carbide,Journal of MaterialProcessing Technology,Vol.115,p.p.344-358.

[8] Payal, Himanshu, Garg, RK.,Sachdeva, A.: Investigation of surface integrity of Hot die steel after EDM, International conference on Advances in material and Manufacturing Technology Chitkara University. 2011.

[9] Payal, Himanshu, Maheshwari, Sachin Bharti,PS.: Effect of tool material on surface roughness in electrical discharge machining, Journal of Production Engineering (2016) Vol.19 (1) Novi Sad, ISSN 1821-4932, pp 27-30.

Author: **Himanshu Payal, Assistant Professor,** Mechanical Engineering, Department ABES, Institute of Technology
E-mail: himanshupayal@rediffmail.com

http://doi.org/10.24867/JPE-2017-02-025

Journal of Production Engineering

Vol.20 No.2

JPE (2017) Vol.20 (2) Original Scientific Paper

Doley, H., Tamang, S.K., Samanta, S.

EXPERIMENTAL STUDY AND DEVELOPMENT OF AN EMPIRICAL MODEL FOR *SR* AND *MRR* IN CNC WEDM OF AZ31B MAGNESIUM ALLOY BASED MMNC

Received: 15 November 2017 / Accepted: 10 December 2017

Abstract: *Magnesium and its alloys reinforced with nano-size reinforcements have attracted the interest of the researchers because of its high strength to weight ratio, high damping capacity and displays improved mechanical property without affecting the ductility. The light weight nature of this structural material makes them a right choice to be used in the automobile and aerospace sector where weight reduction is a primary concern. This work determines optimum process parameters such as pulse on time, pulse off time, peak current, servo voltage and volume of silicon carbide (SiC_p) percentage which influence the wire electro discharge machining (WEDM) process during machining of AZ31B magnesium alloy based metal matrix nano-composite (MMNC) using combined methods of response surface methodology (RSM) and Taguchi-GRA-PCA hybrid method. Taguchi L27 experimental design is used in the experimental investigation, and a predictive model is developed to identify the optimum process parameters in the micro EDM process, which influence two main machining criterions such as surface roughness (*SR*) and material removal rate (*MRR*). Further analysis of variance (ANOVA) is carried out to determine the adequacy of the model and to identify which parameters has most influence on the responses. The proposed method can be used to select optimal process parameters from various sets of combinations of process parameters in a WEDM process.*

Key words: *WEDM, MMNC, RSM, GRA-PCA, SR, MRR*

Eksperimentalna studija i razvoj empirijskog modela hrapavost površine i količine skinute strugotine kod CNC elektroerozione obrade sa žicom AZ31B magnezijumske legure na bazi metalnog nano kompozita. *Magnezijum i njegove legure ojačane nano-armiranijim ojačanjima privukle su interes istraživača zbog svog odnosa visoke snage i težine, visokog kapaciteta prigušivanja i prikaza poboljšane mehaničke osobine bez uticaja na duktilnost. Priroda ovog konstrukcijskog materijala lakog materijala je pravi izbor za korišćenje u automobilskom i vazduhoplovnom sektoru gde je smanjenje težine primarna briga. Ovaj rad određuje optimalne parametre procesa, kao što su impuls u vremenu, vreme impulsa, maksimalna struja, servo napon i volumen protoka silicijum karbida (SiCp) koji utiču na proces obrade kompozita sa metalnom nano osnovom magnezijumske legure AZ31B koristeći kombinovane metode metodologije površine odziva (RSM) i Taguchi-GRA-PCA hibridne metode. U eksperimentalnom istraživanju koristi se Taguchi L27 eksperimentalni model, a razvijen je prediktivni model za identifikaciju optimalnih parametara procesa u mikro EDM procesu koji utiču na dva osnovna kriterijuma obrade, kao što su površinska hrapavost (SR) i količina skinutog materijala (MRR). Dalje analize varijanse (ANOVA) se sprovode kako bi se odredila adekvatnost modela i identifikovali koji parametri najviše utiču na izlazne veličine. Predloženi metod se može koristiti za odabir optimalnih parametara procesa iz različitih skupova kombinacija parametara procesa u EDM procesu.*

Ključne reči: *EDM sa žicom, nanokompozit sa metalnom osnovom, površina odziva, Tagucijeva GRA-PCA metoda, hrapavost površine, količina skinutog materijala*

1. INTRODUCTION

There is need for high-performance and energy efficient materials with light-weight for some demanding applications in the aerospace, automobile, sports and electronics industries. The demand has led to the development of advanced materials like metal matrix composites. Magnesium is lightest of all structural materials. It is about 33% lighter than aluminium, 61% lighter than titanium and 77% lighter than stainless steel. Magnesium and its alloys possesses several good properties like excellent cast-ability suitable for pressure die castings, high damping capacity, good electromagnetic shielding, good machinability compared to other structural metals, less energy requirement in the production of magnesium compared to aluminium and is readily available [1, 2]. This good property of the magnesium and its alloys makes it a preferable candidate to be used in the industries where high strength to weight ratio is required. There is potential application of magnesium based metal matrix composite in automobile industries such as disk rotors, gears, piston ring grooves, gearbox bearings, connecting rods and shift forks [1].

In the recent years the field of research has shifted from conventional metal matrix composites to metal matrix nano composites. It is due to the fact that on addition of micron-size reinforcements, it generally leads to substantial reduction in the ductility of the magnesium matrix due to particle cracking and void formation at particle-matrix interface leading to accelerated failure but on the other hand addition of small volume fraction of nano-size reinforcements

produce results comparable or even superior to that of MMCs reinforced with similar or higher volume fraction of micron size reinforcements [2]. There are number of literatures available on method to develop the mechanical properties of magnesium and magnesium based alloys by reinforcing them with hard ceramic particles to form magnesium metal matrix composites (Mg-MMCs). Cao et al.,[3]found that addition of Si-C nano particles on Mg-(2,4)Al-1Si magnesium alloys enhanced the tensile strength and yield strength while the ductility of magnesium alloy matrix castings was retained. They also postulates that Si-C nano particles bonds well with the Mg-alloy without forming any intermediate phase. Guo et al., [4] revealed that post process treatment like cyclic extrusion compression on as-extruded Mg-SiC nano composite prepared by ultrasonic cavitation based solidification process improved the hardness and grain refinement in the matrix and significantly improving the uniformity of nano particles distributions. Srikanth and Gupta., [5] proposed that the damping capability of the magnesium based composites reinforced with SiC particulates was improved due to the presence of SiC particulates. Ugandhar et al., [6] studied the effects of sub-micron size silicon carbide (SiC) particulate reinforcements used in magnesium matrix composites and found that SiC in sub-micron length scale are more effective in lowering coefficient of thermal expansion, and enhancing hardness when compared to SiC particulates in micron length scale. Since the nano particles reinforced Mg-metal matrix composites (MMC) exhibit promising mechanical properties and can be used for many applications, it is valuable to develop suitable machining methods, to facilitate their industrial applications. However, due to the presence of discontinuously distributed hard ceramic particulate in the matrix makes them highly difficult to machine using conventional machining process like turning, milling, drilling, etc. which may results in poor surface finish and excessive tool wear. With the conventional machining process it hard to machine complex shape geometry. These materials can be machined by many non-traditional methods like water jet and laser cutting etc. but these processes are limited to linear cutting only.On the other hand Wire Electrical Discharge Machining (WEDM) shows higher capability for cutting complex shapes and difficult to cut electrically conductive materials with high precision. Hence the wire electrical discharge machining (WEDM) becomes viable method to these composite materials [3,4]. There are several machining method used against MMCs with particulate reinforcement are reported in the literature. Chalisgaonkar & Kumar [7] investigated the effects of WEDM parameters such as wire type (zinc coated and uncoated brass wire), pulse on time (T_{ON}), pulse off time (T_{OFF}), peak current (IP), wire feed (WF), servo voltage (SV) and wire offset (W_{OFF}) on the responses viz., material removal rate (MRR), surface roughness and wire weight consumption (eroded weight of wire after machining) in machining of pure titanium and developed a model using dimensional analysis and optimizing using utility concept. Gopalakannan and Senthilvelan [8] studied the effect of EDM parameters on metal matrix nanocomposite (MMNC) of Al-7075 reinforced with 1.5 wt% SiC nano particles using copper electrode. Babuand Venkataramaiah [9] applied Analytic hierarchy process (AHP)- combine with TOPSIS to optimize the process parameters in WEDM of Al6061/SiCp composite. The Wire Type (WT), Pulse ON Time (T_{ON}), Pulse OFF Time (T_{OFF}), Wire Feed rate (WF) and Sensitivity (S) is considered as the process parameters. Taguchi L_{18} orthogonal array is used to design the experiments for conducting the WEDM experiments and cutting speed (CS), material removal rate (MRR), surface roughness (SR) and dimensional deviation (DD) is considered as response. They found that sensitivity is the most significant WEDM process parameter among all other parameters. Lu et al., [10] investigated the optimization design of the cutting parameters for rough cutting processes in high speed end milling of SKD61 tool steel. Mehat et al., [11] tried to optimized the process parameters in the plastic injection moulding process through hybrid optimization approach by integrating the Taguchi parameter design, grey relational analysis (GRA), and principal component analysis (PCA). Patil and Brahmankar [12] attempted to determine the metal removal rate (MRR) in WEDM of Al-SiC composites by trying to develop a semi empirical model of MRR by using dimensional analysis technique and compared the model developed by response surface methodology (RSM) and result shows that the there is significant agreement in the predictions. Li et al., [13] investigated the machinability of magnesium metal matrix composites (Mg-MMCs) reinforced with high volume percentage of SiC (5%, 10%, 15%) using micro milling process and compared with the pure magnesium through response surface methodology (RSM) of design. Rao and Krishna [14] applied principal component analysis (PCA), coupled with Taguchi's robust theory for simultaneous optimization of correlated multiple responses of wire electrical discharge machining (WEDM) process for machining SiC_P reinforced ZC63 metal matrix composites (MMCs). Aggarwal et al., [15] formulated an empirical model for predicting cutting rate and surface roughness of Inconel 718 material machined by wire-EDM process with the help of response surface methodology (RSM).

In this paper an attempt has been made to investigate the physics in the machining Mg-SiC using WEDM process. Simultaneous optimization of multiple performance characteristics using Taguchi-GRA-PCA hybrid method and also experimental validation has been attempted.

2. EXPERIMENTAL DETAILS

In this study, the series of machining experiments was performed on SPRINTCUT CNC wire electrode discharge machine (Fig. 1). Zinc coated brass wire of 0.25 mm diameter was selected as the tool material. The length of cut selected on AZ31B magnesium alloy based metal matrix nano-composites was 10 mm. De-ionized water was used as the dielectric fluid which was continuously flushed from upper and lower

nozzles through the gap between the work-piece and the wire. The chemical composition of AZ31B magnesium alloy are Al-2.72%, Si-0.28%, Ti-0.011%, Mn-0.29, Zn-1.11 and Mg is balance. In the present work an experimental investigation was carried out in WEDM on AZ31B magnesium alloy based metal matrix nano-composites. Pulse on time (108−112−116 µs), pulse of time (45−50−55 µs), servo voltage (20−30−40 V), peak current (140−160−180 A), and volume percentage of SiC (5−10−15 %) were considered as process parameters. The surface roughness (*SR*) and material removal rate (*MRR*) were measured in different combination of cutting conditions employed during the experimental work based on Taguchi L_{27} (3^5) experimental design.The kerf width of the specimens was measured using LIECA DMI3000M inverted optical microscope using Q-win software and the *MRR* was computed using the empirical relationship given in equation (1).

$$MRR = \frac{K_f \times t \times l}{T}, mm^3/\min \qquad (1)$$

Where, K_f is the kerf width (mm), t thickness of the work piece (mm), l length of cut of the work-piece (mm) and T time taken to machine (min).

In order to measure the surface roughness, TAYLOR HOBSON Form Talysurf 2D profilometer was used as shown in figure 2. The stylus is placed over the cut surface and a data length of 5 mm is set and then the stylus is allowed to run over the specimen at the speed of 0.25 mm/sec. In order to reduce the errors in the measurements three readings were taken for each specimen at different locations and the average *SR* value of each was calculated.

Fig. 1. Experimental setup of WEDM process

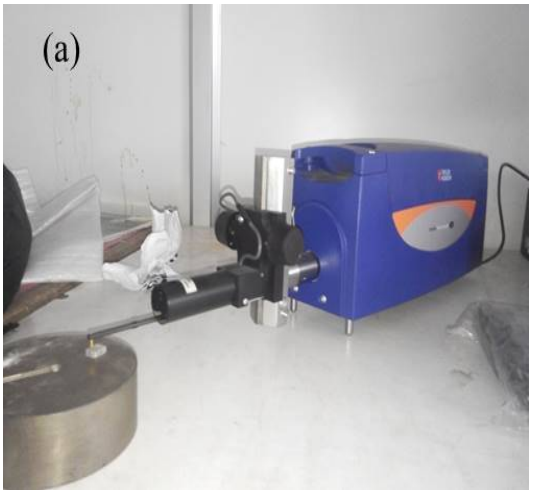

Fig. 2. Taylor Hobson-form talysurf

Sl. No	A (T_{on})	B(T_{off})	C(SV)	D(I_p)	E (V_f)	*SR* (µm)	*MRR* (mm³/min)
1	108	45	20	140	5	2.81	6.81
2	108	45	20	140	10	2.65	6.43
3	108	45	20	140	15	2.52	6.52
4	108	50	30	160	5	3.02	6.79
5	108	50	30	160	10	2.83	6.73
6	108	50	30	160	15	2.31	6.76
7	108	55	40	180	5	2.76	6.99
8	108	55	40	180	10	2.77	6.59
9	108	55	40	180	15	2.54	6.75
10	112	45	30	180	5	3.18	7.22
11	112	45	30	180	10	3.23	6.86
12	112	45	30	180	15	2.49	7.03
13	112	50	40	140	5	3.73	7.11
14	112	50	40	140	10	2.80	6.81
15	112	50	40	140	15	2.67	7.01
16	112	55	20	160	5	3.23	7.07
17	112	55	20	160	10	3.53	6.90
18	112	55	20	160	15	2.60	6.99
19	116	45	40	160	5	3.27	7.24
20	116	45	40	160	10	3.25	7.08
21	116	45	40	160	15	2.73	7.02
22	116	50	20	180	5	3.13	7.18
23	116	50	20	180	10	3.07	6.94
24	116	50	20	180	15	2.40	7.06
25	116	55	30	140	5	3.23	7.17
26	116	55	30	140	10	3.08	6.88
27	116	55	30	140	15	2.85	6.94

Table 1. Experimental results of the responses with the set of process parameters

3. DEVELOPMENT OF MULTIPLE REGRESSION MODEL

A mathematical based multiple regression analysis(MRA) have been attempted to express the complex relationship between process parameters and responses during WEDM process. The developed quadratic model is in the following form.

$$y = \beta_0 + \sum_{i=1}^{k} \beta_i x_i + \sum_{i=1}^{k} \beta_{ii} x_i x_i^2 + \sum_{i} \sum_{j} \beta_{ij} x_i x_j + \varepsilon, \quad (2)$$

Where, y is the performance output terms, $\beta_0, \beta_i, \beta_{ii}, \beta_{ij}$ is the regression coefficients and ε is the machining error.

Based on the experimental performance outputs the model coefficients are evaluated by using MINITAB16® software. The following are the relations obtained for *SR*, and *MRR*.

Since correlation coefficients (R^2) are quite close to 1, which confirm the suitability of the model and the correctness of the evaluated coefficients. As the results obtained from the developed second order polynomial model are found to be in good agreement with the experimental results and also the prediction errors are less than ±5 %. Fig.3 (a) &(b) shows the graphical plot of the model performance for different response characteristics (i.e., *SR* and *MRR*).

$$SR = -205 + 3.692 \times A - 0.194 \times B + 0.000 \times C + 0.0533 \times D + 0.204 \times E - 0.0163 \times A^2 + 0.00193 \times B^2 + 0.000006 \times C^2 - 0.000185 \times D^2 - 0.0094 \times E^2 - 0.00131 \times A \times E + 0.00066 \times B \times E + 0.000064 \times C \times E + 0.000247 \times D \times E \quad (3)$$

$$MRR = -93.7 + 1.668 \times A + 0.077 \times B + 0.0153 \times C + 0.0418 \times D - 0.171 \times E - 0.00724 \times A^2 - 0.00081 \times B^2 - 0.000166 \times C^2 - 0.000124 \times D^2 + 0.00721 \times E^2 - 0.00013 \times A \times E + 0.000469 \times B \times E - 0.000144 \times C \times E + 0.000037 \times D \times E \quad (4)$$

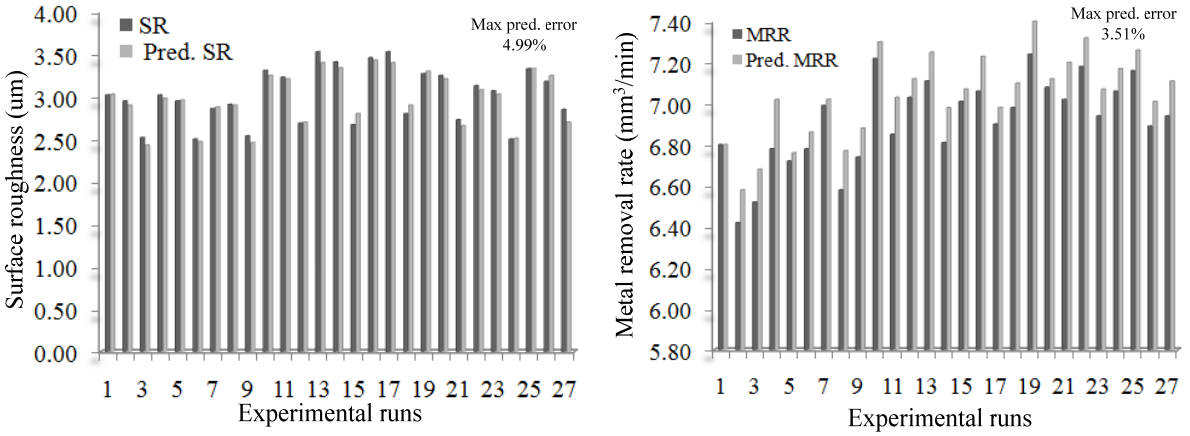

(a) For *SR* (R^2=0.96) (b) For *MRR* (R^2=0.94)

Fig. 3 Predictive performance of both the responses

3.1 Analysis of variance

The ANOVA is a computational technique, which is used to estimate the relative significance of each factor in terms of percent contribution on the overall response. The factors with higher percentage contribution are ranked higher in terms of importance in the experiment and also have significant effects in controlling the overall response. This analysis was carried out for a level of confidence of 95% (i.e., level of significance as 5%). The result shows that SiC vol. % has major contribution (52.72%) followed by T_{on}(21.46%) for *SR* and T_{on} (56.67%) followed by SiC vol. %(28.47) for *MRR* respectively. However, T_{off}, *SV* and I_p has minor effect on both the responses. Fig.4 (a) & (b) show the percentage contribution for *SR* and *MRR*.

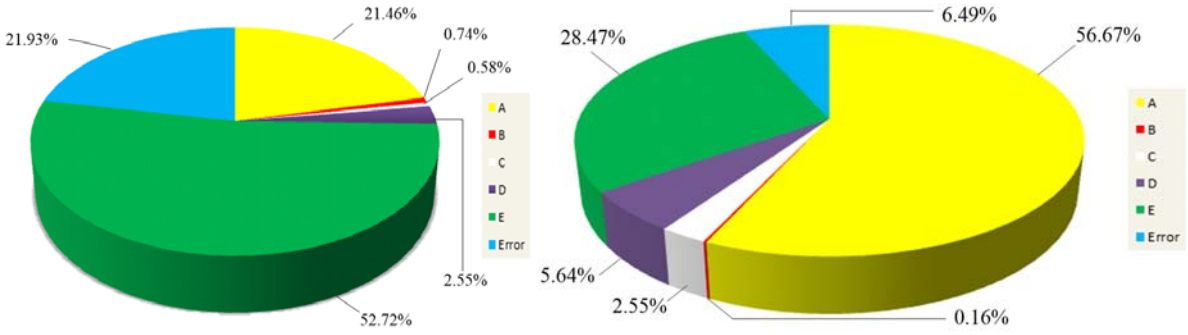

(a) For *SR* (b)For *MRR*

Fig. 4 Bar graph of ANOVA

3.2 Interactive effect of process parameters on *SR* and *MRR*

Figure 5 (a) & (b) depict that with the increase in volume of Silicon Carbide percentage, the surface roughness decreases and with increase in pulse-on time the surface roughness increases. The reason can be attributed that with higher Ton , bigger craters might be generated on the surface of the work piece due to increase in the melting and evaporation rate, and for increase in volume percentage of silicon carbide, it may be due to the grain refinement and uniform mixing of the silicon carbide particle with the magnesium alloy.

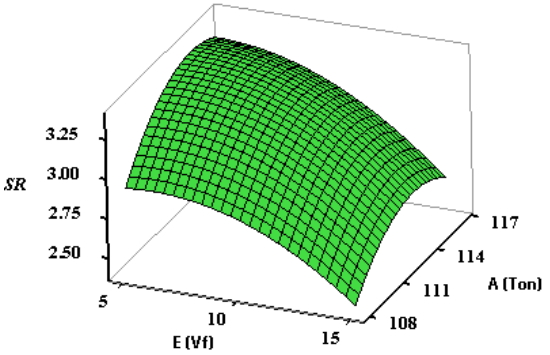

(a) T_{on} Vs V_f

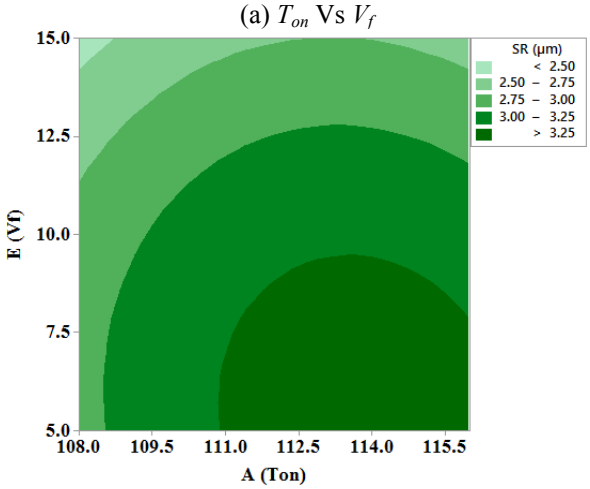

(b) T_{on} Vs V_f

Fig. 5. Showing the variation of *SR* in surface plot and contour plot

Figure 6 (a) & (b) shows that with the low volume of Silicon Carbide percentage, results in higher *MRR*, but as the volume of Silicon Carbide percentage increases the *MRR* relatively decreases.

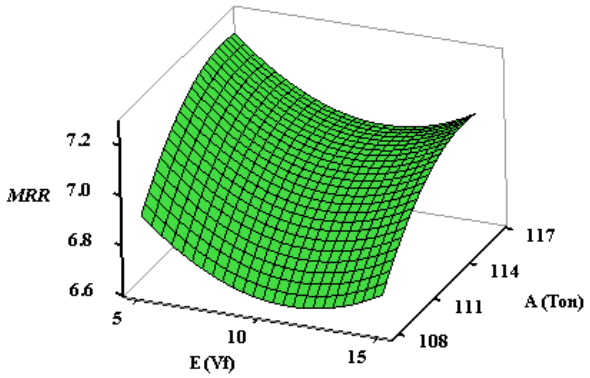

(a) T_{on} Vs V_f

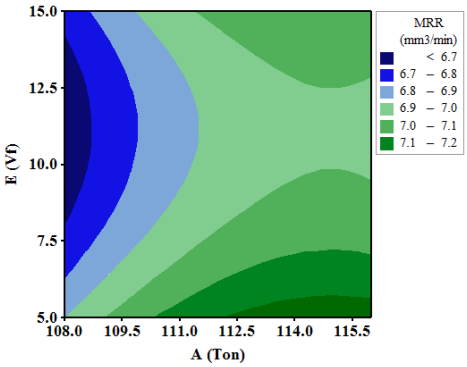

(b) T_{on} Vs V_f

Fig. 6. Showing the variation of *MRR* in surface plot and contour plot

4. MULTI-RESPONSE OPTIMIZATION TAGUCHI-GRA-PCA HYBRID METHODOLOGY

4.1 Taguchi method

The Taguchi method [11] is used to design experiments based on the orthogonal arrays (OA). Taguchi OA designs minimizes the number of experiments can be used to study the whole parameter space with a small number of experiments and it saves time and experimental cost. In analysing the results, the Taguchi method uses a statistical measure of performance known as signal-to-noise (S/N) ratio. The higher the S/N ratio value better is the setting of process parameters. The S/N ratio is a measure of performance to develop products or processes that are insensitive to noise factors in a controlled manner. Noise factors are uncontrollable factors that influence product or process uncertainty. These factors include humidity and weather. Depending on the objective, three different methods can be used to calculate the S/N ratio in the Taguchi method:

(i) Lower the better quality characteristics

$$n_{ij} = -10\log\left(\frac{1}{n}\sum_{j=1}^{n} y_{ij}^2\right) \qquad (5)$$

(ii) Higher the better quality characteristics

$$n_{ij} = -10\log\left(\frac{1}{n}\sum_{j=1}^{n}\frac{1}{y_{ij}^2}\right) \qquad (6)$$

(iii) Nominal the better quality characteristics

$$n_{ij} = -10\log\left(\frac{1}{n\sigma}\sum_{j=1}^{n} y_{ij}^2\right) \qquad (7)$$

Where, y_{ij} is the i^{th} experimental at the j^{th} test, n is the total number of the test, and σ is the standard deviation.

4.2 Grey relational analysis (GRA)

GRA is a method [10, 11] that measures the correlation degree among factors based on the similarity or difference among factors. Grey relational generation involves data pre-processing and calculation according to the quality characteristics. The steps involved in the grey relational generation is as follows.

Normalize the measured results according to the aim of the quality characteristics.

(i) Lower the better normalization method

$$y_i^*(k) = \frac{\max x_i^0(k) - x_i^0(k)}{\max x_i^0(k) - \min x_i^0(k)} \quad (8)$$

(ii) Higher the better normalization

$$y_i^*(k) = \frac{x_i^0(k) - \min x_i^0(k)}{\max x_i^0(k) - \min x_i^0(k)} \quad (9)$$

Where $x_i^0(k)$ is the measured results, $\max x_i^0(k)$ is the maximum value of $x_i^0(k)$ and $\min x_i^0(k)$ is the minimum value of $x_i^0(k)$, i is the number of experiments, and k means the quality characteristics.

We determine the difference sequence $\Delta_{0i}(k)$ and the minimum value $\Delta_{\min}$ and maximum value $\Delta_{\max}$ in the difference sequence. Where $\Delta_{0i}(k)$ is the offset in the absolute values of between the reference sequence $y_0^*(k)$ and the comparability sequence $y_i^*(k)$.

After the data processing, grey relational coefficient is calculated by the following equation,

$$\xi_i(k) = \frac{\Delta_{\min} + \zeta\Delta_{\max}}{\Delta_{0i}(k) + \zeta\Delta_{\max}} \quad (10)$$

Where ζ is the distinguishing coefficient which is normally set as 0.5 in this study, it ranges from 0 to 1.

The grey relational grade is calculated by the following equation

$$\gamma_i = \frac{1}{n}\sum_{k=1}^{n} \beta_k \xi_i(k) \quad (11)$$

Where β_k represents the weighting value of the kth performance characteristics and it is calculated by principal component analysis and $\sum_{k=1}^{n} \beta_k = 1$.

The grey relational grade γ represents the level of correlation between the reference sequence and the comparability sequence. If the two sequences are identically coincidence, then the value of grey relational grade is equal to 1.

4.3 Principal component analysis (PCA)

PCA was developed by Pearson and Hotelling. This approach explains the structure of variance-covariance by the linear combinations of each quality characteristic.

1. The original multiple quality characteristics array

$X_i(j)$, $i = 1, 2, \ldots, m$, $j = 1, 2, \ldots, n$

$$X = \begin{pmatrix} x_1(1) & x_2(2).... & x_1(n) \\ x_2(1) & x_2(2).... & x_2(n) \\ . & . & . \\ . & . & . \\ . & . & . \\ x_m(1) & x_m(2)\cdots & x_m(n) \end{pmatrix} \quad (12)$$

Where m is the number of experiment and n is the number of quality characteristics and x is the grey relational coefficient of each quality characteristics. In the present work m= 27 and n= 2.

2. Correlation coefficient array is evaluated as follows:

$$R_{ij} = \left(\frac{\mathrm{cov}(x_i(j), x_i(l))}{\sigma_{x_i}(j) \times \sigma_{x_i}(l)} \right) \quad (13)$$

Where $\mathrm{cov}(x_i(j), x_i(l))$ are the covariance of sequences $x_i(j)$ and $x_i(l)$ respectively; $\sigma_{x_i}(j)$ is the standard deviation of sequence $x_i(j)$ and $\sigma_{x_i}(l)$ is the standard deviation of sequence $x_i(l)$.

3. Determining the eigen values and eigen vector.

The eigen values and the eigen vector is determined from the correlation coefficient array,

$$(R - \lambda_k I_m) V_{ik} = 0 \quad (14)$$

Where λ_k is an eigen value, $\sum_{k=1}^{n} \lambda_k = n$, k = 1,2,3,4,……,n;

$V_{ik} = \left[a_{k1} a_{k2} ..... a_{kn} \right]^T$ correspond to the eigen vector.

4. Principal components:

The uncorrelated principal component is formulated as:

$$Y_{mk} = \sum_{i=1}^{n} x_m(i).V_{ik} \quad (15)$$

Where y_{m1} is called the first principal components, y_{m2} is called the second principal component and so on.

4.4 Determination of optimal combination

The algorithm of Taguchi-GRA-PCA hybrid optimisation technique to determine the optimal combination of process parameters for WEDM machining process is described step by step in figure 7.

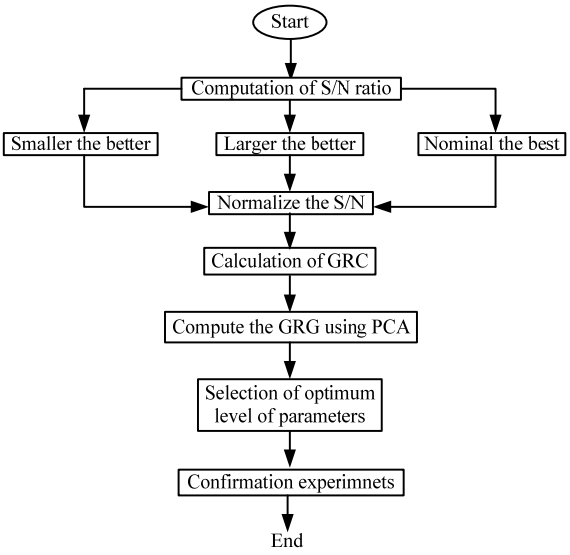

Fig. 7. Flowchart of hybrid Taguchi-GRA-PCA technique

Sl. No	Seq. S/N ratio		Data pre-processing		Deviation sequence		Grey relational coefficient	
	SR	MRR	SR	MRR	$\Delta_{0i}(1)$,*SR*	$\Delta_{0i}(2)$, *MRR*	SR	MRR
1	-9.59	16.65	0.54	0.47	0.45	0.52	0.52	0.48
2	-9.39	16.16	0.47	0	0.52	1	0.48	0.33
3	-8.02	16.28	0.02	0.12	0.97	0.87	0.33	0.36
4	-9.59	16.63	0.54	0.45	0.45	0.54	0.52	0.47
5	-9.40	16.55	0.48	0.38	0.52	0.61	0.49	0.45
6	-7.96	16.63	0	0.45	1	0.55	0.33	0.47
7	-9.12	16.89	0.38	0.71	0.62	0.28	0.44	0.63
8	-9.28	16.37	0.44	0.20	0.55	0.79	0.47	0.38
9	-8.08	16.58	0.04	0.41	0.95	0.59	0.34	0.45
10	-10.38	17.17	0.80	0.98	0.19	0.02	0.72	0.96
11	-10.17	16.72	0.73	0.53	0.26	0.46	0.65	0.52
12	-8.63	16.93	0.22	0.75	0.77	0.24	0.39	0.66
13	-10.96	17.03	1	0.84	0	0.15	1	0.76
14	-10.64	16.66	0.89	0.48	0.10	0.51	0.82	0.49
15	-8.52	16.91	0.18	0.73	0.81	0.26	0.38	0.65
16	-10.77	16.98	0.94	0.79	0.06	0.20	0.88	0.71
17	-10.95	16.78	0.99	0.59	0.01	0.40	0.99	0.55
18	-8.95	16.88	0.32	0.69	0.67	0.30	0.43	0.63
19	-10.29	17.19	0.77	1	0.22	0	0.69	1.00
20	-10.23	17.00	0.75	0.81	0.24	0.18	0.67	0.73
21	-8.70	16.93	0.24	0.74	0.75	0.25	0.39	0.65
22	-9.89	17.13	0.64	0.93	0.35	0.06	0.58	0.88
23	-9.73	16.83	0.59	0.64	0.41	0.35	0.55	0.58
24	-7.97	16.98	0.01	0.79	0.99	0.21	0.33	0.71
25	-10.44	17.10	0.82	0.91	0.17	0.08	0.74	0.85
26	-10.05	16.75	0.69	0.57	0.30	0.42	0.62	0.54
27	-9.09	16.83	0.37	0.64	0.62	0.35	0.44	0.58

Table 2. The sequences of S/N ratio and data processing

The deviation sequence from the results shown in the Table 2 can be calculated as follows

For *SR*

$$\Delta_{01}(1) = x_0^*(1) - x_1^*(1) = (1.000 - 0.541993961) = 0.4580$$

$$\Delta_{01}(2) = x_0^*(1) - x_1^*(2) = (1.000 - 0.4758433) = 0.52416,$$

and so on for the other remaining combinations. The same procedure can be repeated for *MRR* for all 27 runs. The grey relational coefficient can be calculated by using the Eq.10.The result of deviation sequence and the grey relational coefficient is given in Table 2. For the calculation of the grey relational grade Eq.11 is employed. But for these the weighting value is required, which is calculated by applying principal component analysis. The elements of the array for the multiple performance characteristics are the grey relational coefficients, which are listed in Table 2 which is used for evaluating the correlation coefficient matrix and then the eigen values is determined by using Eq.14as shown in the Table 3.

Principal component	Eigen value	Explained variation (%)
First	1.376	68.8 %
Second	0.624	31.2 %

Table 3. The eigen vectors and explained variation for principal components

The eigen vector for principal components corresponding to each eigen values are computed and are listed in Table 4and square of eigenvector can represent the contribution (weight) of the corresponding performance characteristics to the principal component. The contribution of *SR* and *MRR* on the first principal component is shown in Table 5the wights for both the responses as 0.4999 and 0.4999 for *SR* and *MRR* respectively. The variance contribution for the first principal component characterizing the two quality characteristics is as high as 68.8%%.Therefore, for this study, the squares of the respective eigenvectors are selected as the weighting values of the related quality characteristic.

Coefficients β_1 and β_2 in Eq.13 are set as 0.4999 and 0.4999 respectively.

Quality characteristics	Eigen vector	
	First principal component	Second principal component
Surface roughness	0.707	0.707
Metal removal rate	0.707	-0.707

Table 4. The Eigen vector for principal components

Quality characteristics	Contribution
Surface roughness	0.4999
Metal removal rate	0.4999

Table 5. The contribution of individual quality characteristics for the first principal component

Based on Eq.11 the grey relational grade γ has been calculated as follows:

$$\gamma_1 = 0.4999 \times 0.5219 + 0.4999 \times 0.4892 = 0.5054$$

Using the same procedure, the grey relational grade for all the comparability sequence for i = 1 – 27 can be calculated, as shown in the figure 8.

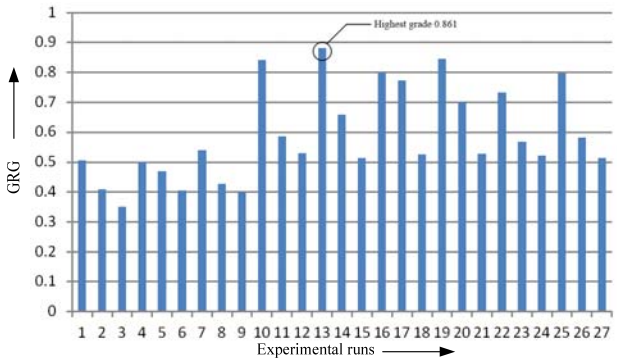

Fig. 8. Grey relational grade

To determine the optimal combination of wire EDM process parameters in machining Mg-SiC MMNC for minimum surface roughness and metal removal rate is done by sorting the average grey relational grade for each cutting parameter level. It is calculated by employing the main effect analysis of the Taguchi method. This process is performed by sorting the grey relational grades corresponding to the levels of the cutting parameters in each column of the orthogonal array and then taking the average of parameters with the same levels.

Generally, a larger grey relational grade indicates that the comparability sequence exhibits a stronger correlation with the reference sequence. A larger grey relational grade results in better multiple quality characteristics. Fig. 9 clearly shows that the multiple quality characteristics of the WEDM process which are significantly affected by the process parameters, selecting the level which have the largest average responses, and thus we get the optimal combination. From the above fig. 9 the optimal combination is A2B3C3D2E1.

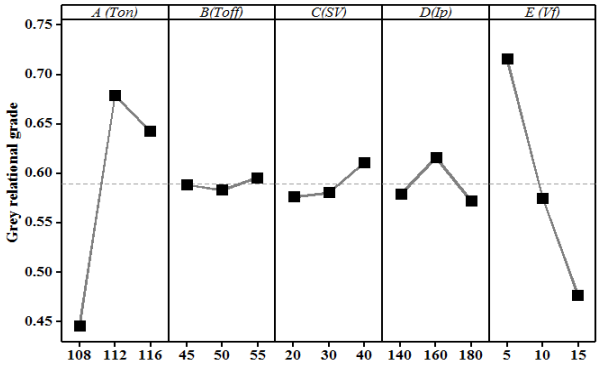

Fig. 9. Effects of process parameters on the quality responses

5. CONFIRMATION TEST

After the optimal level of the parameters is identified by the grey relational analysis, the confirmation test is carried out, that is done by comparing the predicted results with the help of a confirmation experiment. The grey relational grade of the optimal combination can be estimated by the following equation.

$$\sigma = \sigma_t + \sum_{i=1}^{n} \left(\sigma_m - \sigma_t \right) \qquad (16)$$

Where σ_t is the total mean of the grey relational grade, σ_m is the mean of the grey relational grade at the optimum level, and n is the number of the machining parameters.

As mentioned before, the optimal combination of process parameters was A2B3C3D2E1 and the estimated grey relational grade is 0.861, and it is calculated by usingEq.16. The grade of the confirmation experiment and prediction grade is shown in the Table 5. The confirmation experiment shows that the multiple quality characteristics was substantially promoted and the prediction error is within 1% for *SR* and *MRR* respectively which shows the effectiveness of the algorithm.

Optimal WEDM parameters			
	Prediction	Experiment	Error (%)
Level	A2B3C3D2E1	A2B3C3D2E1	
Surface Roughness (SR)	3.421	3.4426	0.66
Metal Removal Rate (MRR)	7.207	7.1832	0.33
Grey relational grade	0.861	0.8737	

6. CONCLUSIONS

In this study, parametric modelling and application of hybrid Taguchi-GRA-PCA for optimizing the cutting parameters of WEDM of machining

magnesium based nano composite was studied. Based on all this work, the following conclusions are summarized:

1. The empirical models for metal removal rate and surface roughness of Mg-SiC metal matrix composites machined by WEDM process have been developed using response surface methodology. The models developed are considered reliable representatives of the experimental results with prediction errors less than ±5 %.
2. The pulse-on time is the most influencing factor for material removal rate and volume percentage content of SiC for surface roughness of the magnesium based composite.
3. The principal component analysis, used to determine the corresponding weighting values of each performance characteristics while applying grey relational analysis to a problem with multiple-performance characteristics, is found to be capable of objectively reflecting the relative importance for each performance characteristic.
4. Based on analysis of variance, the major controllable factor significantly affecting the multiple-performance characteristics is pulse-on time and volume of silicon carbide percentage with a desired total contribution of 88 %.
5. The optimal combination of the cutting parameters obtained from the proposed method is the set with A1, B3, C3, D2, and E1. The confirmation experiment shows that the multiple quality characteristics was substantially promoted and the prediction error is within 1% for *SR* and *MRR* respectively which shows the effectiveness of the algorithm
6. The proposed algorithm greatly simplifies the optimization design of cutting parameters with multiple performance characteristics. Thus, the solutions from this method can be an useful reference for industries and operators who are willing to search for an optimal solution of cutting conditions.

7. REFERENCES

[1] Ye HZ, Liu XY (2004) Review of recent studies in magnesium matrix composites. Journal of materials science39:6153-6171.

[2] GuptaM, Wong WLE (2015) Magnesium-based nanocomposites: Lightweight materials of the future. Materials Characterization 105:30-46.

[3] Cao G, KonishiH, LiX (2008) Mechanical properties and microstructure of SiC-reinforced Mg-(2,4)Al-1Si nanocomposites fabricated by ultrasonic cavitation based solidification processing. Materials Science and EngineeringA 486:357-362.

[4] GuoW, WangQ, YeB, Li X, Liu X, ZhouH (2012) Microstructural refinement and homogenization of Mg–SiC nanocomposites by cyclic extrusion compression. Materials Science & EngineeringA 556:267-270.

[5] Srikanth N, Gupta M (2003) Damping characterization of magnesium based composites using an innovative circle-fit approach. Composites Science andTechnology69:559-568.

[6] Ugandhar S, Gupta M, Sinha SK (2006) Enhancing strength and ductility of Mg/SiC composites using recrystallization heat treatment. Composite Structures72:266-272.

[7] Chalisgaonkar R, Kumar J (2015) Multi-response optimization and modeling of trim cut WEDM operation of commercially pure titanium (CPTi) considering multiple user's preferences.An International Journal Engineering Science and Technology 18:125-134.

[8] Gopalakannan S, Senthilvelan T (2013) Application of response surface method on machining of Al–SiCnano-composites. Measurement 46:2705-2715

[9] AnandBabu K, Venkataramaiah P (2015) Multi-response Optimization in Wire Electrical Discharge Machining (WEDM) of Al6061/SiCp Composite Using Hybrid Approach. Journal for Manufacturing Science and Production 15:327-338.

[10] Lu HS, Chang CK, Hwang NC, Chung CT (2009) Grey relational analysis coupled with principal component analysis for optimization design of the cutting parameters in high-speed end milling.Journal of materials processing technology209:3808-3817.

[11] Mehat NM, Kamaruddin S, Othman AR(2014) Hybrid Integration of Taguchi Parametric Design, Grey Relational Analysis, and Principal Component Analysis Optimization for Plastic Gear Production.Chinese Journal of Engineering 11:351-206.

[12] Patil NG,Brahmankar PK (2010) Determination of material removal rate in wire electro discharge machining of metal matrix composites using dimensional analysis. International Journal of Advanced Manufacturing Technology51:599-610.

[13] Li J, Liu J,Ji Y, Xu C (2013) Experimental investigation on the machinability of SiC nano-particles reinforced magnesium nano-composites during micro-milling process. International of manufacturing research 8:64-84.

[14] Rao TB, KrishnaAG (2013) Simultaneous optimization of multiple performance characteristics in WEDM for machining ZC63/SiCp MMC.Advances inManufacturing 1:265-275.

[15] Aggarwal V, Khangura SS, Garg RK(2015) Parametric modeling and optimization for wire electrical discharge machining of Inconel 718 using response surface methodology. International Journal of Advanced Manufacturing Technology 79:31-47.

Authors: **H. Doley, S.K. Tamang[1]* and S.Samanta**, *corresponding, Department of Mechanical Engineering, NERIST, Nirjuli-791109, India
E-mail: santoshtamang05@yahoo.com

http://doi.org/10.24867/JPE-2017-02-034

Journal of Production Engineering

Vol.20 No.2

JPE (2017) Vol.20 (2) Original Scientific Paper

Cica, Dj., Zeljkovic, M., Sredanovic, B., Tesic, S.

OPTIMIZATION OF MACHINING PARAMETERS WITH MINIMUM SURFACE ROUGHNESS FOR THREE-AXIS MILLING OF SCULPTURED PARTS

Received: 20 September 2017 / Accepted: 11 November 2017

Abstract: *The objective of this study is to identify optimum machining parameters on surface quality of sculptured parts. The effect of various machining process parameters such as machining strategy, feed, depth of cut and spindle speed on surface roughness during three-axis end milling of sculptured parts have been studied by performing a number of experiments constructed according to standard Taguchi's L9 orthogonal array design matrix. Grey relational analysis method was used to find the optimal machining process parameters and analysis of variance was carried out to find the significance and contribution of each machining parameter on performance characteristics. Finally, confirmation test was conducted to indicate the effectiveness of this proposed method.*

Key words: *optimization, surface roughness, grey relational analysis*

Optimizacija parametara obrade troosnog glodanja složenih površina u cilju obezbeđenja minimalne hrapavosti obrađene površine. *Cilj ovog rada je određivanje optimalnih parametara obrade koji obezbeđuju minimalnu hrapavost obrađene površine. Razmatran je uticaj različitih parametara obrade, kao što su strategija obrade, brzina pomoćnog kretanja, dubina rezanja i broj obrtaja glavnog vretena, na hrapavost obrađene površine pri troosnom glodanju složenih površina. U radu je primenjen Tagučijev L9 ortogonalni plan za realizaciju eksperimentalnih ispitivanja, dok je siva relaciona analiza korišćena za rešavanje problema optimizacije. Za određivanje značaja pojedinih parametara na performanse karakteristike kvaliteta korišćena je analiza varijanse. Konačno, u cilju potvrde predloženog modela optimizacije proveden je i konfirmacioni test.*

Ključne reči: *optimizacija, hrapavost obrađene površine, siva relaciona analiza*

1. INTRODUCTION

The rapidly development of the aerospace, automotive die moulding industries brings along the demand of new technological challenges related to the growing complexity of the products. Due to the improved functionality mechanical parts having sculptured surfaces are increasingly important in these industries. Sculptured surface machining, also called freeform surface machining is usually performing on a 3- or 5-axis CNC machining centers with a ball-nosed cutters. However, machining of sculptured surfaces has been a difficult problem addressed by numerous researchers. In this process, several problems such as over- or under-cuts, inappropriate cutting parameters, non-optimized tool paths etc., usually produce inadequate products that require expensive reworking which results in high production costs. Therefore, currently one of major areas of CAD/CAM systems is the representation and manufacture of mechanical parts having sculptured surfaces. In the field of sculptured surface machining, CAM systems allows implementation of various machining strategies (zig-zag, true spiral, back forth, parallel spiral, high speed etc.) for roughing and finishing operation. A machining strategy is a methodology used to compute an operation with the aim of carrying out a geometrical entity in its final form [1]. Nevertheless, implementation and selection of a tool path generation strategy still remains an expert field. Appropriate selection can lead to considerable improvement of surface roughness and tool life, savings in machining time, etc., thereby leading to higher productivity and efficiency.

A large number of research papers about CNC machining of sculptured surfaces have been published. Gologlu and Sakarya [2] concluded that implementation and selection of cutting path strategies with appropriate cutting parameters had significant effect on surface roughness in pocket milling which is often encountered in plastic mould manufacture. Kim and Choi [3] proposed a machining time model that considers the acceleration and deceleration of the CNC machines and compare the machining efficiency of the different tool paths currently employed in molds and dies manufacturing. Ghani et al. [4] applied Taguchi optimization methodology for optimization of machining parameters in end milling process while machining hardened steel AISI H13 with TiN coated P10 carbide insert tool under semi-finishing and finishing conditions of high speed cutting. Mladjenovic et al. [5] analyzed the impact of the chosen machining strategy on roughness of flat surfaces machined with the ball end mill. Ramos et al. [6] analyze different finishing milling strategies of a complex geometry part containing concave and convex surfaces. Krimpenis and Vosniakos [7] developed optimization methodology for obtaining parameter values of sculptured surface parts rough machining. Oktem et al. [8] presents method for determination of optimum cutting parameters leading to minimum surface roughness in milling mod surfaces by coupling neural network and genetic algorithm. Oktem et al. [9]

developed method for determination of the optimum cutting conditions leading to minimum surface roughness in milling of mold surfaces by coupling response surface methodology with a genetic algorithm. Li et al. [10] presents a multi-objective optimization approach, based on neural network, to optimize the cutting parameters in sculptured parts machining. Zain et al. [11] used genetic algorithm technique for estimation of the optimal cutting conditions in end milling machining process that yield the minimum surface roughness value.

The objective of this study is to identify the effects of tool path strategies for rough and finish machining of sculptured surfaces. Furthermore, second objective is to develop an optimization method in order to improve machining quality in CNC finish milling. The machining parameters considered were machining strategy, feed, depth of cut and spindle speed. The both objectives will be addressed by means of using Taguchi parameter design. The surface roughness optimization model was developed by grey relational analysis and a confirmation test was conducted to indicate the effectiveness of this proposed method.

2. EXPERIMENTAL WORK

Traditionally, dies and moulds are machined with a CNC machine where machining operation is usually decomposed in two main steps: rough and then a finish machining. The main objective of rough machining is to remove the maximum amount of raw material as soon as possible, leaving a coarse approximation to the final shape. Finishing operation objective is to meet the requirements of the final shape for best surface quality and outline precision. Since irregular scallops between finishing tool passes are inevitably generated on the machined surface, manual polishing of sculptured surfaces is often required to obtain the desired surface quality. While roughing as well as while finishing, implementation and selection of appropriate machining strategies with proper cutting parameters have significant effect on total production time, costs and product quality. Therefore, matters of support for selection of optimal machining strategy have their actuality in the environments of each CAM system.

Due to surface complexity optimal machining is significantly more complicated for sculptured surface parts comparing to prismatic parts. Sculptured surface parts usually demand long tool paths, which result in high machining times. There are numerous options to efficiently machine a sculptured surface parts which have different impact on cutting process elements wherefore a set of objective function must be defined. Owing to possibility to simulating various alternate machining scenarios and comparing them based on the obtained results the usage of CAM systems is considered today to be the most effective solution for technological preparation of production of sculptured surface parts. Therefore, first impact of machining strategy and machining parameters were examined in rough machining. In practice, in rough machining operations main objective is to achieve minimal costs of manufacturing removing as much material as possible in high removal rates. Thus, minimum machining time of a sculptured surface part is set as an objective. Simulation study was designed based on Taguchi L27 orthogonal array. Machining performance was investigated according to the following machining parameters: machining strategy, feed (*f*), depth of cut (*a*) and spindle speed (*n*). Levels of machining parameters are shown in Table 1. Part having sculptured surfaces used for simulation study is shown on the Fig. 1. Based on simulation analysis minimum machining time of 16 min 35 sec is obtained for parallel spiral machining strategy, f = 650 mm/min, a = 1.5 mm and n = 4000 min^{-1}.

Machining parameter	Levels in coded form		
	1	2	3
Machining strategy	True spiral	Parallel spiral	Morph spiral
Feed, f [mm/min]	350	500	650
Depth of cut, a [mm]	0.5	1	1.5
Spindle speed, n [min^{-1}]	3000	4000	5000

Table 1. Design factors and their levels for rough machining

Fig. 1. Part having sculptured surfaces

Second objective of this paper is identify the effects of machining strategies and cutting parameters employed in finish machining of sculptured surfaces. In pocket milling which is often encountered in mould manufacture, the main demand is associated with minimum surface roughness in order to eliminate as far as possible manual surface grinding and polishing operation. In order to examine the influence of machining parameters on the surface roughness in finish milling, the experiments based on Taguchi L9 orthogonal array have been conducted. The machining parameters selected for the experimental work were machining strategy (*A*), feed (*B*), finish allowance (*C*) and spindle speed (*D*). Rough machining were performed with machining parameters which provides minimum machining time. The milling operations were performed on a 3-axis milling machine EMCO Concept Mill 450 equipped with a Sinumerik 840D CNC controller. The experiments were performed on machining aluminium alloy 7075-T6 with ball nose cutter of diameter 10 mm. The surface roughness of the machined surface of each specimen was measured

using Surftest SJ-210 Mitotoyo. Three measurements were conducted along the longitudinal and transverse direction for each specimen and the average surface roughness parameter values from those reading was recorded. Experimental plan consists values of machining parameters is shown in Table 2 while observed responses are shown in Table 3. Analyzing the results it can be concluded that, depending on the different machining strategy, different values of surface roughness were obtained for the same surface.

Machining parameter	Levels in coded form		
	1	2	3
Machining strategy	Parallel	Radial	Contour
Feed, f [mm/min]	150	250	350
Depth of cut, a [mm]	0.1	0.2	0.3
Spindle speed, n [min^{-1}]	5000	6500	8000

Table 2. Design factors and their levels for finish machining

3. GREY RELATIONAL ANALISYS

Similar to the fuzzy set theory, the grey system theory is an effective mathematical model to deal with incomplete and uncertain information. In grey systems theory, a color spectrum from black to white is used to describe the degree of clearness of the available information. Black color means complete absence of information, whereas white color means having all the information. Grey color is used for intermediate level of information, i.e. for systems with partially known and partially unknown information. Therefore, grey color means the deficiency of information and uncertainty. The intensity of the shade of the grey determines the clarity of the available information, where lower intensity represent higher quality of the known information.

The grey relational analysis can be expressed in the following steps: (i) conversion of experimental data into normalized values, (ii) calculation of grey relational coefficients, (iii) generating grey relational grading. In the procedure of grey relational analysis, the first step is to normalize the data being input in the system in the range between 0 and 1, which is also called grey relational generation. Due to the different measurement units and scales of response attributes, pre-processing of all data in quantitative way into a comparability sequence is very important. The normalized type depends upon the characteristics of attributes including the smaller-the-better, larger-the-better and nominal-the-better characteristic. The second step of grey relational analysis involves the determination of grey relation coefficient to represent the correlation between the desired and actual normalized experimental results. Finally, the grey relational grades were computed by averaging the grey relational coefficient corresponding to selected responses. The overall evaluation of the multiple process responses is based on the grey relational grade. The grey relational grade indicate the degree of similarity between comparability sequence and the reference sequence. Hence, higher grey relational grade for particular comparability sequence shows that this comparability sequence is most similar to the reference sequence.

4. RESULTS AND DISCUSSION

According to the implementation steps of grey relational analysis method presented in the previous section, the experimental results for surface roughness in Table 3 were first normalized according to the "lowest-is-the-best" approach and then, deviations from the reference series were calculated. Afterwards, the grey relational coefficient for each machining response was calculated and listed in Table 3.

No.	Machining parameter				R_a [μm]	Grey rel. coeff.	Rank
	A	B	C	D			
1.	1	1	1	1	0.446	1.000	1
2.	1	2	2	2	0.463	0.970	3
3.	1	3	3	3	0.537	0.856	5
4.	2	1	2	3	0.469	0.959	4
5.	2	2	3	1	0.449	0.995	2
6.	2	3	1	2	0.567	0.817	6
7.	3	1	3	2	1.528	0.333	9
8.	3	2	1	3	1.433	0.354	7
9.	3	3	2	1	1.513	0.336	8

Table 3. Experimental results for finish machining and grey relational coefficients

In this study, it is observed that the experimental no. 1 has the highest grey relational coefficent among the nine experiments in Table 3. The response table was obtained from the average value of the grey relational coefficent for each level of the control parameters in order to find the optimal level of each parameter. The optimal setting of control parameters is to select the level with higher value of grey relational coefficent. From the results shown in Table 4. the optimal level setting of four control parameters for minimizing surface roughness among the nine experiments are identified as surface finish parallel machining strategy, feed as 250 mm/min, depth of cut as 0.2 mm and spindle speed as 5000 min^{-1}, represented as $A_1B_2C_2D_1$.

Level	Machining parameter			
	A Machining strategy	B Feed, f [mm/min]	C Depth of cut, a [mm]	D Spindle speed, n [min^{-1}]
Level 1	0.942	0.764	0.724	0.777
Level 2	0.924	0.770	0.755	0.707
Level 3	0.341	0.670	0.728	0.723
Max-Min	0.601	0.100	0.027	0.054
Rank	1	2	4	3

Table 4. Response table for the grey relational coefficient

Main effects plot of grey relational coefficent is drawn from response table, as shown in Fig. 2. The most influential factors affecting the surface roughness in sequence can be listed as: factor *A* (machining strategy), factor *B* (feed), factor *D* (spindle speed) and factor *C* (depth of cut). The interaction plot between the input parameters over calculated grey relational coefficent is shown in Fig. 3.

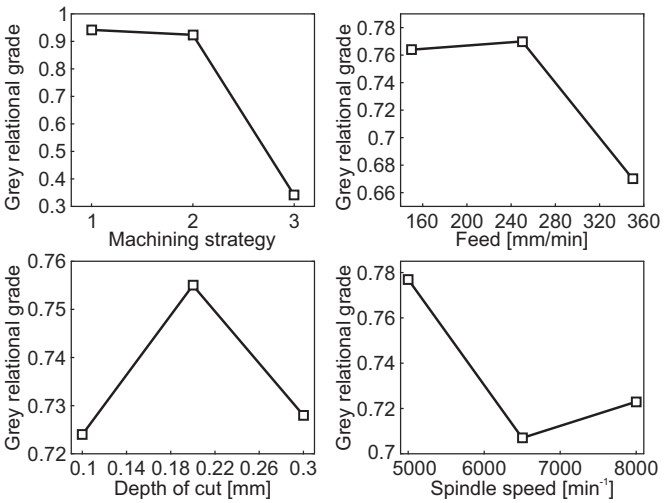

Fig. 2. Main effects plot for grey relational coefficient

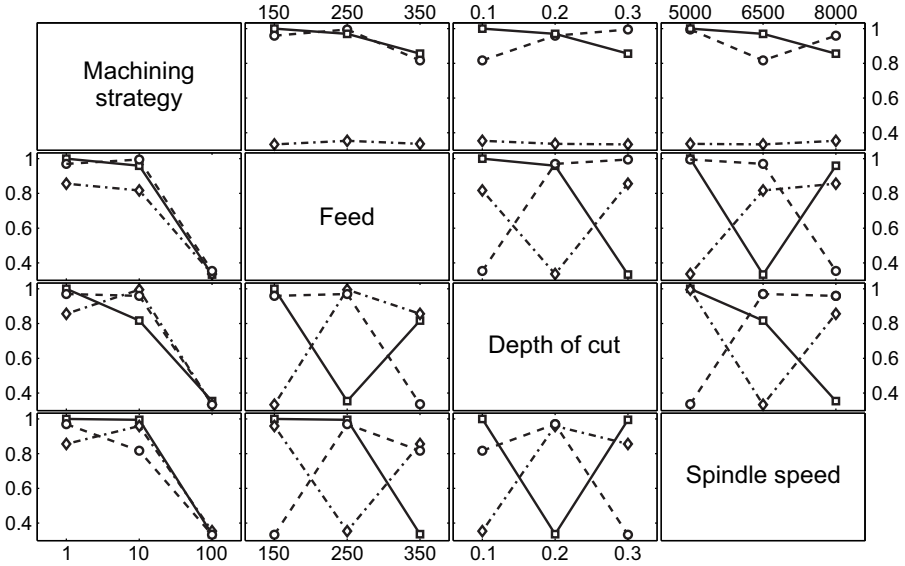

Fig. 3. Interaction plot for grey relational coefficient

In this study, the analysis of variance (ANOVA) is performed to investigate significance of machining parameters that affect the performance characteristics. An ANOVA table consists the parameters such as degree of freedom (*DOF*), sum of squares (*SS*), mean square (*MS*), Fisher's ratio (*F*) and probability value (*P*). In this analysis, depth of cut having the least significant effect on surface roughness, hence it is pooled.

Source	*DOF*	*SS*	*MS*	*F*	*P*
Mach. strategy	2	0.70104	0.35052	405.33	0.0025
Feed	2	0.01966	0.00983	11.37	0.0809
Spindle speed	2	0.00813	0.00406	4.7	0.1754
Residual error	2	0.00173	0.00086		
Total	8	0.73055			

Table 5. Results of the analysis of variance

Results of ANOVA are presented in Table 5. and indicate that the machining strategy is most significant parameter, and feed is the next significant parameter that affecting the total performance characteristics. The error that may due to experiment determined from this ANOVA test was only 0.23%, which is statistically acceptable.

5. CONFIRMATION EXPERIMENT

Finally, after obtaining optimal levels of four machining parameters a confirmation test was conducted to verify the improvement of surface roughness. Using optimal levels of machining parameters the minimal value of surface roughness was calculated as follows:

$$Y = Y_m + \sum_{i=1}^{N} \left(\overline{Y}_i - Y_m \right) \qquad (1)$$

where Y_m is total mean of experimental results for performance characteristic, $\overline{Y_i}$ is the mean of the experimental results at the optimal level and N is the number of the machining parameters. The predicted surface roughness at optimal setting is found to be 0.413 µm.

Finally a confirmation test was conducted to verify the improvement in the required performance characteristic that is surface roughness, using the optimal level of four machining parameters. Table 6 shows the comparisons of initial and optimal levels of machining parameters. The initial designate levels of machining parameters are $A_1B_1C_1D_1$ which is experiment no. 1 in Table 3. Based on the confirmation experiments, for the final optimal combination of parameters $A_1B_2C_2D_1$ surface roughness (R_a) is decreased from 0.446 µm to 0.427 µm. Hence there is a significant improvement in surface roughness after optimization.

Machining parameter	Initial	Optimal	
		Prediction	Exp.
Level	$A_1B_1C_1D_1$	$A_1B_2C_2D_1$	$A_1B_2C_2D_1$
Surface roughness, R_a [µm]	0.446	0.413	0.427

Table 6. Initial and optimal level performance

6. CONCLUSIONS

First objective of this study is to identify the effects of different tool path strategies for three-axis milling of sculptured parts. Simulation study for rough machining was designed based on Taguchi L27 orthogonal array design matrix. Machining performance was investigated according to the four machining parameters (machining strategy, feed, depth of cut and spindle speed) each at three different levels, where minimum machining time is set as an objective. Furthermore, a method for surface roughness optimization using grey relational analysis has been successfully applied. Taguchi L9 orthogonal array design matrix was selected as experimental plan for the four machining parameters, namely machining strategy, feed, depth of cut and spindle speed. The analysis of variance revealed that machining strategy is the most influencing parameter that affect the performance characteristics. Finally, a confirmation test within the optimal machining parameters was conducted to indicate the effectiveness of grey relational analysis methodology. It is found that the performance characteristics, that is surface roughness, is improved using this proposed method.

7. REFERENCES

[1] Sun, G., Sequin, C.H., Wright, P.K.: *Operation decomposition for freeform surface feature in process planning*, Computer Aided Design Vol. 33, pp. 621-636, 2001.

[2] Gologlu, G., Sakarya, N.: *The effects of cutter path strategies on surface roughness of pocket milling of 1.2738 steel based on Taguchi method*, Journal of Materials Processing Technology Vol. 206(1-3), pp. 7-15, 2008.

[3] Kim, B.H., Choi, B.K.: *Machining efficiency comparison direction-parallel tool path with contour-parallel tool path*, Computer Aided Design, Vol. 34(2), pp. 89-95, 2002.

[4] Ghani, J.A., Choudhury, I.A., Hassan, H.H.: *Application of Taguchi method in the optimization of end milling parameters*, Journal of Materials Processing Technology, Vol. 145(1), pp. 84-92, 2004.

[5] Mlađenović, C., Kalentić, N., Zeljković, M., Tabaković, S.: *The influence of milling strategies on roughness of complex surfaces*, Journal of Production Engineering, Vol, 17(1), pp. 51-54, 2014.

[6] Ramos, A.M., Relvas, C., Simoes, J.A.: *The influence of finishing milling strategies on texture, roughness and dimensional deviations on the machining of complex surfaces*, Journal of Materials Processing Technology, Vol. 136(1-3), pp. 209-216, 2003.

[7] Krimpenis, A., Vosniakos, G.C.: *Rough milling optimisation for parts with sculptured surfaces using genetic algorithms in a Stackelberg game*, Journal of Intelligent Manufacturing, Vol. 20(4) pp. 447-461, 2009.

[8] Oktem, H., Erzurumlu, T., Erzincanli, F.: *Prediction of minimum surface roughness in end milling mold parts using neutral network and genetic algorithm*, Journal of Material and Design, 27(9), pp. 735-744, 2006.

[9] Oktem, H., Erzurumlu, T. Kurtaran, H.: *Application of response surface methodology in the optimization of cutting conditions for surface roughness*, Journal of Material Processing Technology, Vol. 170(1-2), pp. 11-16, 2005.

[10] Li, L. Liu, F., Chen, B., Li, C.B.: *Multi-objective optimization of cutting parameters in sculptured parts machining based on neural network*, Journal of Intelligent manufacturing, Vol. 26(5), pp. 891-898, 2015.

[11] Zain, A.M., Haron, H., Sharif, S.: *Application of GA to optimize cutting conditions for minimizing surface roughness in end milling machining process*, Expert Systems with Applications, Vol. 37(6), pp. 4650-4659, 2010.

Authors: **[1]Assoc. Professor Djordje Cica PhD, [2]Professor Milan Zeljkovic PhD, [1]Research Associate Branislav Sredanovic MSc, [2]Sasa Tesic B.Tech,**

[1]Univeristy of Banja Luka, Faculty of Mechanical Engineering, Vojvode Stepe Stepanovica 75, 78 000 Banja Luka, Bosnia and Hezegovina, Phone: +387 51 433 000.

[2]University of Novi Sad, Faculty of Technical Sciences, Institute for Production Engineering, Trg Dositeja Obradovica 6, 21000 Novi Sad, Serbia, Phone: +381 21 450 366.

E-mail: djordje.cica@mf.unibl.org
milanz@uns.ac.rs
branislav.sredanovic@mf.unibl.org
sasa94tesic@hotmail.com

http://doi.org/10.24867/JPE-2017-02-039

Journal of Production Engineering

Vol.20 No.2

JPE (2017) Vol.20 (2) Original Scientific Paper

Madić, M., Radovanović, M., Kovačević, M.

AN OPTIMIZATION APPROACH FOR PRODUCTION TIME MINIMIZATION IN LONGITUDINAL TURNING

Received: 04 September 2017 / Accepted: 17 November 2017

Abstract: *One of the ways for increasing turning efficiency and economics is formulation and solving optimization problems through the use of mathematical models and optimization methods and algorithms. Ability to deal with complex and multi-dimensional optimization problems resulted in the use of a number of different optimization methods and algorithms for solving turning optimization problems, formulated either as single or multi-objective optimization problems with or without constraints. This study promotes the use of conceptually simple and parameter free optimization approach based on the use of exhaustive iterative search. To this aim optimization problem of single-pass turning process was considered. The proposed optimization approach was employed for determining optimal turning conditions, in terms of cutting speed, feed rate and depth of cut, so as to minimize total production time while considering four non-linear constraints. The obtained optimization solutions were compared with those obtained by the previous researchers using different meta-heuristic algorithms including genetic algorithms, simulated annealing, particle swarm optimization, differential evolution etc.*

Key words: *turning, optimization with non-linear constraints, production time*

Jedan optimizacioni pristup za minimizaciju vremena obrade kod uzdužnog struganja. *Jedan od načina za povećanje efikasnosti obrade struganjem je formulisanje i rešavanje optimizacionog problema korišćenjem matematičkih modela, kao i algoritama i metoda optimizacije. Proteklih godina razvijen je veliki broj različitih algoritama i metoda za rešavanje brojnih problema optimizacije, uključujući jednokriterijumske i višekriterijske sa ili bez ograničenja. Ovaj rad promoviše primenu konceptualno jednostavnog, bezparametarskog optimizacionog pristupa zasnovanom na primeni algoritma iterativnog pretraživanja. U tu svrhu razmatran je problem optimizacije uzdužnog struganja za jedan prolaz alata. Cilj je bio da se odrede optimalne vrednosti brzine rezanja, dubine rezanja i koraka kako bi se minimizovalo vreme obrade, uzimajući u obzir i četiri nelinearne funkcije ograničenja. Dobijeni optimizacioni rezultati su upoređeni sa rezultatima autora koji su primenjivali različite metaheurističke algoritme kao što su genetski algoritam, simulirano kaljenje, optimizacija rojem čestica i dr.*

Ključne reči: *struganje, optimizacija sa nelinearnim ograničenjima, vreme obrade*

1. INTRODUCTION

As in other machining process operations, optimization of turning parameters is of great importance. Since adequate turning condition setting can directly minimize production cost and maximize productivity, while satisfying quality and process requirements at the same time, optimization of turning process represents an active field of research. In a given turning operation, optimization aims at selecting the most desirable set of turning parameter values for cutting speed, feed rate and depth of cut so as to obtain maximum productivity (or minimal production time), minimal production cost (or maximal profit) or achieve a certain balance between selected objectives. In some broader optimization problem formulation necessity to include certain constraints, such as allowable machine tool power, cutting tool life, required surface roughness of the workpiece, allowable cutting force, temperature etc., arises. A central place in the optimization process formulation represent mathematical models devoted to establishing relationships between turning parameters (independent variables) and objectives (turning performances).

Upon development of these models, either analytically, empirically or combination of both, these mathematical models are used for formulation of different types of optimization problems including single-objective as well as multi-objective with and without constraints. So far, for solving complex turning optimization problems with several non-linear constraints, a wide spectrum of optimization methods and algorithms has been proposed. Early work in the field of turning process optimization was based on the use of analytical approaches, differential calculus and application of Lagrange multipliers method [1]. Later on, a number of researchers focused on the application of linear, non-linear, geometric, dynamic and goal programming methods [2]. Optimization of parameters in turning process with the use of Nelder Mead simplex search method was discussed by [3]. Mesquita et al. [4] applied Hooke-Jones pattern search method for optimization of multi-pass turning process. Recently, the new trend for solving turning optimization problems considers the use of meta-heuristic algorithms. Saravanan et al. [5] applied genetic algorithm (GA) and simulated annealing (SA) for optimization of turning parameters so as to minimize production time. In a related research Saravanan et al. [6] applied tabu search (TS), memetic algorithm (MA),

ant colony optimization (ACO) and particle swarm optimization (PSO) to minimize production cost. Optimization of multi-pass turning operations using ACO was also attempted by Vijayakumar et al. [7]. The turning parameters were determined by minimizing the unit production cost, subject to various practical machining constraints. Ameur and Assas [8] applied modified PSO for optimization of cutting speed, feed rate and depth of cut so as to achieve desirable compromise between the extent of material removal rate and tool wear. In order to achieve minimum production time in single-pass turning process, Bharathi Raja et al. [9] applied firefly algorithm (FA). The optimization framework was based on the optimization model proposed by Agapiuou [3]. The same algorithm was later applied by Belloufi et al. [10] for determination of optimized conditions in a multi-pass turning process. The optimization problem was formulated so as to achieve minimization of production cost under a set of machining constraints. Chauhan et al. [11] applied LXPM, a real coded GA which uses Laplace probability distribution in the crossover phase, and differential evolution (DE) for determination of optimal machining conditions in CNC turning process. Chauhan et al. [12] proposed the use of totally disturbed PSO (TDPSO) for obtaining optimal turning conditions during multi-pass turning operations subject to various constraints. Mellal and Wiliams [13] applied cuckoo search algorithm (CSA) for minimization of the unit production cost of multi-pass turning operations. Optimization of depth of cut in multi-pass turning using metaheuristic algorithms such as GA, SA and ACO was performed by Satishkumar et al. [14]. The optimization framework was based on the optimization mathematical model proposed by Shin and Joo [15]. Srinivas et al. [16] applied PSO for optimization of multi-pass turning process so to obtain the set of cutting parameters that minimize unit production cost subject to practical constraints. In the optimization study, the mathematical model proposed by Chen and Tsai [17] was selected, which involves multiple rough cuts and a single finish cut. Optimization of multi-pass turning operations using hybrid teaching-learning-based optimization (TLBO) algorithm was considered by Yildiz [18]. The goal was to determine turning parameters considering minimum production cost under a set of machining constraints which were presented and adopted by Shin and Joo [15] and Chen and Tsai [17]. Recently, an improved flower pollination algorithm (FPA) for solving multi-pass turning optimization problem was proposed by Xu et al. [19]. Optimization model proposed by Shin and Joo [15], which takes the unit production cost as the minimizing objective and involves some practical constraints, was used to examine the efficiency of the FPA.

Although traditional optimization methods, based on the use of gradients, can produce acceptable solution, they cannot deal well with integer/discrete independent variables. On the other hand, ability of metaheuristic algorithms to deal with discontinuous, non-differentiable, and multi-dimensional turning mathematical models made them become popular for solving turning optimization problems. However, they posses certain drawbacks, and as primary, inability to prove the optimality of the determined solution, can be listed. In that sense for solving turning optimization problems with nonlinear constraints a more robust approach may be more justified. The motivation of this study is to promote the use of conceptually simpler, and, arguably, easier for practitioners optimization approach based on the use of exhaustive iterative search. In such way optimality of the determined optimization solution would be guaranteed.

2. TURNING OPTIMIZATION PROBLEM FORMULATION

In the present study, optimization model proposed by Agapiuou [3] was adopted and analyzed. Therefore, the production time (T_u), which is the sum of machining time (t_m), tool quick return time (t_R), tool changing time (t_{cs}) and workpiece handling time (t_h), was considered as objective function:

$$T_u = t_m + t_{cs}\frac{t_m}{T} + t_R + t_h \quad (1)$$

The machining time per pass is given as:

$$t_m = \frac{\pi \cdot D \cdot L}{1000 \cdot v \cdot f} \quad (2)$$

where D is workpiece diameter, L is length of the workpiece, v is the cutting speed and f is the feed rate.

Taylor's tool life equation, given by the following power model:

$$v \cdot f^{a_1} \cdot a_p^{a_2} \cdot T^{a_3} = K \quad (3)$$

where a_p is the depth of cut, and a_1, a_2, a_3 and K are empirical constants, can be used for estimation of tool life (T) in Equation 1.

The main turning parameters are ussualy specified by machinist considering past experience and tool maker recommendations. In that sense, maximum and minimum permissible values for these parameters are given as:

$$\begin{aligned} v_{\min} \le v \le v_{\max} \\ f_{\min} \le f \le f_{\max} \\ a_{p_{\min}} \le a_p \le a_{p_{\max}} \end{aligned} \quad (4)$$

During actual turning operation, the cutting power should not exceed the maximal allowable power (P_{max}) provided by the machine tool. Thus the constraint for cutting power may be given using the following empirical relationship in the form:

$$0.0373 \cdot v^{0.91} \cdot f^{0.78} \cdot a_p^{0.75} \le P_{\max} \quad (5)$$

The tool workpiece interface temperature constraint can be given in the following form:

$$74.96 \cdot v^{0.4} \cdot f^{0.2} \cdot a_p^{0.105} \leq \theta_{\max} \quad (6)$$

where θ_{max} is the maximal temperature of tool workpiece interface.

Due to resistance of workpiece material, the cutting force occurs in turning operations. Cutting force in turning is influenced in varying amounts of different factors including cutting parameters, tool related parameters, properties of work pieced material and environment parameters. In terms of main parameters cutting force constraint can be given as:

$$844 \cdot v^{-0.1013} \cdot f^{0.725} \cdot a_p^{0.75} \leq F_{\max} \quad (7)$$

where F_{max} is the maximal allowable cutting force.

The surface quality of turned parts is one of the most frequent customer requirements. In finishing operations, it must not be greater than the maximal specified value (R_{amax}). The surface roughness constraint, in terms of main turning parameters, can be expressed as:

$$14785 \cdot v^{-1.52} \cdot f^{1.004} \cdot a_p^{0.25} \leq R_{a_{\max}} \quad (8)$$

The other necessary cutting data for formulation and solving of the considered turning optimization problem, as proposed by Agapiuou [3], are given in Table 1.

Parameter	Value	Parameter	Value
L	203 mm	P_{max}	5 kW
D	152 mm	θ_{max}	500 °C
v_{min}	30 m/min	F_{max}	900 N
v_{max}	200 m/min	a_1	0.29
f_{min}	0.254 mm/rev	a_2	0.35
f_{max}	0.762 mm/rev	a_3	0.25
a_{pmin}	2 mm	t_h	1.5 min
a_{pmax}	5 mm	t_R	0.13 min
R_{amax}	20 µm	t_{cs}	0.5 min

Table 1. Optimization model data

After setting the values from Table 1 and normalizing constraints, the final formulation of the considered turning optimization problem is reduced to:

$$\text{Minimize: } T_u = \frac{30.856 \cdot \pi}{v \cdot f} + \frac{\frac{15.428 \cdot \pi}{v \cdot f}}{\left(\frac{193.3}{v \cdot f^{0.29} \cdot a_p^{0.35}}\right)^4} + 1.63$$

$$\text{Subject to: } g_1 = 0.0373 \cdot v^{0.91} \cdot f^{0.78} \cdot a_p^{0.75} \leq 5$$

$$g_2 = 14785 \cdot v^{-1.52} \cdot f^{1.004} \cdot a_p^{0.25} \leq 20 \quad (9)$$

$$g_3 = 74.96 \cdot v^{0.4} \cdot f^{0.2} \cdot a_p^{0.105} \leq 500$$

$$g_4 = 844 \cdot v^{-0.1013} \cdot f^{0.725} \cdot a_p^{0.75} \leq 900$$

The final turning optimization problem, as formulated in Equation 9, is the constrained nonlinear optimization problem with three continuous independent variables.

3. RESULTS AND DISCUSSION

For solving the above given turning optimization problem exhaustive iterative search algorithm, provided in the specialized software tool "BRUTOMIZER" [20] was used.

The iterative search algorithm was selected as it represents a parameter free optimization approach that only requires performing a large number of computations that are, however, executed very fast. Moreover, one can take into account techno-technological possibilities of available machine tools in terms of setting particular permissible values for main turning parameter values. The optimization process was run on Intel Core2Duo T5800 with 4 GB RAM.

Table 2 shows the determined optimization values for cutting speed, feed rate, depth of cut and corresponding total production times.

For the purpose of optimization solutions comparison, another set of optimization solutions was determined (Table 3), given that maximal temperature of tool workpiece interface is set to θ_{max}=550 °C in constraint g_3 (Equation 6). Namely, Chauhan et al. [11] applied LXPM and DE for solving this optimization problem with modified constraint g_3.

As could be observed from Table 2, determination of optimal values of cutting speed, depth of cut and feed rate is predominantly conditioned by the maximal temperature of tool workpiece interface constraint (g_3). In the case of solving the optimization problem with modified constraint g_3, i.e. when maximal temperature of tool workpiece interface is set to θ_{max}=550 °C, the most critical constraint to be satisfied is related to maximal allowable machine tool power (g_1).

The optimization solutions obtained using different meta-heuristic algorithms applied by previous researchers are summarized in Tables 4-6.

As could be observed from Tables 4-6, on a first sight the use of different meta-heuristic algorithms provided a set of better optimization solutions for the considered turning optimization problem with constraints. However, after a careful analysis of the given optimization solutions and checking the given constraints as given by Equations 5-8 it turned out that many determined optimization solutions are feasible because of constraints violations. The summary is given in Table 7.

As could be observed from Table 7, it turned out that only DE managed to correctly handle given constraints, while the other meta-heuristic algorithms such as GA, SA, LXPM and PSO were not able to determine feasible solutions which satisfy all proposed conditions.

Solution	a_p (mm)	v (m/min)	f (mm/rev)	T_u (min)	g_1	g_2	g_3	g_4
1	2	109.73	0.762	2.90458	3.648	10.6	499.987	724.181
2	2.5	104.04	0.754	2.99979	4.075	12.024	499.99	854.179
3	3	105.68	0.664	3.18929	4.292	10.816	499.986	891.712
4	3.5	109.16	0.574	3.41487	4.429	9.245	499.994	897.736
5	4	113.61	0.494	3.67288	4.516	7.737	499.986	886.392
6	4.5	116.19	0.444	3.90064	4.633	6.918	499.989	894.134
7	5	119.98	0.394	4.17102	4.703	6	499.993	884.486

Table 2. The production time and corresponding turning parameter values

Solution	a_p (mm)	v (m/min)	f (mm/rev)	T_u (min)	g_1	g_2	g_3	g_4
1	2	139.26	0.762	2.779	4.531	7.378	549.995	706.907
2	2.5	129.07	0.762	2.872	4.999	8.756	546.178	842.147
3	3	121.68	0.685	3.066	4.999	9.007	532.295	899.138
4	3.5	122.69	0.585	3.319	4.999	7.889	525.91	899.466
5	4	123.62	0.51	3.576	4.999	7.027	520.469	899.388
6	4.5	124.41	0.452	3.836	4.999	6.348	515.687	899.535
7	5	125.32	0.405	4.101	4.999	5.773	511.588	898.349

Table 3. Optimization solutions obtained under modified constraint g_3

Solution	GA				SA			
	a_p (mm)	v (m/min)	f (mm/rev)	T_u (min)	a_p (mm)	v (m/min)	f (mm/rev)	T_u (min)
1	2	118.91	0.764	2.85	2	120.39	0.753	2.85
2	2.5	114.15	0.644	3.12	2.5	112.57	0.761	2.93
3	3	114.49	0.665	3.13	3	116.68	0.648	3.15
4	3.5	120.61	0.531	3.46	3.5	118.21	0.582	3.34
5	4	106.16	0.565	3.51	4	122.05	0.507	3.59
6	4.5	104.8	0.454	3.96	4.5	125.41	0.448	3.85
7	5	110.58	0.435	4.14	5	126.28	0.4	4.12

Table 4. The production time and corresponding turning parameter values given by Saravanan et al. [5]

Solution	PSO			
	a_p (mm)	v (m/min)	f (mm/rev)	T_u (min)
1	2	139.9	0.762	2.78
2	2.5	131.94	0.762	2.87
3	3	131.73	0.695	3.04
4	3.5	134.98	0.594	3.29
5	4	134.54	0.517	3.55
6	4.5	133.78	0.458	3.82
7	5	132.15	0.41	4.08

Table 5. The production time and corresponding turning parameter values given by Deep and Bansal [21]

Solution	LXPM				DE				
	a_p (mm)	v (m/min)	f (mm/rev)	T_u (min)	a_p (mm)	v (m/min)	f (mm/rev)	T_u (min)	
1	2	139.26	0.762	2.78	2	139.26	0.761	2.78*	* Corrected values
2	2.5	129.07	0.762	2.87	2.5	129.07	0.761	2.87	
3	3	122.72	0.686	3.06	3	121.56	0.685	3.06	
4	3.5	122.43	0.585	3.32*	3.5	122.61	0.585	3.32*	
5	4	134.54	0.517	3.55	4	123.53	0.51	3.57	
6	4.5	127.92	0.454	3.82	4.5	124.34	0.452	3.84*	
7	5	132.15	0.41	4.07	5	125.08	0.405	4.1*	

Table 6. Optimization solutions as given by Chauhan et al. [11] (modified constraint g_3)

Solution	Meta-heuristic algorithm				
	GA	SA	LXPM	DE	PSO
1	g_3 (516.587)	g_3 (517.663)	OK	OK	g_3 (551.005)
2	g_3 (502.783)	g_3 (516.962)	OK	OK	g_3 (551.004)
3	g_3 (516.414)	g_3 (517.665)	g_1 (5.044)	OK	g_3 (551.059)
4	g_3 (512.305)	g_3 (517.61)	OK	OK	g_3 (548.052)
5	g_4 (983.768)	g_3 (517.222)	g_1 (5.458)	OK	g_3 (539.864)
6	g_4 (918.237)	g_3 (516.423)	g_1 (5.145)	OK	g_3 (532.287)
7	g_4 (958.178)	g_3 (511.878)	g_1 (5.298)	OK	g_3 (523.847)

Table 7. Analysis of constraints violations in the determined optimization solutions by meta-heuristic algorithms

Namely, the most common method for handling linear, non-linear, equality or inequality constraints in the application of meta-heuristic algorithms is the use of penalty functions, i.e. transformation of a constrained to an unconstrained optimization problem. However, as noted by Chehouri et al. [22], the use of penalty functions necessities the definition and proper tuning of specific metaheuristic algorithm parameters, which can be challenging and problematic.

From the analysis of determined optimization results, as well as after checking constraints violations, it is clear that the proposed optimization approach provided the best optimization solutions. As could be observed from the obtained optimization results, the metaheuristic algorithms, i.e. LXPM provided the same optimization results in the case of solution 1 and solution 2 for the modified optimization problem. Thus, one can argue that the proposed optimization approach yielded better optimization results while solving complex turning optimization problem with several nonlinear constraints. Finally, for each depth of cut, the minimal determined production times are given in Figure 1.

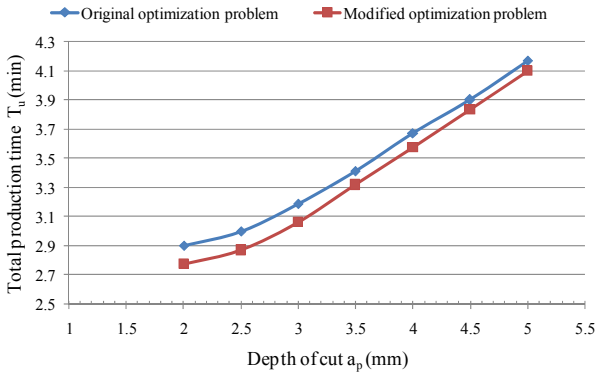

Fig. 1. The set of minimal permissible total production times for different depth of cuts obtained with the proposed optimization approach

From Figure 1 one can observe that in the case when maximal temperature of tool workpiece interface constraint is relaxed one reduces the total production time since higher cutting speeds are allowed. It could be also observed that with an increase in the depth of cut, there is an almost linear increase in the total production time. Although this may seem unusual, one should consider paired values for cutting speed, and especially feed rate, as well as the inevitability to satisfy the set nonlinear constraints.

4. CONCLUSION

So far a number of optimization approaches and methods were applied for solving complex turning optimization problems with constraints. This paper proposed the use of conceptually simple and parameter free optimization approach based on the use of exhaustive iterative search. The optimization model of minimization of production time in single-pass turning process was considered for demonstration of the applicability and suitability of the optimization approach as well as to compare the optimization results with those previously obtained with the use of meta-heuristic algorithms. From the obtained optimization results it can be concluded that the solutions previously determined by past researchers using meta-heuristic algorithms were improved. It has been observed that the presented approach is able to provide reliable and feasible optimization solutions within a reasonable computational time. Optimization solutions obtained in this way can be recorded in the CAD/CAM database for automatic generation of CNC code. On the other hand, after careful and comprehensive analysis of the optimization solution obtained with the use of meta-heuristic algorithms, it turned out that a number of obtained solutions were not feasible because of constraints violation pointing out the necessity of fine tuning of meta-heuristic algorithm parameters so as to be able to handle appropriately nonlinear constraints.

Since turning optimization problems may consider non-smooth and non-convex objective functions in terms of decision variables of continous and discrete type as well as different non-linear and linear contraints of equality and inequality type, the proposed optimization approach seems justified. Moreover, it can be easily extended for solving multi-objective constrained turning optimization problems, as well as other conventional and non-conventional machining processes such as milling, grinding, abrasive waterjet machining etc. and this is the future research scope.

5. REFERENCES

[1] Armarego, E.J.A., Brown, R.H.: *The machining of metals*, Prentice Hall, 1969.

[2] Sundaram, R.M.: *An application of goal programming technique in metal cutting*, International Journalof Production Research, Vol. 16, No. 5, p.p. 375-382, 1978.

[3] Agapiou, J.S.: *The optimization of machining operations basedon a combined criterion, Part 1: the use of combined objectivesin single pass operations*, Transactions ASME, Journal of Engineering for Industry, Vol. 114, No. 4, p.p. 500-507, 1992.

[4] Mesquita, R., Krasteva, E., Doytchinov, S.: *Computer-aided selection of optimum machining parameters in multi-pass turning*, International Journal of Advanced Manufacturing Technology, Vol. 10, No. 1, p.p. 19-26, 1995.

[5] Saravanan, R., Asokan, P., Sachithanandam, M.: *Comparative analysis of conventional and non-conventional optimisation techniques for CNC turning process,* The International Journal of Advanced Manufacturing Technology, Vol. 17, No. 7, p.p. 471-476, 2001.

[6] Saravanan, R., Sankar, R.S., Asokan, P., Vijayakumar, K., Prabhaharan, G.: *Optimization of cutting conditions during continuous finished profile machining using non-traditional techniques*, The International Journal of Advanced Manufacturing Technology, Vol. 26, No. 1, p.p. 30-40, 2005.

[7] Vijayakumar, K., Prabhaharan, G., Asokan, P., Saravanan, R.: *Optimization of multi-pass turning operations using ant colony system*, International Journal of Machine Tools and Manufacture, Vol. 43, No. 15, p.p. 1633-1639, 2003.
[8] Ameur, T., Assas, M.: *Modified PSO algorithm for multi-objective optimization of the cutting parameters*, Production Engineering, Vol. 6, No. 6, p.p. 569-576, 2012.
[9] Raja, S.B., Narayanan, N.S., Pramod, C.S., Ragunathan, A., Vinesh, S.R., Krishna, K.V.: *Optimization of constrained machining parameters in turning operation using firefly algorithm*, Journal of Applied Sciences, Vol. 12, No. 10, p.p. 1038-1042, 2012.
[10] Belloufi, A., Assas, M., Rezgui, I.: *Intelligent selection of machining parameters in multipass turnings using firefly algorithm*, Modelling and Simulation in Engineering, Vol. 1, No. 1, p.p. 1-8, 2014.
[11] Chauhan, P., Deep, K., Pant, M.: *Optimizing CNC turning process using real coded genetic algorithm and differential evolution*, Transaction on Evolutionary Algorithm and Continuous Optimization, Vol 2, No. 2, p.p. 157-165, 2011.
[12] Chauhan, P., Pant, M., Deep, K.: *Parameter optimization of multi-pass turning using chaotic PSO*, International Journal of Machine Learning and Cybernetics, Vol. 6, No. 2, p.p. 319-337, 2015.
[13] Mellal, M.A., Williams, E.J.: *Cuckoo optimization algorithm for unit production cost in multi-pass turning operations*, The International Journal of Advanced Manufacturing Technology, Vol. 76, No. 1-4, p.p. 647-656, 2015.
[14] Satishkumar, S., Asokan, P., Kumanan, S.: *Optimization of depth of cut in multi-pass turning using nontraditional optimization techniques*, The International Journal of Advanced Manufacturing Technology, Vol. 29, No. 3-4, p.p. 230-238, 2006.
[15] Shin, Y.C., Joo, Y.S.: *Optimization of machining condition with practical constraints*, International Journal of Production Research, Vol. 30, No. 12, p.p. 2907-2919, 1992.
[16] Srinivas, J., Giri, R., Yang, S.H.: *Optimization of multi-pass turning using particle swarm intelligence*, The International Journal of Advanced Manufacturing Technology, Vol. 40, No. 1, p.p. 56-66, 2009.
[17] Chen, M.-C., Tsai, D.-M.: *A simulated annealing approach foroptimization of multi-pass turning operations*, International Journal of Production Research, Vol. 34, No. 10, p.p. 2803-2825, 1996.
[18] Yildiz, A.R.: *Optimization of multi-pass turning operations using hybrid teaching learning-based approach*, The International Journal of Advanced Manufacturing Technology, Vol. 66, No. 9-12, p.p. 1319-1326, 2013.
[19] Xu, S., Wang, Y., Huang, F.: *Optimization of multi-pass turning parameters through an improved flower pollination algorithm*, The International Journal of Advanced Manufacturing Technology, Vol. 89, No. 1-4, p.p. 503-514, 2017.
[20] http://www.virtuode.com/?page=SoftwareSolution
[21] Deep, K., Bansal, J.C.: *Performanse analysis of turning process via particle swarm optimization*, Studies in Computational Intelligence, Vol. 129, No. 1, p.p. 453-460, 2008.
[22] Chehouri, A., Younes, R., Perron, J., Ilinca, A.: *A constraint-handling technique for genetic algorithms using a violation factor*, Journal of Computer Science, Vol. 12, No. 7, p.p. 350-362, 2016.

Authors: **[1]Assist. Miloš Madić PhD, [1]Professor Miroslav Radovanović PhD, [2]MSc Marko Kovačević**
[1]University of Niš, Faculty of Mechanical Engineering in Niš, Aleksandra Medvedeva 14, 18 000 Niš, Serbia, Phone: +381 18 500-687, Fax: +381 18 588-244;
[2]University of Niš, Faculty of Electronic Engineering Engineering in Niš, Aleksandra Medvedeva 14, 18 000 Niš, Serbia.

E-mail: madic@masfak.ni.ac.rs
mirado@masfak.ni.ac.rs
marko.kovacevic@elfak.ni.ac.rs

http://doi.org/10.24867/JPE-2017-02-045

Journal of Production Engineering

Vol.20 No.2

JPE (2017) Vol.20 (2) Original Scientific Paper

Mahanta,T., Mishra, A.

OPTIMIZATION OF CUTTING PARAMETERS OF AL-ZRO_2- SIC_P AND GRAPHITE HYBRID METAL MATRIX COMPOSITES

Received: 19 November 2017 / Accepted: 10 December 2017

Abstract: *Paperwork deals with fabrication, cutting parameter optimization as well as the effect of Zirconia on surface roughness and cutting force of hybrid-composites such as Al/7%SiC/1.75%Gr/2.75%ZrO_2, Al/7%SiC/1.75%Gr/4.5%ZrO_2, and Al/7%SiC/1.75%Gr/6%ZrO_2. Considering Depth of cut (d.o.c), Feed and vol.% of ZrO_2 as input parameters. Taguchi experimental design of L27, S/N ratio and ANOVA were conducted. Optimal parameters for cutting force were observed at feed 0.0599 mm/rev, d.o.c 1mm with 6% ZrO_2 and for Surface roughness at feed rate 0.0143 mm/rev, d.o.c 0.5 mm with Zirconia 2.75 %. Relation among the parameters were presented by regression-equation. 3D and contourplots were used to analyse effect of two factors on responses.*

Key words: *Hybrid Al MMC, tool dynamometer, optimization of cutting parameters, Taguchi design of experiment*

Optimizacija parametara rezanja Al-ZrO_2-SiCp i grafitnih hibridnih kompozita metalnih osnova. *Rad se bavi proizvodnjom, optimizacijom parametara rezanja, kao i efektom cirkonije na hrapavosti površine i snage rezanje hibridnih metalnih kompozita kao što su Al/7%SiC/1.75%Gr/2.75%ZrO_2, Al/7%SiC/1.75%Gr/4.5%ZrO_2, i Al/7%SiC/1.75%Gr/6%ZrO_2. Kao ulazni parametri uzeti su obzir dubina rezanja (d.o.c), pomak i težl.% ZrO_2. Izveden je Taguchi eksperimentalni dizajn L27, S/N i ANOVA amaliza. Optimalni parametri za silu rezanja su pomak 0.059 mm/o, d.o.c 1 mm sa 6% ZrO_2 i za hrapavost površine pri pomaku 0.0143mm/o, dubinom rezanja 0.5 mm sa cirkonijom 2.75 %. Veza između parametara predstavljena je regresionom jednačinom. 3D i konturni dijagrami korišćeni su za analizu uticaja dva faktora na izlazne veličine.*

Ključne reči: *Hibrid Al MMC, dinamometar za alat, optimizacija reznih parametara, Taguchi dizajn eksperimenta*

1. INTRODUCTION

There is a growing interest worldwide in manufacturing hybrid metal matrix composites which possesses combined properties of its reinforcement resulting enhanced physical, mechanical and tribological properties.

Tailor-ability of properties, higher ratio strength to density and stiffness, better fatigue resistance, higher electrical and thermal conductivity, better radiation resistance and lower creep rate, wear rate , co-efficient of thermal expansion makes metal matrix composite superior than monolithic materials, common structural materials and polymer matrix materials.. Having desirable attributes of metals and ceramics hybrid metal matrix composites find vast area of application in the field of aerospace, defence, recreation sector, atomic reactor and automobile sector

Al matrix provide better support and distributes the loads homogeneously upon the reinforcement resulting stabilized composite material due to its unique properties i.e. good damping capability, low density, corrosion resistance, non-magnetic nature, thermal conductivity. Earlier researchers have worked on reinforcement of SiCp, Al_2O_3, Gr, TiB_2 and ZrO_2 on Al matrix individually and in combined form and has found enhancement in mechanical and physical properties of the material. Graphite in the form of fibres or particulates, has long been recognized as a high strength, self-lubricating low density materials. Wettability was found to be increasing with addition of Silicon, Manganese Iron and elements of IVA, VA and VI groups with susceptibility for Carbide formation. SiC improves the tribological properties and chemical inertness of composite. ZrO_2 forms an intermetallic disperse of Al_3Zr resulting better wettability, grain refinement, good bonding and corrosion resistance.

The final conversion of composite into engineering products is associated with machining and in production and manufacturing optimal use of resources is a prime issue. This justifies the severe need of optimisation of machining parameter which would affect the production rate, quality and cost of component. The major cutting parameters for cutting force on tool are speed, feed, depth of cut, material, nose radius, lubricants used etc. As hybrid MMCs contain certain amount of hard and abrasive ceramic reinforcement it becomes more difficult for machining leading to severe tool wear and work piece damage. Machining parameters table offered by the manufacturer does not provide data for recent developed material. Hence the parameter for new materials need to be optimized. Improving the machinability of MMCs and developing machining data are the most promising ways to convince designer and manufacturers to use MMCs in their application.

Under above circumstances it has been thought proper to investigate the machinability of composites of Al with SiC, Gr, and Zirconia as reinforcements. The cutting parameters are optimized to give desired surface finish and dimensional stability using cutting force measurement by tool dynamometers and Taguchi

experimental design.

2. LITERATURE REVIEW:

Muthukrishnan and Davim [1] studied the surface roughness of Al-SiC 20 wt % by turning the composite bars using coarse grade polycrystalline diamond (PCD) .Experimental data collected were tested with the analysis of variance (ANOVA) and artificial neural network (ANN) techniques. Depth of cut, cutting speed and feed were considered as input parameters. Multilayer perception model was constructed with back propagation algorithm to analyse surface roughness. In ANOVA it was revealed that feed rate has highest statistical as well as physical influence on the surface roughness (51% to 30 %) followed by the cutting speed (12%).

Radhika [2] optimized the tribological data to find the parameters affecting wear and friction properties. Design of experiment was followed by L_{27}orthogonal array for analysis of parameters i.e applied load, sliding speed and sliding distance on wear rate as well as co-efficient of friction. The influence of parameter was carried out using ANOVA and regression equations for each response as smaller gives better characteristics. Results showed that sliding speed has minimal effect preceded by load and sliding distance.

Rajmohan et al. [3] employed Taguchi method with grey rational analysis to optimise the machining parameters with multiple performance characteristics in drilling hybrid metal matrix Al356/SiC-mica composite. L_{18} orthogonal array was chosen for experiment with input parameters as spindle speed, feed rate, drill type and mass fraction of mica. The parameters were optimized and found that feed rate and type of drill are the most affecting parameters in drilling process. Grey rational analysis is considered more advantageous than the statistical regression analysis.

Tamizharasi and Karthiresan [4] investigated the influence of different cutting parameters on surface roughness during turning of the Al/SiCp/B_4C hybrid composite. Multiple performance analysis (DFA) was performed to combine the multiple performance characteristics followed by ANOVA. The average composite desirability was derived by combining the desirability result of surface roughness, power consumed and cutting force.

Puhan et al. [5] investigated the machinability characteristics of aluminium silicon carbide composite on an electrical discharge machine. To optimize multiple responses simultaneously principal component analysis (PCA) and fuzzy inference system were coupled with Taguchi method. Response parameters selected were material removal rate, tool wear rate, surface roughness and circularity with four influential parameters i.e. discharge current, pulse duration, duty cycle and flushing pressure. Using ANOVA influence of parameters on response were duty cycle, discharge current and flushing pressure.

Sahoo et al. [6] developed composite of Al/SiCp-MMC using stir casting. Experimental investigations were carried out for analysing the flank wear and surface roughness parameters using multilayer coated carbide insert under experimental design consideration of Taguchi L_9 orthogonal array. Regression model and grey relational analysis were carried out for response optimization. It was observed from the analysis that cutting speed acts as the most influential parameter. Flank wear and feed was found to be most significant parameters for surface roughness.

Mahamani [7] studied the influence of machining parameters on cutting force and surface roughness in turning of AA219-TiB_2/ZrB_2. L27 orthogonal layout was used with cutting speed, feed rate and depth of cut as machining parameters. From Minitab package Response graph and analysis of variance showed feed rate has strongest effect on cutting force and surface roughness. Regression model was also developed between machining parameter and response. It was observed that feed rate has the strongest factor with 76.94% contribution.

Kishore et al. [8] performed turning operation on 0 wt. % 2 wt. % and 4 wt. % TiC reinforced in Al6061 composite to analyse the effect on cutting force. Process parameters were speed, feed rate and depth of cut on response to cutting force, flank wear and surface roughness. Using 5 levels for 3 parameters Taguchi design of L25 orthogonal array for design of experiment was followed. From analysis of means of responses at all levels it was observed that addition of TiC reinforcement raises surface roughness. Also increase in feed rate and depth cut results in enhanced responses.

Kumar and Rajendran [9] performed turning operation with opted parameters as cutting speed, feed rate and depth of cut to find the optimum machining parameter i.e. low surface roughness and high material removal rate of CNC turning centre on AL-HMMC reinforced with SiC and Graphite. Design of experiment was followed by Taguchi L27 orthogonal array. To analyse the effect of cutting parameter on surface roughness and MRR signal to noise ratio and analysis of variance (ANOVA) were used. Feed followed by cutting speed and depth of cut were found to be the most significant parameters.

Singh et al. [10] presented an experimental investigation on the effect of cutting force during turning of Al/SiC/Gr hybrid MMC with weight fraction of 10% SiC and 5% Graphite prepared by stir casting method. The experimental design was reported by Taguchi L9 orthogonal array plan for concluding the experiments. The cutting forces were measured with variation of parameters of cutting speed, feed and depth of cut. Results showed that change in depth of cut has the maximum effect on the cutting force than feed and speed.

Kumar et al. [11] considered the process parameters as cutting speed, depth of cut and feed rate during turning of EN19 material for achieving optimum surface finish by the help of Taguchi L27 orthogonal array followed by analysis of variance. Feed rate was having the highest contributing factor followed by depth of cut and speed.

Parihar et al. [12] analysed cutting force by changing spindle speed, depth of cut and feed

performed on conventional HMT lathe using Lathe tool dynamometer. The analysis was done by finite element method using a 3D solid model in ABAQUS/explicit simulator. The study showed that depth of cut has major impact on cutting force.

M. Ay and Altunpak [13] surveyed the drilling of Al/20%SiC/7.5%Gr,Al/20%SiC/10%Gr and Al/20%SiC/5%Gr using Taguchi's L9 orthogonal array, S/N ratio and ANOVA for optimal process parameters for cutting force and surface roughness. Rate of graphite and feed rate was found to have significant impact on surface roughness. The rate of graphite has most significant effect on cutting force i.e. 79.72% followed by feed rate.

Kishore et al. [14] studied the machinability on Al6061-TiC MMC to know the effect of cutting speed ,feed, and depth of cut on surface roughness and cutting forces using Taguchi L-27 orthogonal array. To investigate the contribution of parameters on response ANOVA was used. The contribution of depth of cut is high on the cutting force. In case of surface roughness the contribution of feed is high followed by cutting speed and depth of cut.

Kosaraju and Chandraker [15] investigated the effect of process parameters during tuning of MDN350 steel using cemented carbide tool by optimization using Taguchi method with L9 orthogonal array. Speed, feed, and depth of cut were process parameters whereas cutting force and surface roughness were selected as responses. The degree of influence of parameters on response was derived by the help of Analysis of variance. Cutting speed was the most influential parameter in cutting force and for surface roughness feed rate was found to be most influential.

Ahmed et al. [16] carried out experiment on efficient turning of high performance mild steel material using HSS tool. The process parameters chosen were cutting speed, feed rate and depth of cut to minimise the response i.e. Surface roughness, feed and radial forces. Experimental design and analysis was followed by Taguchi's L9 orthogonal array, signal to noise ratio and analysis of variance with the help of Minitab-16 statistical software. Prediction models were developed with the help of regression analysis method. Depth of cut and cutting speed were found to be the most affecting parameters against variation of feed and radial forces.

Shekar et al. [17] studied the effect of variation in machining parameters like speed, feed, depth of cut and nose radius on Al6063T6 using L9 configuration of Taguchi technique.4 factors and 3 levels for parameters were chosen to develop relation between response and control parameters. Response parameters were surface roughness, material removal rate, machining force and power consumption. From signal to noise ratio analysis for each parameter was done to find the optimum parameter setting. Minimum value for surface roughness were observed with low speed i.e. 500rpm high nose radius of 0.8mm, feed of 10mm/min and depth of cut 0.8mm.

The cutting condition which influence the cutting force and surface roughness in terms of spindle speed, feed rate, axial, radial depth of cut and weight percentage of SiCp in milling operation was investigated by Subramanian et al.[18] using Taguchi L32 ,followed by ANOVA. Response surface methodology has been employed to create the mathematical model. The adequacy of the model has been verified using analysis of variance. Direct and interaction effects of process parameters on different cutting forces were plotted to examine the effect of parameters. Feed rate was found to be the most significant parameter which affect cutting force and surface roughness.

3. SCOPE

- In the present investigation turning experiments are to be conducted on the newly developed Al hybrid composite with SiCp-Graphite and different vol % of ZrO_2 by stir casting method.
- The cutting forces are to be measured using lathe tool dynamometer with the help of strain gauge dial indicator.
- To implement Taguchi's 3 factor 3 level design of experiment technique in the measurement of cutting forces and surface roughness in machining of various vol. percentage of ZrO_2.
- To study the direct and interaction effect of process parameters through contour plots analysed through ANOVA for cutting force and surface roughness.
- To generate mathematical model for cutting force (Fz) and surface roughness (Ra) as response with controllable factors as % of Zirconia, Depth of cut and Feed rate using regression analysis.
- Finally optimum cutting parameters are to be decided based on the results available from both theoretical and experimental investigations

4. MATERIALS AND METHODS

4.1 Materials

Aluminium (AA 6061) was used as matrix material to develop hybrid metal matric composites. The reinforcement added in the hybrid were SiCp, Graphite, and Zirconia(ZrO_2). The particle size of SiCp and Graphite powder were 63µm at an average and that of Zirconia(ZrO_2) was 40µm at an average. The composition of composite was varied by vol. % of reinforcements. Three specimens of different composition i.e. Al/7%SiC/1.75%Gr/2.75%ZrO_2, Al/7%SiC/1.75%Gr/4.5%ZrO_2, Al/7%SiC/1.75%Gr/6%ZrO_2. Aluminium was collected from National Aluminium Company Ltd. Angul, Odisha. Silicon Carbide and Graphite were collected from Suvidhinath Laboratories, Vadodara, Gujrat. Zirconia was collected from High purity laboratory chemicals Pvt Ltd, Sarigam, Gujrat.

4.2 Fabrication of hybrid composite

All composites were fabricated under similar conditions through vortex method followed by conventional casting. The volume percentage and density of raw material were calculated using rule of mixture (Tab.1). Al-the matrix material was placed in the graphite crucible inside muffle furnace and heated

up to its molten state i.e. 750^0C. Reinforcement materials were pre heated up to 450^0C in muffle furnace to remove surface impurities and assist in the adsorption of gases. Constant stirring was done to ensure homogeneity of mixture. The crucible was heated above liquidus temperature up to1000^0C.Then the molten material was poured in to the prepared sand cast mould. The above process was followed for three different variation of composition of reinforcement. After solidification of the composites (Fig.1), these were machined for required specimen size

Fig. 1. Cast specimens

Specimen No	Total Volume in cm^3	Volume Fraction In cm^3				Density **ρc** (gm/c)
		SiC	Gr	ZrO_2	Al	
S1	333.367	0.0598	0.022962	0.01205	0.90457	2.7542
S2	330.226	0.06037	0.023181	0.021325	0.89512	2.7801
S3	327.932	0.06079	0.023343	0.03006	0.8857	2.8

Table 1. Constituents of the composites

4.3 Composite properties

Three different specimens were produced and were subjected to tensile and hardness test with ASTM E8M standard specimen under UTM and micro Vickers hardness tester machines. The properties obtained experimentally are indicated in Tab.2. It is seen that with increased % of ZrO_2 the hardness and tensile strength were found to be increasing.

Specimen	Micro Vickers Hardness	Tensile Strength
Al/7%SiC/1.75% Gr/2.75%ZrO_2	80.25VHN	91 MPa
Al/7%SiC/1.75% Gr/4.5%ZrO_2	103.22VHN	121MPa
Al/7%SiC/1.75% Gr/6%ZrO_2	103.77VHN	132MPa

Table 2. Mechanical properties of composites

4.4 Experimental procedure

To study the effect of Zirconia percentage on cutting force and surface roughness the turning process was carried out using a conventional lathe machine of 2.25 KW (spindle speed 54-1200rpm) motor drive. Entire process was operated at constant speed i.e. 360 rpm. The cutting tool used in the study was HSS(10%) ½ inch x 1/2 inch x 2 inch length with positive rake angle .The work piece used for experiment were with varied % of ZrO_2 (1.75%,4.5%, and 6%) with fixed 7% SiC and 1.75% Gr content by volume. They were in the form of cylindrical bar of diameter 20mm and length 75mm. Experimental trials were carried out in 1 min duration. The cutting force was measured by the Lathe tool dynamometer (Fig.2) connected with the single point cutting tool (SPCT) by the help of a strain gauge dial indicator. The average surface roughness was measured from three different places in the direction of the tool movement using Mitutoyo SJ-210 Surface roughness tester with cut-off and transverse length of 0.8 and 2.5 mm respectively.

4.5 Design of experiment

In order to simplify the parameter design, Taguchi method which is a powerful tool in this regard was used for conducting the experiment for systematised optimization along with quality and cost [11]. Considering the 3 factor and 3 levels L27 orthogonal array with 27 rows (corresponding to the no of experiments) was used for experiment. The opted parameters are presented in Table 3. The experimental results were then transformed into signal to noise (S/N) ratio i.e. the ratio of controlled parameter with the mean of uncontrolled parameters. As recommended by Taguchi the S/N ratio is used to measure the quality characteristics deviating from nominal values. Analysis using S/N ratio has been found to be producing more accurate results for optimisation of parameters [13].The S/N ratio of responses cutting force (Fz) and surface roughness (Ra) were calculated by considering smaller-the-better characteristics. Optimal condition of the cutting parameter levels can only be determined by analysing the significant effect of the parameters which can be obtained by Analysis of variance (ANOVA). The analysis was carried out within 95% of confidence interval along with the frequency test (f-test).The statistical calculations and analysis were made using Minitab Ver.15 software package.

Fig. 2. Machining on lathe with tool dynamometers

Machining Parameters	Unit	Level 1	Level 2	Level 3
% of ZrO_2	Volume Fraction %	1.75%	4.5%	6%
Depth of Cut (D.o.C)	mm	0.5	0.75	1
Feed	mm/Rev	0.0142	0.0313	0.0592

Table 3. Machining parameters and Levels

5. EXPERIMENTAL INVESTIGATION

The turning operation was carried out in conventional lathe machine. The resultant force developed during turning is recorded by the help of lathe tool dynamometer connected with a strain gauge dial indicator. As per the design of experiment the experiments were conducted varying the parameters according to Taguchi L27 orthogonal Array for tabulating the responses resultant force and surface roughness as mentioned in Table 4.

6. RESULTS AND DISCUSSION

Basic purpose of the work is to discuss the influence of cutting parameters and the effect of Zirconia on Cutting force (Fz) and surface roughness during Turning of a Hybrid Al/SiC/Gr/ZrO_2 MMCs.

6.1 Analysis of S/N ratio and ANOVA for resultant cutting force and surface roughness

By considering smaller the better characteristics the S/N ratio for cutting force and surface roughness were calculated to study the control levels produced by each factor on the responses i.e. cutting force and surface roughness as shown in Table 5 and Table 6. It is observed that Feed acts as a prime contributor for both cutting force and Surface roughness. Table 5. Suggests for contribution in cutting force depth of cut and % of zirconia are followed by feed rate. Also from Table 6. It is clear that feed leads the contribution factor followed by % of Zirconia and depth of cut. The experimental results were analysed using ANOVA (analysis of variance). The significant effect of parameters are listed in the Table 7 and Table 8 for cutting force and surface roughness respectively. Table 7 lists the numerical values of ANOVA results with the average values of cutting force (Fz). Present results in Table 7 shows that Zirconia % has least impact on the cutting force. The major significant factor is feed with proportion of 64.4% followed by depth of cut.

Exp. No.	ZrO_2 %	D.O.C	Feed	Fz	SNRA	Ra	SNRA1
1	1.75	0.5	0.0142	4.47	-13.0062	1.011	-0.09502
2	1.75	0.5	0.0313	6.726	-16.5551	1.236	-1.84037
3	1.75	0.5	0.05592	11.661	-21.3347	2.023	-6.11992
4	1.75	0.75	0.0142	13.453	-22.5764	1.075	-0.62817
5	1.75	0.75	0.0313	15.3236	-23.7072	1.45	-3.22736
6	1.75	0.75	0.05592	23.2647	-27.3339	2.611	-8.33614
7	1.75	1	0.0142	10	-20	1.023	-0.19751
8	1.75	1	0.0313	14.038	-22.9461	1.836	-5.27745
9	1.75	1	0.05592	23.2594	-27.332	2.323	-7.32098
10	4.5	0.5	0.0142	9.185	-19.2616	1.106	-0.8751
11	4.5	0.5	0.0313	12.469	-21.9166	2.056	-6.26046
12	4.5	0.5	0.05592	15.212	-23.6437	2.569	-8.19528
13	4.5	0.75	0.0142	12.041	-21.6133	1.168	-1.34886
14	4.5	0.75	0.0313	15.453	-23.7803	2.185	-6.78903
15	4.5	0.75	0.05592	22.186	-26.9216	2.658	-8.4911
16	4.5	1	0.0142	12.747	-22.1082	1.236	-1.84037
17	4.5	1	0.0313	14.866	-23.4439	2.209	-6.88391
18	4.5	1	0.05592	24.186	-27.6713	2.956	-9.41409
19	6	0.5	0.0142	10.63	-20.5307	1.056	-0.47328
20	6	0.5	0.0313	14.689	-23.3398	2.569	-8.19528
21	6	0.5	0.05592	18.62	-25.3996	2.896	-9.23597
22	6	0.75	0.0142	9.65	-19.6905	1.569	-3.91246
23	6	0.75	0.0313	11.661	-21.3347	2.365	-7.47662
24	6	0.75	0.05592	23.124	-27.2813	2.964	-9.43756
25	6	1	0.0142	9.87	-19.8863	2.035	-6.17129
26	6	1	0.0313	12.083	-21.6435	2.778	-8.87464
27	6	1	0.05592	27.318	-28.729	3.025	-9.61451

Table 4. L27 orthogonal array with S/N ratio of responses

Levels	Depth of cut (mm)	% of Zirconia (ZrO_2)	Feed (mm/rev)
1	-4.588	-3.671	-1.727
2	-5.516	-5.566	-6.092
3	-6.177	-7.044	-8.463
Delta	3.25	1.73	6.33
Rank	3	2	1

Table 5. Mean response for S/N ratio of cutting Force (Fz)

.Levels	Depth of cut (mm)	% of Zirconia (ZrO_2)	Feed (mm/rev)
1	-20.55	-21.64	-19.85
2	-23.80	-23.37	-22.07
3	-23.75	-23.09	-26.18
Delta	3.25	1.73	6.33
Rank	2	3	1

Table 6. Mean response for S/N ratio of Surface roughness (Ra)

Factors	Degree of Freedom	Sum of Square	Mean Square	F value	P value	% of contribution
ZrO_2 %	2	18.517	9.259	9.05	0.009	2.13
D.O.C	2	141.082	70.541	68.95	0.000	16.24
Feed	2	560.038	280.019	273.69	0.000	64.4
ZrO_2 %*D.O.C	4	71.729	17.932	17.53	0.001	8.25
ZrO_2 %*Feed	4	16.074	4.018	3.93	0.047	1.8
D.O.C*Feed	4	53.058	13.265	12.96	0.001	6.11
Error	8	8.185	1.023			1.07
Total	26	868.684				100

Table 7. Anova results based on resultant Cutting Force (Fz)

Factors	Degree of Freedom	Sum of Square	Mean Square	F value	P value	% of contribution
ZrO_2 %	2	2.4745	1.2372	28.01	0.000	19.13
D.O.C	2	0.4673	0.2337	5.29	0.014	3.61
Feed	2	9.1045	4.5522	103.07	0.000	70.41
Error	20	0.8833	0.0442			6.85
Total	26	12.9295				100

Table 8. Anova results Based on resultant Surface roughness (Ra)

The ANOVA result of the average values of surface roughness are summarized in the Table 8. Feed with the contribution factor of 70.41 % has the most significant effect followed by Zirconia % with 19.13% contribution factor on the Surface roughness (Ra). However, Depth of cut has little impact on surface roughness. From the interaction plot of control parameters (Fig.3) for the response cutting force it is observed that with increase in feederate the cutting force increases homogeneously. Depth of cut is not as effective as feed rate for cutting force. Experimental results reveal that when depth of cut is increased to 1mm along with feed from 0.03130 mm/rev to 0.05592 mm/rev marginal increase in cutting force is seen.

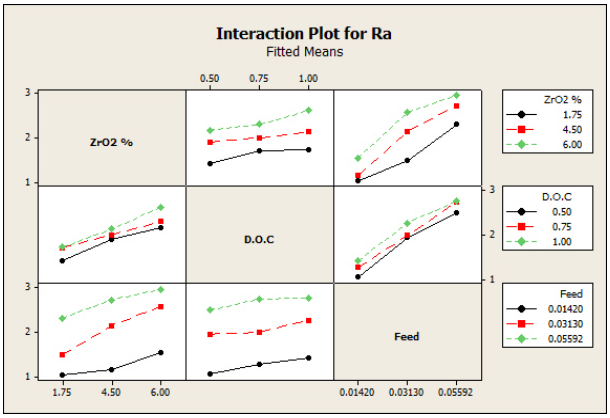

Fig. 3. Interaction plot for Ra

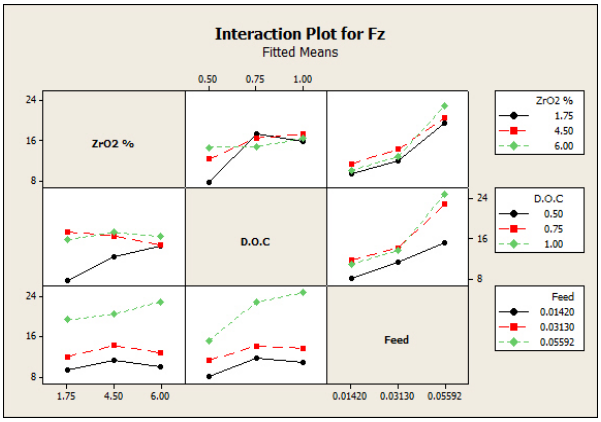

Fig. 4. Interaction Plot for Fz

However, all parameters of surface roughness increases with elevated feed rate as observed from interaction plot for surface roughness (Ra) i.e. Fig.4. With Higher % of $ZrO_2$the feed rate is seen to traverse the work piece rapidly increasing chatter, deteriorating the surface quality. The results prove that surface roughness is highly influenced by feed. It is also observed that Ra value is low with lower % of ZrO_2.

6.2 Analysis of combination of two factors

Analysis for combination of any two factors helps to check the change in effect due to combination of input factors. Comparing the 3-D response surface graph and contour plot for cutting force (Fig.5) against

the two factors % of Zirconia and feed , it is evidently clear that feed is the prime factor for development of cutting force. ZrO_2% has minor effect though highest value for cutting force is observed with high feed i.e. 0.050-0.055 mm/rev

Depth of cut is the primary key for increment of cutting force and ZrO_2% increment ceases to act as a propellant beyond 5% as the insights on Fig.6 suggests. This might be due to inhomogeneity, casting defect in specimen, machine allignment and strain guage calibration. However, for surface roughness Zirconia % was found to be prominent after feed. The 3D- surface plot and contour plots for surface roughness vs the two factor % of $ZrO_2$and feed (Fig.7) depicts the even distribution of contribution of each parameter with increase in value. Feed above 0.030 mm/rev with % of ZrO_2above 3% showed high surface roughness value. Hence for better surface finish low feed in % of ZrO_2should be preferred. Depth of cut along with percentage of Zirconia were analysed with two factor plot for Surface roughness in Fig. 8. It is observed that Depth of cut has very less impact on the surface roughness resulting minute amount of variation in graph. High depth of cut with high percent of Zirconia is producing higher value for surface roughness

6.3 Regression model for Surface roughness and cutting force

Regression model was formed to formulate a predictive equation among the control factors during turning i.e. feed, Zirconia percentage, and depth of cut for different responses. The equation developed for surface roughness (Ra) for this experiment is given below.

Ra = -0.182 +0.165 ZrO2% + 0.545 D.O.C + 32.6 Feed

= 90.6%

Again to produce a predictive equation among the control factors during turning for Cutting force was defined by the below equation as predicted by regression analysis.

Fz = - 3.44 + 0.354 ZrO2 % + 10.4 D.O.C + 277 Feed

= 80.9%

Overall lack of fit test is significant at P = 0.032 the regression equation is found to have 80.9% efficient result. Fig. 8 displays the normal probability plot for surface roughness (Ra) which determines whether the model meets the assumptions of the analysis or not. Verses order and verses fit are found to be in random order. Histogram proves that the data are normally distributed it shows nearly bell-shaped normal distri-bution. Figure 10 displays the normal probability plot for Fz contributing to form the regression equation with random order of versus fit and order. An un-even order of histogram suggests the fluctuation of cutting force resulted due to error during machining which lead to the efficiency of residue equation to 80.9%.

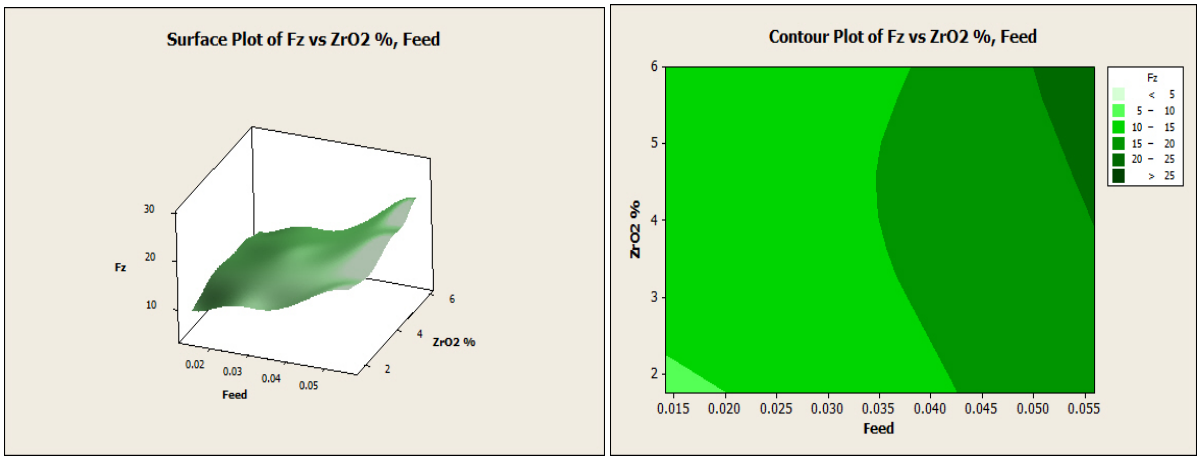

Fig. 5. 3-D response Graph and contour plot for cutting force vs ZrO_2%,Feed

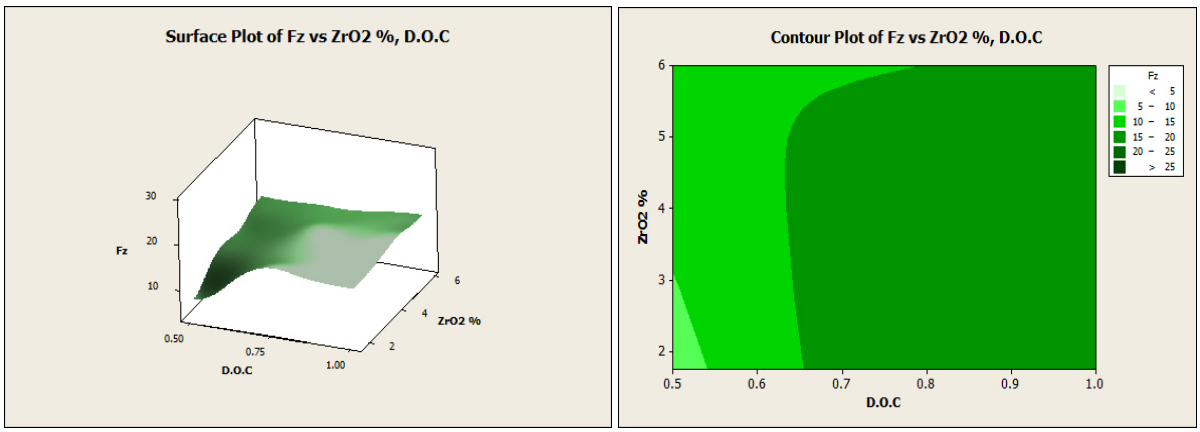

Fig. 6. 3-D response graph and contour plot for cutting force (Fz) vs ZrO_2%, Depth of cut

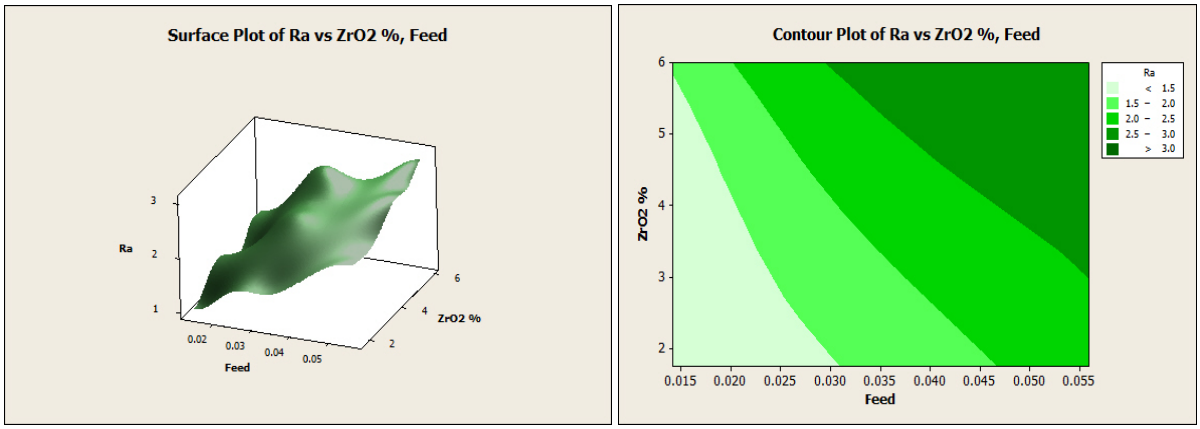

Fig.7 3-D response graph and contour plot for surface roughness (Ra) vs ZrO_2%, Feed

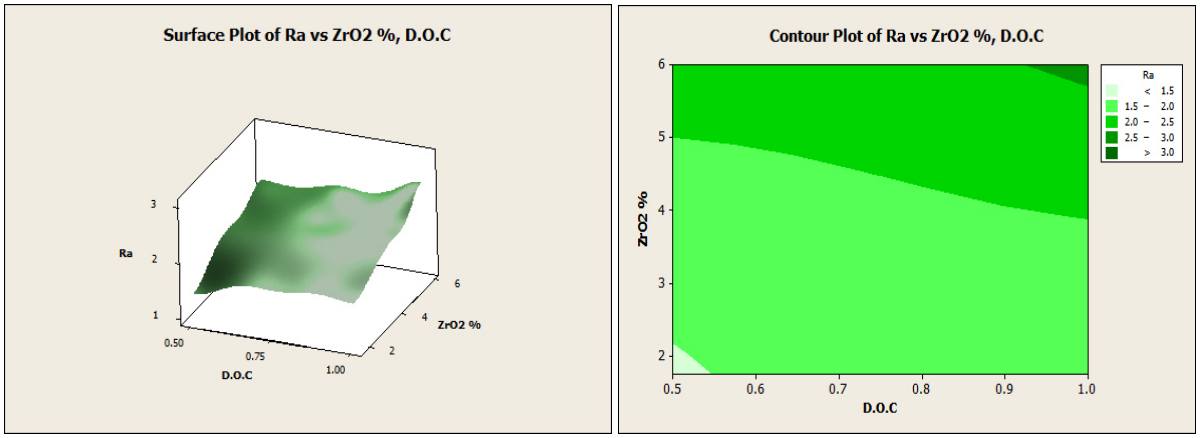

Fig.8 3-D response graph and contour plot for surface roughness (Ra) vs ZrO_2%, Depth of cut

7. CONCLUSIONS

In the present work experimental investigation of turning of

Al/7%SiC/1.75%Gr/2.75%ZrO_2,

Al/7%SiC/1.75%Gr/4.5%ZrO_2,

Al/7%SiC/1.75%Gr/6%ZrO_2

hybrid-metal-matrix composite was carried out at different parameters to study the effect of percentage of Zirconia and machining parameter on resultant cutting force and surface roughness. Taguchi L27 orthogonal array, S/N ratio and ANOVA were used for finding the optimal process parameters for surface roughness and cutting force. Linear regression model was developed to check the adequacy. Two factor 3-D surface plots and contour plots were used for better illustration of contribution of parameters. The following conclusions can be drawn from the analysis of results.

1. From S/N ratios obtained, the optimal cutting parameters for cutting force were observed at feed=0.0599 mm/rev, depth of cut = 1 mm with 6 % ZrO_2. For better Surface roughness recommended parameters were feed rate 0.0143 mm/rev, depth of cut 0.5 mm with Zirconia 2.75 %.
2. Feed rate was found to be the most significant parameter from ANOVA for cutting force with 64.45%followed by depth of cut and zirconia percentage. Also for surface roughness feed rate stood as the most significant parameter with 70.41% contribution followed by % of Zirconia content with 19.13% contribution. Depth of cut has insignificant effect on cutting force.
3. The values obtained from Taguchi analysis and ANOVA analysis are supporting each other justifying the significance of the model.

8. REFERENCES

[1] Muthukrishnan, N. Davim, P. “Optimization of Machining Parameters of Al/SiC-MMC With ANOVA and ANN Analysis,” Journal of Materials Processing Technology vol. 209, pp.225-232, 2009.

[2] Radhika, N. Subramanian, R. Prasat, V. “Tribological Behaviour of Aluminium/Alumina/ Graphite Hybrid Metal Matrix Composite Using Taguchi’s Techniques,” Journal of Minerals & Materials Characterization & Engineering, Vol. 10, No.5, pp.427-443, 2011.

[3] Rajmohan,T. Palanikumar, K. Kathirvel, M. “Optimization of Machining Parameters in Drilling Hybrid Aluminium Metal Matrix Composites,” Transactions of Nonferrous Metals Society of China, Vol.22, pp.1286-1297

[4] Tamizharasi,G. Karthiresan,S. “Optimization of machining Hybrid Metal Matrix Composites using Desirability Analysis,” International Journal of Computer & Organization Trends – Volume 2 Issue 6,pp.12-22,2012

[5] Puhan,D. Mahapatra,S.S. Sahu,J. Das,L. "Hybrid Approach for Multi-response Optimization of Non-Conventional Machining on $AlSiC_p$ MMC," Measurement, Vol.46, 2013, pp.3581-3592,2013
[6] Sahoo,A.K. Pradhan,S. Rout,A.K."Development and Machinability Assessment in Turning Al/SiCp-Metal Matrix Composite with Multilayer Coated Carbide Insert using Taguchi and Statistical Techniques," Archives of civil and mechanical engineering, vol.13, pp.27-35, 2013
[7] Mahamani,A. "Influence of Process Parameters on Cutting Force and Surface Roughness During Turning of AA2219-TiB2/ZrB2 In-situ Metal Matrix Composites," Procedia Materials Science, vol.6, pp.1178-1186,2014
[8] Kishore,D.S.C. Rao,K.P. Mahamani,A. "Investigation of Cutting Force, Surface Roughness and Flank Wear in Turning of In-situ Al6061-TiC Metal Matrix Composite" Procedia Materials Science, Vol.6, pp.1040-1050,2014
[9] Kumar,S. Rajendran,I. "Optimization of CNC Turning Parameters on Aluminum 7015 Hybrid Metal Matrix Composite Using Taguchi Robust Design," International Journal of Engineering and Technology, Vol.6, pp.1675-1682,2014
[10] Singh,G. Singh,B. Singh,K. "Optimization of Cutting Forces During Turning of Al/SiC/Gr Hybrid Metal Matrix Composite," International Journal of Research in Mechanical Engineering & Technology, Vol.4, pp.135-138,2014.
[11] Kumar,A. Chaudhary,G. Kalra,M. Prabhakar,M.S. Jha,B.K. "Optimization of Turning Parameters by Using Taguchi Method for Optimum Surface Finish" International Journal of Mechanical And Production Engineering, Vol.2, pp.42-46, 2014.
[12] Parihar,V.P.S. Saloda,M.A. Nandwana,B.P. Khidiya, M.S. "Effects of Cutting Parameters on Cutting Forces: An Experimental Study and Numerical Modeling of Turning Operation by Finite Element Analysis" Journal of Environmental Science, Computer Science and Engineering & Technology, Vol.4, pp.532-544, 2015
[13] Ay,M. Altunpak,Y. "Optimization of Cutting Parameters and Graphite rate in Drilling of a Hybrid Aluminium Matrix Composites" Journal of Engineering and Fundamentals, vol.2, pp.42-50, 2015
[14] Kishore,D.S.C. Rao,K.P. Ramesh, A. "Optimization of Machining Parameters for Improving Cutting Force and Surface Roughness in Turning of Al6061-TiC in-situ Metal Matrix Composites by Using Taguchi Method" Materials Today: Proceedings, Vol.2, pp.3075-3083, 2015
[15] Kosaraju, S. Chandraker, S. "Taguchi Analysis on Cutting Force and Surface Roughness in Turning MDN350 Steel" Materials Today: Proceedings, Vol.2, pp.3388-3393, 2015
[16] Ahmed, G. M. S. Quadri, S. H. Mohiuddin, S. "Optimization of Feed and Radial Force in Turning Process by Using Taguchi Design Approach" Materials Today: Proceedings, Vol.2, pp.3277-3285, 2015.
[17] Shekar,C. Pattar,N.B.D. Kumar,Y.V. "Optimization of Machining Parameters in Turning of Al6063t6 Through Design of Experiments" International Journal of Mechanical Engineering and Technology, Vol.7, pp.96-104. 2016
[18] Subramanian,A.V.M. NAchimuthu,M.D.G. Cinnasamy,V. "Assessment of Cutting Force and Surface Roughness in LM6/SiCp Using Response Surface Methodology" Journal of Applied Research and Technology, Vol.15, pp.283-296, 2015.

ACKNOWLEDGEMENT

The authors sincerely express their gratitude to the authorities of Mechanical and Metallurgy & Materials Engineering Departments of Indira Gandhi Institute of Technology, Sarang, and Odisha for their support, guidance and motivation to carry out this research work

Author: **M.Tech Scholar Tapapriya Mahanta[1] and Professor Antaryami Mishra[2] Ph.D.,**
Mechanical Engineering Department
Indira Gandhi Institute of Technology, Sarang-759146, Odisha, India
E-mail: tpmahanta18@gmail.com
E-mail: antaryami_igit@yahoo.co
Ph.no:09853-864-364

http://doi.org/10.24867/JPE-2017-02-054

Journal of Production Engineering

Vol.20 No.2

JPE (2017) Vol.20 (2) Original Scientific Paper

Babič, M.

NEW METHOD FOR IMAGE ANALYSIS USING NEW ALGORITHM FOR CONSTRUCTING VISIBILITY NETWORK IN 3D SPACE

Received: 19 September 2017 / Accepted: 10 November 2017

Abstract: *The objective of this paper is to determine the input-output relationship between parameters of robot laser cell for hardening, topological property of materials after hardening and volume of material using method of intelligent system; neural network, multiple regression and genetic programming. Used was method for calculate volume of materials after robot laser hardening. The effects and interaction terms on different responses of these selected parameters of robot laser cell for hardening have been analysed using neural network, multiple regression and genetic programming. Comparison of all technique of intelligent system was done. Shown was that the neural network givs the best predicted results. The genetic programming model is better than the regression model. Specimen P16 has the most volume after robot laser hardening, that is 77.7%. Parameter fractal dimension has most impact on regression model and on genetic programming model. It was noticed that topological property of visibility graph effects have considerable influence on the formation of volume, so it cannot be ignored. Used was topological properties of graphs visibility to analyse SEM images of materials after process of robot laser hardening.*

Key words: *image processing, intelligent system, visibility graphs*

Novi metod za analizu slike uz upotrebu novog algoritma za konstrukciju mreže vidljivosti u 3D prostoru. *Cilj ovog rada je odrediti odnos ulazno-izlaznih parametara robotske laserske ćelije za otvrdnjavanje, topološke osobine materijala nakon otvrdnjavanja i zapremine materijala pomoću metode inteligentnog sistema; neuronske mreža, višestruka regresija i genetsko programiranje. Korišćen je metod za izračunavanje zapremine materijala nakon robotnog laserskog očvršćavanja. Uticaji i uslovi interakcije na različite odgovore ovih odabranih parametara robotske laserske ćelije za otvrdnjavanje su analizirani korišćenjem neuronske mreže, višestruke regresije i genetskog programiranja. Upoređivane su sve tehnike veštačke inteligencije. Pokazano je da neuronska mreža daje najbolje rezultate. Model genetskog programiranja je bolji od modela regresije. Uzorak P16 ima najveću zapreminu nakon robotskog laserskog kaljenja, odnosno 77,7%. Parametar fraktalne dimenzije ima najveći uticaj na model regresije i model genetskog programiranja. Primećeno je da topološka svojstva grafičkih efekata vidljivosti imaju značajan uticaj na formiranje zapremine, tako da se to ne može zanemariti. Korišćena su topološka svojstava vidljivosti grafova za analiziranje SEM slike materijala nakon procesa robotnog laserskog otvrdnjavanja.*

Ključne reči: *obrada slike, inteligentni sistem, grafikoni vidljivosti*

1. INTRODUCTION

Digital images and videos are everywhere these days – in thousands of scientific (e.g., astronomical, bio-medical, mechanical enginering), consumer, industrial, and artistic applications. Moreover they come in a wide range of the electromagnetic spectrum - from visible light and infrared to gamma rays and beyond. We will provide a mathematical framework to describe and analyze images [1]. The image processing program explores engineering issues related to the modeling of signals starting from the physics of the problem, developing and evaluating algorithms for extracting the necessary information from the signal, and the implementation of these algorithms on electronic and opto-electronic systems. Specific research areas include filter design, fast transforms, adaptive filters, spectrum estimation and modeling, sensor array processing, image processing, motion estimation from images, and the implementation of signal processing algorithms using appropriate technologies with applications in sonar, radar, speech, geophysics, computer-aided tomography, image restoration, robotic vision, and pattern recognition.Since only the images obtained by a scanning electron microscope (SEM) and a transmission electron microscope (TEM) were used in this work and since both techniques are well-established, only a brief introduction is given on the principles and instrumentation of SEM and TEM aiming to show what kind of information is expressed through the images obtained by these techniques. An image in SEM is obtained by scanning the fine focused electron beam over the surface of the specimen and the simultaneous registration of the signals from the detectors. At each point of the specimen the beam dwells for some fixed time during which the electrons of the beam interact with the specimen. A series of image processing technologies and geometric measurement methods is introduced to quantify multiple scale microporosity in images. Computer software developed on the basis of these methods was used to quantify the SEM images of clay samples during shear test. According to the quantification result,

total pore area and average pore form factor reduce during the test.

Visibility graphs have been extensively studied. Visibility may be dened among the vertices of a polygon, line segments in the plane, or various other geometric objects in two or higher dimensions. Characterizing visibility graphs of simple polygons and nding algorithms to recognize them seem challenging. There is no polynomial-time algorithm known to recognize visibility graphs. Nor is the problem known to be NP-hard, or even in NP. Solution of problem for constructing visibility graphs was presented in [2].

An intelligent system [3] is a machine with an embedded, Internet-connected computer that has the capacity to gather and analyze data and communicate with other systems. Requirements for an intelligent system include security, connectivity, the ability to adapt according to current data and the capacity for remote monitoring and management. Essentially, an intelligent system is anything that contains a functional, although not usually general-purpose, computer with Internet connectivity. An embedded system may be powerful and capable of complex processing and data analysis, but it is usually specialized for tasks relevant to the host machine. The aim of the paper is presenting new method for image analyzing using new method for constructing visibility graphs in 3D space.

2. MATERIAL PREPARATION AND METHOD

We made patterns of a standard label on the materials according to DIN standard 1.7225. We hardened tool steel with the laser temperature T ∈ [1000, 1400] ° C and different speed v ∈ [2, 5] mm/s. In all these attempts we have made picture of microstructure (Fig. 1).

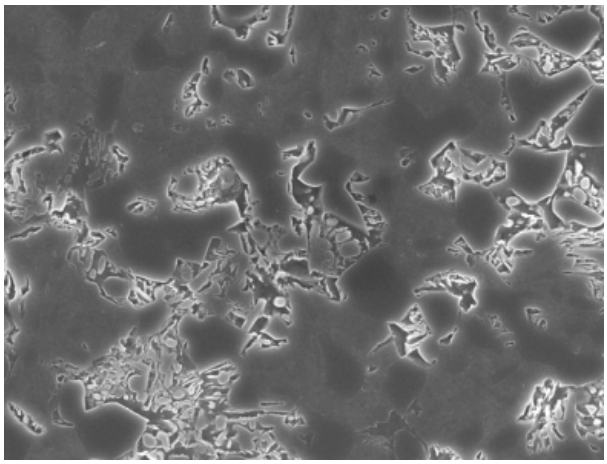

Fig. 1. Microstructure of robot laser hardened specimens

Detailed characterization of their microstructure before and after surface modifications was conducted using a field emission scanningel ectronmicroscope (SEM), JEOL JSM-7600F. The SEM pictures wereconverted into binary images, from which we calculated the density of visibility graph for 3D space, and calculate volume. For each *(x,y,z)* we use only *z* coordinate. Coordinate z have maximal value 256. Also, we calculate volume of robot laser hardened specimens with (1)

$$V = \frac{z_1 + z_2 + \ldots + z_n}{256 \times n} \tag{1}$$

for all *n*.

For image analyze, we use method of visibility graph. We use new method for constructing visibility graphs in 3D space. We calculate topological property; namely density of 3D visibility graphs.

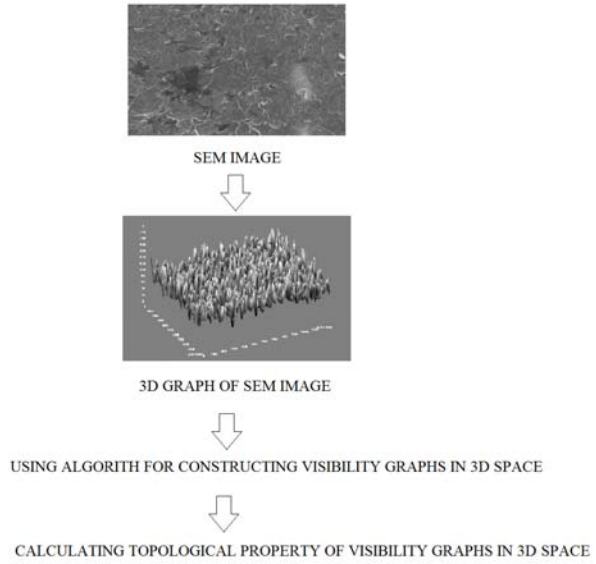

Fig. 2. Intelligent system model

To model the results, we used the intelligent system methods, i.e. the genetic programming method, neural network and multiple regression.

Genetic programming [4] is known to be capable of creating designs that satisfy prespecified high-level design requirements for analog electrical circuits and other complex structures. However, in the real world, it is often important that a design satisfy various non-technical requirements. One such requirement is that a design not possess the key characteristics of any previously known design. Traditional genetic programming ignores the meaning of programs, as the search operators it employs act on their syntactic representations, regardless of their semantics. E.g., subtree swap crossover is used to recombine functions represented as parse trees, regardless of trees repres enting boolean expressions, mathematical functions, or computer programs.

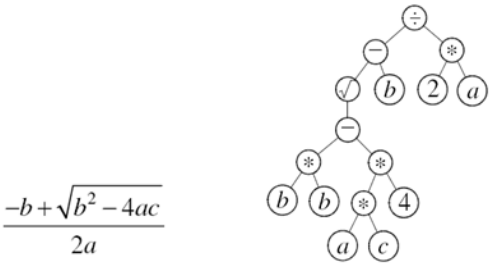

$$\frac{-b+\sqrt{b^2-4ac}}{2a}$$

Fig. 3. Randomly generated mathematical model of genetic programming

These deep learning techniques are based on stochastic gradient descent and backpropagation, but also introduce new ideas. These techniques have enabled much deeper (and larger) networks to be trained - people now routinely train networks with 5 to 10 hidden layers. The idea is to take a large number of handwritten digits, known as training examples, and then develop a system which can learn from those training examples. In other words, the neural network [5] uses the examples to automatically infer rules for recognizing handwritten digits. Furthermore, by increasing the number of training examples, the network can learn more about handwriting, and so improve its accuracy. So while I've shown just 100 training digits above, perhaps we could build a better handwriting recognizer by using thousands or even millions or billions of training examples.

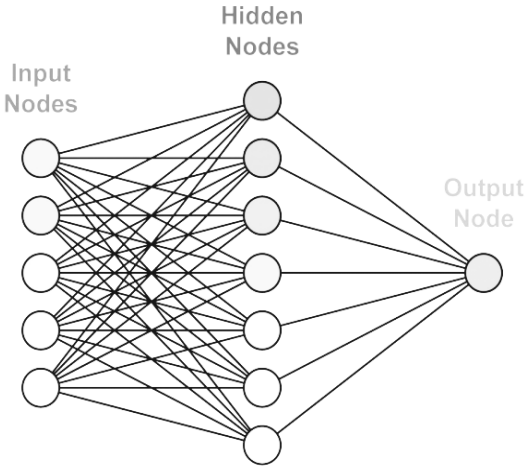

Fig. 4. General multi-layer neural network system

Multiple regression [6] is a flexible method of data analysis that may be appropriate whenever a quantitative variable (the dependent or criterion variable) is to be examined in relationship to any other factors (expressed as independent or predictor variables). Relationships may be nonlinear, independent variables may be quantitative or qualitative, and one can examine the effects of a single variable or multiple variables with or without the effects of other variables taken into account (Cohen, Cohen, West, & Aiken, 2003). Multiple regression is an extension of simple linear regression. It is used when we want to predict the value of a variable based on the value of two or more other variables. The variable we want to predict is called the dependent variable (or sometimes, the outcome, target or criterion variable). The variables we are using to predict the value of the dependent variable are called the independent variables (or sometimes, the predictor, explanatory or regressor variables). A multiple regression equation for predicting Y can be expressed a follows:

$$Y = b + b_1X_1 + b_2X_2 + ... + b_mX_m + c \ ,$$

where α_i is the corrected effect on y given that you are in group *i* (corrected in the sense that the covariates x_1, . . . , x_m are taken into account).

4. RESULTS AND DISCUSSION

In Table 1, the parameters of hardened specimens that impact on volume are presented. We mark specimens from P1 to P21. Parameter X_1 presents the parameter of temperature in degree of Celsius [C], X_2 presents the speed of hardening [mm/s] and X_3 presents density of visibility graphs in 3D space. The last parameter Y is the volume of therobot laserhardened specimens. Table 2 presents experimental and prediction data regarding the volume of laser hardened robot specimens. In Table 2 present symbol S name of specimens, E experimental data, NM1 prediction with neural network with 30% learn set, NM2 prediction with neural network with 50% learn set, NM3 prediction with neural network with method one live out, R prediction with regression and GP prediction with genetic programming. In Table 1, we can see that specimen P17 has the largest density of visibility graphs in 3D; 0.2832, thus specimen P17 have most complex graph. Specimen P16 has maximal volume after hardening, that is 77,7%. The measured and predicted volume of robot laser hardened specimens is shown in the graph in Fig. 5. The genetic programming model is presented on Fig. 3. Under model of genetic programming is presented model of regression. The genetic programming model presents a 14,14% deviation from the measured data, which is less than the regression model, which presents a 31,07% deviation. The best neural network NN3 present 5,22% deviation from the measured data. Neural network NN1 present 40,36% deviation from the measured data and NN2 present 26,49% deviation from the measured data.

S	X_1	X_2	X_3	Y
P1	1000,0	2,0	0,1936	28,0
P2	1000,0	3,0	0,2208	20,6
P3	1000,0	4,0	0,2144	25,4
P4	1000,0	5,0	0,2256	22,5
P5	1400,0	2,0	0,2445	22,9
P6	1400,0	3,0	0,2221	19,3
P7	1400,0	4,0	0,2036	13,2
P8	1400,0	5,0	0,2096	21,0
P9	1000,0	2,0	0,2352	24,0
P10	1000,0	3,0	0,2288	27,5
P11	1000,0	4,0	0,2144	28,7
P12	1000,0	5,0	0,2352	23,7
P13	1400,0	2,0	0,2208	26,3
P14	1400,0	3,0	0,232	22,1
P15	1400,0	4,0	0,1984	20,3
P16	1400,0	5,0	0,1904	77,7
P17	800,0	0,0	0,2832	15,3
P18	1400,0	0,0	0,2688	31,8
P19	2000,0	0,0	0,2416	36,9
P20	950,0	0,0	0,2128	70,8
P21	850,0	0,0	0,208	43,9

Table 1. Parameters of hardened specimens

S	E	NN1	NN2	NN3	R	GP
P1	28,0	27,50742	26,01407	27,90347	44,37732	24,2895
P2	20,6	23,00408	24,39492	22,52183	29,17192	23,1765
P3	25,4	22,33313	23,38383	26,81549	27,6009	23,1482
P4	22,5	24,05944	22,27488	24,59062	18,88807	23,2812
P5	22,9	22,20732	22,13044	22,17005	24,27785	22,8552
P6	19,3	18,75935	21,39192	19,22296	29,1994	21,562
P7	13,2	16,9911	20,66272	14,00208	32,53838	20,432
P8	21,0	18,27011	19,78675	20,92132	25,93563	20,9101
P9	24,0	26,22141	25,34777	25,65762	27,49666	23,6286
P10	27,5	23,22075	24,29008	25,78809	25,92564	23,3662
P11	28,7	22,33313	23,38383	26,81549	27,6009	23,1482
P12	23,7	24,68148	22,20033	14,88504	14,99253	23,6427
P13	26,3	22,29818	22,38205	27,23018	33,89496	21,3368
P14	22,1	19,0925	21,30572	23,30462	25,18213	22,195
P15	20,3	16,6859	20,71165	22,5824	34,64846	20,0704
P16	77,7	16,76278	19,93818	78,04819	33,7267	19,5703
P17	15,3	38,70168	28,79808	15,34632	16,07756	15,3229
P18	31,8	34,44064	23,92898	31,92222	22,75336	32,6352
P19	36,9	26,54524	20,1595	36,94508	34,62322	35,9125
P20	70,8	45,32039	28,75148	70,39741	44,85295	23,3618
P21	43,9	46,97915	29,80684	44,0274	46,66197	44,6988

Table 2. Experimental and prediction data

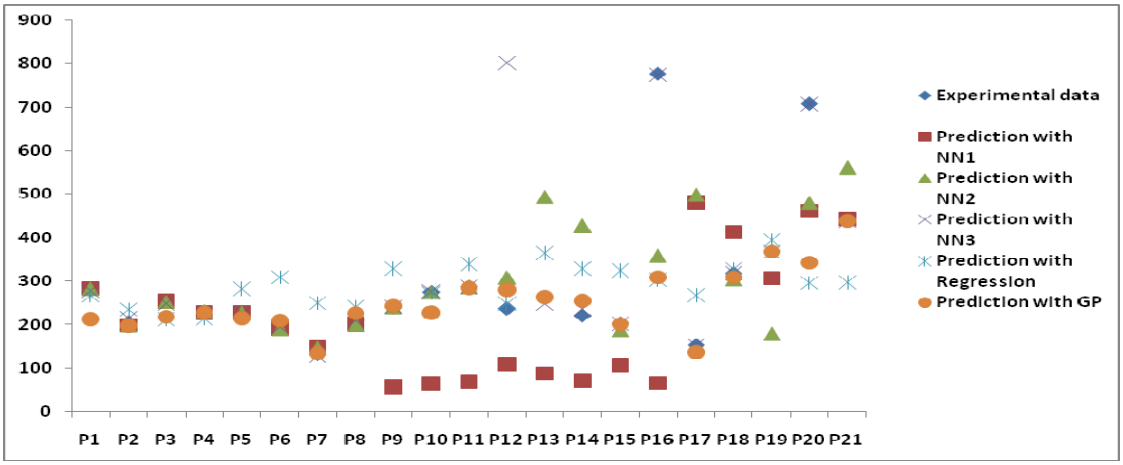

Fig. 5. The measured and predicted volume of robot laser hardened specimens

Model of genetic programming

$$Y=-0{,}728005-7{,}99\frac{X_3^2}{\frac{X_2\times(2\times X_2+\frac{X_3}{X_2})}{X_3}-\frac{(0{,}137367\frac{X_3}{X_2})\times(X_3^2+\frac{X_3}{X_2})}{X_2}}+\frac{2\times X_3\times(X_3+\frac{X_3}{X_2})}{(X_3+\frac{X_3}{X_2})\times(X_3+\frac{(7{,}28005\frac{X_3}{X_2})\times(X_3+\frac{X_3}{X_2})}{1-\frac{2+\frac{X_3}{X_2}}{X_2\times X_3\times(1+\frac{X_3}{X_2})\times(7{,}28005X_2+\frac{(7{,}28005\frac{X_3}{X_2})\times(X_3+\frac{X_3}{X_2})}{X_2+\frac{X_3}{X_2}})}}}+\frac{1}{10}\times\frac{X_2+(\frac{X_3^2}{X_3\times(7{,}28005\frac{X_3}{X_2})}-X_3\times(\frac{X_3}{X_2}+2\times X_2\times X_3+\frac{X_3}{X_2+X_3+X_3})}{X_3\times(X_3+\frac{2\times X_3^2}{X_3\times(7{,}28005\frac{X_3}{X_2})}+\frac{X_3+\frac{X_3}{X_2}}{X_2+\frac{X_3}{X_2}})}}{X_2+\frac{2\times X_3}{X_2\times(X_2+X_3+\frac{2\times X_3}{X_2})\times(7{,}28005-7{,}28005(X_2+X_3))}}+\frac{X_2+X_3^2}{X_3+\frac{X_3}{X_2}}}{X_2+X_2\times X_3-(X_3+\frac{X_3}{X_2})\times(7{,}28005-\frac{X_3}{X_2})}$$

Model of regression

$$Y = 129{,}885900 + 0{,}00138749\times X_1 - 4{,}16804262\times X_2 - 405{,}785107\times X_3$$

A statistically significant relationship was found between volume, the parameters of the robot laser cell and image analysis with new method of graph theory, especially in visibility graphs in 3D space. In addition, image analysis of SEM images of robot laser hardened specimens is an interesting approach. Specimen P16 has the most volume after robot laser hardening, that is 77,7%. Parameter X_3 (fractal dimension) has most impact on Regression model and on genetic programming model. We use method of intelligent systems; genetic programming, neural network and multiple regression to predict volume of robot laser hardened specimens. We show that the neural network give us the best predicted results. The genetic programming model is better than the regression model.

5. CONCLUSSION

In the paper we present the use of an intelligent system method, genetic programming, neural network and multyple regression to predict the volume of hardened specimens, with new method of constructing visibility graphs in 3D space. We describe a method of the visibility graph in a 3D space to analise complexity of the robot-laser-hardened specimens. The main findings can be summarised as follows:

1. We describe the volume of the hardened specimens by using the topological properties of the visibility graphs in a 3D space.
2. We describe the relationship between volume and the parameters of the robot-laser cell by using the topological properties of the 3D visibility graphs. This finding is important with regard to certain alloys that are hard to mix because they have different melting temperatures; however, such alloys have better technical characteristics. By varying different parameters (e.g., temperature), the robotlaser cells produce different patterns with different topological properties of the 3D visibility graphs.
3. To predict the volume of the hardened specimens, we use a neural network, genetic algorithm and multiple regression.
4. Using the presented intelligent system we increase production of the laser-hardening process by decreasing time of the process and increase the topographical property of materials.

6. REFERENCING

[1] R. Kumar, M. Rattan. Analysis of various quality metrics for medical image processing. Int. J. Adv. Res. Comput. Sci. Software Eng., 2 (2012), pp. 137–144.

[2] Matej Babič. Doctoral Thesis. 2014.

[3] Beverly Woolf, "Intelligent Tutoring Systems: A Survey," in *Exploring Artificial Intelligence: Survey Talks from the National Conferences on Artificial Intelligence*, ed. by Howard E. Shrobe and the American Association for Artificial Intelligence (San Mateo, CA.: Morgan Kaufmann, 1988), 1-43.

[4] R. Koza. Course Notes for Genetic Algorithms and Genetic Programming. Spring, (2002).

[5] Graves, Alex; and Schmidhuber, Jürgen; *Offline Handwriting Recognition with Multidimensional Recurrent Neural Networks*, in Bengio, Yoshua; Schuurmans, Dale; Lafferty, John; Williams, Chris K. I.; and Culotta, Aron (eds.), *Advances in Neural Information Processing Systems 22 (NIPS'22), December 7th–10th, 2009, Vancouver, BC*, Neural Information Processing Systems (NIPS) Foundation, 2009, pp. 545–552.

[6] P. Thamilarasi, S. Ragunathan, E. Mohankumar. Development of empirical models for prediction of weld bead geometry in robotic – GMAW. Journal of Achievements in Materials and Manufacturing Engineering. Volume (67), Issue 2, (2014), 72-85.

Author: **Dr. Matej Babič, Bs.M.**
Jožef Stefan Institute, Slovenia,
E-mail: babicster@gmail.com

http://doi.org/10.24867/JPE-2017-02-059

Journal of Production Engineering

Vol.20 No.2

JPE (2017) Vol.20 (2) Original Scientific Paper

Busari, Y.O., Ahmed, I.I., Shuaib-Babata, Y.L.

EFFECT OF HEAT INPUT ON THE MECHANICAL AND CORROSION BEHAVIOUR OF SMAW MILD STEEL

Received: 13 October 2017 / Accepted: 29 November 2017

Abstract: *This study was carried out to assess the effect of heat input on the mechanical properties and corrosion behaviour of mild steel. The intrinsic nature of fusion welding has made it difficult to provide a complete understanding of corrosion behaviour in some systems. Optical metallography was used to determine grain size and HAZ zone, weldment and parent metal. Mechanical properties of the weldment were observed. Corrosion behaviour of mild steel were investigated in air, sea water, alkaline and acidic medium after welding with shielded metal Arc welding SMAW by varying the welding process parameter that leads to power input and monitoring its welding speed with a stop watch. The microstructural characterization of the welded sample carried out through a metallurgical microscope (x100) and the corrosion response rate by weight loss was observed in the different medium, the sample welded with 180A and low voltage displayed the highest Rockwell hardness and the same was observed for impact test. The effect of various heat inputs on the corrosion behaviour of shielded metal arc welded mild steel show thus the as-received sample have the greatest resistance to corrosion in all the medium, at 180 A, high voltage this is closely followed by sample welded with 180 A, low voltage. The sample welded with 90A, low voltage which has the least corrosion resistance in all medium during the exposure period studied. The low heat input welded samples underwent a long period of heating, low heat input could lead to a greater tendency of distortion which may produce a higher weld cracking in the aggressive corrosion medium. The higher the current, the higher the power input and the deeper the penetration. However, the use of too high weld current may cause problems such as excessive spatter, electrode overheating and cracking while too high weld voltage could cause the beads to be wider and flatter. The low arc voltage produces a stiffer arc that improves penetration. If the voltage is too low, a very narrow bead will result.*

Key words: *Heat input, corrosion resistance, weldment, low voltage, high voltage*

Uticaj zagrevanja na mehaničko i korozijsko ponašanje mekog čelika. *Ova studija je sprovedena radi procene uticaja toplotne energije na mehaničke osobine i korozivno ponašanje mekog čelika. Unutrašnja priroda fuzionog zavarivanja otežavala je pružanje potpunog razumevanja korozionog ponašanja u nekim sistemima. Optička metalografija je korišćena za određivanje veličine zrna i HAZ zone, zavarivanja i matičnog metala. Praćene su mehaničke osobine zavarivanja. Korozivno ponašanje mekog čelika ispitano je u vazduhu, morskoj vodi, alkalnom i kiselom medijumu nakon zavarivanja sa zaštićenim metalom Arc varenje SMAV promenljivim parametrom procesa zavarivanja koji dovodi do ulaska snage i praćenja brzine zavarivanja sa štopericom. Mikrostrukturna karakterizacija zavarenog uzorka izvedenog kroz metalurški mikroskop (x100) i stepen korozionog odziva gubitka težine zabeležen je u različitom medijumu, uzorak zavaren sa 180 A i nizak napon dao je najvišu tvrdoću Rockvell-a i isto je primećeno za udarni test. Efekat različitih toplotnih ulaza na korozivno ponašanje zaštićenog mekog čelika zavarenog pomoću luka pokazuje da primljeni uzorak ima najveću otpornost na koroziju u svim sredstvima, na 180 A, visokom naponu, ovo prati i uzorak zavaren sa 180 A , niski napon. Uzorak zavaren sa 90A, niskog napona ima najmanju otpornost na koroziju u svim sredinama tokom istraženog perioda izlaganja. Uzorci zavarenih pri niskim toplotama prošli su dug period zagrijavanja, mala ulazna toplota može dovesti do veće tendencije distorzije, što može dovesti do većeh pukotina vara u agresivnom korozionom medijumu. Što je veća struja, to je veća snaga i dublji prodor. Međutim, korišćenje prevelike struje zavarivanja može izazvati probleme kao što su prekomerno prskanje, pregrijavanje elektroda i pucanje, dok previsok napon zavarivanja može prouzrokovati širi i ravan zavar. Nizak lučni napon stvara čvršći luk koji poboljšava penetraciju. Ako je napon prenizak, rezultiraće vrlo usko.*

Ključne reči: *Zagrevanje, otpornost na koroziju, zavarivanje, niski napon, visoki napon*

1. INTRODUCTION

The importance of mild steel in industrial applications and its development cannot be over-emphasised. Mild steel is the most commonly used steel on account of relatively low and good material and mechanical properties that are suitable for many applications particularly in severe condition such as extreme weather, greenhouse effect, external massive loads and corrosive marine environment. Therefore the material characteristic such as corrosion behaviour under above condition is required.

The weldment of structural steel corrodes due to exposure to moisture in the air, but the process can be strongly influenced by the presence of certain components and change in its microstructure. Corrosion can be localised to form pits, or it can extend across a wide area to produce general

deterioration [1].

Corrosion controlled treatments such as passivation and chromate-conversion may be engineered to enhance material's corrosion resistance. When metal atoms are exposed to an environment containing water molecules, electrons are released from the atoms to become positively charged ions, provided a closed electrical circuit can be established. This phenomena lead to localized corrosion in form of a pit. Pit is often developed when the exist localised anodic cell that is much smaller than cathodic cell. Usually common highly corrosion resistance alloy in contact aggressive electrolyte such as chloride. In extreme case, pit can develop to crack initiation point, which propagates and eventually results to failure such may be found in fatigue failure and stress corrosion cracking [2]. Pitting corrosion may also occur in areas where microstructural changes have occurred due to welding operations [3].

Fusion welding is a common technique for joining structural materials which are predisposed to corrosive environments such as sea water, chemicals in reactors couple with dynamic loading arising from pressure changes and thermal shocks due to start-up and shut down shocks [4].

Corrosion response of welded mild steel embedded in coastal soil environment is higher than the dry land area. This study further carried out the comparative study showing that, thus the corrosion rate is lower in plain mild steel than the welded mild steel in the coastal environment [5].

2. MATERIALS AND EXPERIMENTAL PROCEDURES

A flat bar of mild steel was used for the experiment and its composition is presented in table below.

Element	C	Si	Mn	P	S	Cr	Ni	Mo	Cu	Zn	Fe
Composition (%)	0.191	0.183	0.661	0.048	0.045	0.066	0.090	0.0087	0.0189	0.01	98.4

Table 1. Chemical composition of the material used

The edges of these samples were firmly clamped together with a little gap between them to reduce the warping of the welded joint after welding. Low hydrogen electrode gauge 3.25mm was used for all the welding operation (AWS E7018-1) because of its moisture resistance electrode.

The welding was carried out using shielded metal arc welding (SMAW). The voltage was varied between low voltage and high voltage using the arc length to determine these [6].

Sample were welded to produce five samples for one condition then after current and arc voltage was varied and the constant welding speed was monitored with aid of a stop watch.

The changes in mechanical property of weldment due to welding parameters used can be related to the changes in the microstructures of weld zone. According to following function, the change in fusion/arc welding parameters results in the variations in welding heat input [7]:

$$H = \frac{(60EI)}{(1000S)} \qquad (1)$$

Where:

H = heat input (kJ/mm),
E = Arc voltage (V),
I = welding current (A),
S = welding speed (mm/min)

Varying the heat input typically affect the mechanical properties and microstructure of weld. The amount of heat input influences cooling rate [8].

The six samples were welded in pairs when the current and voltage was varied to give different heat input, and the welding time was observed as much as possible. The current settings used were 180A, 135 A and 90A, the voltage used was assumed to be 20V at low voltage and 30V at high voltage. The range of current used is in accordance with the American Welding Society codes (AWS). During welding, the electrode was run through the gap of the weld piece until the penetration and development of the weld pool were achieved to the thickness level of the bar.

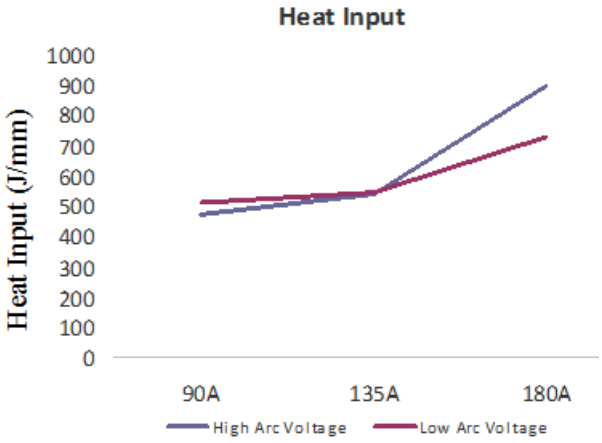

Fig. 1. graphical representation of heat input

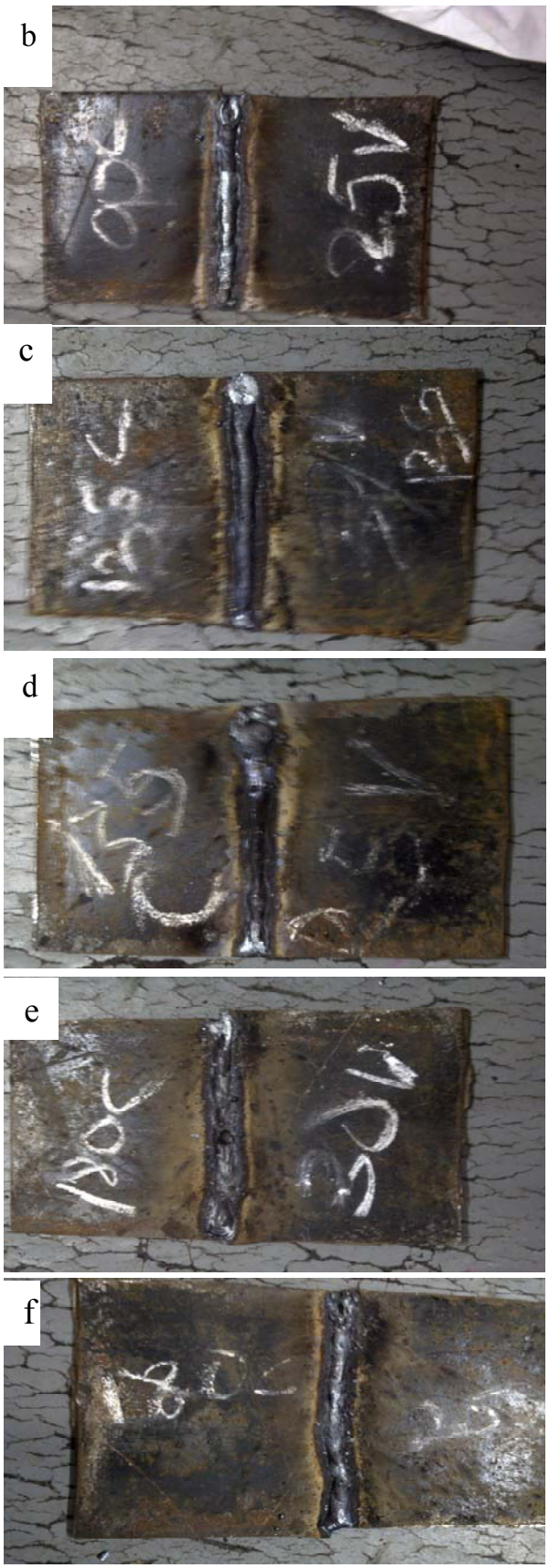

Fig. 2. Weld sample at (a). 90A, High Voltage (b). 90A, Low Voltage (c). 135A,High Voltage (d). 135A, Low Voltage (e). 180A, High Voltage (f). 180A. Low Voltage

The welded samples were cut with hack saw and then machined into shape for microstructural examination, mechanical and corrosion test. It was ensured that the welded portion was captured in the middle of the gauge length. Sample of sea water was obtained from Bar Beach, 1M NaOH (sodium hydroxide) and 0.5M of HCl was prepared in the laboratory.

3. MICROSTRUCTURAL EXAMINATION

The welded samples were first rough ground on a bench vice using a grinder. The samples were later taken for smooth grinding by making use of 220 emery papers. The smoothened surface of these samples was polished in other to remove scratches obtained during the grinding process. Samples were held on the polishing machine containing moist aluminium powder. The samples were then etched at room temperature for about 2 minutes in a V2A etchant solution made of 100 ml hydrochloric acid, 10 ml of ethanol, both of which were dissolved in 100ml of water. The etched samples were finally examined under a metallurgical microscope at a magnification of X100 micron. The steps followed for this metallographic preparation is as spelt out by Zipperian [9].

4. CORROSION

The specimens were immersed in the various prepared media separately; each specimen is then brought out on weekly basis; cleaned, dried and weighed to obtain the weight loss. This is then used to calculate CORROSION PENETRATION RATE (CPR) from the expression:

$$CPR = kw/\rho At \quad (mm/yr.) \qquad (2)$$

Where:

CPR = corrosion penetration rate (mm/yr.)
k = a constant of value = 3.16×10^8
w = weight loss due to corrosion (mg)
t = exposure time (sec)
ρ = density in g/mm^3
A = specimen surface area (mm^2)

After the preparation of the various corrosive medium, the plastic cup was properly labelled, the samples was tied to a wool thread and the required measured quantity of sea water, NaOH and HCl was placed in the cups, then the samples were placed in the prepared corrosive medium, for the HCl the weight loss was measured in the intervals of two (5) days while that of sea water and NaOH was observed at 10 days interval.

5. RESULTS AND DISCUSSION

5.1 Microstructural observation

The microstructures of the weldment were characterized by pseudo-grains and the microstructure are not uniform throughout in composition which is as a result of faster cooling rates. Most of the zone contains ferrite and some pearlites which accout for the relative hardness.

The figure 3(b), (d) and (f) microstructure that

evolved in the weldment are heterogeneous due to the temperature gradient that results from high voltage and the welding process parameter evolves the chemical gradient. Also, the heat affected zone that is between the weldment and base metal contains larger grains.

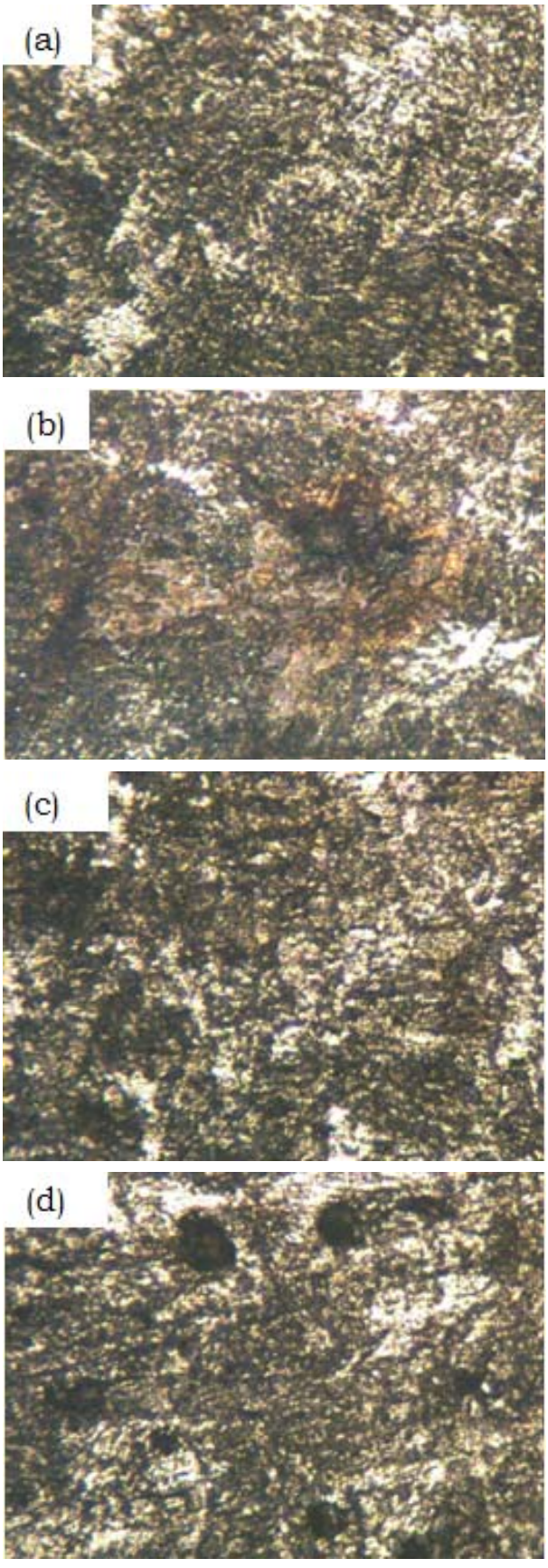

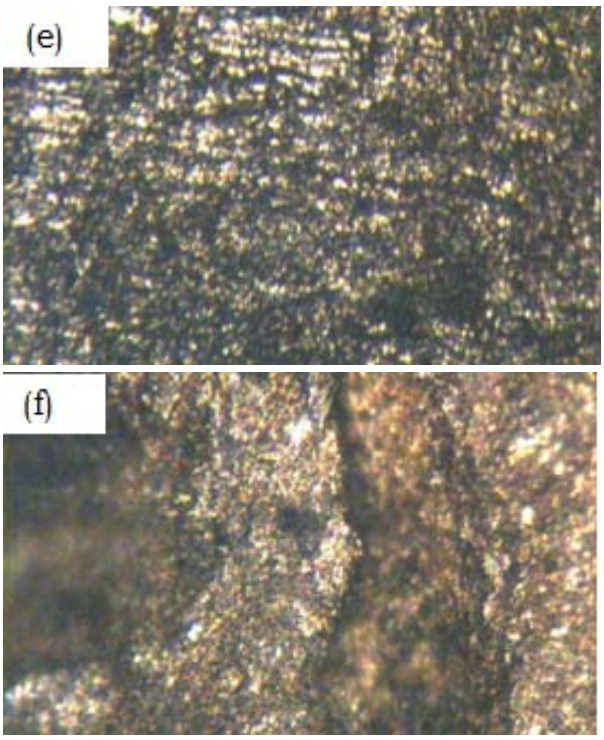

Fig. 3. Microstructure of centre of the weldment produced with different heat input; (a). 90A, Low Voltage, (b). 90A, high Voltage (c). 135A, Low Voltage (d). 135A, High Voltage (e). 180A, Low Voltage (f). 180A, high Voltage (x100)

5.2 Mechanical properties

The Rockwell hardness of the heat affected zone is higher than the various heat input welded samples as represented graphically below. The sample welded with 180A and low voltage displayed the highest Rockwell hardness among the welded sample, There is not much change in hardness of the material observed by increasing the rate of heat input. Although the amount of the heat input increases the size of the heat affected zone, but the value of the hardness remains within a certain range. We have observed that bands of coarse grains grow along a certain preferred crystallographic directions. Moreover, we have found that maximum hardness values are situated in the area of weld metal and HAZ which indicates its specificity. This may be due to the fact that the martenstic transformation.

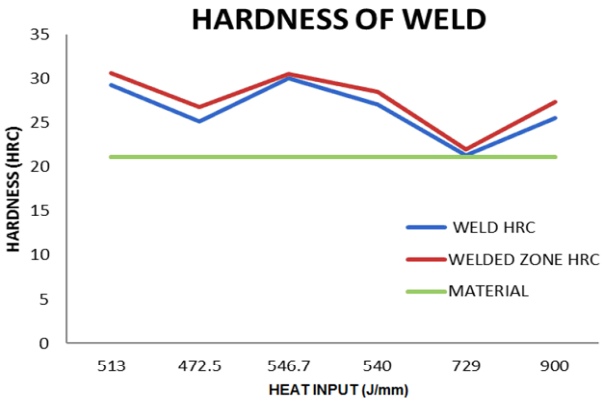

Fig. 4. Graphical representation of hardness of parent metal, weldment and heat affected zone

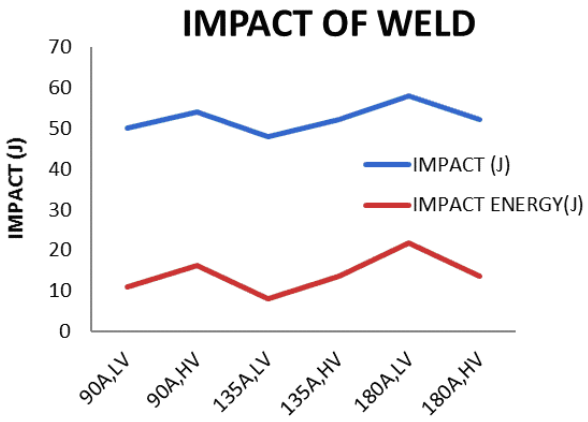

Fig. 5. Graphical representation of impact energy of the weld

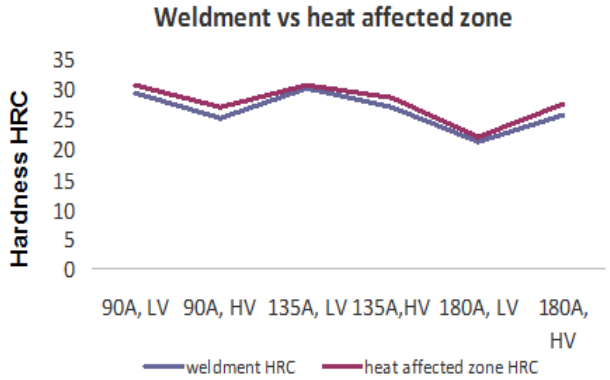

Fig. 6. Hardness value weldment and heat affected zone

6. CORROSION BEHAVIOUR

The effect of various heat inputs on the corrosion behaviour of shielded metal arc welded mild steel. Thus the as-received sample shows the greatest resistance to corrosion in all the medium, at 180 A, high voltage this is closely followed by sample welded with 180A,low voltage. The sample welded with 90A, low voltage which has the least corrosion resistance in all medium during the exposure period studied. Another possible explanation for the above result is that the low heat input welded samples underwent a long period of heating, low heat input could lead to a greater tendency of distortion which may produce a higher weld cracking in the aggressive corrosion medium [10].

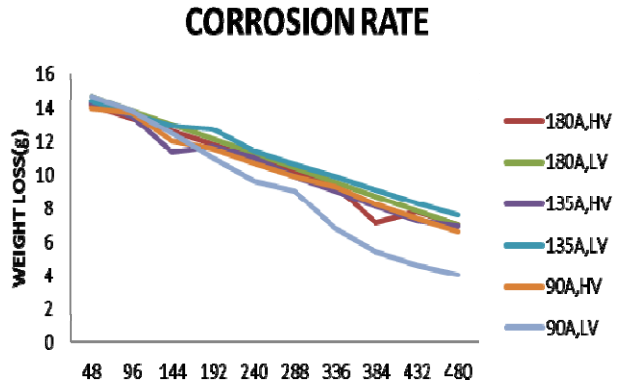

Fig. 7. Graphical representation of weight loss against days

The weld current is the current in the welding circuit during the making of a weld. The higher the current, the higher the power input and the deeper the penetration. However, the use of too high weld current may cause problems such as excessive spatter, electrode overheating and cracking while too high weld voltage could cause the beads to be wider and flatter. The low arc voltage produces a stiffer arc that improves penetration. If the voltage is too low, a very narrow bead will result [11].

7. CONCLUSION

The effects of weld process parameter were carried out and the following conclusions are made at the end of the research:

1. The result of this study have shown that welding process parameters have enormous effects on the mechanical, microstructural properties and corrosion behaviours of shielded metal arc welded mild steel in different corrosive medium.
2. An optimum current value of 135A is required to be maintained to avoid defects like porosity and weld crater.
3. The corrosion resistivity of the material was more at 135A, high voltage and this may be due to decrease grain size structure which may have a positive effect on improving local corrosion resistance. corrosion rate was increased in low current and low voltage.

The sample welded with 180A and low voltage displayed the highest Rockwell hardness and the same was observed for impact test.

8. REFERENCES

[1] Chamberlain, J. ,. (1988). Corrosion for Student of Science and Engineering. London, England.: Longman Scientific and Technology Books.

[2] Fontana, M. (1986). Corrosion Engineering (3rd ed.). New York, NY, USA.: McGraw Hill.

[3] Zhang, G., & Cheng, Y. (2009). micro-electrochemical characterization and Mott-Schottky analysis of corossion of welded X70 pipeline steel in carbonate/bicarbonate solution. electrochimica acta, 55(1), 316-324.

[4] Wahab, M.A., Nguyen N.T., Demir M. (1997), The effect of geometrical parameters, corrosion and residuals, 15th Australasian Conference on the Mechanics of Structures and Material, (pp. 589-595). Melbourne, Vic.

[5] Adeosun S.O., S. O. (2011). corrosion responses of welded mild steel embedded in coastal soil environment. International conference on innovations in engineering and technology. science and education publishing.

[6] Miller, D. F. (1998). Reviewing and Approving Welding Procedure Specifications. The National Steel Construction Conference Proceedings. new orleans.

[7] Gunaraj, V.,. (1999). Application of response surface methodology for predicting weld bead quality in submerged arc welding of pipes.

Journal of Material Processing Technology, 88, 266-275.
[8] Olivera Popovic, m. b.-C. (2010). the effect of heat input on the weld metal toughness of surfac welded joint. 14th international research/expert conference "trends in the development of machinery and associated technology", (pp. 61-64). mediterranean cruise.
[9] Le May, I. &. (1986). Metallography and fractography in corrosion related failures. Metallography and corrosion (pp. 119-130.). houston: National Association of Corrosion Engineers,.
[10] Llewellyn, D. 1.-B. (1992). Steels Metallurgy and Application. . Oxford, England: Heinemenn-Butterworths.
[11] J.W.Elmer, J. T. (2002). 6th international conference of trends in welding research, (pp. 15-19). pine mountain.

***Authors**:* **Y.O Busari, I.I. Ahmed, Y.L. Shuaib-Babata**, Department of Materials & Metallurgical Engineering, University of Ilorin, P.M.B. 1515, Ilorin Nigeria +2348034922296
E-mail:busari.oy@unilorin.edu.ng
sylbabata@gmail.com
shuaib-babata.yl@unilorin.edu.ng

http://doi.org/10.24867/JPE-2017-02-065

Journal of Production Engineering

Vol.20 No.2

JPE (2017) Vol.20 (2) Original Scientific Paper

Sekulić, S.

WEIBULL'S DISTRIBUTION FUNCTION – TERMS FOR MEAN TIME TO FAILURE: STRUCTURES, COMPARISON, DIFFERENCES AND APPLICABILITY

Received: 01 September 2017 / Accepted: 20 November 2017

Abstract: *Two terms for determination mean time to failure, exist, first via gamma function, and second from distribution function for reliability or unreliability R(t) =F(t) = 0,5, are analysed in this paper. Comparison both of terms pointed that the time to failure is direct proportional with position parameter η and the gamma function Γ corespond K value, both in function of shape parameter β also on differences between gamma Γ and K values and their application, to.*

Key words: *reliability, failure, mean time to failure, Weibull's distribution*

Vejbulova funkcija raspodele – izrazi za srednje vreme bezotkaznog rada do otkaza: strukture, poređenje, razlike i primenljivost. *U ovom radu su analizirana dva uslova za izračunavanje srednjeg vremena rada do otkaza, prvo preko gama funkcija, zatim preko funkcije pouzdanosti ili nepouzdanosti R(t) =F(t) = 0,5. Poređenjem može se zaključiti da je vreme bezotkaznog rada direktno proporcionalno parametru razmere η i gama funkciji Γ odgovara vrednosti K, i u oba slučaja su u funkciji parametra oblika β, takođe i razlika između Γ i K vrednosti kao i njihove primene.*

Ključne reči: *pouzdanost, otkaz, srednje vreme rada do otkaza, Vejbulova raspodela*

1. INTRODUCTION

Starting with probability positions mean time to failure can be determined on the basis of observed failures in time [1, 2, 3, 4].

Observed object in time can be described with simple state function

$$x(t)=\begin{cases} 1 & \text{object in available} \\ 0 & \text{object in failure} \end{cases}$$

The time in failure on observed object is not constant and present random value which we can prognose if it is known distribution function parameters and/or approximate - analytical or graphical [3, 5, 6].

For discrete systems if we observe N objects and if after time t is $N(t)$ objects in available and $n(t)$ in failure, the reliability can be expressed as

$$R(t) = N(t)/N = [N - n(t)]/N = n(t)/N \quad (1)$$

and unreliability

$$F(t) =1 - R(t) = [1 - N(t]/N \ \ [N - n(t)]/N=1- n(t)/N \quad (2)$$

From previous equation follows

$$R(t) + F(t) = 1 \quad (3)$$

which indicates complementarities.
Frequency of failure is

$$f(t) = \Delta n/N \quad (4)$$

and intensity of failures

$$\lambda = \Delta n/N(t) = f(t)/R(t) \quad (5)$$

the mean time to failure is

$$T_m = (1/N)\ \Sigma\, \Delta n[(t_{i-1} + t_i)]/2 = \Sigma\, \Delta n\ t_{im}/N \quad (6)$$

where Δn is the number of failures in interval Δt and t_{i-1} is the time on beginning and t_i on the end of interval, and t_{im} the time in the middle of interval [7-9].
If the distribution function is known the reliability is

$$R(t) = 1 - F(t) \quad (7)$$

because it is

$$R(t) + F(t) = 1 \quad (8)$$

The frequency of failure as defined as

$$f(t) = dR(t)/dt \quad (9)$$

and failure intensity

$$\lambda = f(t)/R(t) \quad (10)$$

The mean time to failure by definition is

$$T_m = {}_0\int^{\infty} R(t)\, dt \quad (11)$$

and represent an area under a curve of reliability

$R(t)= f(t)$.

How is known Weibull's distribution function,

$$F(t) = 1- exp(-t/\eta)^{\beta} \quad (12)$$

which finds its application in analysis of reliability of technical systems.

The mean time to failure can be determined analytical via gamma functions

$$T_m = \eta\, \Gamma(1 +1/\beta) \quad (13)$$

As shown in [9,10] mean time to failure correspond reliability i.e. unreliability *R(t) = F(t) = 0,5* and can be determined directly analytically [11].

$T_m = \eta\ [0{,}6931472]^{1/\beta}$ (14)

2. ANALYSYS OF TERMS FOR DETERMINATION OF MEAN TIME TO FAILURE

On the above, mentioned mean time to failure can be determined analytically: [1,2] using Weibull's distribution function (12) for R(t) =F(t) = 0,5.

Staring from Weibull's distribution function (12), mean time to failure T_m can be determined directly from Weibull's distribution function for *R(t) = F(t) = 0,5,* from [11, 12] we have

$t = \eta\ [-\ln(1 - F(t)]^{1/\beta}$

and for F(t) = R(t) = 0,5

$t = T_{R=0,5} = T_m$

$T_m = \eta\ [-\ln(1 - 0{,}5)]^{1/\beta} = \eta\, C^{1/\beta}$

where is C=0,6931472
or

$$T_m = \eta K \quad (15)$$

where is

$K = [-\ln(1-0{,}5)]^{1/\beta} = C^{1/\beta}$

2.1 Applicability terms for determination mean time to failure

How be fore is presented, mean time to failure, with two equation, in analytical form, can be determined

$$T_m = \eta\ \Gamma(1 + 1/\beta)$$

$T_m = \eta\ (0{,}6931472)^{1/\beta} = \eta K$ where is $K = f(\beta)$

By comparing this terms we can conclude that the mean time to failure T_m direct proportional with position parameter of Weibull's distribution function η. Values of gamma functions corresponds to values of K.

Determination mean time to failure via gamma Γ function

$$T_m = \eta\ \Gamma(1 + 1/\beta)$$

demand use gamma function table Γ or table T1

$$\Gamma = f_1(\beta).$$

When in usage is equation

$$T_m = \eta\ [0{,}6931472]^{1/\beta}$$

for calculation needs computer or calculator or slide rule or table T2, $K = f_2(\beta)$, because shape parameter β is in exponent.

But mean time to failure can be determined also, graphically from graphics $R(t) = f_1(t)$ and/or $R(t) = f_2(t)$ or via probalistic paper, for $R(t) = F(t) = 0{,}5$ [12].

β	Γ	β	Γ
0,2	120,00	2,5	0,887
0,35	6,292	3,0	0,893
0,5	2,000	4,0	0,906
0,7	1,266	5,0	0,918
1,0	1,000	6,0	0,928
1,5	0,903	7,5	0,938
2,0	0,886	10,0	0,965

Table T1.

Table T.3, contain differences between gamma function Γ and K values both in function of shape parameter β, are given.

Differences between gamma function and K values for $\beta \geq 2$ are smoler than 10%.

β	K	β	K
0,2	10,160	2,5	0,864
0,35	0,349	3,0	0,885
0,5	0,481	4,0	0,912
0,7	0,592	5,0	0,929
1,0	0,693	6,0	0,941
1,5	0,803	7,5	0,952
2,0	0,833	10,0	0,964

Table T2.

β	Γ	K	Γ - K	%
0,2	120,00	10,160	-40,000	33,3
0,35	6,292	0,349	5,943	94.5
0,5	2,000	0,481	1,519	84,0
0,7	1,266	0,592	0,674	53,2
1,0	1,000	0,693	0,307	30,7
1,5	0,903	0,803	0,100	11,1
2,0	0,886	0,833	0,053	6,1
2,5	0,887	0,864	0,023	2,6
3,0	0,893	0,885	0,008	1,5
4,0	0,906	0,912	-0,006	0,7
5,0	0,918	0,929	-0,011	1,2
6,0	0,928	0,941	-0,013	1,2
7,5	0,938	0,952	-0,014	1,6
10	0,965	0,964	0,001	3,4

Table T3.

3. CONCLUSION

On the basis of before mentioned we can conclude:

- The mean time to failure can be determined:
  - via gamma function Γ and,
  - from veiblle's distribution function, for R(t) = F(t) = 0,5

  in analytical form,

- If comparing terms for mean time to failure in both cases first part is proportional with position parameter η, and second parts of terms are functions of shape parameter β,
- For calculation mean time to failure via gamma function Γ the table of gamma function or table Γ=f1 (β), needs use,
- How mean time to failure correspond to reliability and unreliability R(t) = F(t) = 0,5, the mean time to failure can be determined from graphics R(t) = f_1(t) and/or F(t) = f_2(t) or from probalistic paper,
- Differences between gamma function and K values (table T.3) are consequences of data processing by calculation values for gamma function table.

4. REFERENCES

[1] Todorovic, J., Zelenovic, D., *Effectiveness of Systems in Mechanical Engineering*, Naucna knjiga, Belgrade, 1981. (in Serbian).

[2] Kececioglu, D., *Reliability Engineering Handbook,* Vol. 1 & Vol. 2, PTR Prentice Hall, Englewood Cliffs, New Jersey, 1991

[3] Ivanovic, G., Stanivukovic, D., Beker, I.: *Reliability of technical systems,* Edition: Faculty of Technical Sciences, Novi Sad, 2010 (in serbian: Pouzdanost tehničkih sistema);

[4] Sekulic, S., *Statistical Formulation of a Cutting-tool Reliability in a Working Conditions,* Reports of the 21th Conference of the European Organizations for Quality Control EOQC - Varna 77, Bulgaria, Varna, 1977.

[5] Sekulic, S., *Methodologies for Determination of Cutting-tool Reliability*, Drugie medzynarodove Symozium NARZEDZIA ’84, Krakow - Janovice - Tarnow, Poland, 1984.

[6] Sekulic, S., *Determination of Cutting-tool Reliability on Flexible Automatic Flow Lines,* Towardthe Factory of the Future, Proc. 8th ICPR, Aug., 1985, Springer-Verlag, Berlin- Heilderberg, New-York, okio, 1985.

[7] Sekulic, S., Graphical Procedure for Prognosis of the Cutting-tool Reliability on Flexible Automatics Lines Based on the Number of Work Pieces Machined with Particular Tools. Proc. INTRTRIBO ’90, Sept. 1990, Budapest, 1990.

[8] Sekulic, S., Bogicevic, S., Dudic, S., *Methodologies for Determination of Cutting-tool Reliability Supported by Computer*, Proc. International Computer Science Conference Micro CAD ’96, Febr. 1986, Miskolc, Hungary, pp 75-81.

[9] Sekulic, S., *Reliability which Correspond Mean Time to Failure,* CD-ROM Proc. XXX JUPITER Conference 17th Symposium CAD/CAM, 2004, Belgrade, Serbia, 2004; (in Serbian)

[10] Sekulić, S., Tasić, N., Bogojević, B.: “*Supporting Graphics for Determination of Mean Time to Failure of Technical Systems*”, 5. Life Cycle Engineering and Management, Beograd: Research Center DQM, 27-28 Jun, 2014, Belgrade, Serbia, pp. 46-51, ISBN 978-86-86355-17-1.

[11] Sekulic, S. *About Mean Time to Failure Determination of Technical System*, Proc. XVI International Scientific Conference on Industrial Systems (IS’14), Andrevlje, Novi Sad, Serbia, 15-17 Oct. 2014,

[12] Sekulic, S. *Reliability which correspond to mean time to failure,* Journal of production Engineering, Vol. 18, No 1. Novi Sad 2015.

Autors: **Prof . dr. Sava St. Sekulić**
Department for Industrial Engineering and Management, Faculty of Technical Sciences, University of Novi Sad, 21000 Novi Sad, Dositej Obradović Square 7,
E-mail: nemanja.tasic@uns.ac.rs

APENDIX 1

In goal to determine the mean time to failure of cutting tool T_m and reliability $R(t)$, which corresponding the observation of cutting tool failure, by turning on the lathe, in real production conditions, by different cutting conditions, on operation turning, external, longitudinal, rough-finish, by machining cylinder head of engine "Perkins", type M3. The 25 different cutting conditions was varied (5 different cutting speeds v and 5 different feeds s, in combination each with everyone. By grapho-analytical data processing, the distribution function parameters, for Weibull's distribution function β and η, on the basis of that, the mean time to failure $T_m = \eta\, \Gamma(1 + 1/\beta)$ *and* reliability which corresponding $R(T_m) = exp(-T_m/\eta)^{\beta}$ and $T_{R=0,5}$ which corresponding reliability or unreliability $R(t) = F(t) = 0,5$. are determined. Quoted data are classified in *Table T.4*.

	(n, rev/min)		(160)	(200)	(250)	(315)	(400)
	v, m/min		47,226	59,03	73,79	92,98	118,06
			1	2	3	4	5
	0,8	β η	3,0 600	3,1 320	3,3 158	2,9 70	3,65 38
		$\hat{T}_m$	535,8	286,1	141,7	62,4	34,3
		$R(T_m)$	0,49	0,49	0,50	0,49	0,50
		$\hat{T}_{R=0,5}$	531,0	284,3	141,4	61,7	31,0
			6	7	8	9	10
	1,0	β η	3,28 290	3,07 132	2,48 65	3,2 31,8	3,65 14
		$\hat{T}_m$	260,1	118,0	57,7	28,5	12,6
		$R(T_m)$	0,50	0,49	0,48	0,50	0,50
		$\hat{T}_{R=0,5}$	259,3	117,2	56,1	28,4	16,7
			11	12	13	14	15
s,	1,2	β η	2,72 170	2,76 80	2,72 37,5	2,75 19	1,6 8
mm/rev		$\hat{T}_m$	151,8	71,2	33,3	16,9	7,2
		$R(T_m)$	0,48	0,48	0,48	0,48	0,43
		$\hat{T}_{R=0,5}$	148,6	69,9	32,8	16,6	6,4
			16	17	18	19	20
	1,4	β η	2,91 118	3,0 57	3,0 28	3,0 12,5	1,9 5,5
		$\hat{T}_m$	105,0	50,9	25,0	11,2	4,9
		$R(T_m)$	0,49	0,49	0,49	0,49	0,45
		$\hat{T}_{R=0,5}$	104,0	50,5	25,8	11,1	4,5
			21	22	23	24	25
	1,6	β η	3,54 89	3,2 40	1,62 17	2,01 8	1,4 3.5
		$\hat{T}_m$	80,1	35,8	15,2	7,1	3,2
		$R(T_m)$	0,50	0,50	0,43	0,46	0,42
		$\hat{T}_{R=0,5}$	80,3	35,7	13,6	6,7	2,7

Table T.4. **Estimated values of and correspond mean time to failure $\hat{T}_m$ i $\hat{T}_{R=0,5}$**

The table contains values of mean time to failure given from two equations

$T_m = \eta\, \Gamma(1 + 1/\beta)$

and

$T_m = \eta\, [-ln(1 - 0,5]^{1/\beta} = \eta\, (0,6931472)^{1/\beta}$

which relates on same experimental data.

http://doi.org/10.24867/JPE-2017-02-069

Journal of Production Engineering

Vol.20 No.2

JPE (2017) Vol.20 (2) Original Scientific Paper

Boca, M. L., Kovač, P., Savković, B.

MODEL APPROCH OF AUTOMATION OF BOTTLING AND PACKAGING FOR INDUSTRIAL PROCESS OF BOTTLES

Received: 02 September 2017 / Accepted: 26 November 2017

Abstract: *Industry automation becomes the global trend in manufacturing, packaging process and is one of the most uses in industry; more and more companies are switching to automation. This reasearch is devoted to the use of automatic control system in process machine system; the control system will play a major role in control on all parts of this reasearch. This study report is about design and fabricate an automated packaging machine system The process of bottling and packaging of bottles is only partial part of automate process in one industrial process. Maked was a model using PetriNets for monitoring the process of bottling and packaging and we simulate a model for automation the step of bottling and packaging in the industrial process.*

Key words: *automatization; control; process*

Modelski pristup automatizacije flaširanja i pakovanja u industrijskom procesu flaširanja. *Automatizacija industrije postaje globalni trend u proizvodnji, procesu pakovanja i jedna je od najtraženijih upotreba u industriji; sve više kompanija prelazi na automatizaciju. Ovo istraživanje posvećeno je korištenju automatskog sistema upravljanja u procesnom mašinskom sistemu; kontrolni sistem će igrati glavnu ulogu u kontroli na svim delovima ovog istraživanja. Ova studija je o projektovanju i izradi automatizovanog sistema mašina za pakovanje. Proces flaširanja i pakovanja boca je samo deo automatskog procesa u jednom industrijskog procesu. Izrađen je model koristeći PetriNets za praćenje procesa flaširanja i pakovanja i simuliran model automatizacije faze flaširanja i pakovanja u industrijskom procesu.*

Ključne reči: *automatizacija; kontrola; proces*

1. INTRODUCTION

In the typical systems the model usually does not become an issue either because we will not have a large concurrent number or because our computers are really fast.

Development of society has been conditioned in times with the level and evolution of technologies used to produce goods consumer and goods capital. Big scientific discoveries and inventions of the last century revolutionized and propelled a spectacular economic and social life. It is enough to mention the main achievements in science and technologies (nuclear fission material synthesis substitution - elastomers, fibers, plastics, fertilizers, semiconductors and integrated circuits, biotechnology etc.) to understand that they are the basis of the present and future industrial.

Industry automation becomes the global trend in manufacturing, packaging process and is one of the most uses in industry; more and more companies are switching to automation. This research is devoted to the use of automatic control system in process machine system; the control system will play a major role in control on all parts of theresearch. This study report is about design and fabricate an automated packaging machine system [1].

Packaging machines (Fig. 1) are a vital part of the production process in the consumer goods industry. They often work in multishift operation, and any malfunctions have to be repaired quickly. Proven automation technology provides clear diagnostic and service strategies, and a partner with a global presence can offer prompt on-site support.

High speed is also one important characteristics of packaging machines, and the upper limit for this feature is more linked with the properties of the objects to be wrapped then to the real limits of the mechanism [2].

2. DESCRIPTION OF THE INDUSTRIAL PROCESS

Currently, in the industrial process of packaging and bottling of bottles, only Zone 1 and Zone 2 are fully automated process, Zone 3, needing at least 12 operators (Fig. 2). To increase productivity and decrease costs in this area, we observed the need to develop a project to streamline packaging by complete automation. It is required to be achieved by reconfiguring the master cases are transferred to the introduction in the final packaging and palletizing packs.

Given the above, the following requirements have been defined design:

- Transfer the boxes is automated packaging equipment
- The transfer is automatic storage boxes
- Sealing is automatic boxes
- Transfer the pallets are automatically palletizing area
- Transfer storage boxes, packaged and sealed, is automatic
- Palletizing is done automatically

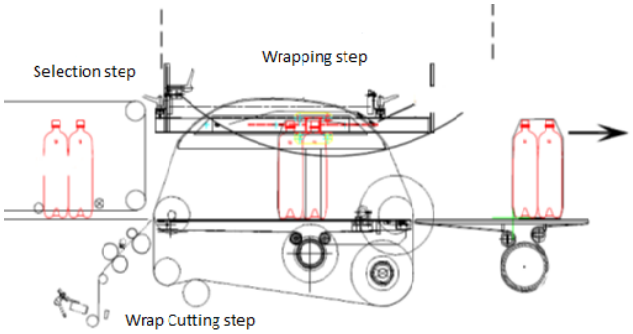

Fig. 1. The process of selection and wrapping for the bottles

To simulate automation solution suggested we used two ways:

- Monitoring technology using Petri networks
- Programming solution, with simulation for automation process in FlexSim.

For the two mentioned steps we followed these steps:

- Identifying required simulation
- Bonding using connections
- Programming each element
- Running the simulation

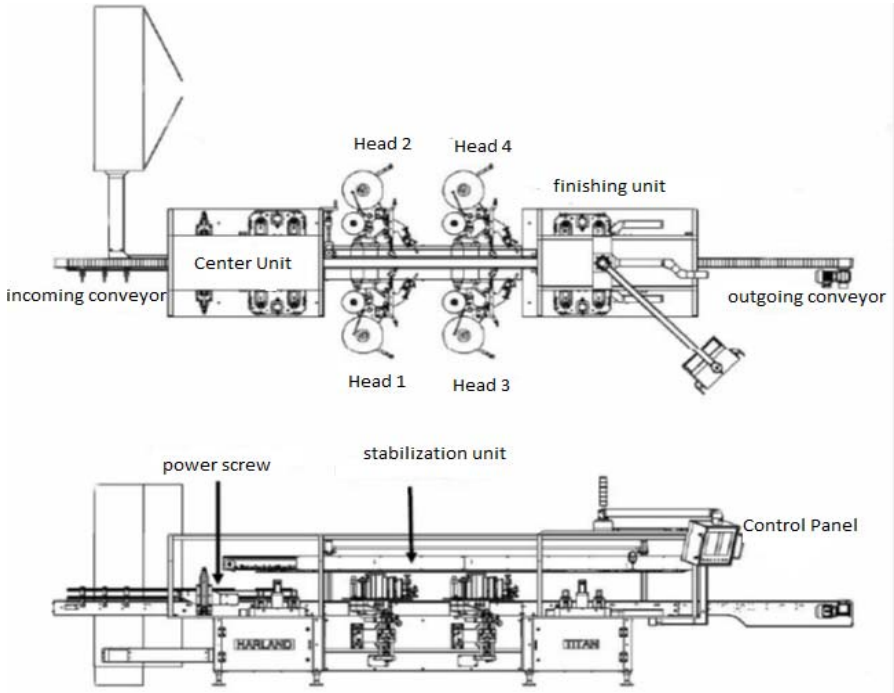

Fig. 2 The componets of the industrial process

Conducting of any technological process involves several elements: raw materials, equipment (plant), energy related technology and manufacturing personnel.

On the other hand, the efficiency of processes is influenced not only by technological factors present, but also a number of economic factors concerning both the costs of raw materials and energy and the selling price of products results, all depending on the economic situation in one time.

To obtain permanent businesses have a positive economic effect to prospect the market and to adapt their technological processes (consumption of materials and energy, working parameters) depending on the quality, accessibility and cost of their raw materials.

So, a technology that aims to obtain a product is subject to a number of technological and economic factors, expressed through physical inputs and outputs, energy and informational materials called variable processes. Calculation and their interdependence are expressed by mathematical relationships mathematical modeling of processes and optimize their default [3].

Since most processes can be achieved by several methods or technological options, perform thorough technical and economic analysis on investment costs, production costs and social and economic effects of each technical ways. It requires choosing the optimal technology, working and economical conditions more accessible as low as possible.

Optimal is to obtain top quality products, the maximum amount possible, with the lowest possible cost, in terms of maximum efficiency.

3. MODEL USING PETRINETS FOR MONITORING THE PROCESS OF BOTTLING AND PACKAGING

As a first step in process automation was achieved technological packing boxes process using PetriNets. These PetriNets had as purpose transport flow optimization of industrial process studied.

Tracking and optimization stages using Petri is in the design / prototyping process technology.

For simulation was used Visual Object Net ++, which was the whole process of packing boxes in preparation boxes or parts for assembly by putting boxes on pallets and storage boxes.

Using this technique tracking packaging process, namely Petri nets, it may consider reducing the space and layout modification work equipment.

In Fig. 3. and Fig. 4. it is the technological process of packing boxes of bottles, using the constraints of time required for each stage and use two robots in different stages of work.

Representation describes the process before and during runtime [4, 5].

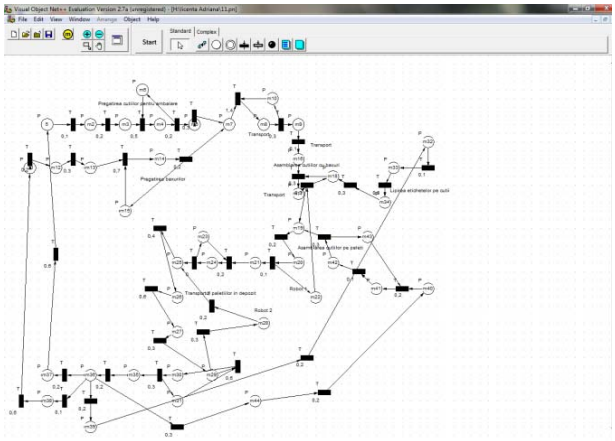

Fig. 3. Reprezentation of technological Flux using PetriNets

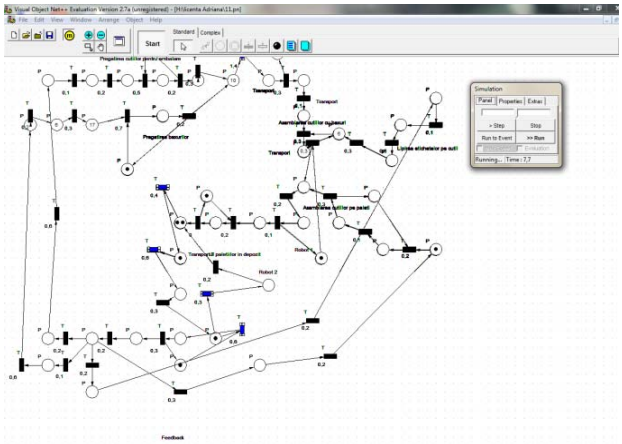

Fig. 4. Reprezentation of technological Flux using PetriNets

In Fig. 5. is the technological flow diagrams relating to the time working for the two robots and assembly stage boxes with boxes. It barely visible stream is linear, so there are no major changes in the technological flow.

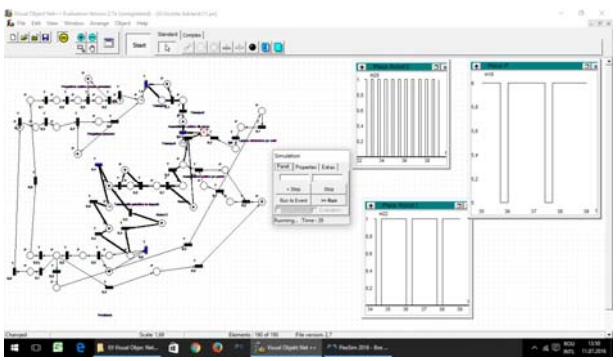

Fig. 5. Tracking and optimization of technological assembly process.

4. SIMULATION OF AUTOMATION IN THE PROCESS OF BOTTLING AND PACKAGING USING FLEXSIM

For the automatically cases transferred packaging, storage boxes will be installed two conveyor belts. At the end of the first bands will be connected a lift that will transfer to the second conveyor belt master cases (Fig.6).

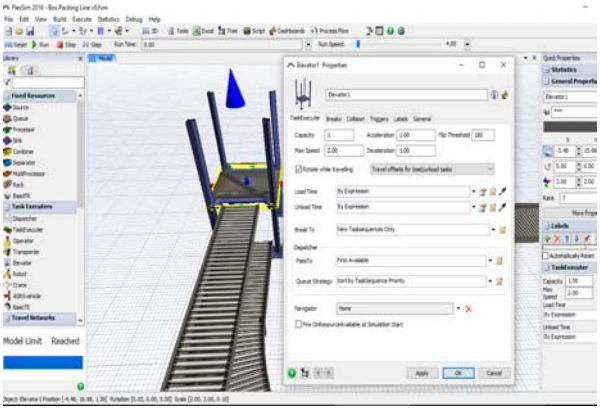

Fig. 6. Parameters setting for Elevator. Preparing the packing boxes

This, in turn, will transfer to the master cases packing boxes.

The pallets needed palletizing area have the same route as master cases until the elevator, with the same settings (Fig. 3.) will transferring the pallets using a third conveyor.

This will ensure the transfer of pallets in palletizing zone.

Also, for the preparation of storage boxes (Fig. 7.) will be install a utility that prepares the boxes, for provide boxes in the packaging using another conveyor.

Packing area will consist of a robot arm (Fig. 10).

Here will be introducing in each storage box one box of water. It is then transported in step sealing and labeling of boxes. Sealed storage boxes are transported to the palletizing area through a conveyor cylinder (Fig. 9).

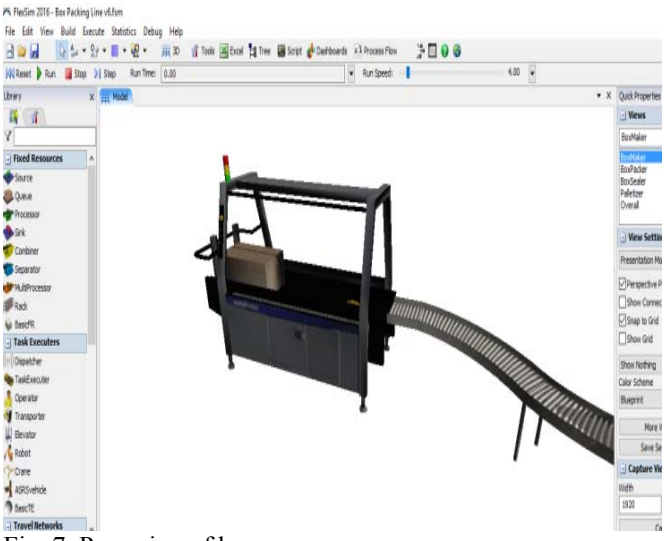

Fig. 7. Preparing of boxes

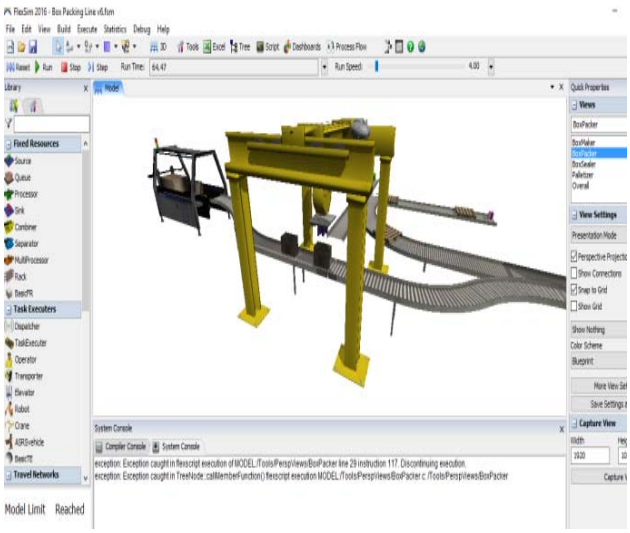

Fig. 8. Preparing of boxes with crane

Palletizing area is driven by a robotic arm that puts on each pallet, a total of 12 storage boxes (Fig.10.).

Fig. 9. Sealing of boxes

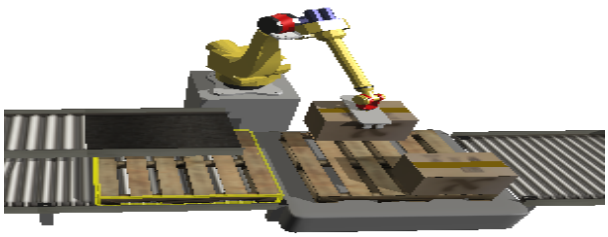

Fig.10. Palletizing robot arm

Take in case the analysis of the following two images (Fig. 11. and Fig. 12) we find major difference between this initial simulation stages through full automation and improved version [6, 7].

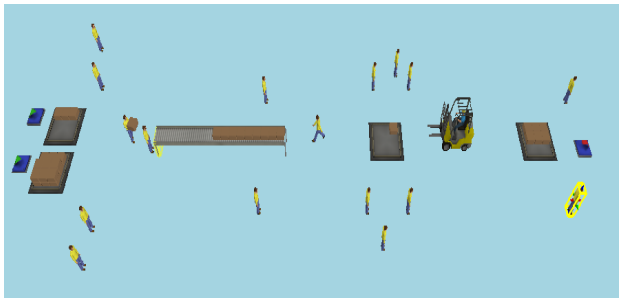

Fig. 11. FlexSim Simulation in initial case

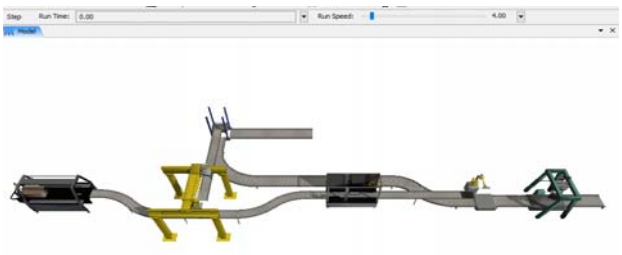

Fig. 12. FlexSim Simulation in final case after automation

5. CONCLUSIONS

Was performed in detail the packaging process flow, by setting specific time in each stage, and thus optimize the process.

Was made the automation packaging stage, initially at certain stages is made by the operator.

There is the possibility of using the model created in other processes involving packaging.

6. REFERENCES

[1] Alhade A. Algitta, Mustafa S., Ibrahim F., Abdalruof N.,Yousef M.: *Automated Packaging Machine Using PLC,* Control Engineering Dep., College of Electronic Technology, Bani Walid 38645, Libya, 2015

[2] Coulouris G., Dollimor., J, Kindberg T.: *Distributed system: concept and design*, 3rd edition, Addison-Wesley, 772, 2001.

[3] Coulouris G., Dollimore J., Kindenberg T. : *Distributed system: concept and design*", E3 Addison-Wesley, 2002.

[4] Gupta V.: *Distributed estimation and control in networked systems*, California Institute of Technology Pasadena, California 2006.

[5] Jack H.: *Automation manufacturing systems- with plc's"*, 2005.

[6] Vânătoru M.: *Conducerea automata a proceselor industriale*, Seria Control Engineering, Vol 1, 2001.

[7] Vişan S., Ghiga C., Panduru V.: *Tehnologii industriale*", Bucureşti, Editura ASE, 2000.

Autors: **PhD Lecturer Boca Maria Loredana** "1 Decembrie 1918" University of Alba Iulia, Romania, Alba Iulia, Gabriel Bethlen No.5, 510009, Phone.: +40 258-80613

Professor Pavel Kovac PhD, Assist. Professor Borislav Savkovic PhD, University of Novi Sad, Faculty of Technical Sciences, Institute for Production Engineering, Trg Dositeja Obradovica 6, 21000 Novi Sad, Serbia, Phone.: +381 21 450-366, Fax: +381 21 454-495.

E-mail: loredana_boca1@yahoo.com
pkovac@uns.ac.rs
savkovic@uns.ac.rs

http://doi.org/10.24867/JPE-2017-02-073

Journal of Production Engineering

Vol.20 No.2

JPE (2017) Vol.20 (2) Original Scientific Paper

Ikubanni, P.P., Komolafe, C.A., Agboola, O.O., Osueke, C.O.

MORINGA SEED DEHULLING MACHINE: A NEW CONCEPTUAL DESIGN

Received: 10 October 2017 / Accepted: 28 November 2017

Abstract: *This work aimed at designing and fabricating a Moringa seed dehulling machine using another design concept. The dehulling mechanisms includes a dehulling shaft that accommodates the dehulling drum of diameter 100mm and thickness 2.5mm and spikes 40mm long. The dehulling machine for Moringa seed processing is powered by an electric motor, pulleys, belts, shafts and bearings. The chaffs leave the machine through a slot created in the dehulling chamber while the seed fall through a screen under the action of gravity to a tray placed under the dehulling chamber. The overall efficiency of this machine on dry basis was 65.9 % and on wet basis was 52.5 %.*

Key words: *dehulling efficiency, dehulling mechanism, moringa dehuller, moringa seed*

Mašina za ljuštenje Moringa semena: Novi idejni projekat. *Ovaj rad je imao za cilj dizajniranje i izmišljanje mašine za dehuliranje semena Moringa koristeći drugi koncept dizajna. Mehanizmi za ljuštenje obuhvataju oslobađajuću osovinu koja se uklapa u bubanj sa prečnikom od 100 mm i debljinom od 2,5mm i šiljciama dužine 40 mm. Mašinu za ljuštenje za preradu semena Moringa pokreće električni motor, kutije, kaiševi, osovine i ležajevi. Pleva odlazi iz mašine kroz prorez koji je stvoren u komori za ljuštenje, dok seme pada kroz sito pod dejstvom gravitacije do ležišta postavljenog ispod komore za ljuštenje. Ukupna efikasnost ove mašine na suvoj osnovi iznosila je 65,9%, a na vlažnoj osnovi bila je 52,5%.*

Ključne reči: *efikasnost ljuštenja, mehanizam ljuštenja, moringa ljuštač, moringa seme*

1. INTRODUCTION

Moringa oleifera, a tree found mainly in the tropic regions, commonly referred to as horseradish or drumstick in English and “ewe ile” in Yoruba. It is the most widely cultivated species of the genus Moringa and has been used by indigenous cultures worldwide for over 4,000 years for various purposes which includes eating, medicinal etc [1] [2]. Moringa is a nutrient-dense plant, rich in calcium, iron, vitamins, and essential amino acids that are found in other complete proteins such as quinoa and meat. Moringa oleifera has many health benefits such as improving energy, lower blood pressure level, lower blood sugar level, improved hair and skin, to name a few [1]. Moringa leaves are believed and reported to prevent over 300 diseases such as diabetes, hypotension, tumour etc., and are used all the time in traditional healing. Moringa, which is the only genus in the family Moringaceae, is an exceptionally nutritious vegetable tree with a variety of potential uses. Every part of Moringa oleifera such as the seed, root and stem are useful. For instance, Moringa oleifera seeds contain flocculants which have tendency to improve water quality. It contains antimicrobial substance and edible oils. The seeds are used to remove lead, iron and cadmium ions from contaminated water [3] [4] [5] [6]. Arthritis, rheumatism, sexually transmitted diseases, hypertension and so on; can be treated using the seed and its oil [7]. The tree itself is rather slender, with drooping branches that grow to approximately 10 metres in height [8]. Moringa is grown in the tropical regions in which Nigeria is part of them. It grows to a height of 5-12 metres with an open umbrella shaped crown, straight trunk and corky, whitish bark, the tree produces a tuberous tap root. The foliage (depending on climate) has leaflets 1 to 2 cm in diameter; the flowers are white or cream coloured. The fruits (pods) are initially light green, slim and tender, eventually becoming dark green, firm and up to 120 cm long, depending on the variety. Fully mature, dried seeds are round or triangular, the kernel being surrounded by a lightly wooded shell with three papery wings [9]. The leaves and seeds of Moringa oleifera are good source of protein, vitamins A, B, C and minerals such as calcium and iron [10]. The root, stem and bark can be used to make medicines, perfumes natural pesticides, fertilizers, cleaning agents etc. The oil extracted from the seed can be used for cosmetics, cooking, soap making and the quality of the oil extracted is as good as that of olive oil. Moringa oleifera, kernels also contains a significant amount of oil which is commonly known as Ben oil or Behen oil due to the high concentration of behenic acid contained in the oil. This was erroneously reported to be resistant to rancidity [11]. Moringa seeds are made up of 40% oil by weight. The cake gotten after the oil has been extracted from the seed can be used as conditioner for the soil or fed to cows to improve their milk production [12].

A lot has been done on the removal of shell for different useful crops such as rubber seed [13], breadfruit seed [14] [15], fluted pumpkin seed [16], melon [17] and so on. However, little design concept has been done on Moringa oleifera seed dehulling as showcased by [2]. Many more design concepts are on-going for high performance of the Moringa oleifera processing machines so as to enhance the industrial revolution of Moringa oleifera seeds.

In order to extract oil from the seed by an oil extractor, partial dehulling of the shell is important and must be

done so as to obtain better and higher quality products. When shells are not removed, there is rapid wear and tear on the oil extractor thus its removal reduces damages to oil extractor presses [2].
Therefore, this work is poised to introduce a new concept in the design and fabrication of Moringa oleifera seed dehuller. This machine will save time and energy. It is designed to be operated by any user.

2. MATERIALS AND METHODS

2.1 Machine Conception

The machine is designed to remove the shell of the Moringa seed. The machine components and system mechanism consist of the following:

1. Hopper: This is the entering point for the seed. It accommodates the seed before moving to the dehulling chamber. The volume of the hopper determines the volume of feed, it can accommodate at once. The hopper is in the shape of frustum of a pyramid.
2. Shaft: This is one of the main components of the machine and is acted upon by weights of material being processed, pulley, impeller blades and the nuts. In operation, the shaft transmits the power being generated by the electric motor through the transmission belt to the dehulling drum which turns the spikes.
3. Main Frame: This is the main body of the machine on which the other members are mounted.
4. Pulley and Transmission Belt: The pulley and belt are transmission system. The belt connects two pulleys. It connects the diving pulley (Electric motor's pulley) to the driven pulley (Shaft's pulley).
5. Dehulling Chamber: This is the place where the dehulling operation occurs. It contains cylindrical drum with spikes attached to it and below it is a screen that lets the seed out.
6. Tray: This is directly below the dehulling chamber and receives the seed after it has been dehulled. The tray is inclined so that the seed roll down under the action of gravity.

2.2 Operation Mode of the Machine

The dehulling cylinder with the attached spikes is rotated by the motion provided by the electric motor. The Moringa seeds are introduced through the hopper. The hopper is pyramidal in shape and it is connected to the dehulling chamber of the seed into the rotating dehulling drum. The dehulling chamber is the unit where the pod of the seed is being removed. It consists of a rotating drum with finger-like spikes, the seeds are dehulled using impact force. Inside the dehulling, there is a screen which allows the seed to go through and prevents the pods from passing through. The pods come out through an outlet created in the dehulling chamber while the seeds leave the screen and land on the tray and roll under the action of gravity. The performance of the machine is dependent on the physical properties of the Moringa seed such as the shape, size, moisture content, speed of the machine, effectiveness of the dehulling surface in the dehulling chamber.

2.3 Material Selection

Locally available materials were used for the construction of the machine while the strength and quality were not compromised. Mild carbon steel plate and angle bar were used for the construction of the machine. The machine was constructed in such a way that it can be easily assembled and disassembled hence making its maintenance easy. A type A, V-belt was selected due to having long and free life; and used in the transmission of power and torque from its prime mover. The belt is connected to the prime mover which drives the shelling drum with spike shaft.

2.4 Design Analysis of the Machine Components

The major design analysis was done on the hopper, shaft, belt drive and power required. The design of the parts of the machine was based on the mechanical and physical properties of the pod.

2.4.1 Hopper Design

It is assumed that the hopper is in the shape of frustum of a pyramid and the formula is given as follows:

$$V = \left(\frac{h}{3}\right)\left(A_1 + A_2 + \sqrt{\left(A_1 + A_2\right)}\right) \qquad (1)$$

Where V is the volume of frustum ($V_{frustum)}$, h is the height of frustum, A_1 is the area of upper base and A_2 is the area of lower base

Trapezium formula was used to find the areas since both the upper and lower base are trapeziums.

$$A = \frac{\left(a+b\right)\times h}{2} \qquad (2)$$

Recall:
Volume of the hopper = Mass of feed that the hopper can accommodate
Mass of feed = Density x Volume of the hopper

$$M = \rho \times V \qquad (3)$$

2.4.2 Belt Drive Calculations

Belts are major type of flexible power transmission equipment. It requires relatively close spacing and precise centre distance. It transmits power from motor to shaft, (and the centre distance between motor and shaft is adjustable).
According to Gupta (2006)

$$\frac{N_1}{N_2} = \frac{D_1}{D_2} \qquad (4)$$

Where N_1 is speed in revolution per minute of motor, N_2 is speed of the shaft in revolution per minute, D_1 is diameter of the motor pulley and D_2 is diameter of the shaft pulley.
Various types of belts exist, however; type A V-belt was chosen.
Therefore, the speed of the driven pulley is calculated using the parameters given in the Table 1.

S/N	Parameters	Value
1	Electric motor speed	1400 rpm
2	Center to center distance	64 cm
3	Coefficient of friction	0.11
4	Angle of Groove	45^0
5	Diameter of driver pulley	70 mm
6	Diameter of driven pulley	205 mm

Table 1. Parameters needed to calculate speed of the driven pulley

According to [18], the following models were used
Velocity of belt

$$V_b = \frac{\pi N_1 D_1}{60} = \frac{\pi N_2 D_2}{60} \quad (5)$$

2.4.3 Belt Length

The length of the belt will be determined using the equation below:

$$L = 2C + \frac{\pi}{2}(D_1 + D_2) - \frac{(D_2 - D_1)^2}{4C} \quad (6)$$

Where L is total length of the belt (mm), D_1 and D_2 are the diameters of the driven and driving pulleys (mm) and C is the distance between the centres of the two pulleys (mm).

2.4.4 Angle of Wrap

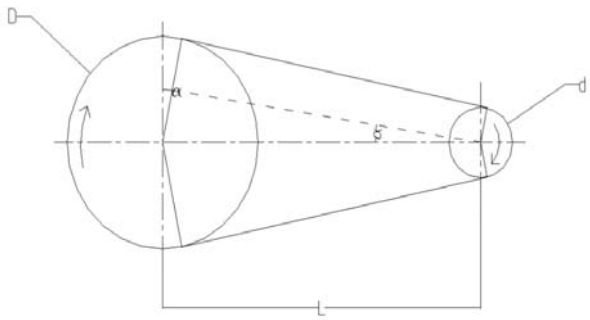

Fig. 1. Open belt drive

A standard belt A type single grooving is selected, whereas the motor can be adjusted horizontally on it supporting slot in other to tension the belt.
For the open belt

$$\sin\infty = \frac{D + d}{2x} \quad (7)$$

$$\text{Where } \theta = (180^\circ - 2\infty)\frac{\pi}{180} rad \quad (8)$$

Where θ= angle of wrap of an open belt, ∞=angle contanct, μ= coefficient of friction, T_1 = Tension in the tight side of the belt, T_2 = Tension in the slack side of the belt, P= Power, and v = velocity

$$P = (T_1 - T_2)v \quad (9)$$

Tension ratio for an open belt:

$$2.3\log\frac{T_1}{T_2} = \mu\theta \quad (10)$$

Where, μ = coefficient of friction between belt and pulley. Coefficient of friction for mild steel pulley and rubber belt, μ= 0.30 [18].

2.4.5 Shaft Design

The shaft is one of the main components of the machine and is acted upon by weights of material being processed, pulley, impeller blades and the nuts. A mild steel rod of diameter 30 mm and length 450 mm was used for the shaft.
The weight of shaft will have effect on the critical speed of the critical shaft.

$$\text{Critical Speed of Shaft } (\omega_s) = \sqrt{\frac{48EI}{ML^2}} \quad (11) \text{ [18]}$$

Where E is Modulus of elasticity of steel, I is Moment of initial ($\frac{\pi d^4}{64}$) and L is the Shaft length.

Calculating the overall critical speed
From Dunkley's formula [19]

$$\frac{1}{\omega^2} = \frac{1}{\omega_1^{\,2}} + \frac{1}{\omega_2^{\,2}} \quad (12)$$

2.4.6 Power Requirement

Power requirement for dehulling drum shaft can be calculated thus;

P = Torque × Angular velocity (13)

Torque = Total weight × radius (14)

2.4.7 Test Procedure

The samples of the Moringa seed pods were collected from the University farm. The samples were divided into two. One part was sun dried for about seven days so as to reduce the moisture content of the pods (dry basis) while the other part was not sun dried but stored in polythene bags to maintain their moisture content before the dehulling process (wet basis). Five runs of experiment was carried out on both the dry basis and wet basis. The Moringa pods were fed into the hopper on a continuous approach because the hopper cannot hold all the required quantity for the period of time of the experiment.

3. RESULTS

The machine has been designed and the materials for its production have also been stated. The engineering drawings required for the production of the machine has been made available based on the design values obtained. The expected machine operation principle has been highlighted. The efficiency of the machine after the fabrication was determined using the moisture content of the Moringa pods.
Testing the hypothesis that the dehulling efficiency for Moringa seeds with high moisture content reduces the efficiency of the machine and with the lower the moisture content in the pod, the higher the dehulling

efficiency i.e. increase in moisture content will reduce dehulling efficiency while reduced moisture content will increase dehulling efficiency. This was confirmed as shown in Tables 2 and 3 in which the higher the moisture content in the Moringa pods, the lower the efficiency of the machine and the lower the moisture content in the Moringa pods, the higher the efficiency of the machine.

Thus, dehulling efficiency could be said to be inversely proportional to the moisture content inside the Moringa pods. i.e. dehulling efficiency $\propto \frac{1}{moisture\ content}$.

In determining the dehulling efficiency, the equation (15) given by [20] can be utilised. This is given as:

$$Dehulling\ Ef\ ficiency = \frac{mass\ of\ the\ dehulled\ beans}{total\ mass\ of\ boiled\ beans} \times 100\% \quad (15)$$

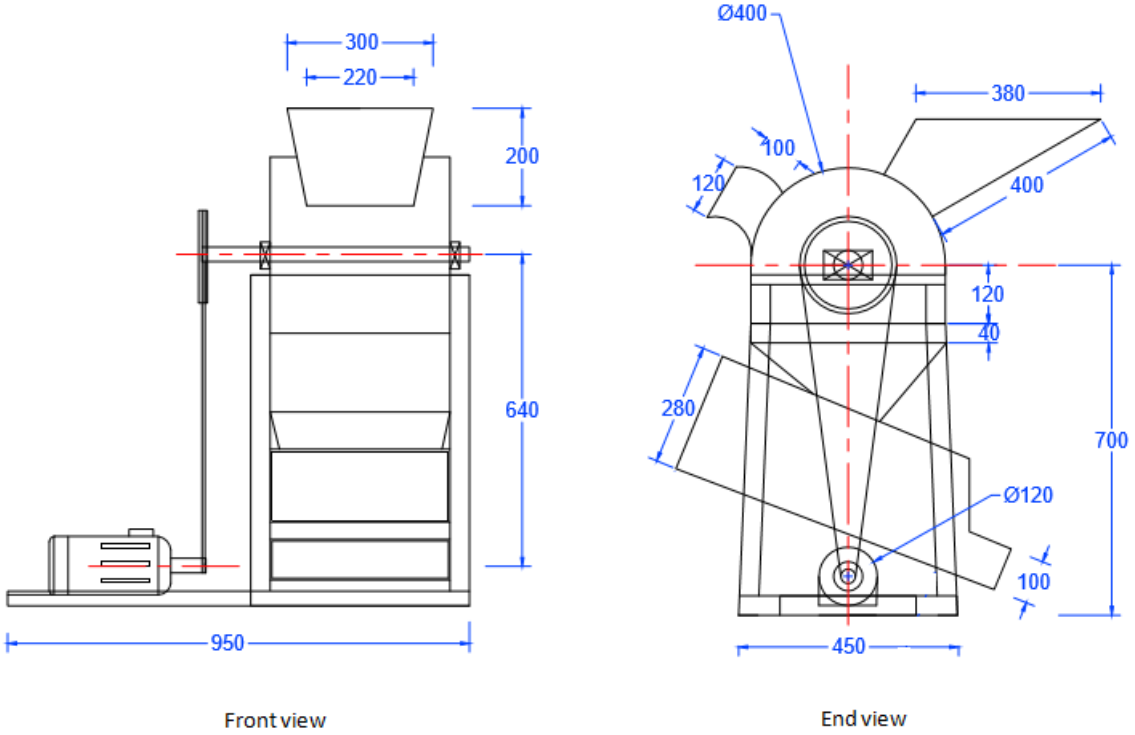

Fig. 2. Orthographic drawing showing the front and end views of the machine

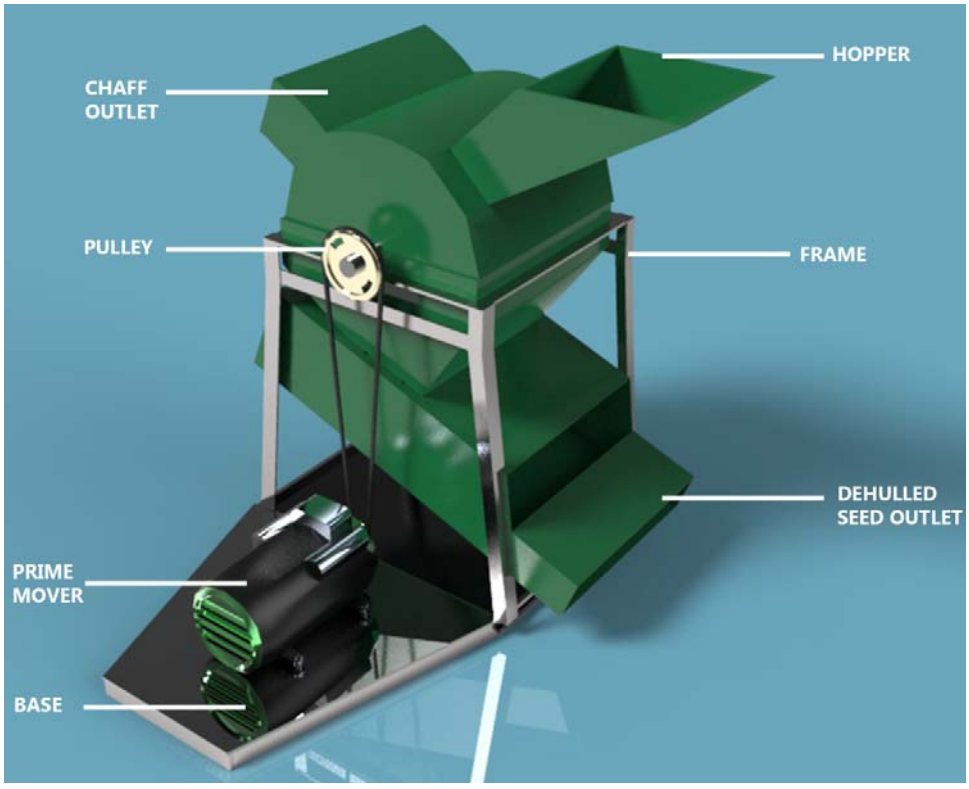

Fig. 3. Isometric drawing of the machine

Adopting [20] equation for efficiency, the dehulling efficiency for the Moringa dehulling machine was derived using equation (16).

$$Dehulling\ Ef\ ficiency = \frac{mass\ of\ dehulled\ seeds}{mass\ of\ pods\ befor\ dehulling} \times 100\% \quad (16)$$

To calculate loss, equation (17) was used.

Loss (kg) = Mass of whole pod -
- [Mass dehulled + Mass of chaff] (17)

4. DISCUSSION

The preliminary testing of the designed and fabricated machine are as shown in Tables 2 and 3. From Table 2, the total mass of the pod used for the experiment was 12.3 kg and the total mass of the dehulled seed was 8.1 kg. Using equation 16, the average efficiency of the machine was derived to be 65.9 % which gave the same value as finding the average value of the efficiency of each run of the performance evaluation.

From Table 3, the total mass of the pod used for the experiment was 12 kg and the total mass of the dehulled seed was 6.3 kg. Using equation 16, the average efficiency of the machine was derived to be 52.5 % which gave the same value as close as finding the average value of the efficiency of each run of the performance evaluation, which was 52.78 %.

The moisture content effect on the dehulling efficiency of the machine was determined. Based on the efficiency calculated, the maximum value of the efficiency at between 9 and 11 % moisture content was 65.9 % while the minimum value at between 12 and 15 % moisture content is 52.78 %. The moisture content effect trend on the dehulling efficiency was not determined as performed by [17] and [2]. However, the efficiency of the machine for both the dry and wet are reasonably high. This may be due to the nature of the shell which is soft when moist and brittle when dry [2].

Test	Mass of whole pod (kg)	Mass of dehulled seed (kg)	Mass of chaff (kg)	loss (kg)	% efficiency
1	2.5	1.2	1.1	0.2	48
2	2.4	1.3	0.6	0.5	54.2
3	2.1	1.2	0.8	0.1	57.1
4	2.3	1.3	0.5	0.5	56.5
5	2.7	1.3	0.6	0.8	48.1
Total	12	6.3	3.6	2.1	263.9
Average					**52.78**

Table 2: Performance evaluation of the machine based on dry basis (% moisture content between 9% and 11%)

Test	Mass of whole pod (kg)	Mass of dehulled seed (kg)	Mass of chaff (kg)	loss (kg)	% efficiency
1	2.5	1.5	0.1	0.9	60
2	2.5	1.6	0.5	0.4	64
3	2.2	1.6	0.28	0.32	72.7
4	2.4	1.5	0.2	0.7	62.5
5	2.7	1.9	0.4	0.4	70.4
Total	12.3	8.1	1.48	2.72	329.6
Average					**65.92**

Table 3. Performance evaluation of the machine based on wet basis (% moisture content between 12% and 15%)

5. CONCLUSION

Based on the design outcome, the Moringa seed dehuller can be used to remove seeds from the Moringa pods and as well separates chaffs/pods from the seeds. In order to maintain simplicity of operation and easy fabrication, the machine is so designed. Due to the simplicity of the machine, it can be conveniently used by Moringa farmers to enable quick and adequate processing of Moringa oleifera seeds. Prior, the Moringa seeds are removed manually which is a serious and laborious task however, by the introduction of this dehulling machine, time energy and cost of production will be saved. Moreover, the components used are strong; the materials are readily available and well selected. The overall efficiency of this machine on dry basis was 65.9 % and on wet basis was 52.5 %. The machine can be improved upon so as to aid its efficiency. Also the usage of Moringa pods with lower moisture contents will also improve the efficiency of the machine.

6. REFERENCE

[1] Kessler, M.: *The Health Benefits of Moringa Seeds.* www.doctorshealthpress.com/general-health-articles/moringa-seeds-benefits/2016 retrieved February 15, 2017.

[2] Fadele, O.K., Aremu, A.K.. *Design, Construction and Performance Evaluation of Moringa Oleifera Seed Shelling Machine*. Engineering in Agriculture, Environment and Food (In press), pp. 1-7, 2016.
[3] Folkard, G., Sutherland, J., Shaw, R.: *Moringa oleifera*. Water and Environment Health at London and Lough Borough, pp. 109-112, 2004.
[4] Rashid, U., Anwar, F., Ashraf, M., Saleem, M., Yusup, S.: *Application of Response Surface Methodology for Optimizing Trans-esterification of Oil: Biodiesel Production.* Energy Conversion Management, Vol. 52, pp. 3034-3042, 2011.
[5] Gupta, R.K., Arora, G., Sharma, R.: *Aerodynamic properties of Sunflower seed (Helianthus annuus L.),* Journal of Food Engineering. Vol. 79, pp.899-904, 2007.
[6] Tende, J.A., Ezekiel, I., Dikko, A.A.U, Goji, A.D.T.: *Effect of ethanolic leaves extract of Moringa oleifera on Blood Glucose Level of Streptozocin-induced Diabetics and Normoglycemic wistar rats.* Br. J. Pharmacol. Toxicol., Vol. 2(1), pp. 1-4, 2011.
[7] Eilert, U., Wolters, B., Nahrstedt, A.: *The Antibiotic Principle of Seeds of Moringa oleifera and Moringa stenopetala tala.,* J. Med. Plants. Vol. 42, pp. 55-61, 1981.
[8] Leone, A., Spada, A., Battezzati, A., Schiraldi, A., Aristil, J., Bertoli, S.: *Moringa oleifera Seeds and Oil: Characteristics and Uses for Human Health*, Int. J. of Mol. Sci., Vol. 17(12), pp. 1-14, 2016.
[9] Orhevba, B.A., Sunmonu, M.O., Iwunze, H.I.: *Extraction and Characterization of Moringa oleifera Seed Oil*, Research and Review J. of Food and Diary Technology, Vol. 1, pp. 22-27, 2013.
[10] Dahot, M.U.: *Vitamins Contents of Flowers and Seeds of Moringa oleifera,* Biochemistry, pp. 2122-2124, 1988.
[11] Nolabigengeser, A., Narasaih, K.S.: *Use of Moringa Seeds as Primary Coagulant in Waste Water Treatment,* Environmental Technology, Vol. 19, pp. 789-800, 1998.
[12] Irénée, M. B.: *Production and Processing of Moringa,* Published by "The Technical Centre for Agricultural and Rural Cooperation and Engineers without Borders", 2016.
[13] Fagbemi, E., Ayeke, P., Chimekwene, P., Akpaka, P., Omonigho, B.: *Design of Dehulling Machine and Rubber Seed Processing*, American Journal of Science and Technology, Vol. 1(4), pp. 206-212, 2014.
[14] Anosike, N., Brown, E., Maduka, C.: *Performance evaluation of a prototyped breadfruit seed dehulling machine*, Machines, Vol. 4(11), pp. 1-6, 2016.
[15] Omobuwajo, T.O., Ikegwuoha, H.C., Koya, O.A., Ige, M.T.: *Design, Construction and Testing of a Dehuller for African Breadfruit (Treculia Africana) Seeds,* Journal of Food Engineering, Vol. 42, pp. 173-176, 1999.
[16] Odewole, M.M., Adesoye, O.A., Oyeniyi, S.K., Isiaka, A.O.: *Development and Performance Evaluation of Fluted Seed Dehulling Machines, Arid Zone Journal of engineering, Technology and Environment*, Vol. 11, pp. 120-130, 2015.
[17] Shittu, S.K., Ndrika, V.I.O.: *Development and Performance Test of a Melon (Egusi) Seed Shelling Machine,* Agric. Eng. Int. CIGR J., Vol. 14(1), pp. 157-164, 2012.
[18] Khurmi, R.S., Gupta, J.K.: *A Textbook of Machine Design*, Eurasia Publishing House Ltd., 7361, Ram Napar, New Delhi, 2006.
[19] Shigley, J.E., Mitchell L.O.: *Mechanical Engineering Design (Ed.)*. McGraw-Hill Book Company, Tokyo, 1983.
[20] Gbabo A., Liberty, J.T., Fadele, O.S.: *Design, Construction and Assessment of African Locust Bean (Parkia biglobosa) Dehuller and Separator*, International Journal of Engineering and Innovative Technology, Vol. 3(5), pp. 438-444, 2013.

Authors: **Engr. Ikubanni Peter Pelumi, Engr. Komolafe Clement Adekunle, Engr. Agboola Olayinka Oluwole, Professor Osueke Christian O.**
Landmark University, College of Science and Engineering, Department of Mechanical Engineering, Omu-Aran, Nigeria.
E-mail: ikubanni.peter@lmu.edu.ng
komolafe.adekunle@lmu.edu.ng
agboola.olayinka@lmu.edu.ng
osueke.christian@lmu.edu.ng

http://doi.org/10.24867/JPE-2017-02-079

Journal of Production Engineering

Vol.20 No.2

JPE (2017) Vol.20 (2) Preliminary Note

Narang, D., Raj, A., Khanna, P.

MATHEMATICAL MODELLING OF A VIBRATORY BOWL FEEDER FOR SPHERICAL WASHER

Received: 09 October 2017 / Accepted: 27 November 2017

Abstract: *Mass production has eliminated the craftwork from a majority of industries and brought about a revolutionary change. Automation has evolved along the past years and has become much more sophisticated due to continual starvation for quality. Feeders play a paramount role on the production line. The present study employs a full factorial design technique to analyse the effect of various parameters and interactions between them on output feed rate in a vibratory bowl feeder using spherical washer. An empirical relation followed the analysis of the model. Finally the validation of the model reflected the correctness of the experimental results.*

Keyword: *Mass Production, Automation, Feeders, Full Factorial design*

Matematičko modeliranje vibraciono kuglične hranilace za sferični perač. *Masovna proizvodnja eliminisala je zanatsku rad iz većine industrija i dovela do revolucionarne promene. Automatizacija je evoluirala poslednjih godina i postala je mnogo sofisticirana zbog kontinuirane potrašnje za kvalitetom. Hranioci igraju najveću ulogu na proizvodnoj liniji. Ova studija koristi pun faktorni dizajn za analizu uticaja različitih parametara i interakcija između njih na izlaznu brzinu prenosa u vibracionom držaču posuda pomoću sferičnog perača. Empirijska relacija je sledio analizu modela. Konačno, validacija modela odražava ispravnost rezultata eksperimenta.*

Ključne reči: *Masovna proizvodnja, automatizacija, hranilice, pun faktorni plan*

1. INTRODUCTION

With the increased demand as well our insatiable thirst for quality has led to the evolution of mass production. Automation is the key ingredient to the success of mass production. On the production line we have different stations, each station responsible for mounting a component on the assembly from the previous station. The parts are to be fed one at a time and it is required to orient them in a particular fashion before mounting onto the assembly. These purposes are quite easily satisfied by feeders. Feeders benefit by saving cost incurred on manual labour, saves time, gives higher production rate and most importantly consistency in quality. There exists a variety of feeders including belt feeders, rotary feeders (drum, table, etc.), centrifugal feeders, vibratory feeders, apron feeders, etc. In this paper, the part feeder of interest is vibratory bowl feeder. Vibratory bowl feeder was patented by Yoshiyuki Hirose [1]. It is the most versatile, robust, reliable and widely used part feeder in the industry. They are generally used for feeding small parts and aligning them. A vibratory bowl feeder generally consists of a bowl (which carries the track via which the part is fed and oriented) and the base. The bowl is mounted onto the base with help of three or four inclined leaf springs. The leaf springs helps to restrict the vibration in the vertical direction. The vibrations are produced with the help of an electromagnet mounted between the base and the bowl. The parts are randomly oriented inside the bowl initially. As the AC supply is turned on the parts, start climbing and moving along the track. The parts are then oriented accordingly by provision of suitable tooling. Each component of tooling either orients the part or pushes it out of the track and hence the same journey of the part begins unless it comes into desired orientation. The base of feeder is provided with a damping material in order to prevent transmission of vibrations to the surroundings. During each vibration cycle the part moves up the track. This upward (slanting) motion can be understood by analysing the motion of bowl and the component. Maul.et al [2] analysed the motion of bowl and the part separately and proposed a model for the same. Lim.et al [3] gave a motion study of the vibratory feeder using turbo C++ language which can be used to determine the position and velocity of the parts at small tie intervals. Though studying the working principle and dynamics of a vibratory feeder is in itself a very engrossing topic and still titillates the minds of researchers, the present paper will be focussing on evolving a model for analysing and optimizing parameters for a certain part being fed to the vibratory bowl feeder.

2. EXPERIMENTAL SETUP

Primary steps of the experiment include-1) Identification of the part, 2) Setting up the track for orienting and feeding the part, 3) Defining the independent parameters (inputs) and dependent parameter (output). The part chosen was a spherical washer. The tooling and obstructions on the track were designed according to the orientation of the part required at the end. The tooling in the track and component can be shown as in fig. 1(a) and (b). The orientation was decided by dropping numerous units of washer on a surface and identifying the orientation that

maximum number of parts adopted. Validation of the drop test has been proved by Ngoi.et al [4]. As far as input variables are concerned, the three controllable variables are-

(i) Size of the part
(ii) Part Population- It is defined as total number of parts present in the bowl at any time.
(iii) Frequency of vibration

The above 3 factors play a crucial role in development of the statistical model using 2^k full factorial design. The range for the parameters was to be decided in order to ensure the working of apparatus within controllable limits and hence were finally drawn out after carrying out many pilot runs. The upper and lower limit of each parameter are depicted in Table 1. Factors like inclination of the spring, coefficient of friction, etc. could not be varied due to mechanical constraints and hence were kept constant for the present experimentation [5].

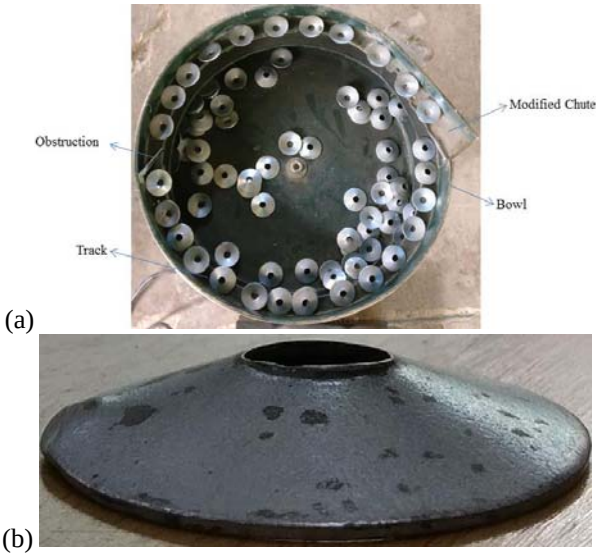

Fig. 1. Track and Component

Factors	Lower Limit	Upper Limit
Diameter of the part(in mm)	15	25
Part population	50	200
Frequency of vibrations(in Hz)	35	50

Table 1. Range of parameters

Run No.	A: Diameter of the part	B: Part Population (PP)	C: Frequency	D: Response
1	-1	1	1	99
2	-1	1	-1	52
3	1	-1	-1	5
4	1	1	1	22
5	1	1	-1	15
6	-1	-1	-1	14
7	-1	-1	1	58
8	1	-1	1	15

Table 2. Response of the run

Since we have 3 parameters which are to be varied, hence the applicable model is 2^3 factorial design. Thus the model requires 8 runs, each run with a particular combination of the parameters at there extreme values i.e. each factor takes either upper or lower limit. The response for the 8 runs are shown in Table 2 with upper and lower limits coded as (+1) and (-1) respectively.

3. RESULT AND ANALYSIS OF THE MODEL

Examination of effect of each factor on the output can easily be understood by obtaining the Cube plot, One Factor plot and Interaction plot. Significance of each factor can be analysed by obtaining the Half-Normal, Normal and Pareto plots. Analysis of Variance (ANOVA) table is obtained which clearly indicates significant factors affecting the feed rate (response).

3.1 Effect of factors on feed rate

The Cube plot (in fig. 2) depicts the average feed rate (in units/mm) at the extremities of the input variables. In coded form, it can be further be explained as a plot indicating feed rates when each variable is either at +1(high) or -1(low) level, or simply it can be stated that cubic plot represents the average feed rate at the critical points. It can be inferred from the plot that a minimum feed rate of 5.8 (approx. 6) parts per minute can be obtained with maximum part size (25mm) coupled with minimum frequency (35Hz) and minimum part population (PP) (50). Similarly maximum feed rate of 98.3 (approx. 99) parts per minute is observed with minimum size (15mm), maximum frequency (50Hz) and maximum PP (200).

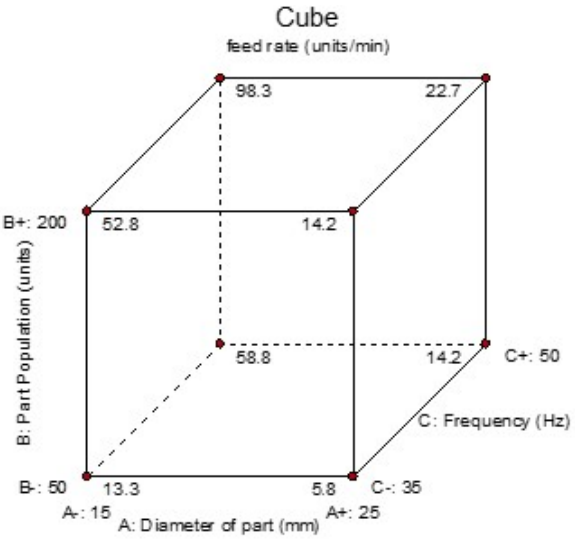

Fig. 2. Cube plot

Fig. 3 shows the feed rate plotted against individual parameters i.e. they give an intimation of how the response would change if only one parameter is varied while the other two are kept constant. These plots are known as one factor plots. The previous study done by authors dealt with graphical analysis based on one factor at a time technique [6]. It can be observed that there exists an inverse relationship between feed

rate and the part size. This behaviour can be attributed to the fact that with increase in part size the number of parts present on any particular length of the track decreases hence causing a fall in the feed rate. Also feed rate is directly proportional to the part population and the frequency. The increase in PP leads to increase in the no. of parts at any time in the bowl hence increasing the feed rate.

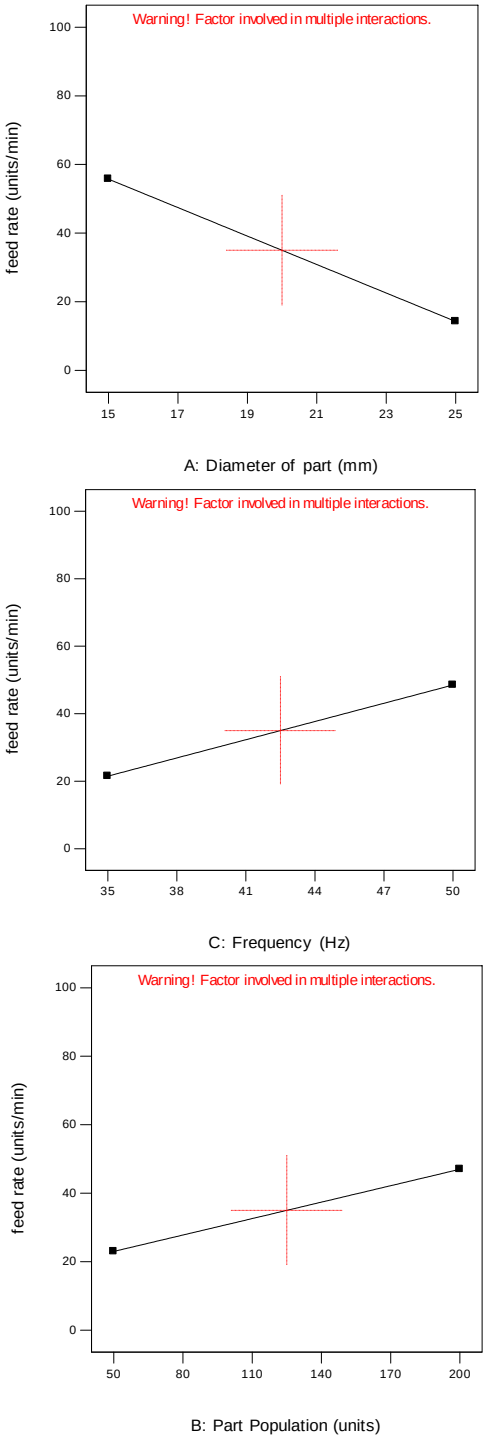

Fig. 3. One Factor plot

Also the increase in frequency gives a greater push or assists in hopping the part to a greater distance. But increase in frequency beyond a limit causes the feed rate to decrease because of collision of parts among themselves. From the slope of the plots, it can firmly be stated that diameter/ size of the part plays a much significant role than the other two. Another type of plot as depicted in fig. 4, 5 and 6 is called the interaction plot. Fig 4, 5 and 6 show the interaction between parameters AB, AC and BC respectively. These plots assist in investigating the effect on feed rate due to change in a particular input factor when that input factor itself is dependent on other inputs. Understanding of a simple statement can fetch us great information about the interaction plots. It can be stated as "greater the deviation of the set of lines from parallelism, more significant will be the interaction between them". At a constant frequency (C) (fig.4) we have feed rate varying with the diameter of the part (A) for the 2 levels of part population (B). The black line indicates feed rate vs diameter when PP=50, while the red line indicates the same relation when PP=200. Similar observation is made in fig. 5 with the interaction shown between diameter and frequency. In both the figs. 4 and 5 we see that lines are non- parallel and tend towards each other thus showing quite significant interactions. On the other hand, fig. 6 shows interaction between PP and frequency is parallel and hence is of negligible significance.

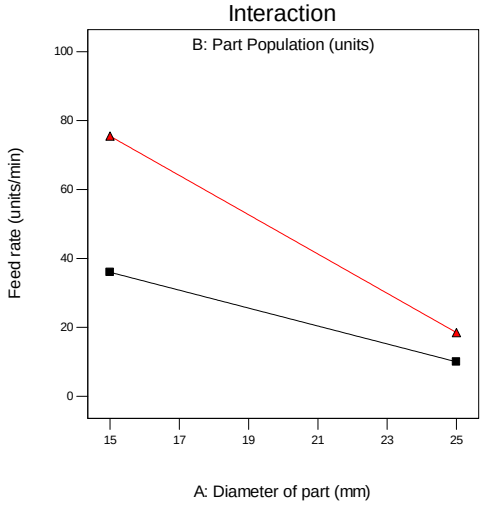

Fig. 4. Interaction plot between diameter (A) and part Population (B)

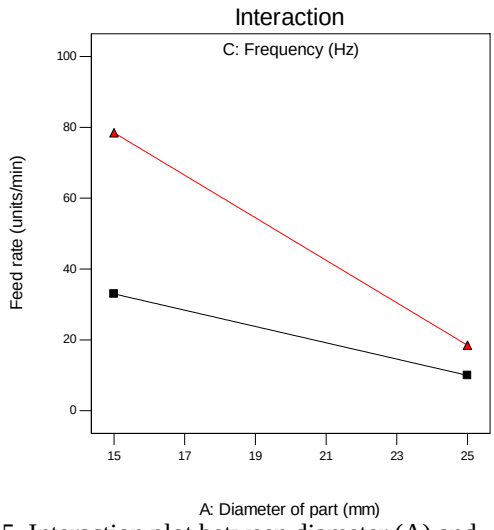

Fig. 5. Interaction plot between diameter (A) and frequency (C)

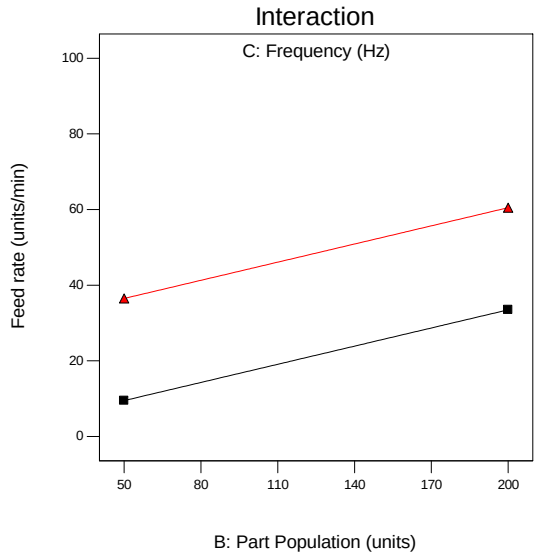

Fig. 6. Interaction plot between part population (B) and frequency (C)

3.2 Significance of various factors

The Half-Normal and Pareto plot also indicate the relative significance of each factor or a group of factors. From Half-Normal (fig. 7) plot we infer that farther the point from the line, more is its significance.

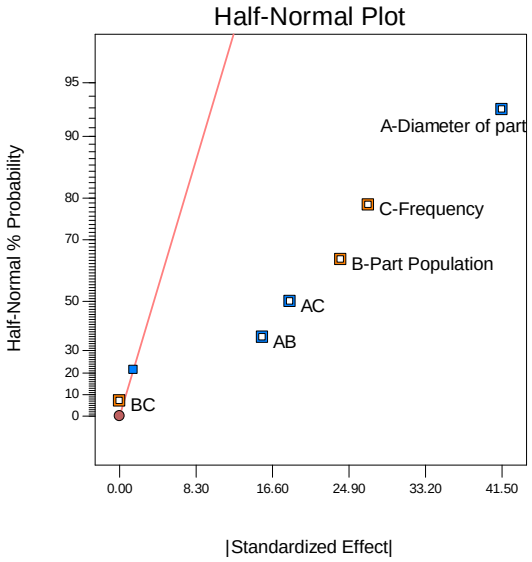

Fig. 7. Half-Normal plot

Thus diagnosis of the two plots gives the sequence of importance of factors as- A, C, B, AC, AB, BC. However we can assume that AC, AB and BC have relatively little importance when compared to A, C and B. Pareto chart (as shown in fig. 8) provides us with the absolute effect values. It draws a reference line at t-value limit. Analysing the chart we draw the same conclusion as from Half-Normal and Normal plots.

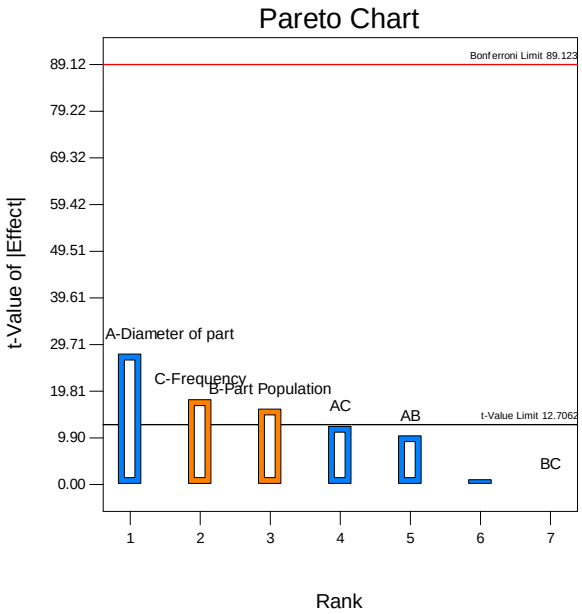

Fig. 8. Pareto chart

As seen from the results in table 3, the terms in the last column (i.e.'Prob>F') having value less than 0.0500 are the significant terms. Hence we get the order of significance as- A, C, B, AC, AB, BC which is same as discussed earlier. The 'F-value' compares the variance of each term with the residual variance. Mean square of a particular term divided by mean square of residual P equals the 'F-value'. P is the probability of 'F- value of the term' [7]. A 3D plot as shown in fig. 9 also gives the epitome of the effect of multiple factors on the response by plotting feed rate against multiple parameters, thus generating a coloured and shaped contour. The colour at various points in space give the magnitude of feed rate.

Source	Sum of Squares	Df	Mean Square	F Value	p-value Prob > F
Model	7219.50	6	1203.25	267.39	0.0468
A-Diameter of part	3444.50	1	3444.50	765.44	0.0230
B-Part Population	1152.00	1	1152.00	256.00	0.0397
C-Frequency	1458.00	1	1458.00	324.00	0.0353
AB	480.50	1	480.50	106.78	0.0614
AC	684.50	1	684.50	152.11	0.0515
BC	0.000	1	0.000	0.000	1.0000
Residual	4.50	1	4.50		
Cor Total	7224.00	7			

Table 3. ANOVA

3.3 Significance of the model

From the model, we obtained 2 empirical relations. However the term ABC, signifying interaction of all 3 factors is ignored to maintain the hierarchical nature of the model. The 2 formulae obtained are as follows-

(i) In terms of coded factors: It contains the coded value of factors ranging from -1 to +1 and thereafter can be used to determine the feed rate for given level of factors. Relative impact of each factor can be determined by the coefficients of the factors.

$$\begin{aligned} Feed\ Rate &= 35.00 - 20.75 \times A + 12.00 \times B \\ &+ 13.50 \times C - 7.75 \times A \times B - 9.25 \times A \times C \\ &+ 0.000 \times B \times C \end{aligned} \quad (1)$$

(ii) In terms of actual factors: It contains factors with there actual values and hence an unknown variable can be found out by putting the value of other known variables. As compared to the coded model, the actual model is less accurate as the terms are rounded off.

$$\begin{aligned} Feed\ Rate &= -239.83333 + 8.91667 \times A \\ &+ 0.57333 \times B + 6.73333 \times C \\ &- 0.020667 \times A \times B - 0.24667 \times A \times C \\ &- 2.76336 \times 10^{-17} \times B \times C \end{aligned} \quad (2)$$

The information in table 4 is obtained from the test runs. The "Pred R- Squared" of 0.9601 is in agreement with "Adj R-Squared" of 0.9956 since the difference between the two is less than 0.2. "Adeq Precision" is a measure of signal to noise ratio. The "Adeq Precision" of 46.616 signifies an adequate signal. "R-Squared" is a statistic which measures the variability associated with the model. Its value comes out to be 0.9994(99.94%). Problem with "R- Squared" is that its value increases as factors are added to the model even if the terms are insignificant. "PRESS (Prediction Sum of Error Squares)" is 288.00 and is useful in computing the value of "Pred R-Squared". A plot between actual and predicted values of the model depicted in fig. 10.

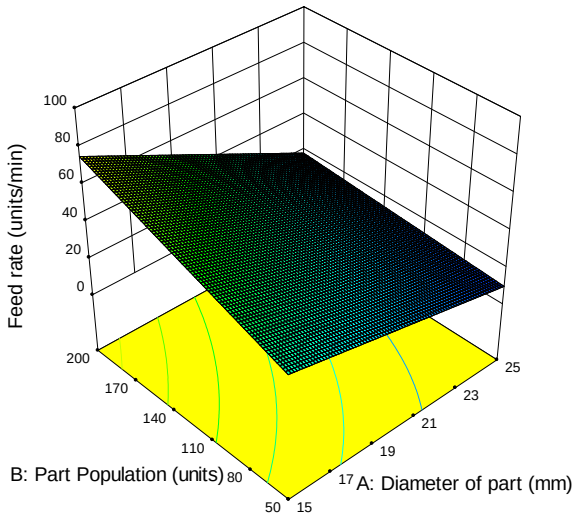

Fig. 10. 3D Surface plot

Std. Dev.	2.12	R-Squared	0.9994
Mean	35.00	Adj R-Squared	0.9956
C.V. %	6.06	Pred R-Squared	0.9601
PRESS	288.00	Adeq Precision	46.616
-2 Log Likelihood	18.10	BIC	32.66

Table 4. Model Results

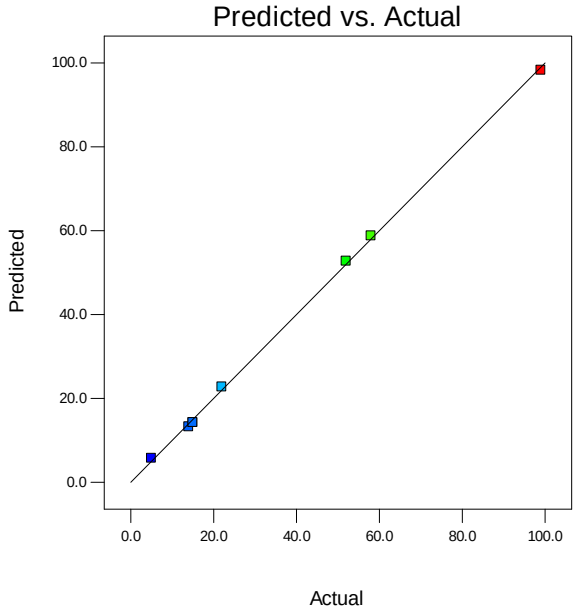

Fig. 11. Predicted vs. Actual plot

4. VALIDATION OF THE MODEL

The correctness of the model can be checked by comparing the experimental value (E.V.) and the theoretical values (T.V.) and thereafter calculating the percentage error. T.V. of the feed rate can be calculated from the equation containing factors with there actual values. Formula for percentage error is given as:

$$Percentage\ Error = \frac{(E.V. - T.V.) \times 100}{T.V.} \quad (3)$$

Table 5 shows the percentage error. By observation of the error values we can state that the values predicted by the model are in accordance with the experimental results.

Average percentage error=5.984%

Accuracy=94.016%

S. No.	Calculated/ Theoretical Value (T.V.)	Experimental Value(E.V.)	Percentage Error
1	86.77	90	3.72
2	73.62	77	4.59
3	44.3	49	10.6
4	29.1	30	3.09
5	87.1	94	7.92

Table 5. Error in the model

5. CONCLUSION

An efficient and reliable model for optimum feed rate was successfully developed using 2^3 factorial design. The "Pred R-Squared" of 0.9601 indicates variability of 96.01% in the new data. The effect of individual parameters on feed rate can be concluded as:

1. The feed rate decreases with increase in size of the part.
2. The feed rate increases with increase in part population.
3. The feed rate increases with increase in frequency up to a particular level.

The model developed not only predicts the effect on output due to individual factors but also due to the interactions between the parameters. Validation of the model indicates an accuracy of 94.016% which signifies that results are in accordance with the model.

6. REFERENCES

[1] Phillips I T S, Costa K D, I R, Chambers T V and Hill R 1994 United States Patent [19]

[2] Maul G P and Brian Thomas M: *A systems model and simulation of the vibratory bowl feeder* J. Manuf. Syst. 16 309–14, 1997

[3] Lim G H: *Vibratory feeder motion study using Turbo C++ language* Adv. Eng. Softw. 18 53–9, 1993

[4] Ngoi B K ., Lim L E . and Ee J T: *Analysis of Natural Resting Aspects of Parts in a Vibratory Bowl Feeder - Validation of "Drop Test"* Int. J. Adv. Manuf. Technol. 300–10, 1997

[5] Kukreja A, Chopra P, Aggarwal A and Khanna P: *Application of Full Factorial Design for Optimization of Feed Rate of Stationary Hook Hopper Int.* J. Model. Optim. 1 205–9, 2011

[6] Raj A, Narang D and Khanna P: *Graphical Analysis of a Vibratory Bowl Feeder for spherical washer* Journal of Material Science and Mechanical Engineering 4 110–3, 2017

[7] Chauhan A: *Mathematical Analysis of U Shaped Components Feeding in a Vibratory Bowl Feeder* International Journal of Electronics, Electrical and Computational System 5 91–9, 2016

Authors: **Research Scholar Daksh Narang, Research Scholar Ayush Raj, Associate Professor Pradeep Khanna**, Division of Manufacturing Processes and Automation Engineering, Netaji Subas Institute of Technology, University of Delhi, New Delhi-110078, India, Phone: +91 9891043115.

E-mail: daksh_narang@yahoo.com
ayushr1995@gmail.com
4.khanna@gmail.com

http://doi.org/10.24867/JPE-2017-02-085

Journal of Production Engineering

Vol.20 No.2

JPE (2017) Vol.20 (2) Preliminary Note

Adekomaya, O., Jamiru, T., Sadiku, R., Huan, Z., Oboirien, B.

EXPLORING THE THERMAL PROPERTIES OF FLY ASHED-BASED GEOPOLYMER MATERIALS FOR COOLING APPLICATION IN BUILDINGS

Received: 11 July 2017 / Accepted: 08 September 2017

Abstract: *Fly ash materials are the by-products of coal combustion process and the volume of this waste alone, accounts for about 80% of the total waste volume from a coal power plant. Part of the reclamation strategy of fly ash material is highly noticeable in the additives for cement production and this approach has recorded significant progress in view of its negative impact on the environment and also the process is generally cleaner due to the significantly low CO_2 emission. In light of the above, a comprehensive and detailed study is therefore needed to explore some of inherent properties of fly ash material for passive cooling in buildings and its adjoining area. Energy consumption in buildings is projected to account for ~50% of world energy demand by 2050 and the underlying point of this research is to x-ray the low thermal conductivity of fly ash geopolymer materials for possible application in passive cooling of buildings and the conclusion drawn from this work may be explored by researchers for further study.*

Key words: *Passive cooling; Building; Fly-ash geopolymer; Phase change materials; environmental waste*

Isključivanje termalnih osobina materijala geopolimera na osnovu letala za hlađenje u zgradi. *Materijali letećeg pepela su nusproizvodi procesa sagorevanja uglja i volumen tog otpada samo, čini oko 80% ukupnog zapreminog otpada iz termoelektrane. Deo strategije reklamiranja materijala za pepeo je vrlo izražen u aditivima za proizvodnju cementa i ovaj pristup je zabeležio značajan napredak s obzirom na negativan uticaj na životnu sredinu, a i proces je generalno čistiji zbog značajno niskih emisija CO_2. U svetlu gore navedenog, stoga je potrebna sveobuhvatna i detaljna studija kako bi se istražile neke od inerentnih svojstava materijala za pepeo koji se pali za pasivno hlađenje u zgradama i njegovoj susednoj oblasti. Projekcija potrošnje energije u zgradama će iznositi ~ 50% svetske potražnje energije do 2050. godine, a osnovna tačka ovog istraživanja je rentgensko ispitivanje niske toplotne provodljivosti geopolimerskih materijala za pepeo za moguću primenu u pasivnom hlađenju zgrada i zaključak iz ovog pregleda rada istraživači mogu koristiti za dalja istraživanja.*

Ključne reči: *Pasivno hlađenje; Building; Geopolimera sa pepelom; Materijali za promenu faze; ekološki otpad*

1. INTRODUCTION AND BACKGROUND STUDY

Coal-fired power plant has remained one of the largest sources of energy worldwide, accounting for about 36% of the world electricity generation and this dominance is likely to remain until the next decade [1]. Many literatures [2, 3] have affirmed that a large volume of fly and bottom ash wastes are generated from coal-fired power plants, in which many these authors described as not environmentally-friendly. Conventionally, these ashes are normally dumped for landfilling or probably used for construction. Recent studies [3, 4] showed that fly ash accounted for between 80-90% of total by-product produced from coal-fired plant, while only between 10-20% volume of bottom ash was generated from the same process. In view of the quantity of fly ash generated, this research study was undertaken in an attempt to further reduce its environmental impact by exploring wider applications of this waste. Figure 1(a) and (b) shows the volume of fly ash waste generated in the USA from 2008 to 2013 and its corresponding area of application. As evidenced in Fig. 1(a), the volume of unutilized fly ash appeared not to have shown considerable decline between 2008 and 2013, while the application of fly ash geopolymer material seems to have gained significant success as additives in Portland cement manufacturing and other materials for construction. Part of the reasons advanced by the construction and building industries are based on the high thermal insulation properties offered by geopolymer materials, which has increased its patronage for construction purposes (Fig.1b). According to Zhang, et al. [5], fly ash geopolymer materials are known for their low thermal conductivities, which may offer good thermal insulation thereby resulting in sustainable binders for most engineering works.

Recent findings in building system, have shown that energy demand in this sector accounts for ~41% of global energy consumption [6] and it is predicted that this demand will rise to ~50% by the year 2050 going by the surge in demands for heating and air conditioning of residential houses, mostly in urban cities. Many authors [7, 8] have reported a lot of progress made in the application of PCM in preserving energy in buildings, but a lot of difficulties have also been attributed to PCMs and most importantly in its practical application. Key of the drawback in the application of PCMs is its high flammability which makes it difficult for them to be exposed to high temperature. This is evident in the numerous papers

(Fig.2) published in recent years as most of the experimental findings in these literatures failed to address this practical application of phase change materials in building. Another disadvantage reported by Konuklu, et al. [9] showed that PCMs sometimes proof difficult to hold in the matrix most especially at liquid state as some PCMs (mostly organic ones) evaporate and sometimes release part of their organic compound. Salt hydrates are typical example in view of their water content. According to Akeiber, et al. [10], PCMs shows some shortcoming that may limit their application in practise. These include high volume variation during transition state and low thermal conductivity which poise a great challenge to be used in passive cooling system.

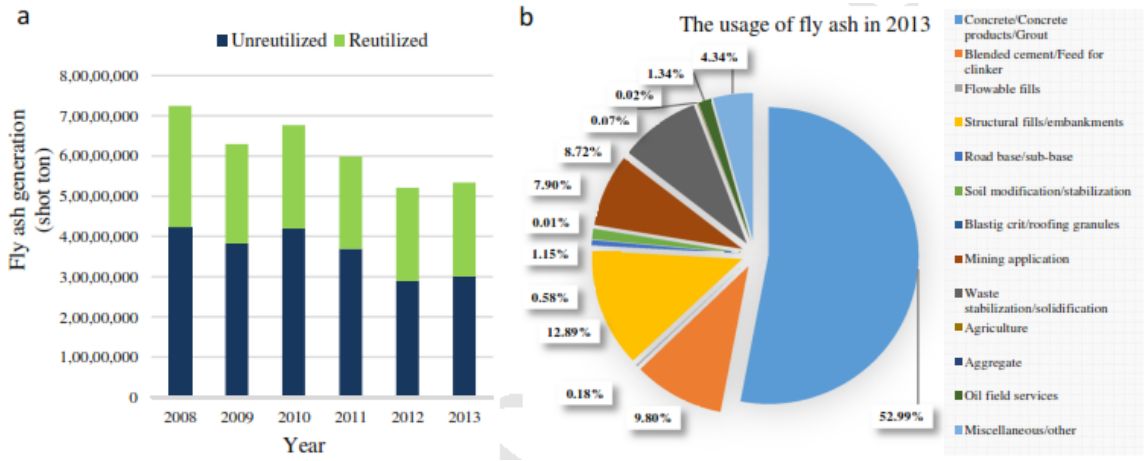

Fig.1. (a) The volume of fly ash generated in the USA between 2008-2013. (b) Applicable area of fly ash geopolymer materials as at 2013. (Adapted from Zhuang et al., 2016)

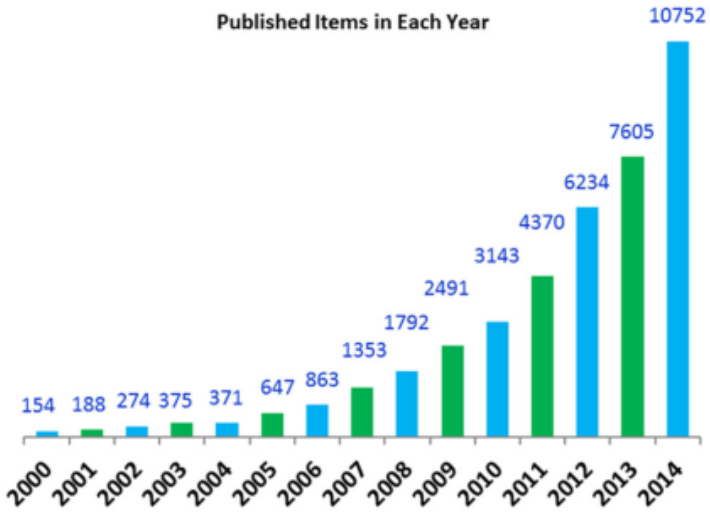

Fig. 2. Available papers published on PCMs from 2000 to 2014. Adapted from Akeiber, et al. [10]

These shortcoming may have informed this study, with the hope of exploring alternative materials with reasonable thermal conductivity for energy conservation in buildings. In order to further justify the relevance of fly-ash geopolymer materials for cooling applications, the research conducted by ul Haq, et al. [11] benchmarked the thermal conductivity values for fly-ash geopolymer materials to be ~0.58 *W/mK* when compared to bottom ash geopolymer, which is ~0.85 *W/mK* . In view of the fact that low thermal conductivity materials are currently being studied for sustainable energy saving [12], this thermal conductivity property of fly-ash geopolymer materials will be explored in this study for possible application in buildings. Although, the density of a typical geopolymer material is considerably high, as reported in past works [13, 14], this physical property may not necessarily be an inhibiting factor, as this strength may be advantageous in reinforcement purposes.

2. SUSTAINABILITY OF PHASE CHANGE MATERIALS (PCMs) IN COOLING APPLICATION

Cooling in building is primarily achieved by using existing pavement improvement either with the introduction of PCMs or novel designs or by introducing new materials to existing pavements [15]. The daily peak of surface temperature of a pavement has been a subject of research in recent times and most of the established conclusion in many literatures

consider this suface temperature as a function of air temperature, solar irradiation and latitude of the building. Correspondingly, the daily peak surface temperature is being minimized by three approaches as shown in table 1 and geopolymer materials could be helpful to reduce the rate of the absorption and also raise the thermal inertia of the building. The prospect of geopolymer materials to enchance the existing cooling methods as predicted in Table 1 is borne out of some of the reported additives geopolymer materials have functioned satisfactorily and one of such application is the binders for concrete production.

Existing cooling method	**Prediction with incorporation of geopolymer materials into the existing cooling mathod**
Absorption	• minimize heat absorptivity by redirecting solar radiation to the sky
Evaporation	• the surface or pavement is reflective at summer and absorptive at low temperature cold weather • Possibility of increase in latent heat
Storage	• Remove heat from the surface and mininize pavement temperature • Reduce pavement or surface temperature by raising conductivity heat

Table 1: Summary of cooling in building and the projection of geopolymer enchancement

Key of the property of phase change materials (PCMs) that have been extensively relied upon in building is their latent heat thermal energy and this property has received a lot of interest in many industries [16]. The concept of energy storage in PCMs is still the most widely used technology, in view of its large energy storage capacity, which presents an isothermal behaviour during the evaporative cooling in building. Although, this approach is seen to have minimized the peak heating and cooling loads with the prospect of keeping the indoor temperature at considerable level, thereby reducing the overall thermal load occasioned by house equipment. The key advantage of PCMs, as reported in literatures, revolves around their storage potential, with reasonable change in the configuration of building designs. Based on the aforementioned conclusion, some researchers [17-19] have expressed divergent views on the sustainability of PCMs in cooling application, as a result of the sudden rise in temperature during summer period, as the temperature rise may hinder complete solidification of PCMs at night, thereby reducing their performance during day. In an extensive literature reviews conducted by Souayfane, et al. [6], these authors affirmed that the astronomical increase in global population coupled with increasing energy demand, may further deepen the deficit in energy demand in the housing sector, thereby worsening global energy shortfall. According to a report released by the International Energy Agency (IEA), the primary energy production has increased from 30% to 49% in the last 20 years, while the CO_2 emissions have equally increased by 43% under the same influence. This may further heighten the cooling demand in locations where urbanization is fast growing, as shown in Fig. 2.

In a similar study developed by IEA in 2010, this agency predicted that the space cooling in buildings in European states alone may reached 220 TWh and it was further reported that an additional increases of about +38% in 2020 and +72% in 2030 are foreseen. In addition, the survey released by European Technology Platform on Renewable Heating and Cooling (RHC) equally collaborated previous report that the cooling demand in the EU and by extension, the world are predicted to rise most importantly in residential sectors, as illustrated in Figure 3.

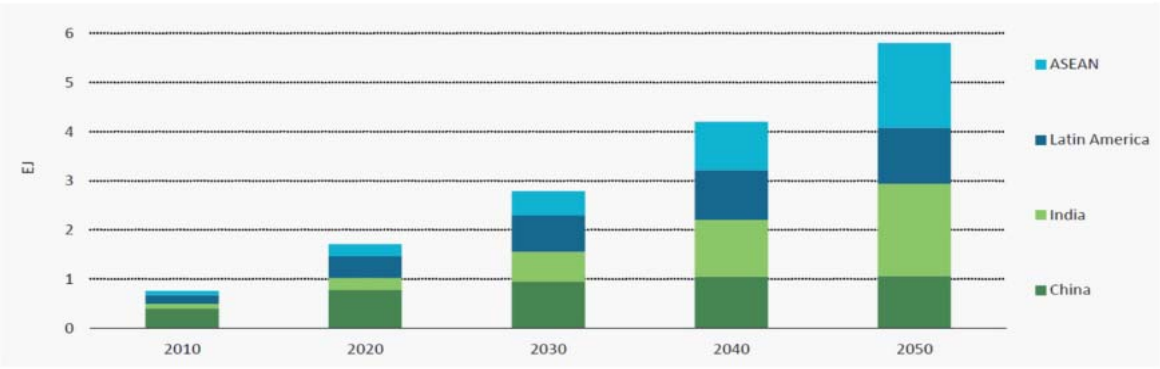

Fig. 3. Prediction of cooling demand in highly populated region of the world. Adapted from Souayfane, et al. [6]

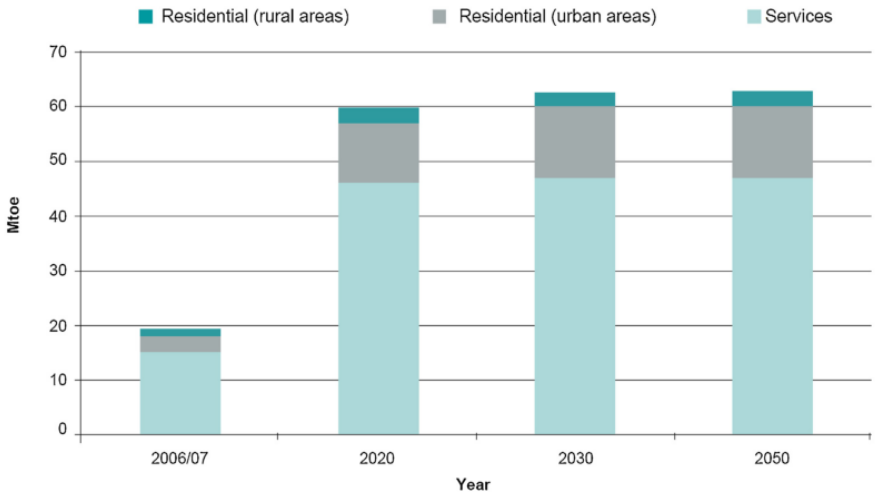

Fig. 4. Illustration of cooling demand and projection in EU for residential and service delivery sectors. Adapted from Souayfane, et al. [6]

In light of the above, the sustainability of PCMs in building may be under serious test in view of increasing world population and emerging housing explosion. Since the thermal load in building is predicted to rise as a result of activities like heating and air conditioning, it may be of interest to study materials of comparable low thermal conductivity like fly-ash geopolymer materials as compliment for passive cooling in building for sustainable comfort.

3. PROSPECT OF FLY-ASH GEOPOLYMER MATERIALS AS PASSIVE COOLING MATERIALS

The possibilities of adopting fly-ash geoplymer materials for passive cooling in buildings with the incorporation of PCMs has received significant attention in some literatures but a lot of gap still exist on the concept of evaporative cooling and absorption using geopolymer materials as additives. According to Emdadi, et al. [20], a lot of low thermal conductivity materials have been extensively studied for this specific application, in which ceramic seems to be a good candidate for potential evaporative cooling application [21]. Part of the conclusion drawn from laboratory analysis of most ceramics, as reported by Costelloe and Finn [22], showed that most porous ceramics demonstrate good mechanical characteristics, sustained chemical and abrasion resistance and most importantly, they are thermally stable. Key to the driving factors in cooling system is principally controlled by variables, such as: porosity of passive materials, configuration and composition of materials and the humidity of the environment [23]. In most cooling structures, several authors [24, 25] have confirmed that a high porosity evaporator, sometimes results in most cooling, while the low-porosity materials may result in virtually negligible levels of cooling. This assertion is evident in the result presented by Okada, et al. [26], where lotus ceramic demonstrated to be cooler, as a result of its heightened capillary rise level (of about 1300mm) above the convectional porous ceramics. The principle evaporative cooling is demonstrated in Figure 4, in which the passive evaporative cooling wall (PECW) is located in a shaded area that is free from both direct and solar influence, while its surface area can therefore be cooled via evaporation.

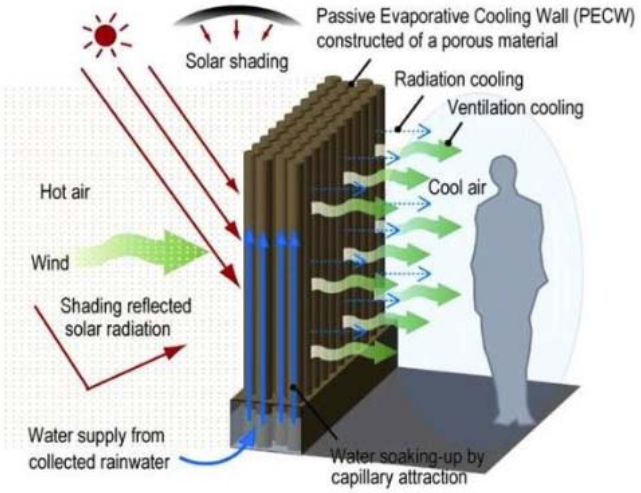

Fig. 5. Diagrammatic description of a passive cooling wall constructed with porous material with high tendency for water soaking-up ability. Adapted from Emdadi, et al. [20]

The application of geopolymer materials for these specific purposes may not be necessarily far-fetched, going by its purported potentials. Several studies embarked upon by these authors [27, 28], have proved beyond any reasonable doubt that fly-ash geopolymer materials have good prospect at low temperature (<100 °C) condition and their production technique releases six times less CO_2 when compared to other additives in cement production. Of critical consideration in this research is that geopolymer materials seem to have derived its composition from by-products and fly-ash, which is to a larger extent, is more environmentally-friendly when compared to other porous ceramics. This salient property may give further consideration for geopolymer materials to be considered as passive cooling materials and the authors suggest further experimental analysis to validate these potentials.

4. AREAS FOR FURTHER RESEARCH

From the concept of evaporative cooling and absorbtion technique, it can be found that there is a broad potential for future studies in these techniques particularly the integration of geopolymer materials for cooling purposes. Based on the shortcoming of PCMs under this context, a brief list of potential future research is offered for further experimental validation.

- ❖ Cost and economic evaluations of PCMs seem not to have been thoroughly addressed in many studies as it relates its application in building. Even though significant progresses have been recorded as per high capability of PCMs in sustaining comfort in building, only handful of these journals considered the economic sustainability. The construction industry must be convinced of their financial return of the initial investment to improve its patronage.
- ❖ As reported earlier, passive cooling techniques alone may not be adequate to reduce high energy demand in building as daily peak of surface temperature is dependent on climatic conditions among other factors. Therefore, a combination with geopolymer materials could be a potentially novel topic for future studies.

5. CONCLUSIONS

Going by the prospect of geopolymers materials as enunciated in the body of this work, it can therefore be inferred that this material remains a potential candidate for evaporative cooling system application. Key of the reason adduced to this fact, is that its manufacturing approach is more environmentally-friendly and in most cases, low firing temperatures are needed. In view of the fact that fly ash-based geopolymer materials are primary raw materials for the production of geopolymer materials, renders this research topic a promising and novel area that should be further explored. This development could serve as a way of addressing some of the environmental and energy issues that are currently bedevilling developing countries, via the reduction of waste volume of fly-ash and most importantly, reducing the global CO_2 emissions. Meanwhile, lot of researches are still needed to validate the potential of introducing industrial and agricultural waste materials into fly-ash geopolymer for passive cooling application.

6. REFERENCES

[1] J. Weber, S. Strączyńska, A. Kocowicz, M. Gilewska, A. Bogacz, M. Gwiżdż*, et al.*, "Properties of soil materials derived from fly ash 11years after revegetation of post-mining excavation," *Catena,* vol. 133, pp. 250-254, 2015.

[2] J. Van Jaarsveld, J. Van Deventer, and G. Lukey, "The characterisation of source materials in fly ash-based geopolymers," *Materials Letters,* vol. 57, pp. 1272-1280, 2003.

[3] A. Bilodeau and V. M. Malhotra, "High-volume fly ash system: the concrete solution for sustainable development," in *CANMET/ACI. Séminaire international*, 2000.

[4] A. Yilmaz and N. Degirmenci, "Possibility of using waste tire rubber and fly ash with Portland cement as construction materials," *Waste Management,* vol. 29, pp. 1541-1546, 2009.

[5] Z. Zhang, J. L. Provis, A. Reid, and H. Wang, "Mechanical, thermal insulation, thermal resistance and acoustic absorption properties of geopolymer foam concrete," *Cement and Concrete Composites,* vol. 62, pp. 97-105, 2015.

[6] F. Souayfane, F. Fardoun, and P.-H. Biwole, "Phase change materials (PCM) for cooling applications in buildings: A review," *Energy and Buildings,* vol. 129, pp. 396-431, 2016.

[7] N. Zhu, Z. Ma, and S. Wang, "Dynamic characteristics and energy performance of buildings using phase change materials: a review," *Energy Conversion and Management,* vol. 50, pp. 3169-3181, 2009.

[8] C. Chen, H. Guo, Y. Liu, H. Yue, and C. Wang, "A new kind of phase change material (PCM) for energy-storing wallboard," *Energy and Buildings,* vol. 40, pp. 882-890, 2008.

[9] Y. Konuklu, M. Ostry, H. O. Paksoy, and P. Charvat, "Review on using microencapsulated phase change materials (PCM) in building applications," *Energy and Buildings,* vol. 106, pp. 134-155, 2015.

[10] H. Akeiber, P. Nejat, M. Z. A. Majid, M. A. Wahid, F. Jomehzadeh, I. Zeynali Famileh*, et al.*, "A review on phase change material (PCM) for sustainable passive cooling in building envelopes," *Renewable and Sustainable Energy Reviews,* vol. 60, pp. 1470-1497, 2016.

[11] E. ul Haq, S. Kunjalukkal Padmanabhan, and A. Licciulli, "Synthesis and characteristics of fly ash and bottom ash based geopolymers–A comparative study," *Ceramics International,* vol. 40, pp. 2965-2971, 2014.

[12] O. Adekomaya, T. Jamiru, R. Sadiku, and Z. Huan, "Minimizing energy consumption in refrigerated vehicles through alternative external wall," *Renewable and Sustainable Energy Reviews,* vol. 67, pp. 89-93, 2017.

[13] P. Duxson, J. L. Provis, G. C. Lukey, S. W. Mallicoat, W. M. Kriven, and J. S. Van Deventer,

"Understanding the relationship between geopolymer composition, microstructure and mechanical properties," *Colloids and Surfaces A: Physicochemical and Engineering Aspects,* vol. 269, pp. 47-58, 2005.
[14] H.-C. Wu and P. Sun, "New building materials from fly ash-based lightweight inorganic polymer," *Construction and Building Materials,* vol. 21, pp. 211-217, 2007.
[15] Y. Qin, "A review on the development of cool pavements to mitigate urban heat island effect," *Renewable and Sustainable Energy Reviews,* vol. 52, pp. 445-459, 2015.
[16] Z. Zhang and X. Fang, "Study on paraffin/expanded graphite composite phase change thermal energy storage material," *Energy Conversion and Management,* vol. 47, pp. 303-310, 2006.
[17] S. Hasnain, "Review on sustainable thermal energy storage technologies, Part I: heat storage materials and techniques," *Energy Conversion and Management,* vol. 39, pp. 1127-1138, 1998.
[18] G. A. Blengini and T. Di Carlo, "The changing role of life cycle phases, subsystems and materials in the LCA of low energy buildings," *Energy and Buildings,* vol. 42, pp. 869-880, 2010.
[19] L. F. Cabeza, A. Castell, C. Barreneche, A. De Gracia, and A. Fernández, "Materials used as PCM in thermal energy storage in buildings: a review," *Renewable and Sustainable Energy Reviews,* vol. 15, pp. 1675-1695, 2011.
[20] Z. Emdadi, N. Asim, M. A. Yarmo, and R. Shamsudin, "Investigation of More Environmental Friendly Materials for Passive Cooling Application Based on Geopolymer," *APCBEE Procedia,* vol. 10, pp. 69-73, 2014.
[21] E. Ibrahim, L. Shao, and S. B. Riffat, "Performance of porous ceramic evaporators for building cooling application," *Energy and Buildings,* vol. 35, pp. 941-949, 2003.
[22] B. Costelloe and D. Finn, "Thermal effectiveness characteristics of low approach indirect evaporative cooling systems in buildings," *Energy and Buildings,* vol. 39, pp. 1235-1243, 2007.
[23] V. Fabi, R. V. Andersen, S. Corgnati, and B. W. Olesen, "Occupants' window opening behaviour: A literature review of factors influencing occupant behaviour and models," *Building and Environment,* vol. 58, pp. 188-198, 2012.
[24] S. Wei, R. Jones, and P. de Wilde, "Driving factors for occupant-controlled space heating in residential buildings," *Energy and Buildings,* vol. 70, pp. 36-44, 2014.
[25] K. Fong, T. T. Chow, C. K. Lee, Z. Lin, and L. Chan, "Comparative study of different solar cooling systems for buildings in subtropical city," *Solar Energy,* vol. 84, pp. 227-244, 2010.
[26] K. Okada, S. Uchiyama, T. Isobe, Y. Kameshima, A. Nakajima, and T. Kurata, "Capillary rise properties of porous mullite ceramics prepared by an extrusion method using organic fibers as the pore former," *Journal of the European Ceramic Society,* vol. 29, pp. 2491-2497, 2009.
[27] S. Wang and H. Wu, "Environmental-benign utilisation of fly ash as low-cost adsorbents," *Journal of hazardous materials,* vol. 136, pp. 482-501, 2006.
[28] E. Diaz, E. Allouche, and S. Eklund, "Factors affecting the suitability of fly ash as source material for geopolymers," *Fuel,* vol. 89, pp. 992-996, 2010.

ACKNOWLEDGEMENTS

The authors would like to thank some of the literatures whose contents have helped to establish the prospect of geopolymer as a candidate for passive cooling materials. Although, the usual disclaimer applies, the views expressed in this study are primarily the opinion of the authors.

Authors: **Oludaisi Adekomaya,** Olabisi Onabanjo University, Agricultural and Mechanical Engineering, Faculty of Engineering, College of Engineering and Environmental Studies, Nigeria
Oludaisi Adekomaya, Tamba Jamiru, Zhongjie Huan, Department of Mechanical Engineering, Mechatronics and Industrial Design, Faculty of Engineering and Built Environment, Tshwane University of Technology, Pretoria 0001, South Africa.
Rotimi Sadiku, Department of Chemical and Metallurgical Engineering, Faculty of Engineering and Built Environment, Tshwane University of Technology, Pretoria 0001, South Africa.
Bilianu Oboirien, Council for Scientific and Industrial Research (CSIR), Pretoria South Africa.
E-mail:
(Corresponding author: oludaisiyetunde@gmail.com, adekomaya.oludaisi@oouagoiwoye.edu.ng, adekomayao@tut.ac.za)

http://doi.org/10.24867/JPE-2017-02-091

Journal of Production Engineering

Vol.20 No.2

JPE (2017) Vol.20 (2) Preliminary Note

Shuaib-Babata, Y. L., Abegunde, A. J., Abdul, J.M.

SUITABILITY OF ADO-EKITI (NIGERIA) NATURAL MOULDING SANDS FOR USE AS FOUNDRY SANDS IN PRODUCTION OF ALUMINUM ALLOY CAST

Received: 22 September 2017 / Accepted: 12 November 2017

Abstract: *Adequate application of sand casting processes in Aluminum casting can improve the economic activities of Nigeria through industrialization. Samples of natural moulding sand were collected from three different moulding sand deposits within Ado-Ekiti metropolis. The samples' properties were evaluated using American Foundry Society standards. The samples were used to produce aluminum alloy cast specimens and their mechanical properties were evaluated. The results revealed that the properties compared favourably with standard values as indication that the moulding sands are suitable materials for aluminum casting. Thus, effective application of the sample sands will enhance industrialization, job creation and the nation self-reliance.*

Key words: *Aluminum, casting, foundry, moulding and sand*

Primenljivost ado-ekiti (Nigeria) prirodnog peska za livenje, upotreba peska za podlogu u proizvodnji aluminijumskih livenih legura. *Adekvatnom primenom procesa livenja aluminijuma u pesku se može poboljšati ekonomske aktivnosti Nigerije kroz industrijalizaciju. Uzorci prirodnog livenog peska sakupljeni su iz tri različita depozita peska za livenje unutar Ado-Ekiti metropoli. Osobine uzoraka ocenjivane su korišćenjem standarda American Foundri Societi. Uzorci su korišćeni za proizvodnju livenih uzoraka legure aluminijuma i procenjena su njihova mehanička svojstva. Rezultati su pokazali da su osobine pozitivno upoređene sa standardnim vrednostima kao indikacija da je pesak za kalupovanja odgovarajući materijali za livenje aluminijuma. Stoga će efikasna primena peskovitih uzoraka poboljšati industrijalizaciju, otvaranje novih radnih mesta i samopouzdanje nacije.*

Ključne reči: *Aluminijum, livenje, podloga, kalupovanje i pesak*

1. INTRODUCTION

Foundry technology is one of the vital bases for rapid industrial development of any nation. Rapid industrial development is very essential to positively address the problem of economic recession in Nigeria. Sand cast is found suitable in casting of all metals of different sizes, ranging from very small to extremely large sizes [1, 2]. Sand is used in sand casting as a manufacturing process to produce a mould in which molten metal is poured to produce a cast. This is due to the fact that the sand particle size is packed finely and tightly together in such a way to provide excellent surface for the mould [3]. In manufacturing of engineering goods, tools, devices and equipment (such as engine blocks, machine tool bases, cylinder heads, pump housings, and valves), metal casting process is employed. In metal casting, sand casting is the most widely used [4]. Sand casting is found to be relatively cheap and adequate refractory for use in foundry applications [2]. Adequate utilization of sand as a resource will help towards enhancement of Nigeria's industrialization. Thus, rapid production of different locally needed devices, tools, utensils and equipment in Nigeria can be achieved through indigenous small and medium scale enterprises. Rapid growth in production was earlier reflected in the rising importance of manufacturing in the economies of virtually all countries [5].

Industrialization greatly depends on production capacity from availability of locally available raw materials used in development of technology in the transformation of the raw materials to finished products [6]. Hughes also identified the bases for the development of an industrial sector to include access to raw materials, labour force, funds and technology [7].

Raw Material Research and Development Council (RMRDC) in 1990 delved into geological survey of Nigeria resources and found sand to be the major mineral deposits in the country [8]. Sand covered an estimated proven reserve of billions of tones, out of which petroleum, gas and coal resources exploration had only received sufficient attention [9]. Studies have shown that majority of the available natural sands in Nigeria have not been receiving sufficient attention [10, 11, 12, 13, 14].

Researchers had discovered through their various studies that most Nigerian Moulding sands, such as Azare foundry sand, Alkaleri, Barkin-ladi and Ilorin moulding sands were suitable for foundry applications [13, 15, 16]. Thus, it is essential to investigate the suitability of various Nigerian moulding sands for casting applications.

Shuaib-Babata and Olumodeji noted that the strength of foundry rests on the fundamental behaviour of sand, since casting quality depends on sand quality [13]. Sand often determines the quality of cast [17]. The choice of moulding sand for casting processes depends on its properties, such as strength, permeability, refractoriness, collapsibility [18].

Foundry sands were abundantly available and scattered all over the towns and villages in Nigeria

which had been in use for past decades for casting of aluminum cooking utensils, decorative ornament and others without any evidence or trace of determining the mechanical properties or carrying-out any effect of sand on the product cast [13]. Hence, it is very essential to investigate the suitability of natural moulding sands in Ado-Ekiti (Nigeria) for Aluminum casting for its effective and appropriate usage in enhancing production of equipment, devices and home utensils, and at long run assist in solving the problem of unemployment in Nigeria.

Aluminum, the most abundant metal in the earth's crust is widely used as results of its excellent qualities [19, 20]. Aluminum is known with high strength-to-weight ratio, high thermal and electrical conductivity, high toughness with good strength at low temperature, high resistant to corrosion, non-toxic, excellent reflector of radiant energy, ease to form and fabricate, low weight, bright colour, and readily recycled [19, 20, 21]. It is also the lightest metal other than magnesium, with a density of about one-third of that of steel. These qualities made the material to be considered most suited for wide usages in transportation vehicles (such as aircraft, rocket, trucks, ships, automobiles), suitable structures (like ladders, scaffolding, gangways), heating and cooling applications (automobile radiator, refrigerator evaporator coils, heat exchangers, engine components), piping and vessels, cooking utensils, food processing and packaging of food and beverages, heat and lamp reflectors and for cryogenic vessels.

Scraps of Aluminum alloys (such as automobile engine piston scraps, cooking utensils, in dry-battery cell, among others) are commonly seen as waste products in major towns and villages in Nigeria. This material can be recycled to be used as raw material for aluminum casting in producing different items.

Application of sand casting processes in Aluminum casting can improve the economic activities of the country through industrialization, most especially during the present economic recession which requires shifting attention from over dependency on oil and gas as main economic source.

There is no doubt that the efficient and economic production of quality sand castings in the modern foundry requires a thorough knowledge of foundry sand technology [22]. This can be appropriately achieved through effective testing and analysis of sand mould in casting of device or any product; and analysis of the cast product properties. This study therefore is to determine the suitability of Ado Ekiti moulding sands for Aluminum casting and investigate the cast desirable properties and effectiveness in meeting appropriate casting materials' standards. Information from this study will at long run will enhance industrialization, job creation and the nation self-reliance through reduction in importation of foundry sand and Aluminum products into the country.

2 MATERIALS AND METHODS

2.1 Materials

The sand samples for this study were collected from Oke Ureje river banks (Sample A), Omisanjana river bank (Sample B) and Odo Ayo river bank (Sample C) within Ado-Ekiti metropolis. Ado-Ekiti is located in Ekiti state of Nigeria; situated in between longitude 5^0 11' and 5^0 25' and latitude 7^0 11' and 7^0 37'.

Aluminum alloy scraps (Automobile engine piston) were obtained within Ado-Ekiti, Ekiti State, Nigeria and analysed at National Geosciences Research Laboratory, Kaduna, Nigeria.

2.2 Methods

2.2.1 Preparation of natural moulding sand

The sand samples collected from the above named locations were washed, sun-dried, filtered in order to separate the debris that was collected with them and kept in desiccators for further laboratory/experimental analysis, in accordance with American Foundry Society (AFS) standards. The details of the procedures had earlier been discussed [2].

2.2.3 Production of sand specimens for laboratory analyses

Sands obtained from the four selected sites were dried naturally to remove the free water and the specimens were prepared from each samples of the sand from these locations. A quantity of the sand was sieved through 2 mm British Standard (BS) sieve to obtain grain size required for the experiment. The sand grains pebbles were broken into pieces using foundry flat edge rammer, the powdered-moulding sand were thoroughly mixed with clean water for about 10 minutes to have homogeneous sand water mixture and sieved with 2mm British standard sieve. The samples were then moulded in a specimen tube to produce standard test specimen of diameter 50mm by average height of 85 mm using standard sand rammer that delivered a compaction blow of 6.4 kg thrice from a height of 50 mm. The specimens were classified for various foundry tests. In accordance with the American Foundry-Men Society standards, AFS guidelines [23], the sands' foundry properties were obtained and recorded.

2.2.4 Determination of chemical and Physico-mechanical properties of the natural moulding sands

The chemical constituents of the samples of the sand samples were determined using x-ray fluorescence (XRF) spectrometer and atomic absorption spectrophotometer (AAS). The Physic-mechanical properties of the moulding sands (such as moisture content, clay content, flowability, bulk density, permeability, shatter index, Compression strength, Green compression strength of natural moulding sand, dry compression strength, hot compression strength, refractoriness value of moulding sand) were also determined in line with AFS recommendations [23] and the details of the procedures were adequately discussed Shuaib-Babata and Abegunde [2].

2.2.5 Melting and Casting Processes

Pattern of the shape of object to be produced was made with core box. The sands prepared for analysis were made into moulds and filled into a wooden

rectangular box prepared (molding). The pattern was pressed into the fine sand mixture to form the mold into which aluminum was to be poured. The pattern was made to be larger than the part to be made to give room for aluminum shrinkage during solidification and cooling. Cores were inserted into the casting box and properly set, after the pattern was removed. Gating/feeding system was then created to direct the metal into the mold cavity created by the pattern.

Melting of the aluminum alloy scraps was done using a fuel-fired crucible furnace for more than one hour at temperature of 700 ^{o}C and held at the temperature for 30 minutes to attain homogeneous composition. The melt was stirred and the mould was filled by pouring the melted aluminum from transfer ladles. It was allowed to cool thoroughly. The sand mold was then broken and casting was removed. The cast was then cleaned by removing the gates and risers, adhering sand, scale, parting fins and other foreign materials. Grinding of the object was carried out and subsequently inspection and testing to detect defects in the casting to attain better surface finishing and dimensional precision of the cast. The processes involved in the sand casting (production) of the aluminum cast (melting, casting and fettling processes) are as shown in Plates 1 - 3.

(a) Placing of pattern on the moulding board

(b) Filling and ramming of mould

(c) Top filling of the drag

(d) Placing of cope over drag.

(e) Removing of runners & riser

(f) Venting of the mould.

(g) Opening to remove patterns

(h) Dressing and gating of the mould

(i) Covering of the mould ready for casting

Plate 1. Preparation of mould for casting aluminum

(a) Preparation of Furnace

(b) Charging of scraps for melting.

(c) Addition of fluxes

(d) Removing of molten metal from furnace

Plates 2. Melting of Metal

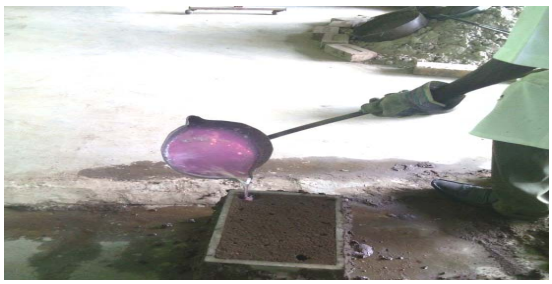

(a) Pouring of Molten Metal

(b) Mold Filled with Molten metal.

(c) Removal of cast product

(d) Cast sample

(e) Fettled casts.

Plates 3. Casting of mould.

3. DETERMINATION OF TENSILE STRENGTH AND HARDNESS OF THE CAST ALUMINUM SAMPLES

The tensile specimens were prepared to required ASTM E-8 standard [24, 25] shape and sizes (50 mm gauge length) as shown Plates 4. The tensile properties of the specimens were determined on a Testometric Materials Testing Machine (Model 0500-10080, Win test analysis; 100 kN capacity, England made) showing in Plates 5 and 6.

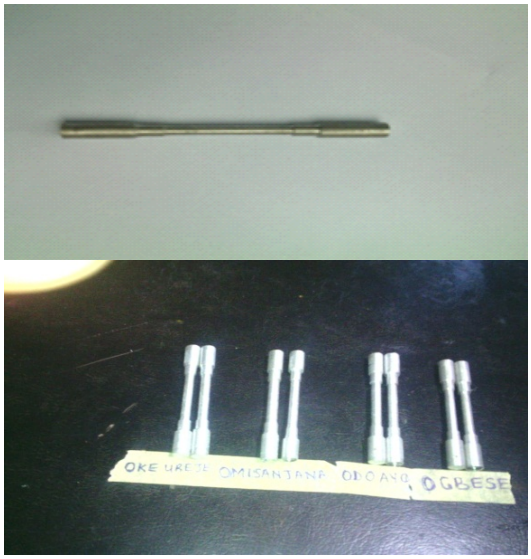

Plates 4. Specimens for tensile test

Plate 5. Testometric Materials Testing Machine Used

5.a) Fixing of a specimen unto the tensile testing machine

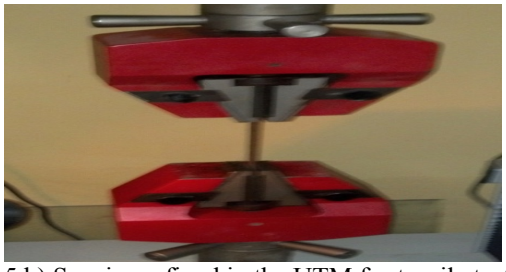

5.b) Specimen fixed in the UTM for tensile test

The hardness test was also done using each of the four samples of cast aluminum on the Tensometeric Materials Testing Machine. The surfaces of the machined specimens were ground to remove the skin or scale present on them. A hardened steel ball is pressed for a time of 10 to 15 seconds into the surface of the material with the Testometric machine but using another gripping device. After the load and ball have been removed, the diameter of the indentation was measured. The Brinell hardness number, signified by HB, was obtained and read on the computer screen attached to the machine

3.1 Determination of impact strength value of cast aluminum

The Charpy impact test, also known as the Charpy V-notch test is the form used in this analysis. Test pieces which were machined to 60 mm long and 10 square millimeters notched on the notching machine; principally to assure fracture by a stress concentration introduced at the notch area (Plates 6).

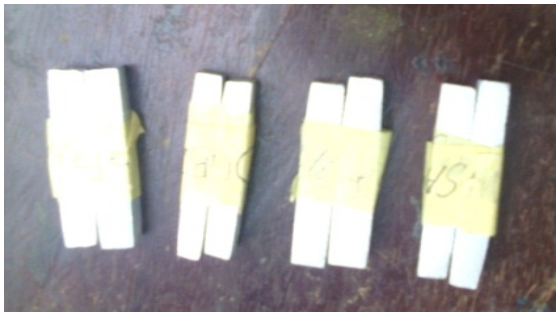

(a) Test pieces in different sizes

(b) Notching of test piece

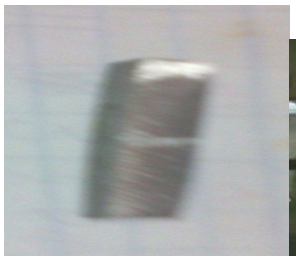

(c) Notched test piece

(d)Test-Piece on Impact machine

Plates 6. Impact Test

The notched specimen was fed into impact machine. The notched in the sample was of regular dimensions and geometry. The standard machine has the pendulum hitting the test piece with energy of 300 ±10J. The test

piece was supported at each end with the notched side face directly opposite to where the pendulum strikes the test piece in line with the view of Bolton [23]. The specimens were fixed one after another to receive the fast moving hammer blow when released from a fixed height on the machine. Upon released, the pendulum hammer struck and fractured the specimen at the notched region.

4. MICROSCOPIC STRUCTURE OF CAST ALUMINUM

The micro examination of the cast pieces was carried out in accordance with the practice of Dibiezue using 2% of trioxonitrate (v) acid as an etchant and viewed from metallurgical microscope of magnification X50.

5. RESULTS AND DISCUSSION

The results of chemical composition analysis for the selected moulding sands in Ado-Ekiti are as presented in Table 1. This result is significant since at the foundry, the chemical composition of the foundry sand relates directly to the metal moulded [26].

Table 1 revealed that the sample sands are of high proportion of silica, with 75.22 % - 79.23 % silicon oxides, which are within the American Foundry Society, AFS standard. According to AFS, most metal casting sand (foundry sand) is high quality silica with physical characteristics [27].

The results of the physico-mechanical properties of the selected natural moulding sands in Ado-Ekiti are presented in Table 2.

Sample	Elemental Composition by Weight (%)									
	SiO_2	Al_2O_3	CaO	MgO	Na_2O	Fe_2O_3	TiO_2	K_2O	MnO	LOI
A	78.67	12.20	0.35	0.40	1.87	1.69	1.76	0.17	1.89	0.81
B	75.22	16.03	3.70	1.54	1.14	0.64	0.23	0.22	0.15	0.76
C	79.23	12.20	0.35	0.40	1.80	1.66	1.75	0.13	1.72	0.75

Table 1. Chemical Composition of Natural Moulding Sand

Sample	AFS GFN (%)	Clay content (%)	Bulk density (g/cm^2)	Moisture content (%)	Permeability (%)	Green strength (kN/m^2)	Drycompression strength (kN/m^2)	Green shatter index (g)	Dry shatter index (g)	Refractoriness (^oC)	Flowability (%)
A	63.27	12.0	12.04	7.36	86.2	120.9	203.0	0.50	0.22	>1200	67.87
B	61.08	13.0	12.25	5.75	87.5	63.6	101.8	0.03	0.05	>1200	68.50
C	66.98	10.0	12.23	6.79	86.3	70.9	191.0	0.12	0.30	>1200	67.40

Table 2. Some properties of the natural moulding sand samples

The result of AFS GFN analysis for the various specimens is presented in Table 2, which is a useful parameter with the average grain size of the sand with which its choice should be based on particle size distribution [28]. The values of the sand samples AFS-GFN are within the standard ranges values of 35 to 90 fineness number for non-ferrous metal [29]. Sand with AFN 50 – 60 with average grain size of 220 – 250 microns and fines content (below 20 microns) 2% maximum yields good surface finish at low binder levels; allows low binder level to be used; and allows low binder levels [30].

The samples' clay contents range between 10 and 13%, an indication that the natural molding sand is expected to contain sufficient amount of binder material [31]. The specified clay content for moulding sand is between 10 - 12% [32]; while American Foundrymen's Association satisfactory proved values for aluminum, brass and bronze, iron and steel castings is between 12 and 18% clay contents [32].

Moisture content is the amount of water present in the moulding sand. In Table 2, the percentages of the moisture contents of the specimens are between 5.75 and 7.36 %, which are within the satisfactory AFS moulding sand moisture content for various types of castings [29].

The specimens' flowability values are between 67.25 and 68.50%. It varies in sand with moisture and clay contents [31]. The AFS satisfactory mould sand percentage flowability for casting aluminum is 65 [33,34,35,36]. The high flowability value in the sands is as a result of rounded grains nature of the sand, which enhances the ease compaction of the sand [37]. Flowability increases with decrease in grain size of sand [31].

The permeability test results recorded for the tested natural moulding sands range between 86.2 and 87.5. The experimental results of the green permeability for the specimens in Table 2 indicate that the sand samples had good natural green permeability for casting a good number of ferrous and non-ferrous metals [32]. The recommended green permeability for green sand is within 80 – 110 [28]. This implies that the study sands green permeability values are within the stated standard ranges. The high permeability is due the amount of well spread grain distribution and rounded-grains of the sand. The permeability depends on grain size, grain shape, grain distribution, binder

and its content, degree of ramming and water content of the moulding sand the [3, 31, 38].

Ureje sand with the highest moisture of 7.36% has the lowest % permeability (86.2); Omisanjana sand sample with 5.75 % MC also possess the highest % permeability of 87.5. while Odo Ayo sand sample has 6.79 % MC and 86.3 % permeability. The trend of these results is in line with the principle that high moisture content (MC) decreases permeability [39].

The green and dried shatter index of the specimens ranges between 0.03- 0.50 and 0.05- 0.22 respectively as shown in Table 2. The shatter index values also indicate that the sand samples are tough enough to aid satisfactory lift during pattern withdrawal. The content of clay and corresponding moisture content are attributed to this high value [16].

The sands' bulk density values are 12.04, 12.25 and 12.23 g/cm^3 for sample A, B and C respectively. These values are within the recommended AFS specification [16]. Ihom *et al.* also gave recommended bulk density for green moulding sand as 1.49 g/cm^3 and above [28].

Moisture (MC) in moulding sand has influence on the sand permeability. High moisture content decreases permeability [39]. Moisture content affects the other properties of the mixture such as strength [40]. It was made known that too much moisture can cause steam bubbles to be entrapped in the metal casting. Though, there was opinion that low moisture content in the moulding sand does not develop strength properties [39].

Compression strength of natural moulding sand is the ability of the sand casting mixture to hold its geometric shape under the conditions of mechanical stress imposed during the sand casting process is the sand's strength [40]. Dry compression strength is the strength of the moulding sand in dry condition. The natural sand's dry compression strength increases as the moisture content of the sand increases [28]. The Oke-Ureje, Omisanjana and Odo Ayo sand samples exhibited dry compression strength values of 203, 101.8 and 191.0 kN/m^2 respectively. The results in Table 2 show that the higher the MC, the higher the dry compression strength. This is in line with the Ihom *et al* [28]'s assumption that dry compression strength increases with the MC of sand. The sand's strength depends on the clay and water content, type of clay, the clay size distribution, among other factors [28].

Green compression strength is the strength of the sand in the green or moist condition. A mould having adequate green strength will retain its shape; it will not distort or collapse even after the pattern has been removed from the moulding box. It helps in making and handling the moulds unless the mould is hardened in contact with pattern surface, it will not be possible to achieve dimensional stability and high accuracy of the required size. Oke-Ureje, Omisanjana and Odo Ayo sand samples exhibited green compression strength values of 120.9, 63.5 and 70.9 kN/m^2 respectively. The recommended green sand's strength ranges between 70 – 100 kN/m^2 [28]. The sand samples possess adequate green strength that will retain its shape and will not distort or collapse even after the pattern has been removed from the moulding box, but Omisanjana moulding sand's strength may needs to be enhanced.

5.1 Chemical composition of aluminum scrap

The chemical composition of the aluminum alloy obtained from scraps is presented in Table 3.

Element	Al	Fe	Si	Mg	Cu	Zn	Cr	LOI
Percentage Composition (Wt %)	88.50	0.60	6.80	0.26	0.2	0.03	0.21	3.1

Table 3. Elemental chemical composition of the Aluminum alloy

5.2 Mechanical Tests Results

Sands used in casting of metals are proved to have effects on the cast alloy's properties due to the conditions the cast subjected to. Since the strength of these casts rest on the fundamental behavior of the foundry sand that was basically used in making the moulds and cores [13].

Aluminum alloys that were cast by these various sands were made into laboratory specification and subjected them to various mechanical tests.

Table 4 shows some tensile properties of the Aluminum alloy cast samples, while the hardness test results are graphically presented in Figure 1. The properties such as yield strength, ultimate tensile strength, plastic deformation limit and toughness are important, most especially for design engineers to determine the quantity of force the material can withstand with reference to the cross-section used without deforming permanently.

SAMPLES	Stress @ Yield (N/mm^2)	Stress @ Break (N/mm^2)	UTS (N/mm^2)	Energy @ Break (J)	Elog @ Break (mm)	Elog @ Yield (mm)	Strain @ Break	Strain @ Max.	Modulus of elasticity (N/mm^2)
A	1.9	1.9	1.8	6.4	66.0	5.0	2.1	2.0	35.0
B	5.0	1.7	1.7	6.6	74.0	5.0	3.8	4.0	85.0
C	5.7	2.2	2.2	10.0	61.0	5.0	2.1	2.0	83.0

Table 4. Some mechanical properties of cast Aluminum samples

As presented in Table 4, the aluminum cast samples from Oke Ureje (moulding sand A), Omisanjana (moulding sand B) and Odo Ayo (moulding sand C) respectively are with tensile strength average values of

1.9, 1.7 and 2.2 N/mm^2; while with the Ultimate tensile strength values are 1.8, 1.7 and 2.2 N/mm^2 and average ductility (elongation) values of 66, 74 and 61 mm for sample A, B and C respectively. The aluminum cast samples A, B and C respectively also exhibited average toughness (the amount of the energy absorbed before failure) of 6.4, 6.6 and 10.0 J.

The average Brinell hardness number (BHN) of the cast aluminum samples from various tested moulding sands as presented in Figure 1 are 116.9, 101.9 and 114.1 BHN for cast from Oke Ureje (moulding sand A), Omisanjana (moulding sand B) and Odo Ayo (moulding sand C) respectively. These values fall within AFS standard value ranges of 100-120 kN/mm^2 [17].

5.3 Microscopic Structure of Cast Aluminum

The metallographic results showing microstructure of aluminum alloy casts are presented in Plates 7.

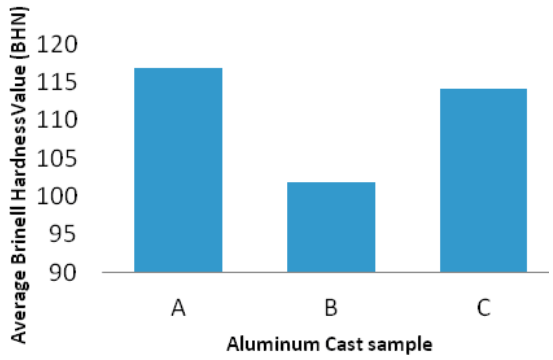

Fig. 1. Average Hardness of the Aluminum Cast from the Moulding Sand Samples

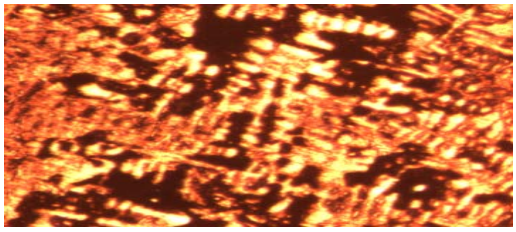

a) Oke Ureje (Sample A) x 50

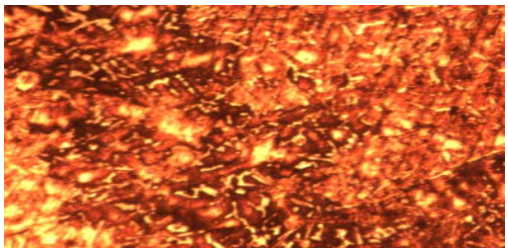

b) Omisanjana (Sample B) x50

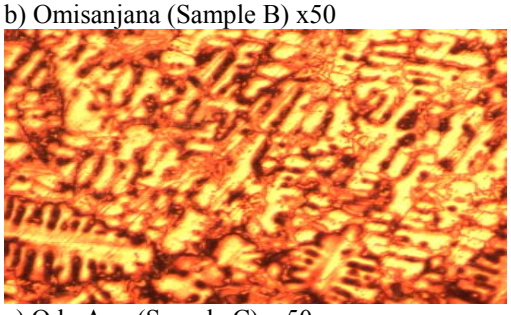

c) Odo Ayo (Sample C) x 50

Plates 7. Microscopic Structure of Cast Aluminum samples

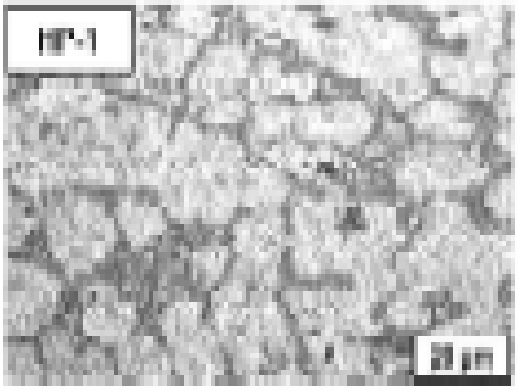

Plate 8. The microstructure of un-treated Al-7Si alloy [41]

The microstructures generally consist of fine crystals of aluminum (Al), magnesium silicide (Mg_2Si) and Al Mg_2Si phases. Interestingly, the microstructure of un-treated Al-7Si alloy from a literature [41] that consists of large primary α-Al grains is favorably compared with the microstructures of the cast aluminum samples.

6. CONCLUSION

From this study the following conclusions are drawn:

i. The chemical and physico-mechanical properties of the studied natural moulding sands were compared with AFS mould sand properties for casting of low meting temperature metals
ii. The sands had the potential for use in sandcasting process for non-ferrous metals.
iii. The properties of the aluminum casts from the sand samples were favourably compared with standard ranges for aluminum alloy cast from sand moulding process. This study therefore revealed that all the sand samples at green state were suitable for casting of aluminum alloy.
iv. Ekiti State in Nigeria has potentials of foundry sands and has to take the advantage with suitable conversion technologies.

7. REFERENCES

[1] Sand casting for manufacture – manufacturing process, Retrieved from http://thelibraryofmanufacturing.com/metalcasting_sand.html, accessed on February 22, 2017.

[2] Shuaib-Babata, Y. L., Abegunde, A. J. and Ambali, I. O.: Evaluation of chemical and physico-mechanical properties of Ado-Ekiti (South West, Nigeria) natural moulding sands for foundry applications, Arid Zone Journal of Engineering, Technology and Environment (AZOJETE), Vol. 13, No. 4, 2017, accepted for publication.

[3] Aweda, J. O., Jimoh, Y. A.: Assessment of properties of moulding sands in Ilorin and Ilesha, Nigeria, USEP: Journal of Research Information in Civil Engineering, Vol. 6, No. 2, pp 68-77, 2009.

[4] Sand Casting. Retrieved from: http://thelibraryofmanufacturing.com/metalcasting_sand.html, accessed on 22 January, 2017.
[5] Industry: Producing more with less, Report of the World Commission on Environment and Development: Our Common Future, Retrieved from: http://www.un-documents.net/ocf-08.htm, accessed on July 02, 2017.
[6] Chete, L. N., Adeoti, J. O., Adeyinka, F. M. and Ogundele, O.: Industrial Development and Growth in Nigeria: Lesson and Challenges, Leaning to Complete Working Paper No. 8, African Growth Initiative at Brookings Institute /African Development Bank Group / United Nations University UNU-Wider World Institute for Development. Retrieved from https://www.brookings.edu/wp-content/uploads/2016/07/L2C_WP8_Chete-et-al-1.pdf, accessed 0n August 22, 2017
[7] Hughes, J. R. T.: Industrialization. International Encyclopedia of the Social Sciences, Thompson Gale, Canada. Retrieved from http://www.encyclopedia.com/history/united-states-and-canada/us-history/industrialization#B, accessed on July 02, 2017
[8] Raw Material Research and Development Council (RMRDC), 1st ed, pp 18-22, 1990.
[9] Abegunde, A. J.: Analysis of moulding sand in Ado-Ekiti, Unpublished M.Eng Thesis, Ekiti State University, Ado-Ekiti, 2017.
[10] Abolarin M. S., Olugboji O. A. and Ugwuoke I. C.: Determination of Moulding Properties of Locally Available Clays for Casting Operations. Journal of AU Journal of Technology, Vol.9, No. 4, pp 238-242, 2006.
[11] Isah, B. K.: Solid Mineral Resource Development in Sustaining Nigeria's Economic and Environmental Realities of the 21st Century. Journal of Sustainable Development in Africa, Vol.13, No. 2, pp 210-214, 2011
[12] Adeoye, B.: Fallacy of Oil Wealth, Resource Curse and Economic Development: Oil Wealth and Income Inequality in Nigeria, Retrieved from https://adeoyebabatola.wordpress.com/2014/02/03/fallacy-of-oil-wealth-resource-curse-and-economic-development/, accessed on July 02, 2017.
[13] Shuaib-Babata, Y. L. and Olumodeji, J. O.: Analysis of Ilorin Sand Moulding Properties for Foundry Applications, International Journal of Engineering Research and Technology (IJERT), Vol. 3, No. 1, pp1520 – 1526, 2014.
[14] Ovat, F. A. and Bisong, M. A.: Analysis and categorization of Akparavini and Okwuboyere clay deposits in Biase LGA of Cross River State-Nigeria. Engineering and Technology, Vol. 4, No. 2, pp16-21, 2017.
[15] Abolarin, M. S., Olugboji, O. A. and Ugwuoke, I. C.: Experimental Investigation on Local Refractory Materials for Furnace Construction, Proc. of the 5th Annual Engineering Conf., Federal University of Technology, Minna, Nigeria, pp. 82-85, 2004.
[16] Tokan, A., Adelemoni, E. A. and Datau, S. G.: Mould Characteristics of Azare Foundry Sand, Journal of Raw Material Research (JORMAR), Vol.1, No. 1, pp 67-78, 2004.
[17] Nwajagu C. O.: Foundry Theory and Practice, 1st Ed., ABC Publisher Ltd, Enugu Nigeria, pp. 418-419, 1994.
[18] Bala, K. C. and Khan, R. H.: Characterization of Beach/River sand for foundry application, Leonardo Journal of Sciences, Vol. 12, Issue 23, pp 77-83, 2013.
[19] James, K. W.: Hanabook of advanced materials enabling new designs. A John Wiley & Sons Inc., Publisher, New Jersey, 2004
[20] Degarmo, E.P., Black, J. T. and Kosher, R.: Mineral processes in manufacturing, McMillan, New York, 1988.
[21] Sanders, R. E.: Technology innovation on aluminum casting, Microsoft Corporation, United State of America, 2001.
[22] Le Serve F.L.: Sands and Sand Preparation, In: Beadle J.D. (Eds) Castings. Production Engineering Series. Palgrave, Londonhttps://doi.org/10.1007/978-1-349-01179-7_5, accessed on Jyly 02, 2017.
[23] American Foundry-Men Society Standards (AFS): Mould and Core Testing Handbook, 2nd Ed: Foseco Ltd Permgamon Press Oxford England, 1989.
[24] ASTM E8/E8M – 16a: Standard test methods for tension testing of metallic materials, ASTM International, West Conshohocken, PA, 2015.
[25] Bolton, W.: Engineering materials technology, 4th ed., Butterworth-Heinemamn, Linnacre House, Jordan hill, Oxford, 2003.
[26] Akinyele, J.O. and Oyeyemi, K. S.: Strength Behaviour of Concrete using Foundry Sand as Aggregate, Journal of Natural Science, Engineering and Technology, Vol. 13, pp 99-108, 2014.
[27] Introduction to foundry sand, Retrieved from: http://www.afsinc.org/content.cfm?ItemNumber=7075, accessed on August 27, 2017.
[28] Ihom, A. P., Agunsoye, J. Anbua, E. E. and Ogbodo, J.: Effects of Moisture Content on the Foundry Properties of Yola Natural Sand, Leonardo Electronic Journal of Practices and Technologies, Vol.9, pp 85-96, 2011.
[29] Burns T. A.: Foseco Foundryman's Handbook, 9th ed, Foseco (F.S.) Ltd. Tamworth Staffordshire Permgamon Press Oxford England, pp 435, 1986.
[30] Tuncer, B. E.: Foundry Sand: Characteristics, Specifications, Environmental Considerations, Availability, Recycled Materials Resource Center (RMRC), University of Wisconsin-Madison, 2017.
[31] M E Mechanical. Molding Sand: Constituents, Types and Properties, Retrieved from https://me-mechanicalengineering.com/molding-sand/, accessed on July 02, 2017
[32] Burns T. A. (Eds.): Foseco Ferrous Foundryman's Handbook. Butterworth

Heinemann., New Delhi, India, pp. 1- 352, 1989
[33] Brown, J. R. (Ed.): Foseco ferrous foundry's man handbook, Butterworth, Heinemann, Oxford, 2000.
[34] Mikhailov, A. M.: Metal Casting, Mir Publishers, Moscow, 1989.
[35] Ademola, N. A and Abdullah, A. T.: Assessment of Foundry Properties of Steel Casting Sand Moulds Bonded with the Grade 4 Nigeria Acadia Species (Gum Arabic). International Journal of Physical Sciences, Vol. 4, No 4, 238-241, 2009.
[36] Dielert, H. W.: Foundry Core Practice, American Foundry Men's Society. 3rd Ed. Des Plaines Furnace lining. Nigerian Journal of Engineering Management. Vol. 2, No. 3, 1966.
[37] Casting and Welding: Lecture Notes on advanced casting and welding (ACW), SSM College of Engineering and Technology, Department of Mechanical Engineering. Retrieved from: https://ssmengg.edu.in/weos/weos/upload/EStudy Material/Mechanical/4thSem/production-techonology/CastingAndWelding.pdf, accessed on May 25, 2017.
[38] http://www.iitbhu.ac.in/faculty/min/rajesh-rai/NMEICT-Slope/lecture/c6/l3.html), accessed on July 02, 2017.
[39] Mechanical Engineering: A complete online guide for every Mechanical Engineer-Sand testing methods sand testing equipment, Retrieved from http://www.mechanicalengineeringblog.com/2997-sand-testing-methods-sand-testing-equipment/, accessed on July 02, 2017
[40] Sand Casting: Retrieved from: http://thelibraryofmanufacturing.com/metalcasting_sand.html, accessed on January 22, 2017.
[41] Choi, H., Konishi, H., & Li, X.: Microstructure and mechanical properties of cast hypereutectic Al-Si alloy nanocomposites, Materials Science and -Technology Conference and Exhibition 2010, MS and T'10, pp692-701, 2010.

***Authors**:* Senior Lecturer, **Shuaib-Babata, Yusuf Lanre**, PhD, PE, Department of Materials and Metallurgical Engineering, University of Ilorin, Ilorin, Nigeria Nigeria +2348033945977
Senior Technologist, **Abegunde, Abayomi Johnson,** M. Eng; Department of Mechanical Engineering, The Federal Polytechnic, Ado-Ekiti, Nigeria
Chief Lecturer, **Abdul, Jimoh Mohammed**, PhD, R.Eng, Federal Polytechnic, Offa, Nigeria
E-mail: sylbabata@gmail.com
shuaib-babata.yl@unilorin.edu.ng

http://doi.org/10.24867/JPE-2017-02-101

Journal of Production Engineering

Vol.20 No.2

JPE (2017) Vol.20 (2) Preliminary Note

Edibo, S., Ofuyekpone, O., Edoziuno, F.O., Adediran A.A.

MOULDING PROPERTIES OF RIVER NIGER SAND (*IDAH* DEPOSIT) BONDED WITH *IYOLOKO* CLAY AND CASSAVA STARCH

Received: 02 November 2017 / Accepted: 12 December 2017

Abstract: *The foundry properties of river Niger sand (Idah deposit) bonded with Iyoloko clay and cassava starch were evaluated. Impurities and other foreign objects were removed by washing and sorting, sieve analysis of Idah sand deposit revealed a grain fineness number (GFN) of 40.03 which belongs to the group of grain fineness number that has wide application in sand casting. Above 95% bulk of the sand was retained after the first few sieves, hence the sand was considered to have met the American Foundrymen's Society (AFS) standard specification for moulding sand. Energy Dispersive X-Ray Fluorescence Spectrometer was used to carry out the chemical analysis of the sand and clay samples. From the results obtained, the sand was of high silica content (95.93%) while the clay was rich in silica and alumina contents (65.40% and 20.30% respectively). It was further observed that the sand deposit also maintained its refractoriness at above 1000 ^oC. Moulding properties investigated are green compression strength, dry compression strength, green shear strength, dry shear strength, permeability and compactibility were determined using a motor driven universal sand strength machine and its accessories and electric permeability meter. The mechanical and physical properties of the aluminium alloy casting produced with the local sand compared favourably with typical mechanical properties for aluminium alloys. Therefore, foundry moulds produced from this sand deposit bonded with Iyoloko clay and cassava starch is suitable for casting aluminium alloys.*

Key words: *Binder, Permeability, dry compression strength, green compression strength, compactibility.*

Osobine peska reke Niger za pravljenje kalupa (idah deposit) spojeni sa Iioloko glinom i kasava skrobom*. Ocenjene su osobine peska reke Niger za livenje (deponije Idah) spojene sa Iioloko glinom i kasava skrobom. Nečistoće i ostali strani predmeti uklonjeni su pranjem i sortiranjem, sito analiza deponije peska Idah otkrila je broj zrna (GFN) od 40.03 koji spada u grupu čestice zrnatosti zrna koja ima široku primenu za livenje u pesku. Veća količina od 95% peska zadržano je posle prvih nekoliko sita, pa se smatra da je pesak dostigao standardnu specifikaciju američkog livačkog društva (AFS) za oblikovanje peska. Energetski disperzivni rentgenski fluorescentni spektrometar korišćen je za izvođenje hemijske analize uzoraka peska i gline. Iz dobijenih rezultata, pesak je bio visokog sadržaja silicijuma (95,93%), dok je glina bila bogata sadržajima silike i glinice (65,40% i 20,30% respektivno). Dalje je primećeno da depozit peska zadržava i svoju refraktornost na preko 1000* ^oC*. Ispitane osobine livačkih karakteristika su zelena jačina kompresije, jaka kompresiona čvrstoća, jačina čvrstoće smicanja, čvrstoća na suvom smicanju, prepustljivost i kompaktibilnost korišćenjem univerzalne mašine za čvrsto širenje peska i njegovog pribora i merača električne propusnosti. Mehaničke i fizičke osobine livenja aluminijumske legure proizvedene sa lokalnim peskom u poređenju sa tipičnim mehaničkim svojstvima aluminijumskih legura. Zbog toga, livački kalupi proizvedeni iz ovog depozita od peska vezanog sa Iioloko glinom i kasava skrobom pogodan je za livenje aluminijumskih legura.*

Ključne reči: *Vezivo, permeabilnost, čvrstoća na suvom smicanju, jačina kompresije, kompatibilnost.*

1. INTRODUCTION

Sand is the principal material in sand casting operation. Moulding sand ingredients consist essentially of silica sand, clay, water and other additives [1-3]. Sand is the base refractory material, while clay serves as suitable bonding agent for moulding mixtures. Water is added to develop strength and plasticity, hence, the moisture content is regulated between 4-6% [4]. Above 6% causes decrease in permeability, while below 4% does not provide sufficient plasticity and bond strength to the mould [5-7]. Other addictive serve special purposes, ranging from bonding, improving high temperature plasticity and hot strength, producing anti-metal penetration properties and impart good surface finish to the casting [1,8,9]. Moulding sand can be classified into natural and synthetic moulding sands. Natural moulding sand are obtained directly from the source, particularly from the river or dug from the pit and used essentially as it is. It contains about 10-15% clay in contact with the silica sand. Natural moulding sand is not suitable for steel casting because K_2O, Na_2O, FeO present reduce its refractoriness, hence the need for composition of synthetic moulding sand from locally available raw materials [10-11]. One reason for the resort to use of synthetic moulding sand is attributed to its economy and ease of control. The sand is blended with clay, water and other required additives in the right proportion before use. It can be employed for ferrous casting moulds and others that require high refractoriness.

A variety of casting methods is available, the choice of methods depending on a numbers of factors, including size of casting required, surface finish and cost per component. Sand casting process involves low capital

cost and cost of operation, possibility of large tonnage casting, near net shape casting, reusable characteristics of sand and surface finish achieved by proper sand control. It is this process flexibility that have resulted in the continuous use of sand casting method [12,5].
The quality of casting produced depends largely upon the properties of sand utilized. To ensure good casting, the sand must satisfy specifications as to refractoriness, bond strength, permeability, grain fineness, and moisture content [10,8]. Hence, this work explores the foundry properties of Niger sand (Idah deposit) bonded with Iyokolo clay and cassava starch.

2. MATERIALS AND METHODS

2.1 Materials

The materials used in this research includes silica sand from river Niger (Idah deposit), Iyoloko clay, cassava starch sediment and aluminum alloy from motorcycle hub. The equipment used include stack of standard sieves mounted on a sieve shaker, standard sand rammer, electric motor driven universal sand strength machine, electric permeability meter, laboratory core baking oven (40 ^{o}C - 240 ^{o}C), heat treatment furnace of 1100 ^{o}C capacity, energy dispersive X-ray fluorescence spectrometer, metallurgical bench microscope, electric Rockwell hardness testing machine and universal tensile strength testing machine.

2.2 Methods

Silica sand was collected from river bed some 320 m from river bank was washed thoroughly, sun dried and sorted ready for sieve analysis. Iyoloko clay dugged form Iyoloko stream bed in lumps was spread and dried in the sun. The sun dried clay was crushed and finely ground to pass through a sieve of 200-250 mesh size. Fresh tuber of cassava were selected, peeled and grate using a motorized grater. The grate paste on the screen was washed and as much starch as possible passed through the screen into a little water. The white milky water was channeled into a shallow container where sedimentation took place. Excess water was removed and the sediment (starch) was sun dried and reduced into powdered form, ready for use.

2.2.1 Sieve Analysis

100 g of sand sample was weighed and passed successively through an arrangement of set of sieve mounted on a sieve shaker. Each sieve oversize retained on the sieves was collected. The sieves set were arranged in a descending order in a stack with the coarsest sieve on top and the finest at the bottom. The sample was turned into the uppermost sieve and the sieve shaker was allowed for a shaking time of 15 min. The result of sieve analysis shown on Table 3 was used to compute the grain fineness number (GFN).

2.2.2 Chemical Analysis of the Samples

Energy dispersive x-ray fluorescence spectrometer (ED-XRFS) was used for the chemical analysis of the aluminum alloy cast, the silica sand and the clay samples. In this process, high energy x-ray beam was allowed to pass through the samples, which caused the samples to generate x-ray characteristics of the atoms in the sample. Elements present in the sample were identified from the energies of the characteristics radiation, while the concentration were evaluated from the intensity measurement of the radiation. The result of the ED-XRFS chemical analysis (Tables 1 & 2) were reported in percentages for minor and major concentrations of element.

2.2.3 Mixing Procedure

The sand, clay, cassava starch and water were all mixed in a laboratory sand mixer. This was made possible by weighing the quantity of the sand, clay, starch, and measurement of a suitable liter(s) of water. The mixing proportions of the sample is shown in Table 1.
Weight of composed moulding mixture = 1000 g

Sample	Sand	Clay	Starch	Water
Wt.%	80	12	4	4

Table 1. Samples mixing proportions

2.2.4 Specimen Preparation

AFS standard specimen of moulding sand was used with Ridsdale laboratory sand rammer. 170 g weight of moulding sand was compacted in the specimen tube by inserting the tube under the plunger and rammed with three drops of the sliding weight of the cam by turning the cam handle three revolutions. The specimens were then stripped from the tube by inverting over the stripping post and pushing the tube gently downward.

2.2.5 Green Compression Strength (GCS) Test

GCS test was carried out in a universal sand strength machine (USSM) the rammed standard specimen was carefully inserted in between the compression heads at the lower arm of the machine. The machine was put on and the magnetic rider gradually moves along the reading scale. The compression proceeds until fracture at the maximum strength of the specimen. The machine reverses and returns to zero automatically, while the magnetic rider remains in the position of the ultimate strength. The green compression strength is then read from the scale.

2.2.6 Dry Compression Strength (DCS) Test

Here, the AFS standard specimen was dried in a laboratory core baking oven for a period of 2 h at a temperature of 110 ^{o}C and then allowed to cool in ambient air. The test was carried out in the same manner as explained in GCS test. But in this case, the dried specimen was inserted into the compression heads place in the upper arm of the machine. This position increases the load applied by a factor of 5. The dry compression strength is read from the scale marked “dry compression strength” at the point of specimen fracture and multiplied by 5.

2.2.7 Green Shear Strength (GSS) Test

The green shear strength test is carried out in the same way as explained for dry compression strength, but the compression heads was replaced will shear

heads.

The dry shear strength multiplied by the factor of 5 was recorded at the point where the specimen shears by reading the scale designated "dry shear strength".

2.2.8 Permeability Test

AFS standard specimen retained in the specimen table was mounted on the electric permeability meter which employs the orifice method for the rapid determination of moulding sand permeability. The equipment operates by passing air at constant pressure through the standard test specimen, and the drop in pressure is measured in a pressure gauge which is calibrated directly in permeability number.

2.2.9 Compactibility Test

The test was run by filling the AFS standard specimen tube with sand. The sand stuck level with the top of the tube and then the sand was rammed the standard 3 ramming blows by the rammer. The reduction in the height of sand from the top of the tube to the level of the rammed sand is read as the percentage compatibility, by dividing the decrease in height by the initial height.

2.3 Refractoriness Test

The test was carried out on 50 g of the River Niger sand (Idah deposit) the sample was place in a stainless steel cup and heated at about 14.3 ^{o}C/min in a heating furnace up to 1100 ^{o}C and held for 1.13 h. The sand sample was then observed for fusion of the particles.

2.4 Mechanical Analysis Of Aluminum Alloy Cast

The mechanical properties considered include hardness test, tensile strength test and microstructural examination of the cast material.

2.5 Metallography Examination

Microscopic examination was carried out on a prepared cast sample to determine the grain size and the distribution of various phases present in the aluminum alloy cast as well as the inclusions.

The sample was view under a metallurgical bench microscopic with the following magnification of lenses.

Objective lens = X 10

Viewing eye piece = X10

Camera eye piece = X 12.5

Magnification, M = objective lens X viewing eye piece (during structural viewing)

M = 10 × 10 = X100

Magnification in photomicrograph (Plate 1)

M = 10 × 12.5 = X125

3. RESULTS AND DISCUSSION

3.1 Results

3.1.1 Hardness Test of Cast Product

The Rockwell hardness testing machine make use of a diamond penetration 'c' scale for hard materials and hardened steel ball (as used in this work) for softer steels and non-ferrous metals. The diameter of the steel ball used is 1.78 mm. The load applied is 998 RHB which is equivalent to 100 kg force. The Rockwell hardness machine used is electrically operated and has a scale for reading the hardness values with the sample rigidly held on the supporting head, the load was applied and hardness recorded as shown in Table 7.

3.1.2 Tensile Strength Test

The universal tensile strength testing machine was used. 0.2% proof stress was used to determine the tensile strength. During the experiment, the following data were used to calculate the tensile strength.

Initial gauge length (G_o) = 50 mm

Final gauge length (G_f) = 50.9 mm

Initial diameter (D_o) = 11.9 mm

Final diameter (D_f) = 11.75 mm

Proof load (Y_L) = 14658 N

Maximum load (M_L) = 18094 N

The following relations are used to calculate the results of various tensile strength properties

Proof stress (P_s) = $\frac{Y_L}{A_O}$,

Ultimate tensile strength UTS = $\frac{ML}{A_O}$

Percentage Elongation (%E) = $\frac{G_f - G_O}{G_O}$ x100 %

reduction in cross-sectional Area (% RCSA) = $\frac{A_O - A_f}{A_O}$ ×100

$A_o = \frac{\pi(D_O)^2}{4}$, A_o = 111.22 mm^2

$A_F = \frac{\pi(D_r)^2}{4}$, A_F = 108.43 mm^2

% E = $\frac{G_f - G_O}{G_O} \times 100$ = 1.8 %

% R.C.S.A= $\frac{A_O - A_f}{A_O} \times 100$ = 2.51

(0.2%) Proof Stress, $P_s = \frac{Y_L}{A_O}$ = 131.79 N/mm^2

UTS = $\frac{ML}{A_O}$ = 162.69 N/mm^2

3.2 Discussion

The representative values of constituents compounds in Iyoloko clay and Idah sand are presented in Table 2, Table 3 shows the various trend in values of moulding properties of Idah silica sand while Tables 4-7 shows the sieve analysis against grain fineness number, composition of casting of cast Al alloy, result of tensile test of Al alloy cast with Idah silica sand and hardness test result of Al alloy cast with Idah silica sand respectively.

The results of chemical analysis (Table 2) showed that Idah sand deposit is high in silica (95.93%) and have good foundry properties. The standard properties of silica sand for foundry use includes 95-96% minimum silica (SiO_2) content, 0.3% maximum Fe_2O_3 content, 0.2% maximum CaO content, 0.5% maximum K_2O content 0.5% maximum Na_2O content [11]. While the percentages of the various constituent of the silica sand obtained from the analysis indicate that the sand have met the silica content standard.

Compounds	Iyoloko Clay	Idah Sand
Al_2O_3	20.30	1.58
SiO_2	65.40	95.93
K_2O	1.05	0.83
CaO	0.79	0.14
TiO_2	3.17	0.07
ZnO	0.02	-
MnO	0.13	-
Fe_2O_3	6.03	0.5
MgO	0.18	-
Fe_2O_3	6.03	0.5
Na_2O	0.05	0.15

Table 2. Chemical compositions of Idah silica sand and Iyoloko clay deposits

The $\%Fe_2O_3$ from the chemical analysis indicate that the sand has not met the Fe_2O_3 content standard. The $\%k_2O$ obtained from the analysis is 0.83, thus this have not met the required standard for k_2O content. The value of Na_2O content in the sample is 0.15%, thus the sand deposit has met the specified standard for Na_2O content. The refractoriness of the sand was maintained even at above 1000 ^oC as there was no fusing observe and the sand particles were independent despite the presence of this fusion inducing oxides in the sand deposit. Therefore, this sand can be used to produce mould for casting of aluminum alloys and other non-ferrous alloys.

Properties	**Iyoloko clays as binder**	**Bentonite as binder**
GCS (kN/m^2)	16.8	123.2
GSS (kN/m^2)	(sand too weak for strength determination)	29.4
DCS (kN/m^2)	546	1974
DSS (kN/m^2)	266	252
Compatibility (%)	33%	45%
Permeability (NO)	600	863

Note: GCS = Green compression strength
GSS = Green shear strength
GCS = Dry Compression Strength
DSS = Dry Shear Strength

Table 3. Moulding properties of Idah silica sand.

Results of moulding properties obtained using Iyoloko clay and cassava starch as binders (Table 3) did not compare favourably with those obtained using bentonite as binder, except the dry shear strength (DSS) which is higher than that obtained using standard industrial binder (bentonite). It could be inferred that Iyoloko clay and cassava starch require other additives or increasing the clay content for improved moulding properties, such as the dry and green strength and the permeability.

$$GFN = \frac{Total\ product}{Total\ \%\ Sand\ retained}$$

$$GFN = \frac{3997.394}{99.86} = 40.03$$

The sieve analysis (Table 4) revealed that the sand has met the American Foundrymen's society (AFS) standard specification for moulding sand, since above 95% of the bulk sand was retained on the first few sieves. The grain fineness number is 40.03 and this grade of fineness have wide range of application in sand casting [11].

S/N	**SIEVE APERTURE (µm)**	**BSS NO**	**% SAND RETAINED (g)**	**PRODUCT**
1	1600	-	4.606	-
2	1000	10	5.607	56.07
3	710	20	12.17	243.4
4	630	30	4.15	124.3
5	400	40	55.8	2232
6	315	50	9.26	463
7	200	70	7.55	528.5
8	160	100	0.48	48
9	125	140	0.2	28
PAN	-	200	0.7	14
TOTAL			99.86	3997.394

Table 4. Sieve analysis and grain fineness number (GFN) of Idah silica sand

Element	Al	Cu	Mg	Si	Fe	Mn	Zn	Pb	Sn	Ti
Percentage	90.59	1.5	0.6	5.5	0.6	0.5	0.1	0.1	0.05	0.21

Table 5. Chemical composition of cast aluminium alloy

0.2 % proof stress	131.79
U.T.S N/mm^2	162.69
% Elongation	1.8
% Reduction in CSA	2.51

Table 6. Tensile value of Al alloy cast with Idah silica sand

Property	**Hardness (RHB)**			**Average (RHB)**
Sample	A	B	C	48.1
	48.8	48	47.5	

Table 7. Hardness value result of aluminium alloy cast with Idah silica sand

It is evident from the tensile strength results (Table 6) that 0.2% proof stress of the cast aluminium alloy is 131.79 N/mm^2 with a % elongation of 1.8. This result compared favorably with the standard, 0.2% proof stress of 130 N/mm^2 with corresponding percentage elongation of 1.3 [11].

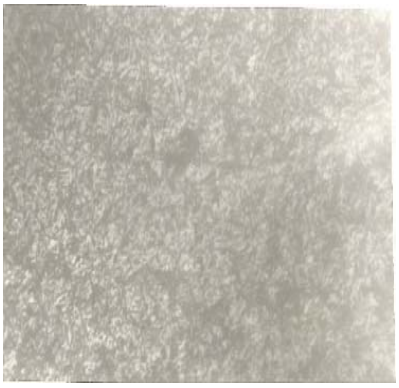

Plate 1. Photomicrograph of cast aluminium alloy using Idah silica sand (X100)

The microstructural examination result (Plate 1) confirms the justification of the mechanical properties and the inference that harder materials have fine grain structure, while ductile materials have coarse grain structures. The photomicrograph is coarse, which is also a direct effect of the coarseness of the sand grains and permeability of the sand deposit.

4. CONCLUSION

From the results of this comparative evaluation, the following conclusions were made:

1. sand deposit met the minimum silica content requirement (95-96%) for moulding sand. The sand also met the maximum Na_2O content (0.5%) requirement, but failed to meet the maximum content requirement for the other oxide contents. Nevertheless, the refractoriness of the sand was maintained at above 1000 ^oC.
2. moulding properties of the sand bonded with Iyoloko clay and cassava starch is not suitable for adequate mould handling when compared with those obtained using bentonite.
3. microstructure of the cast aluminium alloy correspond with the permeability effect of the sand on the cast alloy.
4. the mechanical properties of the cast aluminium alloy from the sand deposit (proof stress of 131.79 N/mm^2 and 1.8% elongation) compared favourably with the typical mechanical properties for aluminium alloys.

5. REFERENCES

[1] American Foundrymen's Society, AFS. *Moulding Methods and materials*, AFS handbook, 1968.

[2] Edoziuno, F.O., Oyibo, A.O., Nwaeju, C.C. *Preparation of Synthetic Moulding Sand Using Local Raw Materials*. International Journal of Advanced Engineering and Technology, Vol.1(1), 2017, pp. 28-31.

[3] Edoziuno, F.O., Oyibo, A.O., and Odo, J.U. *Effects of Particle Size, Clay and Moisture Contents on the Properties of Synthetic Moulding Sand*. Proceedings of the 33rd Annual Conference of the Nigerian Metallurgical Society (NMS), Warri. Nov. 01-04, 2017, pp.100-110.

[4] Edoziuno, F.O., Utu, O.G., and Nwaeju, C.C. *Variation of Moisture Content with the Properties of Synthetic Moulding Sand Produced from River Niger Sand (Onitsha Deposit) and Ukpor Clay*. International Journal of Research in Advanced Engineering and Technology, Vol.3(2), 2017, pp.102-106.

[5] Beeley, P.R. Foundry Technology, Butterworth – Heinemann, 2001.

[6] Atanda, P.O., Olorunniwo, O. E., Alonge, K. and Oluwole, O. O. *Comparison of Bentonite and Cassava on the Moulding Properties of Silica Sand.* International Journal of Materials and chemistry, Vol. 2 , No.4 , 2012, pp. 132-136

[7] Edoziuno, F.O., Odo, J.U., and Nnuka, E.E. Effect of Ukpor Clay Content on the Properties of *Synthetic Moulding Sand Produced from River Niger Sand*. International Journal of Research in Advanced Engineering and Technology, Vol. 1(3), 2015, pp.12-16.

[8] Jain, P.L. Principles of Foundry Technology, 4th ed, Tata McGraw-Hill Publishing Company Limited, Inddia, 2006

[9] Turkeli, A. Sand, Sand Additives, Sand Properties and Sand Reclamation, MSE-432 (Foundry Technology), Lecture Notes, 2008.

[10] Mclaws, I. J. Uses and Specifications of Silica Sand. Research council of Alberta, Report 7-41, 1971.

[11] Brown, J.R. Foseco Foudryman's handbook, 10th ed, Butterworth Heinemann, Britain, 1994.

[12] American Foundrymen's Society, AFS: Foundry Sand Handbook; The America Foundrymen's Society. Des Plaines, Illinois, 7th ed, 1963.

Authors: **Edibo, S., Ofuyekpone, O., Edoziuno, F.O.**, Department of Metallurgical Engineering, Delta State Polytechnic, Ogwashi-Uku, Nigeria

Adediran, A.A., Department of Mechanical Engineering, Landmark University, Omu-Aran, Kwara State, Nigeria

e-mail: emmanueledibo78@gmail.com
francisedoziuno@gmail.com
dladesoji@yahoo.com

http://doi.org/10.24867/JPE-2017-02-106

Journal of Production Engineering

Vol.20 No.2

JPE (2017) Vol.20 (2) Preliminary Note

Sahu, B., Nayak, N.C.

DEVELOPMENT OF A NEW METHODOLOGY FOR PERFORMANCE EVALUATION OF GREEN SUPPLY CHAIN MANAGEMENT IN ALUMINIUM INDUSTRY

Received: 14 September 2017 / Accepted: 08 November 2017

Abstract: *This research considers seven critical practices from the production phase for implementing Green supply chain management (GSCM) practices. The study aims to describe the prominent factors responsible for GSCM practices and their priorities with productivity approach. The questionnaire has been developed to capture these prominent factors on a five point likert scale. A case study has been carried out. Data has been collected and analyzed using a balanced Analysis of Variance (ANOVA) method. It has been observed that recovery of the end-of-life products affect much for improving GSC practices.*

Key words: *Green Supply Chain, Inbound greening, Outbound greening, Reverse logistics, ANOVA, Optimization*

Razvoj nove metodologije za vrednovanje performansi zelenog lanca upravljanja u aluminijumskoj industriji. *Ovo istraživanje razmatra sedam kritičnih običaja iz proizvodne faze za sprovođenje upravljanja zelenim lancem snabdevanja (GSCM) u praksi. Studija ima za cilj da opiše istaknute faktore odgovorne za praksu GSCM-a i njihove prioritete sa pristupom produktivnosti. Upitnik je razvijen tako da ove istaknute faktore uhvati na skali od 5 tačaka. Sprovedena je studija primera. Podaci su sakupljeni i analizirani pomoću balansirane metode analize varijanse (ANOVA). Primećeno je da oporavak proizvoda na kraju života značajno utiče na poboljšanje GSC-a prakse.*

Ključne reči: *Zeleni lanac snabdevanja, ulazno zeleno, izlazno zeleno, obrnuta logistika, ANOVA, optimizacija.*

1. INTRODUCTION

Greening of the supply chain is one such innovative idea that is fast gaining attention in the industry. This may be primarily because many companies want to do something more than just taking typical measures such as implementing waste reduction strategies, installing pollution control technologies, replacing hazardous material inputs with environment-friendly alternatives, and so on.

Green supply chain management defined as "integration of environmental issues and burden into supply chain management in order to improve the environmental impact of the activities of supply chain i.e. product design, raw material sourcing and selection, manufacturing processes, delivery of the final product to the consumer as well as end-of-life of the product, while maintain the economic and operational performance" [1, 2].

GSCM is an important organizational philosophy, plays an important role in promoting efficiency and synergy between partners, facilitating environmental performance, minimal waste, while it improves the ecological efficiency of organizations and their partners. Before knowing the GSCM practices we should know about the various barriers to implementing GSCM in Indian manufacturing industry. The following four main barriers of GSCM implementation have been identified from the literature i.e. information gap, insufficient society pressure, poor legislation and capacity constraints [3].

In developing countries the increase of industrialization and globalization creates more opportunities for manufacturing industries but simultaneously increases environmental pressures. The aluminium industry shows a constant improvement and development of new technologies [4]. It fulfills an important role in our ordinary life. Three most properties characterize this metal: low density, high mechanical properties and good corrosion resistance. From an ecological point of view the metal is not consumed but simply reused during the product life time. This motivation justifies its nickname as green metal.

1.1 Factors of GSCM

Recently green supply chain management contains many logistics topics from in-bound logistics and supplier management, where logistics focuses on the movement of material and supplier management focuses on the relationships with the suppliers, in other words purchasing and its functions. This has grown to include the internal supply chain, production and outbound logistics [5] and even reverse logistics where the products after customer use are remanufactured and brought back to the incoming phase. For better understanding three factors are briefly described below; *Reverse Logistics:* is defined as the process of planning, implementing, and controlling the efficient, cost-effective flow of raw materials, in-process inventory, finished goods and related information from the point of consumption to the point of origin for the purpose of recapturing value or proper disposal [6].The variables fall into this category are; using re-

manufacturing and recovery of the end-of-life products. The main purpose behind reverse logistics is economical – cost minimizing and increasing profits.

Inbound Greening: It is fundamentally about green purchasing strategies adopted by the firms in response to ever-growing concerns of environmental sustainability all over the world [7]. This greening phase incudes choosing suppliers by environmental criteria, use of waste of other companies, urging suppliers(s) to take environmental actions.

Outbound Greening: In order to green this stage of the supply chain, the organization has to deal with green marketing, environment-friendly packaging, environment-friendly transportation, and environment-friendly waste management. The critical practices belongs to this stages are recycling of waste material internal to the company and informing consumers on environmental friendly products.

The main objective of this research work is to find out the main critical factors and various hindering effect/barriers in GSCM practices in the production phase. This study identifies the effect of different variables on the quality of the product and correlates them with quality and the performance.

2. REVIEW OF LITERATURE

There are many factors which have a major effect on the performance of the industry/firm. It is necessary to study all the factors which have a direct impact on the performance of the enterprise and productivity [8]. Green supply chain plays an important role in improvement of the service performance and productivity of the firm. A brief observation on the literatures regarding green supply chain management (GSCM) over the last twenty to thirty years hasbeen discussed and the keydrivers for green initiatives to reduce the ecological impacts on industrial activity [9].

Performances in an industry i.e. economic, environmental, and social [10]; implementing the GSCM practices in industry has a positive impact on performances [11, 12]. Increasing environmental concern in ISO14001 certified manufacturing industries in a developed and developing countries has been the main business strategy for economic performances [13]. The initiatives for environmental enhancement, economic performance and competitiveness among the manufacturing industries like chemical, Electronics, automotive, furniture, computers, wind energy sector, aluminium, steel etc. [14, 15]; different sustainable and GSCM issues in supply networks in different economic sectors like utilities, transport, information and communication technology, retail, tourism, construction, food and farming, and public sector [16,17] has been observed.

The various important hindering factors for implementing the GSCM practices in different manufacturing industries have been categories and the interaction between these factors in different phases of the industry has been summarized [18].

The researchers have used different methods i.e. Structural Equation Modeling (SEM) by [19], hypothesis test and multiple regression analysis by [20], fuzzy set theory and Decision Making Trial and Evaluation Laboratory (DMTEL) by [21], Interpretive Structural Modeling (ISM) by [22, 23], Analytical Hierarchy process by [24], sensitivity and reliability analysis by [25], ANOVA [26] to analyze the survey data and find the appropriate solution for the GSCM practices implementation in a manufacturing industry.

3. THEORY AND METHODOLGY

3.1 Critical Practices of GSCM

This research constitutes different critical practices for implementing GSCM practices. From the literature, seven critical practices have been selected which affect the GSCM practices in the industry. The various critical practices are described in Table.1.

In order to measure the critical GSCM practices and for a better understanding of seven GSCM practices are grouped into three factors i.e. reverse logistic greening, inbound greening and outbound greening; which has been discussed in introduction phase.

Variables	Critical Practices	References
VAR01	Use of waste of other companies	Rao (2007)
VAR02	Recycling of material internal to the company	Mohanty&Prakash (2014)
VAR03	Use of remanufacturing	Handfield et al. (2005)
VAR04	Choosing suppliers by environmental criteria	Yunang and Kielkiewiez (2001)
VAR05	Recovery of end-of-life product	Handfield et al. (2005)
VAR06	Urging supplier(s) to take environmental action	Rao (2007)
VAR07	Informing customers ofenvironmentally friendly products	Yunang and Kielkiewiez (2001)

Table 1.Critical practices selected from literatures

3.2 Analysis of Variance

Deco-positioning of total variability into its components is called ANOVA. It is a very important technique in the discipline of experimental statistics. Moreover, ANOVA can be very much used for analyzing the result of enquiries conducted in the field of industrial engineering. ANOVAs assess the importance of one or more factors by comparing the response variable means at the different factor levels. ANOVA uses F-tests to statistically test the equality of means. The F-statistic is simply a ratio of two variances. Variances are a measure of dispersion, or how far the data are scattered from the mean. Larger values represent greater dispersion. The procedure works by comparing the variance between group means versus the variance within groups as a way of determining whether the groups are all part of one larger population or separate populations with different characteristics.

4. DATA COLLECTION

The following section describes the administration and the findings of this research. An empirical research has been conducted in an aluminium industry, which is a manufacturing sector.

4.1 Sampling Frame

There are many aluminium industries in Odisha, due to the accessibility in XYZ Ltd. The above industry was selected for this research work. Respondents were drawn from across three sections of the industry, i.e. Port room, Casting house and Research and Development.

4.2 Sample Size

In this research work the senior most professionals, technicians, junior engineers, senior engineers, Asst. manager in various departments have been considered as the respondents for the first hand data collection. A total of 110 questionnaires were distributed, out of which 40 were rejected because some of the questionnaires were unfilled, some were wrongly filled and half-filled. Finally 70 completely filled questionnaire was considered and based on this responses further study was conducted.

4.3 Data Collection Method

The data has been collected from questionnaires administered from 21 December 2016 to 10 February 2017. The questionnaire used in this research had seven statements (appendix) for design the profile of the target respondents in terms of environmental actions taken by their organization in the past 5 years, where the respondents had to agree on a five-point Likertscale, where 1 = Very low, 2 = Low, 3 = Moderate, 4 = High and 5 = Very high.

5. DATA ANALYSIS, RESULTS AND DISCUSSIONS

Pertinent data has been collected from various respondents using the questionnaire developed in chapter 3, with specific reference to an aluminium industry (XYZ Ltd.). A total number of 110 responses have been received in the process. Out of the total 70 number of useful data sets (attached in the appendix) were used in this research after outlier detections. Then the core/scaled data were normalized for further statistical analysis. The steps are described as follows:

5.1 Measuring Implementation of Critical Practices

With the objective of measuring the extent of implementation of the green supply chain initiatives, the ratings from survey responses were considered the three factors representing phases of the green supply chain. To assess the reliability of responses, Cronbach alpha coefficient was calculated. It is defined as a measure of internal consistency, i.e., how closely related a set of items are as a group. It is considered to be a measure of scale reliability. A commonly accepted rule for describing internal consistency using Cronbach alpha is as follows:

Internal consistency is considered excellent for $\alpha \geq 0.9$, good for $0.9 \leq \alpha < 0.8$, acceptable for $0.8 \leq \alpha < 0.7$, questionable for $0.7 \leq \alpha < 0.6$, poor for $0.6 \leq \alpha < 0.5$ and unacceptable for $\alpha < 0.5$.

The Cronbach alpha values for three factors have been calculated using SPSS software table 2.

FACTORS	CRONBACH ALPHA
Reverse logistics	0.896188
Inbound greening	0.990452
Outbound greenin	0.779299

Table 2.Reliability analysis for factors

Checking on the internal consistency, the values of Cronbach alpha are high indicating that the critical practices under each factor are strongly correlated and thus they measure the same attribute.

5.2 ANOVA Test

In this approach, the goodness-of-fit statistics model has been examined for the summarized ANOVA tables of three factors of GSCM practices and the output of the model are evaluated. The data has been analyzed using the Minitab-2017 software. The respondents' opinions has been analyzed for identifying the factors deeply and how it's affects the performance of the industry. The ANOVA was carried out for significance level of $\alpha = 0.05$, i.e. for the confidence level of 95%.

5.2.1 Reverse Logistics

From the ANOVA table, it is cleared that differences between the means are statistically significant; the value of p=0.00 (<0.05). In these results, the factor explains 100% of the variation in the response,so the data fitsbest in the model. S indicates that the standard deviation between the data points and the fitted values is approximately 0.001866 units. The last column of the table-3 shows the percentage of contribution of critical practices out of total variation, indicating the degree of influence on the result. The percentage of contribution of the critical practices is 44% of the use of remanufacturing and 56% of Recovery of the end-of-life product towards reverse logistics.

Sources	DF	SS	Adj. SS	Adj. MS	F	p	% Contribution
VAR04	4	29.977	29.977	7.494	22.17	0.00	44
VAR05	4	38.534	38.534	9.633	40.71	0.00	56
Error	16	0.000	0.00	0.00	-	-	0
Total	24	68.52	-	-	-	-	100

Note: S =0.001866 R-Sq =100.00% R-Sq(adj) =100.00%

Table 3. ANOVA for Reverse logistic, using Adjusted SS

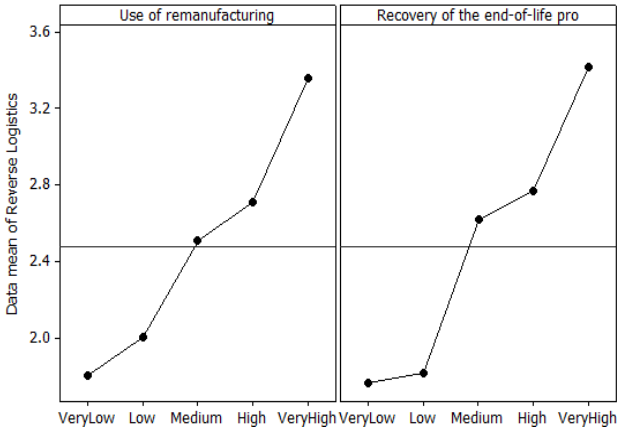

Fig.1. Main effect plot for Reverse logistics

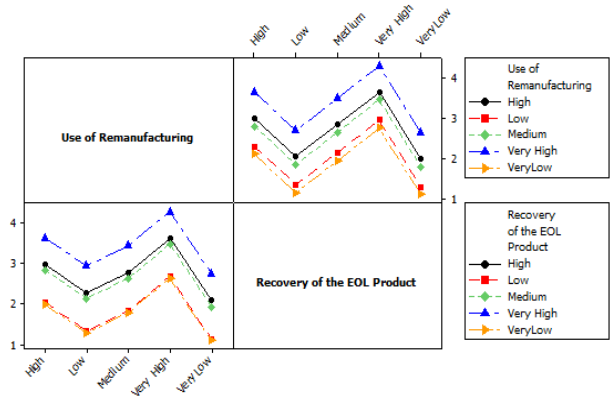

Fig.2. Interaction plot for Reverse logistics

In fig. 1 the mean values of the two critical practices have been compared. The graph indicates that both the critical practices of the reverse logistic, i.e. recovery of the end-of-life product and use of remanufacturing shows that the slope of the line is not steeper, so there is less magnitude of the main effect. In this interaction plot (fig. 2) the two variables show a greater degree of interaction at the high and medium level.

5.2.2 Inbound Greening

From the ANOVA the table.4, it is found that all the individual critical practices have significant effects on the inbound greening. All the interaction effects among the individual critical practices except one express significant effects towards the inbound greening at a significance level of 0.05. In these results, the factor explains 98.27% of the variation in the response, so the data fits better in the model. The standard deviation between the data points and the fittedvalues is approximately 0.0813235 units. As compared to two critical practices of GSCM, i.e. choosing suppliers by environmental criteria and urging suppliers (s) to takeenvironmental actions, the third one i.e. use of waste of other companies gives less percentage (26%) of contributiontoward inbound greening. Fig.3 shows the main effect plot for inbound greening. From the main effect plot, the effect of individual critical practices on inbound greening has been defined subsequently. The slop lines indicatethat choosing a supplier by environmental criteria toslope line is steeper than the other two variables slop line, so the magnitude of the main effect is greater for choosing a supplier by environmental criteria. Fig. 4 shows the interaction effect between the critical practices.

Sources	DF	SS	Adj.SS	Adj.MS	F	*p*	% Contribution
VAR04	4	34.907	34.907	8.727	31.56	0.00	34
VAR01	4	26.787	26.787	6.696	12.61	0.00	26
VAR06	4	39.446	39.446	9.862	49.14	0.00	38
VAR04* VAR01	16	0.705	0.705	0.044	6.67	0.00	1
VAR04* VAR06	16	0.163	0.163	0.010	1.54	0.11	0
VAR01* VAR06	16	0.978	0.979	0.061	9.24	0.000	1
Error	64	0.423	0.423	0.007	-	-	0
Total	124	103.412	-	-	-	-	100

Note: S = 0.0813235 R-Sq = 99.59% R-Sq(adj) = 99.21%

Table 4. ANOVA for Inbound Greening, using Adjusted SS

5.2.3 Outbound Greening

Sources	DF	Seq SS	Adj.SS	Adj.MS	F	*p*	% contribution
VAR02	4	9.596	9.596	2.399	18.51	0.00	34.009
VAR07	4	16.545	16.545	4.136	31.91	0.00	58.639
Error	16	2.074	2.074	0.129	-	-	7.531
Total	24	28.216	-	-	-	-	100

Note: S = 0.360053 R-Sq = 92.65% R-Sq(adj) = 88.97%

Table 5. ANOVA for Outbound Greening, using Adjusted SS for Tests

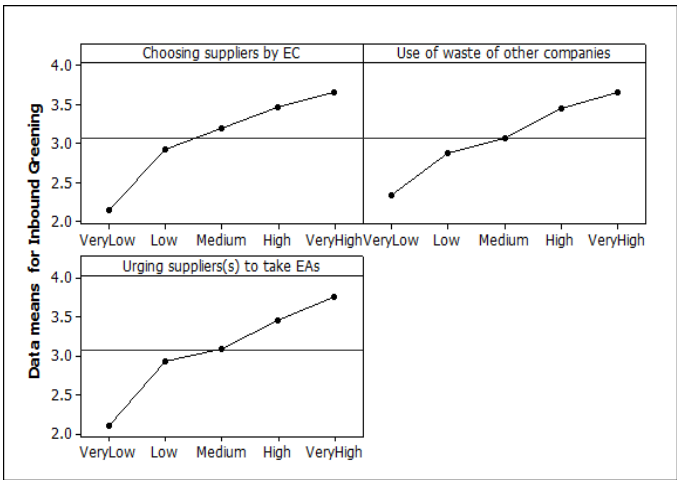

Fig. 3. Main effect plot for inbound greening

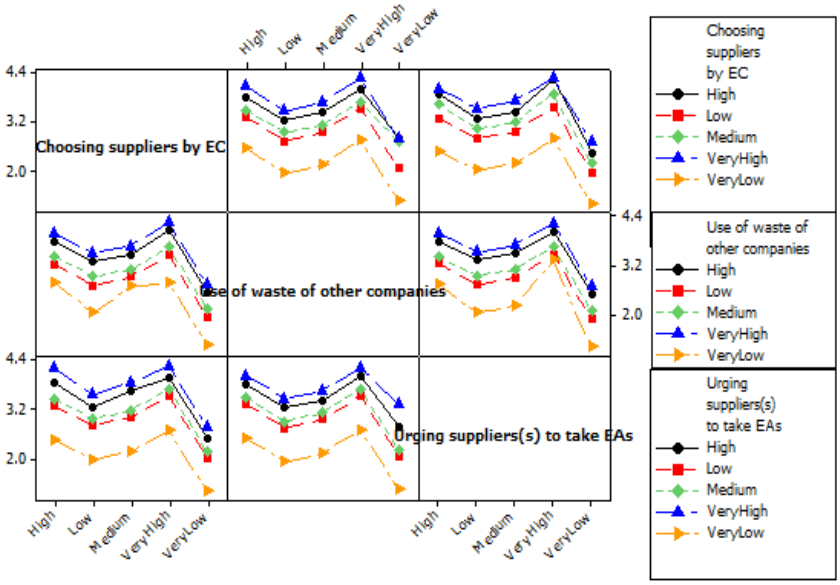

Fig. 4. Interaction plot for inbound greening

From the table it is cleared that differences between the means are statistically significant; the value of p=0.00 (<0.5). In these results, the factor explains 92.65% of the variation in the response,so the data fits better in the model. The percentage of contribution of the critical practices is 34% of recycling of waste materials internal to the company and 58.64% of informing consumers on environmentally friendly products towards outbound greening.

The graph (fig. 5) below indicates that both the critical practicesshow that the slope of the line is steeper, so there is the greater magnitude of the main effect.In the above interaction plot (fig. 6) the two variables show a greater degree of interaction.

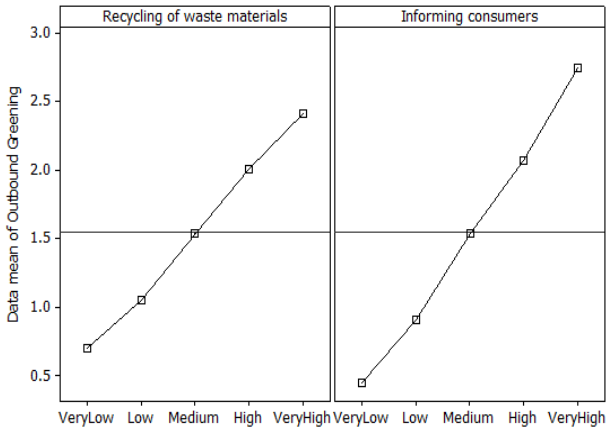

Fig. 5. Main effect plot for outbound greening

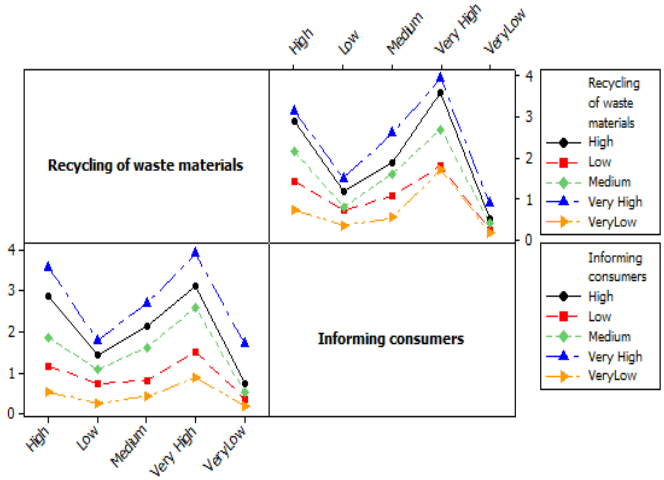

Fig. 6. Interaction plot for Outbound greening

6. CONCLUSIONS

Greening has been understood to be linked with a strong colour often associated with life, fertility and health. Being green has become an important marketing tool for economic performance. In a developing country like India, there is a rapid growth in industries which gives more opportunities for manufacturing sector but also increase the environmental burden.From the reliability analysis, the values of Cronbach alpha are found to be high. Thus, it indicates that the critical practices under each factor are strongly correlated and the internal consistency is good for all the three GSCM factors. From the ANOVA table of three factors, using adjusted sum of squares for tests shows that the probability values are less than the level of significance i.e. α=0.05, which means the model is statistically significant. R-Sq is the percentage of variation in the response that is explained by the model. The higher the R-sq value, the better the model fits the data. In this analysis, R-sq value for all the six factors is in between 90% to 100%.

- As far as the reverse logistic is concerned both the input variables significantly affects the output. However, recovery of the end-of-life products affects much for improving reverse logistics.
- As far as the inbound greening is concerned three input variables significantly affects the output. However, urging supplier(s) to take environmental actions affect more for improving inbound greening.
- Insofar as the out bound greening is concerned both the input variables significantly affects the output. However, informing consumer on environmental friendly products affect much for improving the outbound greening.

For the complete implementation of GSCM practices in the industry, users may focus their attention to the above mentioned practices for more productivity, less/zero waste, with improved product quality.

7. SCOPE FOR FUTURE RESEARCH

This research has certain limitations. The research has covered only three important sections in a leadingaluminium industry. The critical practices for GSCM implementation has been captured only in production phase initiatives using the questionnaire survey. Thus, further research work may be carried out in the other sections of the above industry and the data may be collected from other more industries (like mining, steel, electronics, automotive etc.) as well for validating the results as has been obtained in this research. In the case of large data sample, Structural Equation Modeling (SEM) method may be used/constructed in this research work.

8. REFERENCES

[1] Beamon, B. M.: *Designing the green supply chain*, Logistics Information Management, Vol. 12, No. 4, p.p. 332-342, 1999.

[2] Mutingi, M.: *Developing green supply chain management strategies: A taxonomic approach*, Journal of Industrial Engineering and Management JIEM, 6(2), p.p. 525-546, 2013.

[3] Jayant, A., Azhar, M.: *Analysis of the barriers for implementing green supply chain management (GSCM) Practices: An Interpretive Structural Modeling (ISM) Approach*, Procedia Engineering, vol97, p.p. 2157-2166, 2014.

[4] Ferretti, I., Zanoni, S., Zavanella, L., Diana, A.: "Greening the aluminium supply chain", *Int. J. Production Economics*, 108, p.p. 236-245, 2007.

[5] Srivastava, S. K.: *Green supply-chain management: a state-of-the-art literature review*, International Journal of Management Reviews, 9 (1), p.p. 53-80, 2007.

[6] Olariu, I.: *Conceptual issues regarding reverse logistics*, Studies and Scientific Researches Economics Edition, vol.18, p.p. 326-331, 2013.

[7] Chen, Y.: *The driver of green innovation and green image–green core competence*, Journal of business ethics, 81.3, p.p. 531-543, 2008.

[8] Mishra, D., Gunasekaran, A., Papadopoulos, T., Hazen. B.: *Green supply chain performance measures: A review and bibliometric analysis*, Sustainable production and consumption, vol.10, p.p. 85-99, 2017.

[9] Dubey, S. A., Gawande, Dr. R. R.:*Green supply chain management - A literature review*, International Journal of Computer Applications, p.p.0975 – 8887, 2011.

[10] Geng, R., Mansouri, S. A., Aktas, E.: *The relationship between green supply chain management and performance: A meta-analysis of empirical evidences in Asian emerging economics*, Int. J. Production Economics, 183, p.p. 245–258, 2017.
[11] Vanalle, R. M., Ganga,G. M. D., Filho. M. G.: *Green supply chain management: An investigation of pressures, practices, and performance within the Brazilian automotive supply chain*, Journal of Cleaner Production, 151, p.p. 250-259, 2017.
[12] Sulaiman, Z., Tat, H. H., Zainon, S. N., Muhamad, L.:*Green supply chain management practices and sustainability performance*, Journal of Management and Sustainability, vol. 5, No.1, p.p. 149-157, 2015.
[13] Hazikhani, M., Wahiza, N., Bin, K.: *Considering on Green Supply Chain Management Drivers, as strategic organizational development approach, Malaysian perspective*, Australian Journal of Basic and Applied Sciences, 6(8), p.p. 246-265, 2012.
[14] Poulsen, T., Lema, T.: *Is the supply chain ready for the green transformation? The case of offshore wind logistics*, Renewable and Sustainable Energy Reviews, vol.73, p.p. 758-771, 2017.
[15] Azevedo, S. G., Carvalho, H., Machado V. C.:*The influence of green practices on supply chain performance: A case study approach*, Transportation Research Part, vol. 47, p.p. 850-871, 2011.
[16] Das, P. K., Nayak, N. C.:*Assessment Modeling and Optimization of efficiency in Rice Supply Chain from a Farmers' Perspective: Study of Rice Supply Chain in Indian*, International Journal of Operation And Logistic Management, Vol. 5, No.3, p.p. 164-189, 2016.
[17] Young, A., Kielkiewicz-Young, A.: *Sustainable supply network management*, Corporate environmental strategy, 8.3, p.p. 260-268, 2001.
[18] Mehar, A.N., Agi, Rohit, N.: *Understanding influential factors on implementing Green Supply Chain Management practices: An Interpretive Structural Modeling analysis*, Journal of Environmental Management, vol. 188, p.p. 351-365, 2017.
[19] Mohanty, R.P., Prakash, A.: *Green supply chain practices in India: a confirmatory empirical study*, Production & Manufacturing Research: An open Access Journal, Vol. 2, No. 1, p.p. 438-456, 2014.
[20] Chang,B., Kenzhekhanuly, Y., Park, B.:*A Study on Determinates of Green Supply Chain Management Practices*, International Journal of Control and Automation, vol.6, No.3, p.p. 199-208, 2013.
[21] Li Ai, Q., Found, P.: *Lean and Green Supply Chain for the Product-Service System (PSS): The Literature Review and A Conceptual Framework*, Procedia CIRP 47, p.p. 162-167, 2016.
[22] Das P. K.,Nayak N. C.: *Modeling supply chain of rice, uncertainty factors & strategic supply management*, Int. Jrl. of Logistics Systems & Mgt, vol. 27, no. 3, pp. 343-362, 2017.
[23] Dubey, R., Angappa, G., Thanos, P.:*Green supply chain management enablers: Mixed method research",* Sustainable Production and Consumption, vol.4, p.p. 72-88, 2015.
[24] Kamolkittiwong, A., Phruksaphanrat, B.: *An Analysis of Drivers Affecting Green Supply Chain Management Implementation in Electronics Industry in Thailand*, Journal of Economics, Business and Management, vol. 3, No. 9, p.p. 864-869, September 2015.
[25] Sharma, V. K., Chandna, P., Bharadwaj, A.: *Green supply chain management related performance indicators in agro industry: A review*, Journal of Cleaner Production, 141, p.p. 1194-1208, 2017.
[26] Rao, P.: *Greening of the supply chain: An empirical study for SMES in the Philippine Context*, Journal of Asia Business Studies, 1.2, p.p. 55-66, 2007.

Authors: **Bandita Sahu**, M.Tech Scholar in Mechanical Engineering Department, Indira Gandhi Institute of Technology (An Autonomous Institute of Govt. of Odisha), Sarang, India-759146.
Dr. Narayan C. Nayak, Phd, Reader in Mechanical Engineering Department, Indira Gandhi Institute of Technology (An Autonomous Institute of Govt. of Odisha), Sarang, India–759146 (Corresponding Author).
E-mail: nayak.iem@gmail.com

APPENDIX

Questionnaire

On the basis of past 5years, the respondents are requested to rate on a scale of **1** to **5**, where **1 = Very low, 2 = Low, 3 = Moderate, 4 = High, 5 = Very high.**

Respondents are also requested to add any variables, if any, relevant to Green Supply Chain Management.

Name:

Designation:

Variables	Critical Practices (description of the variables)	1	2	3	4	5
VAR01	Use of waste of other companies					
VAR02	Recycling of material internal to the company					
VAR03	Use of remanufacturing					
VAR04	Choosing suppliers by environmental criteria					
VAR05	Recovery of end-of-life product					
VAR06	Urging supplier(s) to take environmental action					
VAR07	Informing customers ofenvironmentally friendly products					

IN MEMORIAM

Teach. Ass. IVAN SOVILJ-NIKIĆ, MSc. Eng. (1981 – 2017)

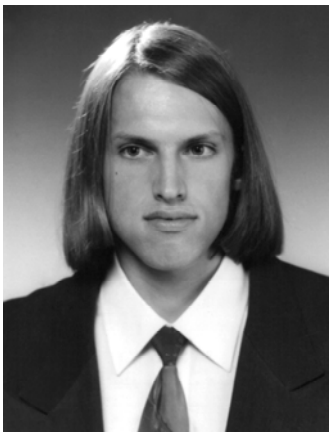

On Sunday, July 2, 2017, high-minded heart of Ivan Sovilj-Nikić at the age of 37 stopped working. Ivan Sovilj-Nikić was assistent-master at the Faculty of Technical Sciences in Novi Sad. He abandoned his colleagues and associates prematurely, without experiencing the realization of many ideas and goals for which he constantly advocated. By ethnicity Serb, Ivan Sovilj-Nikić was born on 17.05.1981. in Novi Sad from mother Ljiljana Nikić, a native of Fruška Gora, and father Bogdan Sovilj, a native of Lika. After finishing elementary school "Ivo Lola Ribar" and Gymnasium "Isidora Sekulić" in Novi Sad with an average grade of 5.00 and received the Vuk's diploma, he enrolled at the Faculty of Technical Sciences in Novi Sad at the Department of Production Engineering. Graduated-master thesis titled "Application of the genetic algorithm in optimizing the geometrical parameters of the hob milling tool" was defended on July 10, 2007. He was one of the best students since the founding of the Faculty of Mechanical Engineering in 1960 and the best student in the promotion of graduate engineers with an average grade of 10.00 (ten) in December 2007 at the Faculty of Technical Sciences in Novi Sad. In April, 2015, he planned to start the procedure for defense of his doctoral dissertation, but on April 6, he started a great battle for his health and life, which prevented him from defending his doctoral dissertation.

From early childhood he had the gift for making different models of various materials. The title of his dissertation also begins with the word Modeling. He imagined the last model on the Easter holiday on April 16, 2017. He designed a carriage and made its model from baked bread dough. You can see the photo of this model with this text.

In the final years of the Gymnasium, Ivan showed affinity for scientific research. His final examination in physics that was highly rated contained elements of research work and indicated that he was a young and promising researcher. In October 1999 he presented his first scientific paper as a co-author in Timisoara at a conference of young researchers. In the autumn of 2000, Ivan was a participant at the First Mediterranean Conference on Tribology in Jerusalem where he presented his work as a co-author, too. Ivan then picked up the applause of the attendees at the conference for a witty approach to the presentation of scientific research. As one of the top 100 students of all universities in Serbia, Ivan was a participant in the trip to Europe organized by the European Movement in 2005.

Along with the steps in education, Ivan cleared his way into the sport. He won a large number of medals in all ages and in all racing disciplines. He was the champion of the state and the representative of Vojvodina and the state in the most difficult technical discipline-steeplechase.

In professional work, Ivan has been a research scholar of the Ministry of Science and Technological Development since 2007 on the project Development of progressive technology for the back machining of profile tools on CNC machines at the Faculty of Technical Sciences in Novi Sad. During his doctoral studies, he gained his first pedagogical experience by engaging in exercises on Cutting tools, Tribology, Tribology and tools for CIM systems. Ivan was elected in the title assistent-master in 2012 for the narrow scientific field Tribology, maintenance and cutting tools. Ivan participated in the preparation and teaching in the following subjects: Tribology, Tribology and Maintenance, Cutting tools, Biotribology, Evolutionary Methods, Tribology and modern tools for CIM systems, Measurement and tools in precision engineering, Modern tools for CIM systems. Among the students he enjoyed high reputation, popularity and respect both as an expert and as a human being. He participated in the organization of several professional excursions for the students of Production Engineering, from which excursions to Prague, Ljubljana and Boljevac are set out.

Ivan was a young scientific researcher of great potential, which unfortunately did not fully develop. Despite his academic career premature stopped, Ivan achieved an outstanding number of scientific papers for his young age. During his work at the Faculty of Technical Sciences within the Department of Production Engineering at the Chair of Metrology,

quality, ecological-engineering aspect, tools and fixtures he participated in several scientific and research projects of international and national significance where he achieved significant results. During his scientific and pedagogical career he has published over 70 scientific papers, from which four monographs of international importance can be distinguished, 5 original scientific papers in international journals on the SCI list, more than 50 papers published and presented at international and national congresses, symposiums and conferences, more than 10 papers published in national journals. In the framework of doctoral studies and engagement at CEEPUS international projects, he stayed at technical faculties and institutes in Poland, Slovakia, Romania, Hungary, Bulgaria, Moldova, Macedonia, Croatia, Bosnia and Herzegovina.

Ivan Sovilj-Nikič's personality was characterized by numerous human and moral values, among which the most important honesty, the culture of behavior and behavior, the tendency to listen and appreciate a different opinion. Ivan was a well-educated, witty young man, an intellectual, a fan of sports and music. In everyday life he liked socializing, honest and friendly conversations. He had nice manners and spread positive energy. He was cheerful and well-off. He was a cordial and attentive colleague. Whenever he traveled somewhere, he traveled a lot, thought about others, and especially liked to treat friends and colleagues with gifts and small signs of attention.

At work among his colleagues at the Chair, Department, Faculty and University he was decorated by constructiveness and readiness for cooperation, that is, teamwork. His giftedness, intellectual and research capacity have put him in a group of highly capable and creative researchers. In a mountain called scientific research, Ivan did not stray, but he deliberately cleared his way to clearly defined goals.

Ivan has contributed immensely to the education and encouragement of young scientists in his country and abroad. Ivan was an energetic and active expert in the field of tribology. The originality and importance of his work, the success in applying the results of the research in practice and the promotion of tribology had a great significance at the national and international level. He constantly encouraged and influenced the scientific research work of students. As a creative engineer and scientist, he designed, constructed and executed several devices for testing the tribological characteristics of hob milling tools and gears.

Ivan successfully built a solid bridge between university researchers and engineers in industry. As an assistant, he significantly contributed to the graduation of engineers in tribology, tribodiagnostics, maintenance and cutting tools that they are now working in key positions in the Serbian and Republic of Srpska industries. As an author, Ivan prepared material for two patents that did not succeed to be formalized.

Ivan was the first to have the idea of forming Tribological Society of Vojvodina, but he was not able to carry it out. His influence on the development of tribology in Vojvodina was significant. Also, Ivan's tireless work on obtaining support for research projects of national importance and his efforts for the benefit of engineers have a lasting significance in the field of tribology.

Ivan loved history, theater and literature. He was able to express himself orally and in writing. He wrote and published novels. In his desk there were more notes and sketches for new novels, and in one of them he pointed out that he shared his Christian goodness with others without leaving anything to him.

The family, Chair, Department, Faculty and University have lost their valuables and wealth that cannot be compensated with anything. Ivan was a young man for an example that by his goodness, honesty, work, responsibility and, above all, high moral, labor and human qualities can never be forgotten and erased from the memory of parents, sister, colleagues, associates and friends.

A patient, thoughtful and just man, a strong person, a creative and curious intellectual, an outstanding pedagogue and a scientific researcher left us. His contribution to the education of engineers and the formation of scientific disciplines is irreplaceable. We will all remember Ivan for a long time.

Our Ivan went on Heavenly Tribological Congress to present a part of tribological results from his dissertation entitled by Modeling and Optimization of Hob Milling Process.

Journal of Production Engineering

PUBLICATION ETHICS AND PUBLICATION MALPRACTICE STATEMENT

The statement is based on the worldwide recognized Elsevier's Publishing ethics resource kit (http://www.elsevier.com/ethics/toolkit) and on the Committee on Publication Ethics (COPE) Code of Conduct (http://publicationethics.org/resources/guidelines). Full detailed guidelines of international standards for authors and editors can be found here: http://publicationethics.org/international-standards-editors-and-authors.

1. Authors' duties

Reporting standards. Authors of original research reports should present an accurate account of the work performed as well as an argumentatively coherent discussion of its significance. Underlying data should be represented accurately in the paper. A paper should contain sufficient detail to permit others to judge the academic and scientific merits of the work. Fraudulent or knowingly inaccurate statements constitute unethical behaviour and are unacceptable.

Data access and retention. Authors may be asked to provide the raw data in connection with a paper for editorial review, and should be prepared to provide public access to such data, if practicable, and should in any event be prepared to retain such data for a reasonable time after publication.

Originality and plagiarism. The authors should ensure that they have written entirely original works, and if the authors have used the work and/or words of others that this has been appropriately cited or quoted. Plagiarism takes many forms, from 'passing off' another's paper as the author's own paper, to copying or paraphrasing substantial parts of another's paper (without attribution), to claiming results from research conducted by others. Plagiarism in all its forms constitutes unethical publishing behaviour and is unacceptable.

Multiple, redundant or concurrent publication. An author should not in general publish manuscripts describing essentially the same research in more than one journal or primary publication. Submitting the same manuscript to more than one journal concurrently constitutes unethical publishing behaviour and is unacceptable. In general, an author should not submit for consideration in another journal a previously published paper.

Acknowledgement of sources. Proper acknowledgment of the work of others must always be given. Authors should cite publications that have been influential in determining the nature of the reported work. Information obtained privately, as in conversation, correspondence, or discussion with third parties, must not be used or reported without explicit, written permission from the source.

Authorship of the paper. Authorship should be limited to those who have made a significant contribution to the conception, design, execution, or interpretation of the reported study. All those who have made significant contributions should be listed as co-authors. Where there are others who have participated in certain substantive aspects of the research project, they should be acknowledged or listed as contributors. The corresponding author should ensure that all appropriate co-authors and no inappropriate co-authors are included on the paper, and that all co-authors have seen and approved the final version of the paper and have agreed to its submission for publication.

Disclosure and conflicts of interest. All authors should disclose in their manuscript any financial or other substantive conflict of interest that might be construed to influence the results or interpretation of their manuscript. All sources of financial support for the project should be disclosed.

Fundamental errors in published works. When an author discovers a significant error or inaccuracy in his/her own published work, it is the author's obligation to promptly notify the journal editor or publisher and cooperate with the editor to retract or correct the paper.

2. Editors' duties

Publication decisions. The editors of a peer-reviewed journal are responsible for deciding which of the articles submitted to the journal should be published. The editors may be guided by the policies of the journal's editorial

board and constrained by such legal requirements as shall then be in force regarding libel, copyright infringement and plagiarism. The editors may confer with other editors or reviewers in making this decision.

Fair play. An editor should evaluate manuscripts for their intellectual content without regard to race, gender, sexual orientation, religious belief, ethnic origin, citizenship or political philosophy of the authors.

Confidentiality. The editors and any editorial staff must not disclose any information about a submitted manuscript to anyone other than the corresponding author, reviewers, potential reviewers, other editorial advisers, and the publisher, as appropriate.

Disclosure and conflicts of interest. Unpublished materials disclosed in a submitted manuscript must not be used in an editor's own research without the expressed written consent of the author. Privileged information or ideas obtained through peer review must be kept confidential and not used for personal advantage.

3. Reviewers' duties

Contribution to editorial decisions. Peer review assists the editors in making editorial decisions and through the editorial communications with the author may also assist the author in improving the paper.

Promptness. Referees who feel unqualified to review the research reported in a manuscript or knows that a prompt review will be impossible, should notify the editor and excuse themselves from the review process.

Confidentiality. Any manuscripts received for review must be treated as confidential documents. They must not be shown to or discussed with others except as authorized by the editors.

Ethics. Reviews should be written respectfully. Personal criticism of the author is inappropriate. Referees should express their views clearly with supporting arguments. Sweeping general remarks that disfavour the author's paper is unacceptable and such remarks needs to be backed up with clear arguments and concrete references to the content of the paper reviewed.

Acknowledgement of sources. Reviewers should identify relevant published work that has not been cited by the authors. Any statement that an observation, derivation, or argument had been previously reported should be accompanied by the relevant citation. A reviewer should also call to the editors' attention any substantial similarity or overlap between the manuscript under consideration and any other published paper of which they have personal knowledge.

Disclosure and conflict of interest. Unpublished materials disclosed in a submitted manuscript must not be used in a reviewer's own research without the express written consent of the author. Privileged information or ideas obtained through peer review must be kept confidential and not used for personal advantage. Reviewers should not consider manuscripts in which they have conflicts of interest.

INSTRUCTIONS FOR CONTRIBUTORS

No. of pages:	4 DIN A4 pages
Margins:	left: 2,5 cm
	right: 2 cm
	top: 2 cm
	bottom: 2 cm
Font:	Times New Roman
Title:	Bold 12, capitals
Abstract:	Italic 10
Headings:	Bold 10, capitals
Subheadings:	Bold 10, small letters
Text:	Regular 10
Columns:	Equal column width with 0,7 cm spacing
Spacing:	Single line spacing
Formulae:	Centered and numerated from 1 in ascending order. Equations must be typed in Equation Editor, with following settings: Style>Math – Times New Roman Size>Full 12pt, Subscript/Superscript 7pt, Symbol 18 pt
Figures:	High quality, numerated from 1 in ascending order (e.g.: Fig.1, Fig. 2 etc.); Figures and tables can spread over both two columns, please avoid photographs and color prints
Tables:	Numerated from 1 in ascending order (e.g..: Tab. 1, Tab. 2, etc.)
References:	Numerated from [1] in ascending order; cited papers should be marked by the number from the reference list (e.g. [1], [2, 3] ...)
Submission:	**Papers prepared in MS Word format should be e-mailed to: pkovac@uns.ac.rs, savkovic@uns.ac.rs**
Notice:	**Papers are to be printed in Journal of Production Engineering** Sample paper with detailed instructions can be found at: **http://www.jpe.ftn.uns.ac.rs/**

FOR MORE INFORMATION, PLEASE CONTACT:

Prof. Pavel Kovač, PhD, MEng.
Assist. Prof. Borislav Savković, PhD, MEng.
FACULTY OF TECHNICAL SCIENCES
Department for Production Engineering
Trg Dositeja Obradovica 6
21000 Novi Sad
Serbia

Tel.: (+381 21) 485 23 24; 485 23 20 ; 450 366;
Fax: (+381 21) 454 495
E-mail: pkovac@uns.ac.rs, savkovic@uns.ac.rs
http://www.jpe.ftn.uns.ac.rs/